REFERENCE ONLY

UNIVERSITY OF LONDON THESIS

Degree PhD Year 2005 Name of Author CHAMSHAM

Systematic Approaches For Modelling and Optimisation of Chromatographic Processes

Sharon Hui Min Chan

November 2005

A thesis submitted for the degree of Doctor of Philosophy
of the University of London

Department of Chemical Engineering
University College London
London WC1E 7JE, United Kingdom

ProQuest LLC
789 East Eisenhower Parkway
P.O. Box 1346
Ann Arbor, MI 48106-1346

Abstract

Chromatography is an increasingly important separation technique in the fine chemical, pharmaceutical and biotechnological industries. The development of accurate, reliable mathematical models for chromatography is necessary for an efficient optimisation of the process. The past decade has seen a tremendous advance in the mathematical modelling and optimisation of the chromatographic processes, with the increase in computational power that is now available. The purposes of this work are to (1) compare chromatographic models, (2) examine the choice of chromatographic models employed and (3) compare different chromatography configurations applied to the same process.

With the variety of chromatography models available, there is a need to decide which model is best suited to a given process and the means by which the model parameters can be determined. A novel approach is proposed in this thesis for the model parameter and model selection for chromatographic processes to address both these issues and is illustrated using three case studies. This work highlights the differences in using simulated, theoretical data (which most modelling work commonly illustrated with) and experimental data, particularly data of complex bio-mixtures. Model selection is conducted using a recent graphical interpretation method, discussing the advantages and disadvantages of this method.

Over the years, the operation of the chromatographic process in these industries has undergone some changes and it is no longer limited to batch processing. Whilst the single column is still popular in preparative chromatography, multi-column processes are now becoming increasingly popular in industrial-scale chromatography to produce large amounts of highly purified products.

In light of the diversity of operational policies now available to chromatography, the second half of this thesis addresses examines the differences between the single column and the multicolumn chromatographic processes. Preliminary work is done on developing a detailed model of the simulated moving bed (SMB) chromatographic

process, presenting both a dynamic model and two cyclic steady state (CSS) models. A theoretical case study is then optimised for the operation of the SMB process.

The simulated moving bed (SMB) process and its recent variation, the Varicol process, are particularly well known. Such processes are continuous and are able to produce large quantities of high purified products. The decision of choosing either a single column or multi-column process for a separation is not a clear cut one. As the configurations and process operations in these processes are vastly different, an economic comparison between the optimised process alternatives is thus necessary to properly assess the strengths and weaknesses of each system, particularly from an industrial point of view. In column chromatography, a single column, as well as a single column with recycle and peak shaving operations, are considered, whilst for the multi-column alternative, the SMB process and its variations (Varicol, Powerfeed etc.) are examined.

Acknowledgements

I would like to express my deepest gratitude to both my supervisors, Dr Eva Sørensen and Professor Nigel Titchener-Hooker. Both of them been extremely supportive of the work that I have done, and have done much to encourage me broaden my horizons and explore things outside of my PhD study. They were also very reassuring and helpful, especially when my confidence level was low. I cannot thank them enough.

Special thanks also go to Dr Daniel Bracewell, who helped me immensely in understanding many practical aspects of chromatography in bioprocesses and also for helpful pointers in developing this work. A word of thanks is also due to Simon Edwards-Parton in helping me solve problems I encountered during this work. In addition, I owe some heartfelt thanks to Derek Hill of Novasep and Marc Bisschops from Univalid, who were very kind to spend some time to talk me through about industrial costing data.

I would also like to take this opportunity to thank my colleagues and members of staff of the Chemical Engineering and Biochemical Engineering departments at University College London for their help and suggestions when I encountered problems during the course of my research. Special acknowledgements in particular go to Taj Barakat and Kashif Ali Zahoor for their invaluable feedback on my work at all stages of this research, in both oral and written presentation. In particular, I would really like to thank Kashif for not only assiduously checking every single reference and notation of this work, but also helping me with the printing of this thesis.

This work also could not have been done without the financial support from the Centre for Process Systems Engineering in my first year of research and subsequent financial aid from University College London Graduate School and the Overseas Research Council.

My dearest parents have to be thanked for as well the countless trips they have made to the UK during my study to not only cook and clean for me whilst I studied

(I honestly do all this on my own usually!), but also to encourage me in my work. They have always been willing to spend extra time with me, and I am glad that they are happy with this work.

Finally, though last but certainly not least, I wish to thank the members of New Life Bible-Presbyterian church of Queens Park and other Christian friends in London and Singapore, for the years of prayer and encouragement through my course, right up to the very end, without which I could not have done this work. I especially owe John Poh much thanks for his patience in listening to me and constantly praying for me during this time. Thanks be to the good Lord God for leading me to do this PhD and through it, for helping me to run the race and to finish it well (and in time!). I am also ever thankful for my great Comforter Jesus Christ during the personal dark times I went through whilst I was doing my PhD. At the end of it all, may this work bring honour to His Name.

Jeremiah 31:3 *The LORD hath appeared of old unto me, [saying], Yea, I have loved thee with an everlasting love: therefore with lovingkindness have I drawn thee.*

Contents

List of Figures

List of Tables

Chapter 1

Introduction

In this chapter, the background to this project is given. First, the main processes and applications of chromatography are briefly introduced together with an overview on the history of chromatography (Section 1.1). Background information on the scale of operation, separation and operation techniques used in chromatography are subsequently reviewed (Section 1.2). The different mechanisms of chromatographic separation are also studied (Section 1.3). The motivation and objectives of this research are discussed (Section 1.4), and an outline of the thesis is delivered (Section 1.5). Finally, the main contributions of this research work are summarised (Section 1.6).

1.1 Introduction

Chromatography is a separation technique in which a mixture is separated into its constituents, usually by passing it through a surface of some adsorbent (McKetta, 1979). Chromatographic methods are characterised by their high selectivity and their ability to achieve separation between components of very similar physical and

chemical properties (Coulson and Richardson, 1991). Analytical chromatography is used extensively in areas such as the analysis of art objects, quality control in industry, analysing biological materials and in forensics. However, chromatography is also used as a commercial separation process known as *production chromatography.* Production chromatography is a relatively new unit operation in the process industries and its use is increasing with the growing demand for high purity materials (Coulson and Richardson, 1991). Development of accurate and reliable mathematical models for chromatography is thus necessary for an efficient optimisation of the design and operation of the process. The increase in computational power available over recent years has seen a tremendous advance in research within mathematical modelling and optimisation of chromatographic processes. With the variety of chromatography models available, there is, however, a need to decide (i) *which* model is best suited to describe a given separation process and (ii) the means by which the model parameters can be determined.

In addition, over the last decade, the operation of chromatographic separations in industry has undergone several changes and is no longer limited to batch processing. Whilst the single column is still popular in preparative chromatography, multi-column processes are now increasingly favoured in industry to produce large amounts of highly purified products. Choosing between a single column or multi-column process for a separation, and the different operating strategies for each, is not a clear cut decision, given the vastly different configurations and operating policies within these alternatives.

In view of these needs, this work sets out to address (1) the choice of which chromatographic models to employ in optimisation of design and operation and (2) to compare different chromatography configurations, and operating strategies, applied to the same separation to determine which is the most suitable for a given separation. To be able to attend to these issues, one requires a clear understanding of the background to chromatography.

1.1.1 History of chromatography

The first scientific reports demonstrating the chromatographic phenomena appeared in the 1890s but it was not until 1906 that the era of analytic chromatography began.

This was due to the publication of a paper by Mikhail Tswett, a Russian botanist, describing the separation and identification of the components of a mixture of structurally similar green and yellow chloroplast pigments in leaf extracts. A solution of these extracts on carbon disulphide was passed through a column packed with chalk. Through this experiment, the mechanism by which separation occurred was identified to be adsorption. In addition, the application of a pure solvent to the development of a chromatogram was discovered. It was then that the potential of the technique of adsorption as a means of identifying compounds by properties other than colour was realised (Kirk-Othmer, 1993). Tswett is credited as "the father of chromatography" because he coined the term chromatography, (coming from the combination of two Greek roots "chroma", meaning colour,and "graphe", meaning writing), and because he scientifically described the process (McNair and Miller, 1998).

In the 1940s, Martin and Synge introduced liquid-liquid partition chromatography using silica gel loaded with water as a chromatographic stationary phase. These separations took place due to a combination of adsorption and partition. Martin suggested in this paper (Martin and Synge, 1941) the possibilities of using gas as a mobile phase; the work of which he only undertook nearly a decade later with James (James and Martin, 1952). Around the same time, Tiselius independently developed frontal analysis and displacement analysis (Scott, 1976).

In 1949, Maclean and Hall introduced a starch binder into an alumina absorbent to make the first effective form of Thin-Layer Chromatography (TLC). It was discovered that TLC had advantages over paper chromatography due to the larger forces between the component molecules and adsorbent relative to component molecules and a liquid. TLC was developed extensively and became an extremely effective

separation technique with a wide field of applications (Scott, 1976).

With the publication of James and Martin's work on using gas as a mobile phase (James and Martin, 1952), gas-liquid chromatography techniques were developed and Gas-Liquid Chromatography (GLC) rapidly replaced analytical low-temperature distillation in the petrochemical and petroleum industries. It had a phenomenal rate of development as the basic chromatograph was simple and inexpensive, simple methods of detection could be employed and effective separations could be obtained with basic coating and packing (Scott, 1976).

Despite its wide range of applications, GLC had a large number of problems, especially where thermally labile and highly polar materials in the high molecular field had to be separated. Attention was therefore turned to the development of liquid column chromatography (Scott, 1976).

Modern liquid chromatographic techniques originated in the late 1960s and early 1970s. The recent development of modern liquid chromatography with special column packings and fully automated equipment has renewed the interest in liquid column chromatography. High Performance Liquid Chromatography (HPLC) now utilises adsorbent particles having diameters of 20μm or less to achieve faster and sharper separations. The use of smaller-diameter particles requires pressures to be about 14 to 140 bar to force the feed and solvent through the tightly packed bed, and the technique is therefore sometimes referred to as High Pressure Liquid Chromatography (Schweitzer, 1996).

1.1.2 Theory of chromatography

In this section, the basic concept of a chromatographic process is explained to provide an a understanding of the fundamentals of the chromatographic technique.

A summary of important terms generally used when describing chromatographic processes is given in Appendix A.

What is chromatography?

The definition of chromatography given by the International Union of Pure and Applied Chemistry (IUPAC) is: "Chromatography is a physical method of separation in which the components to be separated are distributed between two phases, one of which is stationary (stationary phase) while the other (the mobile phase) moves in a definite direction" (McNair and Miller, 1998).

Chromatographic separations depend on fundamental differences in the affinity of the constituents of a mixture for the phases of the chromatographic system (Kirk-Othmer, 1993). The constituents separate by distributing themselves between two phases present in the chromatographic unit. These phases, so named because of their motions relative to one another, are known as the *mobile* phase and the *stationary* phase. The separation of the constituents results primarily from the differences in their affinity for the stationary phase.

There are a great many different types of chromatography and these can broadly be classified according to the nature of the mobile and stationary phases (gas or liquid) as well as the technique (planar or column) used in separation. There are generally two large classes of chromatography, *gas chromatography* (GC) and *liquid chromatography* (LC) and their names derive from the nature of the mobile phase under which the chromatography is carried out. In this thesis, the focus is on liquid chromatography.

When to choose chromatography?

The chromatographic process

Figure 1.1 is a schematic representation of the chromatographic process. The horizontal lines represent the column and time is zero at the top and increases downwards. Each line represent what is happening in the column as time progresses.

A mixture of components A and B is introduced into the column and it is then carried along the column (from left to right) by the mobile phase. It is thus in

contact with two phases, the stationary phase and the mobile phase. The stationary phase is contained in a column or sheet, through which the mobile phase moves in a controlled manner relative to the stationary phase. The components in the mixture which have a greater preference for the stationary phase compared to the mobile phase, is adsorbed. In Figure 1.1, component B has a higher *affinity* for the stationary phase and is adsorbed. The unadsorbed part of the mixture is carried along by the mobile phase (Component A). An equilibrium is established between the adsorbed components (peaks below the lines in Figure 1.1)and what remains in the mobile phase (peaks above the lines).

Due to the differences in the affinity of the components for the stationary phase and the mobile phase, the components tend to be swept along the column with the mobile phase at different rates. This selective interaction of the constituents with the two phases is known as *partitioning* (Kirk-Othmer, 1993), while varying rates of movement of different constituents in the column is known as *differential migration* (Snyder and Kirkland, 1974).

In Figure 1.1, each component partitions between the two phases, as is shown by the peaks above and below the line. The peaks which are above the line represent the amount of a particular component in the mobile phase, while the peaks below represent the amount in the stationary phase. From Figure 1.1, it is observed that component A has a greater distribution in the mobile phase, while component B has a greater affinity in the stationary phase. Consequently, component A is swept down the column faster than component B, which spends more time in the stationary phase. Thus, separation of the components occurs as they travel through the column. Eventually, each component leaves the column and pass though the detector. The output signal gives rise to the *chromatogram* shown at the right side in Figure 1.1 (McNair and Miller, 1998). The chromatographic peaks in the figure widen or broaden as the separation progresses. The is known as *band broadening.* (Refer to Appendix A for more details on terms relating to chromatography.)

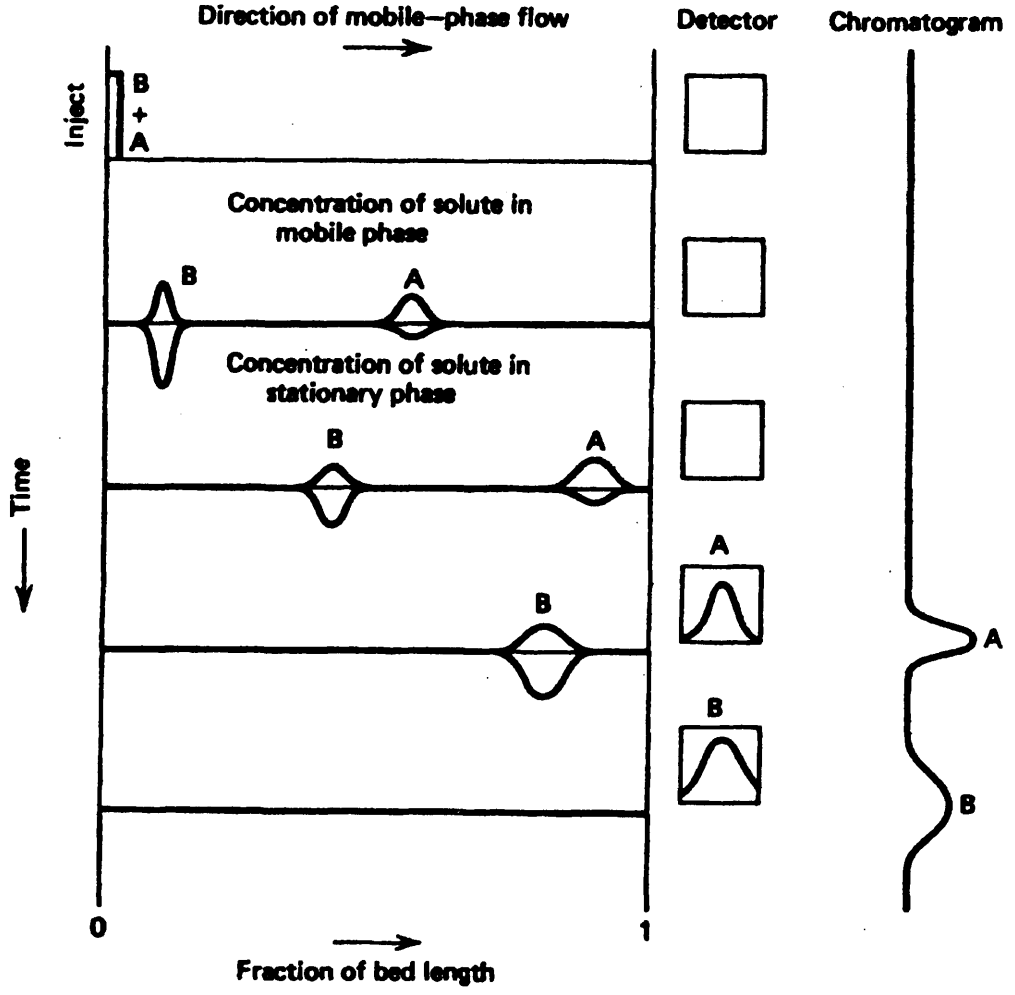

Figure 1.1: Chromatographic Separation of A and B (MacNair and Miller, 1998)

1.2 Chromatographic operations and methods

Chromatography is a versatile separation tool which can be characterised by its scale of operation (Section 1.2.1), operation modes (Section 1.2.2), design configuration and operating policies (Section 1.2.2), and the equilibrium between the phases in the column (Section 1.2.3). The following sections will summarise the main features of these characteristics.

	Analytical	**Preparative**	**Production**
Performance criteria and basis for design	Resolution and speed of analysis	Throughput for specified purity	Production cost, *i.e.* throughput/cost per year, for specified purity
Processing rate	—	0.1g - 1kg	0.02-0.3 kg/h(100mm diameter), 0.2-3.0 kg/h(300mm diameter)
Column diameter	0.3-5mm	3-40mm	>30mm
Column length	>0.03m	0.1-2m	0.2-2m
Particle size†	3-8μm	8-60μ	20-70μm

Table 1.1: Comparison of analytical, preparative and production chromatography (Coulson and Richardson, 1991) † except for proteins, which are about 30-300μm

1.2.1 Scale of operation

Depending on the scale of operation, liquid chromatography can generally be divided into analytical, laboratory-scale preparative and process-scale chromatography. The fundamentals of all chromatography systems are basically the same whichever category they fall in. In analytical systems, the objective is to *identify* the components present in a small sample volume (Subramanian, 1995). It is frequently used in fields dealing with forensic and biomedical studies. At the other end of the scale, in process chromatography, the end goal is to *purify* one or more components in the mixture and to simultaneously maximise the throughput. Lab-scale chromatography falls in the mid-range and can be semi-analytical or preparative. It is the size of operating equipment and the quantity to be collected that will define the operating scale of the chromatographic separation. A comparison of the different categories of scale is given in Table 1.1 (Coulson and Richardson, 1991).

1.2.2 Chromatography modes and techniques

Tiselius defined three distinct modes in which a chromatographic column can be operated: elution, displacement and frontal (Subramanian, 1995). In addition, there are other means of operation which are intermediate (*e.g.* gradient elution) and other operating techniques which have been used to improve the operation of chromatography (*e.g.* recycling, peak shaving, simulated moving bed *etc.*). These modes and techniques are discussed in this chapter.

Elution chromatography

Elution is the most widely utilised technique among the three main modes. In elution chromatography, a mixture is transported by the mobile phase through a fixed bed of sorbent, which is the stationary phase, as illustrated in Figure 1.2. Each component in the mixture migrates at a different rate along the column; those that travel faster elute from the column bed faster, enabling a separation to be achieved. The rate of migration of each component depends mainly on its distribution between the stationary phase and the mobile phase (McKetta, 1979). This distribution is a result of the interactions between the component and both the mobile and the stationary phase and an equilibrium between the two is established. The time which one constituent spends in the mobile phase, compared with the time it spends on the stationary phase, is different for different constituents. Components which interact less with the stationary phase are eluted from the column faster than those which interact more strongly with the stationary phase. In elution chromatography, all of the sample material is usually removed from the column during the chromatographic process and the column can thus be reused without regeneration (Kirk-Othmer, 1993).

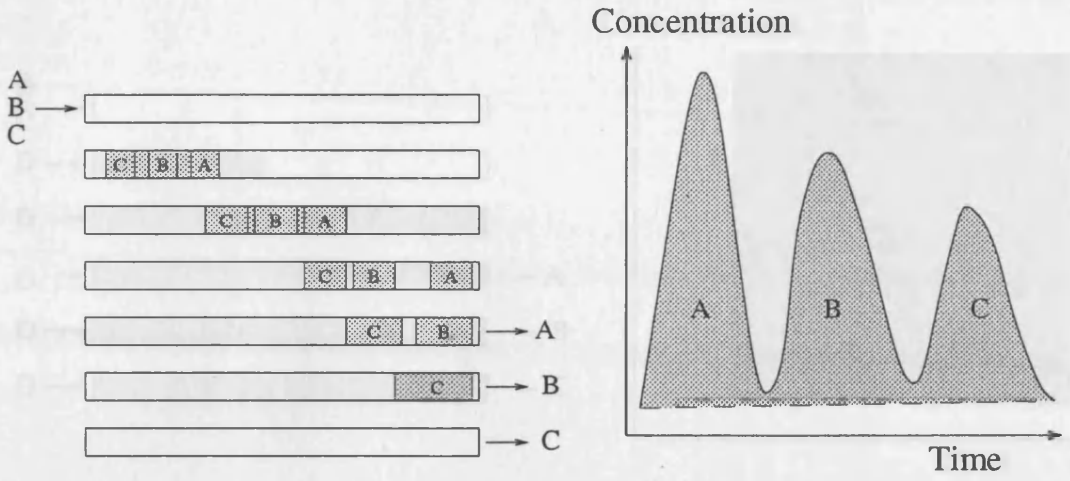

Figure 1.2: Elution Chromatography (Subramanian, 1995)

Displacement chromatography

In displacement chromatography, there is minimal interaction between the mobile phase and the stationary phase. As the mixture is loaded into the column, components with the weaker affinity for the stationary phase are displaced by components with a stronger affinity (In Figure 1.3, component A is displaced by component B, which is then displaced by component C). By adding a substance to the mobile phase which has a much stronger affinity for the stationary phase than the most strongly adsorbed component in the sample, the latter will be displaced. This results in a series of bands being set up across the column, each band being displaced by a band which is more strongly attracted to the stationary phase, as shown in Figure 1.3 (Subramanian, 1995).

This technique is useful for the generation of pure material, especially in the application of environmental analyses. However, it has the disadvantage that once the column has been used, some of the sample remains on the column and the column has to be regenerated before it can be reused (Kirk-Othmer, 1993), which presents additional costs in terms of time and materials.

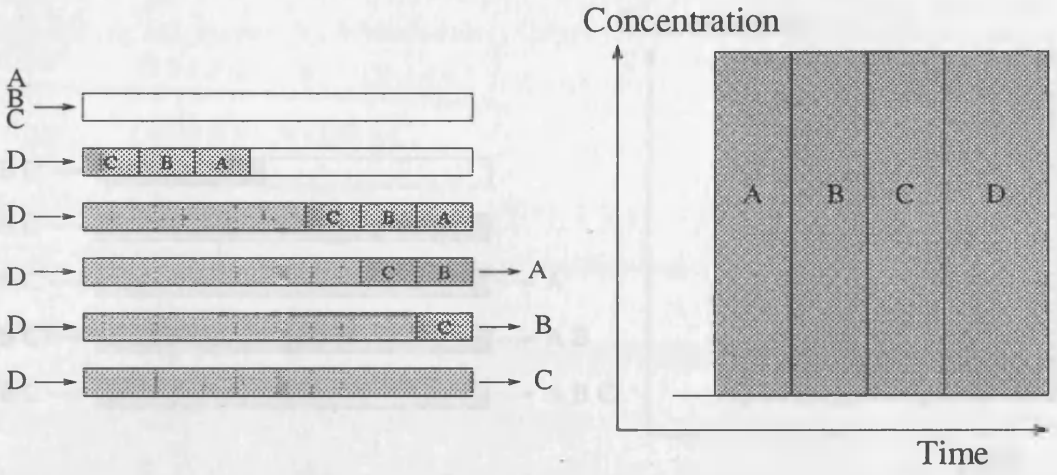

Figure 1.3: Displacement Chromatography (Subramanian, 1995)

Frontal chromatography

Frontal analysis is a special form of displacement chromatography in which the sample is continuously introduced into the column. From Figure 1.4 one can observe how frontal chromatography works. The eluent collected first at the end of the column is the mobile phase, free of the material that is adsorbed on the column. When all the adsorption sites on the stationary phase are occupied, the component which has the weakest affinity for the stationary phase (Component A) begins to elute from the column. Eventually, with increased loading, all the adsorption sites are occupied by the component in the mixture with the highest affinity for the stationary phase (Component C).

Subsequently, the column can be washed free of the unadsorbed material. The remaining component can then be displaced using an appropriate substance which has a higher affinity for the stationary phase than the remaining component. Frontal chromatography is not well suited to the production of high quality materials and this limits its general applicability, although there are occasions when it is used, such as for adsorption isotherm studies.

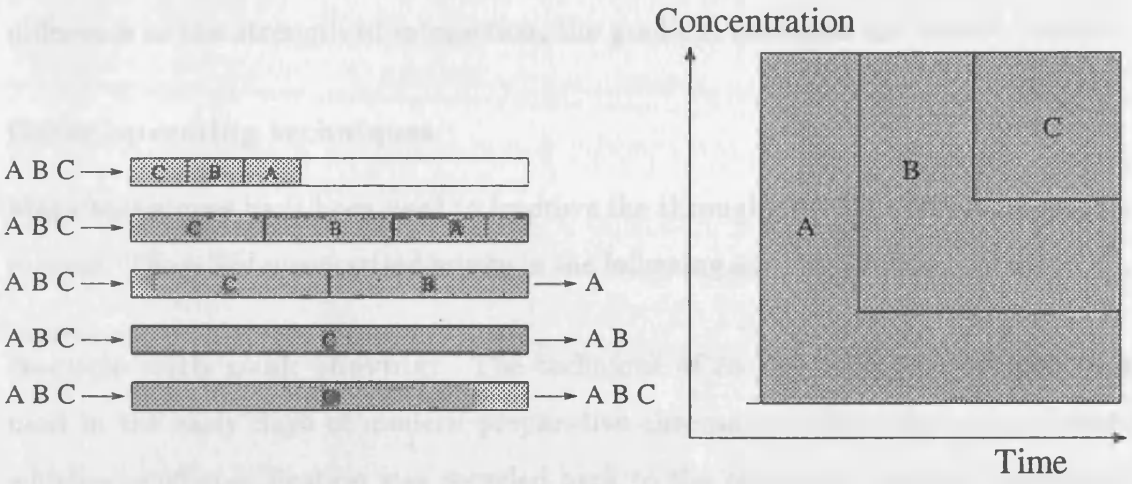

Figure 1.4: Frontal Chromatography (Subramanian, 1995)

Other operating modes

In most cases, the three modes of chromatography described above are not sharply defined (Subramanian, 1995). Under elution conditions, if the concentration of the component is increased, the equilibrium between the mobile and stationary phase is changed. Competitive interaction between the constituents with the stationary phase takes place, depending on their affinity for the stationary phase. As such, the interaction of the components between the mobile phase and the stationary phase decreases. The dominant mechanism is then displacement chromatography and this is the so-called "self-displacement" effect. Where the concentration of the constituent is higher in the column, the predominant mechanism is displacement chromatography. At the back of the band, where the concentration is lower, the predominant mechanism becomes elution.

Changing the composition of the eluent is referred to as *gradient elution.* Increasing the strength of the mobile phase concentrates the band and induces a displacement mechanism, and also maintains the high concentration of component required for the displacement train in the column. For lower concentrations, gradient elution works by an elution mechanism. When the constituents have a large

difference in the strength of interaction, the gradient increases the rate of elution.

Other operating techniques

Many techniques have been used to improve the throughput of the chromatographic process. These are summarised briefly in the following sections (Subramanian, 1995).

Recycle with peak shaving: The technique of recycle with peak shaving was used in the early days of modern preparative chromatography, where the product which was off-specification was recycled back to the column to improve the purity. It has recently been revived for use in preparative enantiomeric separations (Subramanian, 1995). Work involving recycle with peak shaving has demonstrated significantly better purification compared with conventional recycling operation (Teoh, 2002). While it was useful in one-off operations, it is not a good method for process operations as it may be slow and difficult to automate (Subramanian, 1995).

Overlapping sequential injections: Sequential injections onto a column can be overlapped to use the window before the fastest component begins to elute from the column in order to collect fractions from the previous injection. Column usage is maximised in this manner and solvent usage can be reduced (Subramanian, 1995).

Reverse directional flow: Another technique to improve column operation is to reverse the direction of the flow in the column and to inject the sample alternately at either end of the column. This has been demonstrated to provide higher throughputs with reduced solvent consumption for elution chromatography (Subramanian, 1995). This approach, however, requires a column where the stability of the packed bed is unaffected by the direction of flow.

True moving bed chromatography: The true moving bed (TMB) process refers to the technique where the stationary phase ("bed") is moving countercurrent to the flow of the mobile phase. Due to the circulation of a solid adsorbent, or stationary

phase, it is immensely difficult mechanically to operate a TMB process, in spite of the benefits of a countercurrent operation (Subramanian, 2001). Thus, the true moving bed concept is implemented in a different way, using the simulated moving bed (SMB).

Simulated moving bed chromatography: Simulated moving bed (SMB) chromatography refers to the technique where a continuous countercurrent operation is simulated to avoid the actual movement of the solid (the stationary phase), which is what happens in a true moving bed (TMB). In this mode, the bed is not moving. However inlet (desorbent and feed) and outlet (extract and raffinate) lines are shifted at a fixed time frequency, thus simulating the flow of the bed.

This technique was not commonly used in the past due to patent restrictions, although it has been around since the 1960s. Subsequently, when these restrictions were lifted, due to a lack of understanding of the complex process dynamics, there were engineering problems developing SMB units. With the recent development in instrumentation and understanding of the SMB process, its prospects for wider acceptance in industry is fast improving given its ability to produce large amounts of purified products very efficiently.

1.2.3 Linear and non-linear chromatography

Chromatographic separation may be divided into linear and non-linear chromatography depending on the operating region of the isotherm involved. An *isotherm* describes the relationship between the component concentration in the mobile and the stationary phases, and thereby characterises the component's behaviour during separation. Different isotherms are discussed in more detail in Section 1.2.4.

Linear chromatography

Linear chromatography assumes that the concentration of the sample component in the stationary phase is proportional to its concentration in the mobile phase, and the

isotherm is summarised by a proportionality coefficient. This assumption is usually valid for analytical applications of chromatography, where the sample size is small and the concentration is low.

Non-linear chromatography

In non-linear chromatography, the separation is carried out under overloaded conditions (either concentration or volume overloaded), in order to maximise the process throughput. As the component concentration increases the ratio of component concentration in the stationary phase (q) to that in the mobile phase (C_i^m) decreases. This is because with an increase in concentration, there is a decrease in the number of adsorption sites on the stationary phase available for further chromatography separation. Thus, the saturation of column capacity will cause intense competition between components of interest for the availability of free adsorption sites. As a result, the retention factor and solute (or component) velocity (refer to Appendix A for definitions) will *not* vary proportionally with respect to the changes in component concentrations. In such a scenario, a more complex isotherm model is required to account for these deviations from linearity.

1.2.4 Adsorption equilibria

The two phases of a chromatographic system are never truly at equilibrium. As the continuous flow of the mobile phase pushes the sample components along the column, a difference in chemical potential of the component between the two phases is maintained and equilibrium is therefore not achieved (Guiochon *et al.*, 1994). This gives rise to local concentrations in both phases, which can be expressed numerically by an isotherm relationship, a function defining the behaviour of the component concentration between the mobile and stationary phase.

The Linear isotherm The linear isotherm is the simplest relationship describing the adsorption equilibrium and can be represented by:

$$q_i = K_i C_i^m \tag{1.1}$$

which means that the concentration of component i adsorbed on the stationary phase q at equilibrium is proportional to the component concentration in the mobile phase, C_i^m, and K_i is the proportionality constant (also known as the Henry's constant).

This isotherm is widely used in analytical chromatography as it simplifies calculations of their elution profiles. Moreover, it does not include the influence of thermodynamics on the shape of the band profile, and thus the influence of the kinetic parameters (such as mass transfer parameters) can be isolated for study (Guiochon *et al.*, 1994).

The Langmuir isotherm The Langmuir isotherm is derived from simple mass-action kinetics, assuming chemisorption (an adsorption by means of *chemical* forces, rather than physical). The underlying assumptions behind the Langmuir isotherm are:

1. The adsorbent presents a set of equivalent, distinct and independent binding sites.

2. Each site binds with one molecule only.

3. There are no interactions between the bound molecules.

The classical form of the Langmuir isotherm is given as:

$$q_i = \frac{a_i C_i^m}{1 + b_i C_i^m} = \frac{b_i q_{i,s} C_i^m}{1 + b_i C_i^m} \tag{1.2}$$

where b_i is the ratio of the rates of adsorption and desorption where $b = k_a/k_d$ and $q_{i,s}$ is the saturation capacity of the stationary phase.

Experience shows that the Langmuir isotherm is an excellent approximation for single-component adsorption equilibrium in liquid-solid chromatography (Guiochon *et al.*, 1994).

The Bi-Langmuir isotherm In most cases, the surface of the adsorbent used in chromatographic separations is not homogenous, but rather contains several different kinds of sites which behave independently. For the bi-Langmuir isotherm, it is assumed that two different kinds of sites exist and the equilibrium isotherm thus results from the addition of the two independent contributions of the two types of sites:

$$q_i = \frac{a_1 C_i^m}{1 + b_1 C_i^m} + \frac{a_2 C_i^m}{1 + b_2 C_i^m} = \frac{q_{s,1} b_1 C_i^m}{1 + b_1 C_i^m} + \frac{q_{s,2} b_2 C_i^m}{1 + b_2 C_i^m} \tag{1.3}$$

where the subscripts 1 and 2 denote the different binding sites.

The Competitive Langmuir isotherm The Langmuir isotherm can be extended to multicomponent systems as well. With the presence of other components in the solution, the amount of each component adsorbed at equilibrium is less than if that component were alone. This is due to the interference of the different components. A kinetic derivation of the competitive isotherm for a binary mixture can be found in Guiochon *et al.* (1994). For the ith component of a multicomponent system, the competitive isotherm can be written:

$$q_i = \frac{a_i C_i^m}{1 + \sum_{j=1}^{n} b_j C_j^m} \tag{1.4}$$

where n is the number of components in the system. The coefficients a_i and b_i are the coefficients of the single-component Langmuir equilibrium isotherm for component i.

The Competitive bi-Langmuir isotherm This isotherm is analogous to the competitive Langmuir isotherm, except in this case, the surface of the adsorbent is covered by two different kinds of sites, and thus the competitive behaviour of the two components is accounted for by using the bi-Langmuir isotherm:

$$q_i = \frac{a_{i,1} C_i^m}{1 + b_{A,1} C_A^m + b_{B,1} C_B^m} + \frac{a_{i,2} C_i^m}{1 + b_{A,2} C_A^m + b_{B,2} C_B^m} \tag{1.5}$$

1.3 Principles of separation

In this section, the different retention mechanisms or principles encountered in chromatographic separation are discussed. In all chromatographic separations, with the exception of size exclusion chromatography (SEC) (gel filtration), the components adsorb to the surface of the stationary phase. The following sections discuss each retention mechanism in detail. Note that the emphasis of this work is on adsorption chromatography.

Adsorption chromatography

Adsorption is based primarily on the differences in the relative affinity of compounds for the solid adsorbent used as a stationary phase. This affinity is determined almost entirely by polar interactions, molecules are retained by the interaction of their polar functional groups with the surface functional groups. Component molecules which have greater interaction with the stationary phase, and are thus more retained in the column to elute later. Figure 1.5 illustrates the principle behind adsorption.

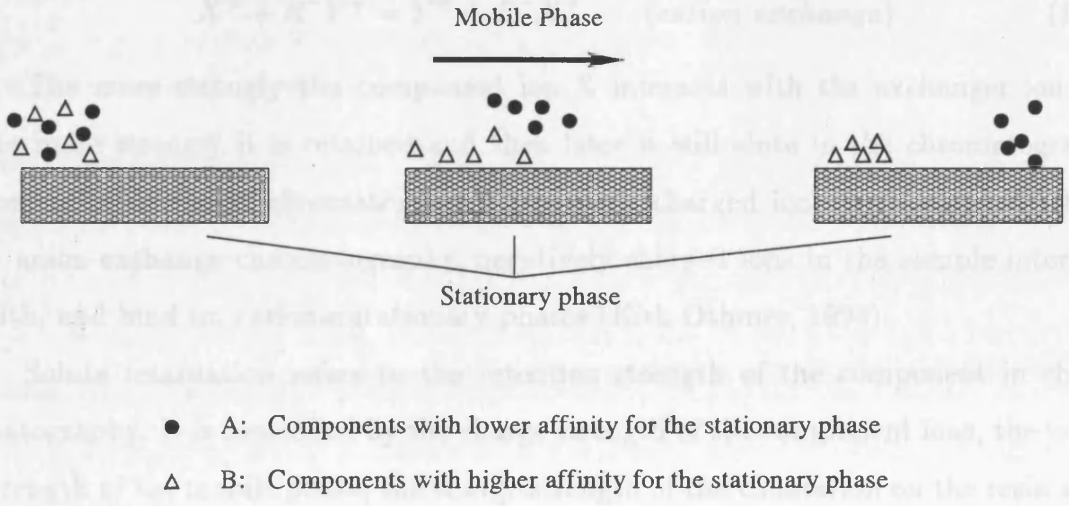

Figure 1.5: Adsorption chromatography of two components

Ion-exchange chromatography

Ion-exchange chromatography (IEC) is an adsorption process in which a reversible exchange of ions occurs between the aqueous carrier, the mobile phase, and the charged surface of the ion-exchange resin (the stationary phase). The ion-exchanger consists of an insoluble matrix to which fixed charged groups *e.g.* sulphonate or carboxylate, have been covalently bound. The charged groups are associated with mobile counter-ions, such as sodium or potassium. These counter-ions can be reversibly exchanged with other ions of the same charge without altering the matrix.

The ionic feed is introduced into the mobile phase and when introduced into the column, results in retardation in movement due to ion-exchange between component ions X and mobile phase ions Y with the charged groups R of the stationary phase (Coulson and Richardson, 1991):

$$X^- + R^+Y^- = Y^- + R^+X^- \qquad (anion\ exchange) \tag{1.6}$$

$$X^+ + R^-Y^+ = Y^+ + R^-X^+ \qquad (cation\ exchange) \tag{1.7}$$

The more strongly the component ion X interacts with the exchanger ion R, the more strongly it is retained and then later it will elute in the chromatogram. For cation-exchange chromatography, positively charged ions are separated while in anion-exchange chromatography, negatively charged ions in the sample interact with, and bind to, cationic stationary phases (Kirk-Othmer, 1993).

Solute retardation refers to the retention strength of the component in chromatography. It is controlled by the charge strength of the component ions, the ionic strength of the mobile phase, the charge strength of the counterion on the resin and the pH of the mobile phase. Retardation can be decreased by increasing the ionic strength of the mobile phase or decreasing the charge strength of the counterion. In addition, by adjusting the mobile phase pH in such a way that dissociation of either the component, the counterion on the mobile phase or both occurs, the retardation

can decreased (McKetta, 1979). As IEC can be carried out with an aqueous mobile phase near physiological conditions, this is an important technique used in the purification of proteins (Coulson and Richardson, 1991).

Partition chromatography

Partition chromatography, also known as liquid-liquid chromatography, is based on the relative solubility characteristics of components between the mobile phase and a liquid phase held stationary by impregnation on a porous, inert support. The stationary phase is normally more polar than the mobile phase, but sometimes it may be more beneficial to have the roles reversed and to have a stationary phase that is less polar than the mobile phase. This is known as *reversed phase partition chromatography* (Perry *et al.*, 1972).

In practice, the range of stationary phases which can be used is restricted. As the component molecules arefree to diffuse within both the mobile and the stationary phase, the thickness and viscosity of the mobile phase are relevant properties affecting the speed of separation (McKetta, 1979).

Exclusion chromatography

Size exclusion chromatography (SEC), also known as gel permeation chromatography (GPC) or gel filtration chromatography (GFC), separates molecules by size in solution. The sample is passed through a column which has been tightly packed with a porous permeable gel in the mobile phase which fills the gel pores and interparticle spaces. Small molecules can diffuse into all of the gel's pores while molecules which are too large to enter the pores are totally excluded from the pores and remain in the interstices.

As the mobile phase passes through the column, molecules inside the pores are left behind until they can diffuse back out of the pores into the mobile phase. Large molecules which cannot enter the pores are swept along with the mobile phase and are thus eluted first from the column. Small molecules permeate the gel's pores to a

varying extent depending on molecular size and are retained in the pores to varying extents in order of size. Small molecules which spend the longest time in the pores, are eluted last.

Bonded-phase chromatography

In bonded-phase chromatography, the stationary phase is chemically bonded to a support (usually silica-based particles). This changes the surface functionality and chemical nature of the packing material, imparting a hydrocarbon phase to the silica support. This maintains the mechanical strength and high surface area of the support. The bonded phase material contains polar functional groups such as amino (NH_2) or cyano (CN) groups to which the sample molecules are attracted.

Most bonded phase packings are designed for use in reversed phase modes, but normal modes are also available. The degree of retention on the column is a function of the polarity of the bonded phase, the particle size, and the pore diameter of the substrate particles. The range of packings can be used to modify the system and gives bonded-phase chromatography its flexibility and advantage over partition chromatography (Schweitzer, 1996).

Bonded normal phase A mode of chromatography in which a polar organic phase is chemically bonded to the silica substrate. The bonded phase material contains polar functional groups such as amino (NH_2) or cyano (CN) groups to which the sample molecules are attracted. The degree of retention on the column is a function of the polarity of the bonded phase, particle size, and pore diameter of the substrate particles.

Reverse phase A mode of chromatography in which the solvent or mobile phase is more polar than the stationary phase. Reverse phase chromatography is generally used for the separation of non-polar or weakly polar water-soluble molecules; however, more polar molecules can also be separated by using a more polar bonded

phase or such special techniques as ion pairing.

Affinity chromatography

When the region of one molecule is complementary to another region on a different molecule, this gives rise to "co-operation interactions", similar to how a lock and key work (Coulson and Richardson, 1991). Affinity chromatography utilises these interactions to carry out the separation process.

One molecule is chemically bonded to the support matrix, or stationary phase, to form the *ligand*, while the other molecule is the *ligate*, the component to be adsorbed. The interaction between the two molecules is very specific as the adsorption of the two molecules depends on molecular "recognition".

Bio-affinity chromatography uses a number of such complexes which occur in biological systems, *e.g.* antibody-antigen and enzyme-cofactor. Affinity chromatography can also be used where synthetic ligands such as dyes or electron donors are used, although this technique has been applied almost exclusively to biological ligates (Coulson and Richardson, 1991).

Chiral chromatography

The chirality of many biochemical molecules is increasingly being recognised as crucial to their activity and toxicology. Pure enantiomers, also known as optical isomers, are two mirror forms of the same compound where the physical properties are the same, however, one form of the compound may be bioactive whilst the other may be toxic (Kirk-Othmer, 1993).

Chiral chromatography can be used to separate a racemic mixture (mixture of two enantiomers) to its individual components and is useful in separating pharmaceuticals and biochemical compounds. There are various types of chiral stationary phases used for chiral chromatography which utilise either attractive interactions, metal ligands, inclusion complexes or protein complexes to carry out the separation(Kirk-Othmer, 1993).

Thin layer chromatography (TLC) and paper chromatography (PC)

These are very similar and are both simple, rapid techniques which uses inexpensive and portable equipment. A chamber is used to isolate the "column" which is a piece of paper in paper chromatography and a glass plate coated with an adsorbent such as silica gel in thin layer chromatography. The chromatogram is developed by allowing a mobile phase to move through the column, carrying with it materials to be separated which are soluble in the "column" to various extents. The "column" is subsequently removed and the mobile phase evaporated. The separated components are then visualised, for example by using a ultraviolet lamp (Kirk-Othmer, 1993). TLC is widely used in forensic, chemical and pharmaceutical analytical work, whilst PC is mainly used in analytical work separating and identifying substances such as such as sugars, amino acids, and natural pigments.

Supercritical fluid chromatography (SFC)

Supercritical fluid chromatography was developed in the 1960s but not used extensively until the early 1980s. The mobile phase is a supercritical fluid which has physical and chemical properties which are intermediate between a gas and a liquid. It is these properties which are strong factors in determining the selectivity and sensitivity towards individual components and the efficiency of the separation. Supercritical fluids can be viewed as dense gases which cannot become liquids. At constant temperature, an increase in pressure increases the density of a supercritical fluid. The solubility of materials in a solvent increases with density, thus the solvating power of the supercritical fluid increases as pressure increases. In this manner, retention can be changed in supercritical fluid chromatography.

Supercritical fluid chromatography can be performed using either capillary or packed columns. Usually, carbon dioxide is used as the supercritical mobile phase as it is compatible with chromatographic hardware, is readily available and is non-corrosive. The most important detector used for supercritical fluid chromatography

is the flame-ionisation detector as the mobile phase does not give a significant background signal (Kirk-Othmer, 1993).

Recent applications of supercritical fluid chromatography include separations in the drug and food industries as it has the advantages of low operating temperatures, selective detection and its sensitivity to the molecular weight of the feed components (Kirk-Othmer, 1993)

1.4 Motivation and objectives

The background and history of chromatographic separation has shown it to be well established as an analytical technique since the 1950s. As a large-scale unit operation it is still, however, a relatively new entrant. The high selectivity and efficiency of chromatography render it an attractive separation tool for demanding purification problems, especially in downstream processing applications in the biotechnological, pharmaceutical and fine chemical industries. As such, detailed mathematical modelling is necessary to obtain insight into the dynamics and equilibria of chromatographic separations, in order to reduce the time and effort required to develop new chromatographic processes. The dynamic and interactive nature of chromatography make it difficult, however, to model the separation efficiently. A *dynamic* mathematical model employs a system of partial differential and algebraic equations to describe the chromatographic process. The solution of such a complex model is a challenging matter and in the past, a number of assumptions were introduced to simplify the model to reduce the computation effort required. With the recent advances in computational power and availability of robust algorithms, more complex models can be solved.

With a range of chromatography models of varying complexity presented over the years, the difficulty now lies in the correct *choice* of model for a given application. It is important that an appropriate model is selected in order to represent the process dynamics accurately but without excessive computational time. While both the

equilibrium-dispersive model and the general rate model have been widely used, little work has been done to compare these models properly and the criteria to be used as a basis for model selection has not been considered. A systematic approach for model parameter estimation and model selection utilising numerical parameter estimation and little experimental effort is therefore proposed (Chapter 3).

Optimisation of the chromatographic separation is an even more complex task given the non-linear characteristics of the separation and the high inter-dependency between column design parameters and operating conditions of the process. Having selected an appropriate model which represents the column process dynamics adequately, optimisation of the process can now be conducted using newly developed optimisation tools (Teoh *et al.*, 2001; Teoh, 2002).

Multi-column chromatographic separations such as simulated moving bed (SMB) processes are becoming popular in industry to meet the demand for large amounts of purified products. With its complex process dynamics, the efficiency of the separation is highly dependent on its operating parameters. However, due to the switching nature of the SMB process, it may take many cycles to reach steady state, depending on the separation involved. Ideally, the process should be examined at steady-state conditions. As such, the optimisation of this process is examined in this work using a cyclic steady state (CSS) model developed using a *dynamic* optimisation technique to determine the optimal operating conditions (Chapter 4).

The development of single and multi-column chromatographic processes in recent years provides a wide range of choice in separation systems. However, given a particular separation, it is not always clear which of these systems should be employed as all may be suitable but all have certain trade-offs associated with them. An approach for the determination of the most suitable single or multi-column process for a given separation is proposed where the optimal design and operation of each alternative is compared based on a common economic objective function (Chapter 5).

1.5 Outline of the thesis

This thesis focuses on the modelling and optimisation of chromatographic processes. Detailed, dynamic mathematical models previously presented in the literature, are developed from experimental data using a novel systematic approach. These models are then compared against the experimental data using a graphical method for model selection. Subsequently, these models, coupled with a dynamic optimisation technique, are used to determine the optimal design, and operating policy for different chromatographic processes.

The history and background of chromatography has been examined in Chapter 1, detailing the mechanism of chromatographic separation and the different modes of operation within chromatography.

Different chromatography models available in the literature and the work that has been done using these models over the years are detailed in Chapter 2. Optimisation work done in the area of chromatography is also reviewed.

The choice of which model to use for a given chromatographic process is explored in Chapter 3. A systematic approach for model parameter estimation and model selection is proposed by comparing the performances of different models to allow the determination of the most appropriate model. This approach is demonstrated through a theoretical case study and further illustrated with two experimental case studies of complex mixtures.

The modelling and optimisation of a simulated moving bed (SMB) chromatography unit is examined in detail in Chapter 4. The dynamic SMB model is reformulated as a cyclic steady state (CSS) model, and is demonstrated that the CSS model describes the steady state of the dynamic SMB model adequately. The CSS model is then used to determine the optimal operating parameters for an industrial-scale case study.

In Chapter 5, an investigation of different single column and multi-column chromatographic processes - a single column, a column with recycling, a simulated mov-

ing bed process and a Varicol process - is carried out. The selection of the most appropriate separation system means that the best design and operation of each candidate process must be determined first. To allow a fair comparison between such different alternatives, an overall economics objective function that encompasses capital investment, operating costs and production revenues is used. The approach developed is illustrated using a verified case study.

1.6 Main contributions of this thesis

The following summarises the main contributions of this thesis:

- A systematic approach for model parameter estimation and model selection has been proposed and verified using different case studies.
- A comparative study on the dynamic and steady-state model of a simulated moving bed model and their optimisations for operation has been performed.
- A method developing the economic optimisation of different chromatographic processes, including a single column, a column with recycling, simulated moving bed process and Varicol process, in order to select the optimal separation system for the same separation task.

Chapter 2

Literature review

In this chapter, the importance of modelling in chromatography (Section 2.1) and the mathematical models available in chromatographic separation (Section 2.2) is discussed. The modelling work of these models in the literature is then reviewed (Section 2.3), followed by the optimisation efforts in the past on such models (Section 2.4). Finally, some concluding remarks are discussed in Section 2.5. The lack of detailed comparative work between different chromatographic models and that between different chromatographic processes is highlighted.

2.1 The importance of modelling in chromatography

Chromatography is increasingly being used as a purification method in many pharmaceutical separations, including the purification of enantiomers, peptides and proteins. As the optimisation of a chromatography separation involves optimising many experimental parameters, it is thus necessary to model the separation (Felinger and Guiochon, 1995).

A *process model* is a set of equations, including the necessary input data to solve these, that *allows* the prediction of the behaviour of a chemical process system. A *simulation* then solves this set of equations to give a theoretical prediction of the expected behaviour of the system with the given input data.

Process models are used for different purposes such as

1. Understanding the effects of the operating variables on process behaviour and the main parameters influencing the separation
2. Prediction of column behaviour
3. Investigation of the influence changes these parameters have on the performance of the column
4. Determination of optimal design and operating conditions

In preparative chromatography, where the aim is usually to improve the production rate, large amounts of sample are used in the chromatographic column. As a result, the adsorption isotherms deviate from linear behaviour, generally resulting in competitive isotherms for multicomponent mixtures. Thus, the amount of one component adsorbed at equilibrium is dependent on the presence and concentration of other components.

The modelling of chromatography is therefore a difficult task given the complex attributes of non-linear chromatography, in addition to the inherent dynamic nature of the process and the interactions between the process variables. Hence, it is difficult to predict the elution profiles accurately, especially when the process is subject to disturbances (*e.g.* changes in feed concentrations and loads).

Thus, overcoming these challenges in mathematical modelling and computer simulation of chromatographic processes is an important area of study, to enable a more efficient use of chromatographic columns. Modelling provides valuable information about the physical and thermodynamical kinetics, as well as the flow phenomena

through the granular media that makes up the stationary phase in the chromatographic column.

Modelling the chromatographic process does not eliminate experimental work, as some real data is required to develop a reliable model. However, experimental work and modelling complements each other in developing a better understanding of the separation process and accurate and reliable models allow for a reduction in the time and effort required to make a process concept a reality.

2.2 Mathematical models in chromatography

Over the years, many chromatography column models have been developed and used in the literature, with the study of the more complex models rendered possible with advances in computational power and technology. In this section, these models and their assumptions are described, and some of the work done in the literature using these models is reviewed. The models may be divided into two categories - microscopic and macroscopic models.

2.2.1 Microscopic modelling

Microscopic modelling, sometimes known as atomistic models or stochastic models, usually take into account *all* the molecules in the system (Lipkowitz, 1995). The work done in this area is considered separately for the molecular model and the stochastic (or statistical) model, although the former is a subset of the latter.

Molecular modelling

In recent years, molecular modelling has made its foray into chiral chemistry in order to understand where and how the chiral selection takes place in chromatography. Such an understanding is vital in the quest for improvements in design of chromatographic systems. The precision in which the intermolecular forces work in

concert to promote the component binding to the stationary phase is not clear, and is the focus of much research in the area of molecular recognition (Lipkowitz, 1995). Atomistic modelling of this type is done in two different ways:

Fitting procedures: The fitting procedure is a rationalisation between *molecular structure* and *physico-chemical properties* with *biological response* (Lipkowitz, 1995). The response is regressed to a set of molecular descriptors for the molecules, and these are used in the model to predict an unknown molecule's property or anticipated response. Molecular descriptors often include information about molecular size and shape, electronic effects and lipophilicity. Existing data is required to create the model and allow the user to interpolate or extrapolate new properties/activities of the unknown molecules within the same class of compounds.

Computational tools: The model can be developed using 5 major computational tools together with sample data which are summarised in Table 2.1:

Weinstein *et al.* (1980) proposes a molecular inter-calculation model to account for the discrimination in the interactions within the series of chiral secondary amides. The model explains the gas-liquid chromatography resolutions which occur when these amides are used as the chiral stationary phase and energy computations conducted support the stability of the molecular structure which follow from the model.

Lipkowitz (1995) provides a detailed review on atomic-level modelling in chiral chromatography, focussing on chiral stationary phase (CSP) types II to V, where regression models are more common (using fitting procedure). This stems mainly from the fact that the shape of these CSPs is largely not well-defined or not known at all. Despite such models lacking the atom-by-atom details of the interactions occurring in chromatography, they nevertheless provide important information concerning where and how chiral recognition takes place. Furthermore, they are capable of making predictions.

A later review by Lipkowitz (2001) focussed on CSP types I to V and high-

Model tools	**Characteristics**
Quantum mechanics (QM)	Spatial positions of electrons and nuclei described with an iterative calculation to minimise energy forces in the molecule.
Molecular mechanics (MM)	Non-quantum mechanical way of computing structures, energies and some properties of molecules using an empirical force field (EFF)
Molecular dynamics (MD)	The Newtonian laws is applied to the motion of atoms, and the equations integrated using the same EEF as in MM
Monte Carlo (MC) simulations	The same EEF used in MM and MD is used to obtain a large number of energetically feasible states for various molecule configurations, providing averaged energies and properties
Molecular graphics	Renders the data from QM, MM, MD and MC manageable for simulation, showing four or five attributes in a single image

Table 2.1: Computational tools used for molecular modelling studies

lighted the need for adequate samples on the potential energy surfaces (PES) of the diastereomeric complexes. The methods used for sampling PES implementing different methodologies is compared. The care to be taken to have adequate samples of the important regions of the diastereomeric PES and to perform a statistical averaging of results is also stressed upon. Lipkowitz also reviews the work in the literature involving the use of molecular modelling tools (Table 2.1, mostly in gas chromatography to understand component behaviour in the cavity (of the stationary phase) and evaluate detailed stractual features of the "guest-host" complex formed during the process. With good agreement with experimental data, the computational tools are a valuable adjunct to the existing experiment in providing information on atom-atom interaction, as well as being a predictive tool.

The statistical model

In molecular modelling, a great deal of the focus is on the structure and detail of the interactions that take place during the bonding of the component to the stationary phase. The statistical model on the other hand, uses the observations on the molecular level to obtain a concentration distribution to model the chromatographic process.

Giddings and Eyring (1955) introduced a statistical model to describe the molecular migration in chromatography. This dynamic molecular approach is based on statistics, where the chromatographic process is treated as a Poisson distribution process. The random migration of a single solute along a chromatographic column (described by the "random walk" approach) is considered to derive an expression for the elution profile or the residence time of a molecule in a column. Some of the assumptions for this model include:

- random adsorption and desorption processes
- single type site on a stationary phase
- impulse injection is used

- axial dispersion is negligible
- mass transfer kinetics approximated using a random walk model

The moment of the peak is a mathematical equation that describes a characteristic of the distribution function. The relationships between the statistical moments and chromatographic parameters are summarised by Wheelwright (1991) as follows:

Zeroth moment → band area or the injected sample

First moment → retention time or retention volume

Second moment → peak width or variance of profile

Third moment → symmetry of peak

Fourth moment → flatness or peakedness (kurtosis) of peak

The research using such models include the works of Karger *et al.* (1973), Horvath (1983), Dondi and Remelli (1986).

In the past, statistical models were limited to linear isotherm systems as the interactions between molecules are not taken into account. The recent advances in the theoretical work in statistical modelling have lead to these models being extended to more complex models. The work of Dondi and Remelli (1986) applied a characteristic function to the stochastic theory of chromatography, allowing the formulation of a general model to take into account the random mass transfer phenomena occurring in the mobile phase.

Dondi *et al.* (2002) developed a general stochastic theory of size exclusion chromatography (SEC), where the SEC models are solved by means of the characteristic function method and chromatographic parameters like plate height, peak skewness and excess are derived. The peak shapes are obtained by numerical inversion of the characteristic function under the most general conditions of the exploited models. The approach presented is able to account for more complex SEC conditions such as continuous pore size distributions and mixed retention mechanism.

Felinger *et al.* (2004) theoretically compared the elution band profiles produced

by the microscopic and macroscopic models in chromatography, using a stochastic-dispersive model (microscopic) and a lumped kinetic model (macroscopic). An exponential distribution for the time during adsorption-desorption step and a Poisson distribution for the number of adsorption events is assumed. Without these, the microscopic model would no longer be equivalent to the macroscopic model.

2.2.2 Macroscopic models

The microscopic models are limited by the assumptions of the probability distributions, which is the basis on which they are formulated. Whilst they aid an understanding of what is happening at a molecular level, they are unable to account for disturbances or large changes taking place in the process dynamics of the chromatographic process. Conversely, the macroscopic model is able to account for the process dynamics happening in the column.

The macroscopic model describes the coarse-grain features of the system or process (Lipkowitz, 1995). Some aspects of the process, such as the variation in the concentration of the components, mass transfer kinetics, and the equilibrium relationship across the phases, is considered but without including the structural features of the individual molecules.

The plate models

Plate models divide the column into a number of theoretical plates, or equilibrium stages. These plates are identical and are placed in series. Thus, they represent a continuous column of finite length by a discrete number of cells.

The advantages of the plate model are its capability to describe the elution profile, peak shape and band broadening. However, the plate model fails to predict plate height and plate number and cannot quantify the individual contributions each as diffusion, flow pattern and mass transfer on band broadening (Kirk and Othmer, 1993). Refer to Table 2.2 for the work done in the literature using these models and

their characteristics.

The Martin and Synge plate model The Martin and Synge plate model is a continuous plate model (Guiochon *et al.*, 1994). This model assumes that the column is equivalent to a series of continuous flow mixers. The mobile phase is transferred from one plate to the next as the new mobile phase is added to the first plate. Thus, the volumes of the mobile and stationary phase remain constant, while the mobile phase flows continuously. Other assumptions are that the column is loaded with the sample and that there are no other sample components in the other plates.

The Craig plate model The Craig model is a discontinuous plate model (Guiochon *et al.*, 1994). It assumes that initially, the first stage contains all the solutes used, while the other stages are entirely free of solute, and that all further amounts of the mobile phase introduced in the first stage are pure mobile phase. After equilibrium is reached in the first stage, the amount of mobile phase contained in the last stage is withdrawn from that stage and collected. Subsequently, the volume of mobile phase in each stage is moved from that stage to the next, and the same amount of pure mobile phase is added to the first stage. When equilibrium is reached in all the stages containing solute, the mobile phase contained in one stage is moved again to the next stage, the volume in the last stage collected and the first stage is replenished. This is repeated so as to sweep the sample components from the column.

References	Models	Assumptions	Advantages	Limitations
Karol (1989), Guiochon *et al.*, (1994) Li *et al.* (1995), Jungbauer (1996)	Craig model, Martin & Synge model	Refer to Section 2.2.2 (The plate models)	1) Simple 2) Able to describe the elution profile and zone broadening effect 3) Analytical solution can be easily obtained	1) Unable to quantify the contribution of different physical phenomena in zone broadening effect 2) Restricted to linear adsorption 3) Limited success, *i.e.* error up to 100% Fails to predict plate height and plate number
Synder *et al.* (1989a,b)	Knox-Pyper model coupled with Craig model (Discontinuous plate model)	1) Band deviation from "right triangle" shape at higher loading is ignored 2) Band migration for individual component proceeds independently in the presence of other components in the sample	Provide a simple and clear description of the interrelationship between optimum plate number and experimental conditions	Under mass overloaded conditions, deviation from actual elution profiles are significant, especially for low plate numbers, small values of separation factor and large sample.
Jungbauer & Kaltenbrunner (1996)	Craig model	Refer to Appendix B	A strategy to derive the distribution coefficient from experimental results was developed	Unable to predict the variation in plate numbers with different separation conditions. More complex algorithm is required for multicomponent system.

Table 2.2: The chromatography column plate models and their characteristics

The rate models

The limitations of the plate model means that it fails to consider contributions of effects such as diffusion and mass transfer resistance during migration. It is also generally not suited to multicomponent chromatography since the equilibrium stages may not be assumed equal for different components (Gu, 1995). The plate theory also does not provide any *a priori* information on the relationships between column efficiency and the various parameters which control or may influence it (Guiochon *et al.*, 1994).

Rate models are models which also consider non-equilibrium conditions in the column and address the causes of band broadening in chromatography. The individual contributions of mass transfer mechanisms (*e.g.* eddy diffusion, mass transfer resistance, axial dispersion) are quantified. Variations of the rate models include the ideal model, equilibrium-dispersive model and general rate model, which are discussed in more detail in Section 2.3.2. Work done in the literature using rate models and their characteristics are summarised in Table 2.3.

There are many variants of the rate model, including the ideal model, the equilibrium-dispersive model, transport-dispersive model, lumped kinetic and the general rate model to name a few. Some of these models will be examined in further detail in Section 2.3.2.

The mass balance equations The derivation of the differential mass balance equations can be found inthe literature (Guiochon *et al.*, 1994). Further details of its derivation and the assumptions which it is based on may be found in Appendix B. The basic mass balance equation is:

$$\frac{\partial C_i}{\partial t} + F\frac{\partial C_{P_i}}{\partial t} + u\frac{\partial C_i}{\partial z} = D_L\frac{\partial^2 C_i}{\partial z^2} \tag{2.1}$$

where F is the phase ratio, V_s/V_m, equal to$(1-\epsilon)/\epsilon$, and V_s and V_m are the volumes of the stationary and mobile phases, respectively. C_{P_i} and C_i are the concentrations of the component i on the stationary and mobile phases, respectively.

Relationship between the concentrations in both phases If the mass transfer kinetics across the mobile and stationary phases are very fast, these phases are close to equilibrium and this can be used as an approximation to obtain:

$$C_{P_i} = q_i = f_i(C_1, C_2, ..., C_i, ..., C_n) \tag{2.2}$$

When the mass transfer kinetics are slow, the following relationship takes this into account:

$$\frac{\partial C_{P_i}}{\partial t} = g_i(C_1, C_2, ..., C_i, ..., C_n, C_{P_1}, C_{P_2}, CP_i, ..., CP_n) \tag{2.3}$$

where g_i depends on both the rate constants of adsorption and desorption and the isotherm equations.

References	Models	Assumptions	Advantages	Limitations
Ghodbane & Guiochon (1988), Golshan-Shirazi & Guiochon (1989a, b), Gallant *et al.* (1996)	Ideal model	Infinite column efficiency	1) Simple 2) Analytical solution easily available	Unable to account for axial dispersion and mass transfer effects for columns with finite efficiency.
Bellot & Condoret (1993a), Charton *et al.* (1993), Seidel-Morgenstern & Guiochon (1993), Charton *et al.* (1994), Heuer *et al,* (1995), Heuer *et al.* (1999), Quiñones *et al.* (2000), Teoh *et al.* (2001)	Equilibrium dispersive model	Refer to Appendix B	Able to capture the dispersion and mass transfer effects in the column using an apparent dispersion coefficient as long as the column efficiency is greater than several hundreds HETP.	1) Unsuitable for column with low HETP 2) Unable to account for intra-particle diffusion for large particle size.
Gu *et al.* (1990), Gu *et al.* (1991), Colby *et al.* (1996), Ma *et al.* (1996), Gu & Zheng (1999)	General rate model	Refer to Appendix B	1) Detailed model of the system 2) Able to capture the mass transfer, axial dispersion, inter- and intra-diffusion effects for large scale separation	1) Difficult to obtain the model parameters 2) Difficult to identify or quantify the most important design parameter(s) and operating conditions that will affect the separation performance.

Table 2.3: The chromatography rate column models and their characteristics

2.2.3 Summary

In this section, the two main areas of modelling the chromatographic processes have been introduced - the microscopic and macroscopic. Both methods handle the modelling of the process to different levels. The microscopic models are demonstrated to be useful in understanding the finer detail of the adsorption-desorption mechanics of chromatography. In the case of the statistical models, they are shown to be equally capable of predicting the elution profiles for chromatography.

However, these models are limited by the assumptions of the probability distribution employed to formulate the model, and are also lacking in the insight into the disturbances on the chromatographic system which the macroscopic model can provide. With large-scale processes, it is important that the process dynamics are reflected in the chosen model. This leads to the focus on macroscopic models.

2.3 Review of modelling work in the literature

In this section, the different types of macroscopic models used in the literature is discussed. The assumptions that define the models and the work presented in the open literature employing them is also outlined (For full details of the equilibrium-dispersive model and the general rate model, refer to Appendix B.).

2.3.1 Plate models

Whilst plate models can be used to describe elutions profiles and some zone broadening effects, they are limited by their inability to effectively quantify the kinetic contributions of the varied physical phenomena present (such as mass transfer resistance) as the separation occurs. As such, their applications in modelling liquid chromatographic processes are limited to linear chromatography. Reviews of the modelling work done with such models may be found in Guiochon *et al.* (1994) and Jungbauer (1996).

Karol (1989) used the differential rate model to derive both the Martin and Synge plate model and Craig plate model. In the latter model, the ad hoc manner in which the plate number is related to the chemistry and physics of the process renders it severely deficient. In spite of this, however, the work demonstrates that the Craig model is a phenomenologically valid approximation to the Martin and Synge plate model and to the rate model.

Snyder *et al.* (1989a) and Snyder and Cox (1989) used the Craig model to successfully simulate isocratic high-performance liquid chromatographic (HPLC) separation in a mass-overload mode. This was then extended to the case of gradient elution for large samples (Cox *et al.*, 1989; Snyder *et al.*, 1989b, c). These simulations support earlier conclusions drawn that so-called "corresponding" isocratic and gradient separations provide similar sample resolution when the sample size is the same. The Craig simulations reported in collaborations of Synder *et al.* (1989a,b,c), Snyder and Cox (1989) and Cox *et. al.* (1989) also provide further insight into the factors that affect preparative HPLC separations under mass-overload conditions.

Jungbauer and Kaltenbrunner (1996) employed the Craig model to model and optimise a protein separation using ion-exchange chromatography. The main objective was to maximise the production rate whilst maintaining the desired resolution. The distribution coefficient, which is a strong function of the protein and the salt concentration, was found to determine the system performance under overloaded conditions.

2.3.2 Rate models

The three rate models examined in this section are among the most prolific in the open literature for modelling the chromatographic process: the ideal, equilibrium-dispersive and general rate models. The work done on chromatographic processes using these models is reviewed and discussed. Table 2.4 gives a summary of the modelling work done for rate models.

The ideal model

This model is the simplest nonlinear chromatography model and assumes that the column efficiency is infinite (Guiochon *et al.*, 1994). Axial dispersion is neglected and the two phases are constantly at equilibrium. The stationary phase concentration is given by Equation 2.2. The mass balance for component i in Equation 2.1 is simplified to:

$$\frac{\partial C_i}{\partial t} + F\frac{\partial q_i}{\partial t} + u\frac{\partial C_i}{\partial z} = 0 \tag{2.4}$$

Thus, the influences of mass transfer kinetics and axial dispersion on the band profiles are completely neglected.

This model has been used in the literature to study the elution profiles of components in single columns, in works such as *e.g.* Ghodbane and Guiochon (1988), Golshan-Shirazi and Guiochon (1989a, b), Gallant *et al.* (1996), Hägglund and Ståhlberg (1997), Zhong and Guiochon(1998). In recent years, the ideal model has been studied in multi-column chromatographic processes such as simulated moving bed (SMB) chromatography (Zhong and Guiochon, 1997a,b; Zhong and Guiochon, 1998; Klatt *et al.*, 2000).

A variant of the ideal model of chromatography is used in a study of the separation of a binary mixture in the work of Ghodbane and Guiochon (1988). This model incorporates the column efficiency and predicts the individual elution profiles of the components of a mixture. These elution profiles are then used to study the influence of the relative concentrations of the two components of a binary mixture on their overloaded elution profiles. The effect of column efficiency is also discussed.

Hägglund and Ståhlberg (1997) employed the ideal model to calculate the elution profile of hydrophobic charged solutes injected on a reverse-phase chromatography column (Hägglund and Ståhlberg, 1997). (Reverse-phase chromatography describes a mode of chromatography when the mobile phase is more polar than the stationary phase, and is the opposite of normal-phase chromatography.) It was demonstrated

that by combining the ideal model of chromatography and an electrostatically modified linear adsorption isotherm, the concentration profile of an eluting peak from a reversed-phase column can be described for an amphiphilic ion, which is an ion which contains both hydrophilic (water-loving) and hydrophobic (water-hating) properties. The theoretical calculations and the experimentally obtained concentration profile show very good agreement at high solute concentrations. However, this agreement gradually decreases with the decrease in injected solute concentrations.

Zhong and Guiochon (1998) applied the ideal model to the operation of a simulated moving bed (SMB) to predict the concentration profile of the solutes along the column as well as the concentration profiles at the raffinate and extract ports. Comparing these ideal model results with numerical solutions of more realistic, nonideal models showed that in most practical cases, the speed at which the profiles tend toward steady state was the same. Significant differences were observed, however, when the efficiency of the column was poor.

The equilibrium-dispersive model

This model includes mass transfer resistance and axial dispersion and Equation 2.1 can be replaced with the following:

$$\frac{\partial C_i}{\partial t} + F\frac{\partial q_i}{\partial t} + u\frac{\partial C_i}{\partial z} = D_{a,i}\frac{\partial^2 C_i}{\partial z^2} \tag{2.5}$$

where q_i is the equilibrium concentration of component i in the stationary phase and $D_{a,i}$ is the apparent dispersion coefficient. The equilibrium-dispersive model assumes that all contributions due to the non-equilibrium can be lumped into an apparent axial dispersion term, $D_{a,i}$, and that the $D_{a,i}$ of the solutes remain constant, independent of the sample component concentrations. This is a reasonable assumption, given that concentrations in nonlinear chromatography usually remain low, rarely exceeding 10% (w/w) (Guiochon *et al.*, 1994).

The simple nature of the equilibrium-dispersive model enabling it to be easily

solved by a number of established numerical methods, has resulted in it being the most widely employed chromatographic model in the literature (Bellot and Condoret, 1993a; Charton *et al.*, 1993; Heuer *et al.*,1996, 1998; Mihlbachler *et al.*, 2001; Teoh *et al.*, 2001; Gritti *et al.*, 2003). As a good approximation, this model allows an accurate prediction of the self-sharpening and dispersive phenomena due to thermodynamics and kinetics of phase equilibria generally found in a column (Guiochon *et al.*, 1994).

Bellot and Condoret (1993a) theoretically considered preparative ion-exchange chromatography of a two-protein mixture using numerical simulations. The mathematical model is a combination of the semi-ideal model for the chromatographic process, with the stoichiometric displacement model for the basic interactions between proteins and the stationary phase. Special emphasis is put on the effect of overloading the column by pointing out displacement effects between proteins. The influence of important adsorption parameters, such as the characteristic charge or maximum loading capacity, was investigated by considering criteria of production rate, recovery yield and enrichment of products.

Heuer *et al.* (1996) used thermodynamic parameters from preliminary investigations to simulate separation behaviour in larger columns using the equilibrium-dispersive model. Experimental studies involving the separation of α- and β-isomers of a steroid compound using columns with increasing diameters were conducted for verification. Chromatograms for larger columns could be qualitatively predicted and this demonstrated the applicability of the model as a tool for design and optimisation of preparative chromatography. This same applicability was demonstrated in another publication (Heuer *et al.*, 1995), for the simulated moving bed (SMB) process.

The work of Mihlbachler *et al.* (2001) discusses the effects on the SMB process performance caused by column-to-column fluctuations of the column porosity. Both the ideal and the equilibrium-dispersive models are used in this work; the former to formulate general conditions easily, whilst the latter model was used to correct the

conditions in order to account for banding broadening.

Teoh *et al.* (2001) employed the equilibrium-dispersive model for the high performance liquid chromatography separation of an aromatic mixture of four components (nitrobenzene, naphthalene, fluorene and fluoranthene). The isotherm parameters and the height equivalent to a theoretical plate (HETP) of this separation were estimated. Good agreement in terms of peak positions and heights were obtained between the simulated and experimental elution profiles, thus verifying the model.

The general rate model

The general model is the most comprehensive model of chromatography presented so far, as it takes into account all the phenomena which may have an influence on the band profiles such as axial dispersion, external mass transfer, intraparticle diffusion and the kinetics of adsorption-desorption (Guiochon *et al.*, 1994). However, as its use requires the independent determination of many parameters, it requires much more computational time to calculate, compared to the ideal or equilibrium-dispersive model. The general rate model consists of two partial differential equations for each component, which expresses its mass balances; the first one in the mobile phase flowing between packing particles, and the other in the fluid contained inside the particles.

The model is expressed with three dimensionless kinetic parameters (Guiochon *et al.*, 1994):

- The axial Peclet number, $Pe = uL/D_L$, where L is the column length and D_L is the axial diffusion coefficient,
- The particle Peclet number, $Pe_p = ud_p/D_p$, where d_p is the particle size and D_p the diffusion coefficient inside the particles,
- The Biot number, $B_i = k_f d_p/2\epsilon_p D_p$, where k_f is the film mass transfer coefficient and ϵ_p the internal porosity.

Gu *et al.* (1990) displayed the capability of the general rate model in visualising the interference effects in a multicomponent chromatographic process when subjected to mass transfer limitation. This numerical investigation was conducted for the elution, frontal and displacement modes in chromatography. It was concluded that the elution profile of a component is sharpened by the displacement effect from another component, whilst the leading front of the displacer is usually diffused.

Ma *et al.* (1996) employed the general rate model to investigate the effects of pore and surface diffusions in a multicomponent liquid chromatographic process. Experimental and simulation results demonstrated that in the linear region of a single component system, both surface and pore diffusions cause a symmetric spreading in the elution profiles. In the non-linear region, however, surface diffusion causes profound tailing in the elution curves, whilst the relatively symmetric elution profiles are due to the pore diffusion. In a multicomponent non-linear system, the elution order can change if the pore diffusion dominates for a low affinity component (usually elutes first) and the surface diffusion dominates for a high affinity component (usually elutes later).

The general rate model has also been applied to the modelling and scale-up of reversed-phase liquid chromatography (RPLC) (Gu and Zheng, 1999). Human growth hormone and a recombinant human growth hormone analog (hGHG120R) are used as samples in experiments to obtain the isotherm parameters. The work presented demonstrates that the general rate model and the parameter estimation protocol presented can be used for RPLC scale-up and gradient elution profiles can be predicted without *a posteriori* data from the preparative column.

The mass transfer kinetics of bovine serum albumin (BSA) in ion-exchange chromatography were evaluated using the general rate model of chromatography by Kaczmarski *et al.* (2001). The results were compared to that of a simple transport-dispersive model and a lumped pore diffusion model and demonstrated the importance of using an appropriate model, otherwise erroneous interpretations of experimental data may occur.

Reference	Models	Isotherm	Mode	Numerical solution	Remarks
Ghodbane & Guiochon (1988)	Ideal model	Langmuir isotherm	Overloaded elution	Finite difference	Concentration was optimised in overloaded liquid chromatography
Golshan-Shirazi & Guiochon (1989a, b)	Ideal model	Competitive Langmuir	Overloaded elution	Analytical solution	Experimental conditions for a liquid chromatographic separation determined using the model.
Gallant *et al.* (1996)	Ideal model	Equilibrium constant (linear isotherm)	Gradient elution	Analytical solution	Elution profiles for a protein ion-exchange chromatographic separation predicted using the ideal model.
Bellot & Condoret (1993a)	Equilbrium dispersive model	Competitive Langmuir, LeVan-Vermeulen	Displacement	Finite difference	Investigation of applying different competitive adsorption isotherms for the modelling of displacement chromatography.
Charton *et al.* (1993)	Equilibrium dispersive model	Competitive bi-Langmuir, competitive LeVan-Vermeulen	Elution	Finite difference	Successful application of the model for describing the purification of methyl-mandalate enantiomers.

Table 2.4: Examples of work done in modelling chromatography

Reference	Models	Isotherm	Mode	Numerical solution	Remarks
Seidel-Morgenstern & Guiochon (1993)	Equilibrium dispersive model	Competitive Langmuir	Elution	Finite difference	Use of the equilibrium-dispersive model for the modelling of recycling chromatographic separation, and demonstrated that the recycling can improve the recovery yield and increase the rate of production.
Charton *et al.* (1994)	Equilibrium dispersive model	bi-Langmuir	Elution	Forward-backward finite difference	Investigation of recycling different cuts of purified sample of the performance of the chromatographic separation.
Heuer *et al.* (1995)	Equilibrium dispersive model	Langmuir	Elution	Finite difference	Experimental investigation and modelling of a closed-loop recycling preparative chromatography on a mixture of TTB and PHL were performed.
Heuer *et al.* (1999)	Equilibrium dispersive model	Competitive bi-Langmuir	Elution	Finite difference	The model was used as a design tool for recycling chromatography, neglecting mixing effects in pumps and tubings.
Quiñones *et al.* (2000)	Equilibrium dispersive model	Competitive Langmuir	Elution	Forward-backward finite difference	The model was used to describe the band profiles of a racemic pharmaceutical intermediate on a closed-loop steady-state recycling chromatographic unit, with the extra column band broadening effect accounted for using correction terms.

Table 2.4: Examples of work done in modelling chromatography (continued)

Reference	Models	Isotherm	Mode	Numerical solution	Remarks
Gu *et al.* (1990)	General rate model	Competitive Langmuir	Frontal elution, displacement	Orthogonal collocation finite element	The interference effect in multicomponent chromatography was studied.
Gu *et al.* (1991)	General rate model	Competitive Langmuir	Displacement	Orthogonal collocation finite element	The effect of varying the displacer concentration on a desorption chromatography process was studied.
Colby *et al.* (1996)	General rate model	Second order kinetic	Step elution frontal	Orthogonal collocation finite element	The compression effect during the scale-up of an ion-exchange chromatography separation was investigated.
Ma *et al.* (1996)	General rate model	Second order kinetic	Elution	Orthogonal collocation finite element	The effects of pore and surface diffusions in multi-component adsorption for liquid chromatography were examined.
Gu & Zheng (1999)	General rate model	Second order kinetic	Gradient elution	Orthogonal collocation finite element	The model was used in the scale-up of a reversed-phase chromatographic separation.

Table 2.4: Examples of work done in modelling chromatography (continued)

2.3.3 Comparing chromatographic models

Other work have compared the other available models of chromatography such as the transport-dispersive model (which uses a lumped dispersion coefficient and the lumped mass transfer coefficient) (Antos *et al.*, 2003; Piątkowski *et al.*, 2003) and lumped pore diffusion model (a simplified form of the general rate model employing a lumped overall mass transfer coefficient) (Kaczmarski and Antos, 1996) with the equilibrium-dispersive model and general rate model. Refer to Table 2.5 for a more detailed comparison of the work in some of these papers.

Much of the comparative work done on these models, however, compares them on a theoretical basis only or examine the conditions under which the models are applicable using experimental results at an analytical scale for simple systems. There is thus a need for a systematic approach to discern which of the models are appropriate to describe complex experimental separations, such as those found in biochemical and pharmaceutical applications, and how to determine the parameters in these models from experimental data.

Reference	Models	Numerical solution	Remarks
Lee *et al.* (1989)	Detailed rate equation model (Yu & Wang, 1989) and local equilibrium models	Gradient-directed moving finite element technique (Yu & Wang, 1989)	Isocratic elution of lysine and proline compared with the models for verification. Conditions for which local equilibrium model is applicable is identified. Rate model is deemed better when 1) mass transfer resistances are important 2) effects of changing particle size/flowrate needed 3) isotherms are complex.
Kaczmarski & Antos (1996)	General rate lumped pore diffusion & equilibrium-dispersive models	Forward-backward finite difference scheme	Modification of Rouchon algorithm to eliminate error associated with components with vastly different retention factors. Simulations carried out for mixture of components for each model. This numerical solution was found to be less accurate but required less computational time compared with othogonal collocation on finite elements. Conditions for applicability of modelsformulated based on Peclet number.

Table 2.5: Work comparing different mathematical models in chromatography

Reference	Models	Numerical solution	Remarks
Antos *et al.* (2003)	General rate, equilibrium-dispersive and transport-dispersive models	Othogonal collocation on on finite elements (OCFE)	Models used to simulate band profiles for different isocratic and gradient conditions. General rate model was used as a basis of comparison for the other two models. Both models can be used in a broad range of column efficiencies. Equilibrium-dispersive model performed better than the transport-dispersive model at gradient elution simulations.
Piątkowski *et al.* (2003)	Extended general rate model (to include surface diffusion kinetics) & transport-dispersive models	Orthogonal collocation on finite elements (OCFE) for general rate model; Backward-forward finite difference for transport-dispersive model	Experimental profiles of methyl deocycholate and cholate were examined and compared with the computer simulations under linear and non-linear conditions. Good agreement confirm that the simplified model can service as a basis to examine mass transport mechanism, provided lumped coefficient is adjusted to include concentration dependence of the surface diffusion coefficient.

Table 2.5: Work comparing different mathematical models in chromatography (continued)

2.3.4 Multi-column chromatography modelling

Multi-column processes, such as simulated moving bed (SMB) chromatography, are now becoming increasingly popular in industry. Companies such as UCB (Belgium), Lundbeck (Denmark) and Bayer Chemicals have been known to purchase SMB units for processing large amounts of racemic mixtures, indicating its rising popularity in the pharmaceutical industry. Research work done in the open literature on SMB has also looked at extending and varying the SMB process, employing the ideas of switching feed and product lines but in an irregular pattern, known as the Varicol process.

In the literature, the mathematical modelling of multi-column processes such as simulated moving bed (SMB) is divided into two camps: (1) the true moving-bed (TMB) model which treats the SMB process as an TMB equivalent (2) the dynamic SMB model, which includes the *process dynamics* of the SMB system. This includes process complexities such as the various sections with a number of chromatography columns in each, and whose boundary conditions change with time (Hassan *et al.*, 1995).

Storti *et al.* (1993) presented the *Triangular theory* in this paper, which was a means of estimating the flowrates for the inlet and outlet lines based on the coefficients of the isotherms used in the system. This considered the flowrate in each section of the SMB unit in the form of flowrate ratios, based on a TMB model. It has since been extremely widely used in the literature, *e.g.* Mazzotti *et al.* (1997), Migliorini *et al.* (1998), Migliorini *et al.* (1999), Biressi *et al.* (2000) *etc.*, as a means of establishing the flowrates for the SMB process.

Mazzotti *et al.* (1997) examined the effect of feed concentration on the SMB process, as a means of controlling the nonlinearity of the system in order to adapt the operation of the SMB unit. Experimental work carried out showed that while the optimal operating point established in theory exhibits a good separation, the expected complete separation was not achieved. Whilst this was attributed to the

lack of robust operating conditions and uncertainties in the adsorption equilibrium, another contribution may be the failure of the TMB model to capture the dynamics involved in the SMB process.

Beste *et al.* (2000) considered the optimisation of an SMB process with stationary phases with low efficiency. Optimisation was done to improve purity and yield, followed by productivity and decreasing desorbent consumption. The optimisation results obtained from the TMB model employed were then assessed against that of the SMB model, as the latter was considered more realistic.

Strube *et al.* (1997) optimised the SMB process for minimal desorbent requirement, product dilution and maximal feed throughput using a TMB model. However, employing these optimum results on a dynamic SMB model has showed that the parameters obtained were not the real optimum operating conditions.

Minceva and Rodrigues (2002) recently employed the TMB and the SMB models for a separation of *p*-Xylene using the SMB process. The results were very similar, and showed that the TMB model could be used in prediction of the performance of the SMB operation. The TMB model was then used to examine the effects of the switching time period, adsorbent capacity and mass-transfer resistances on the SMB performance. The conclusions from this paper were that mass-transfer resistances had a significant effect on the separation region, and that the choice of the flowrate rate in the four sections of SMB affect the size of the separation region, echoing the findings of Storti *et al.* (1993). However, the results of the TMB-SMB comparison also showed that, at best, the TMB model gives an approximation of the SMB behaviour.

Schmidt-Traub and Strube (1996) gave a summary of the comparisons between TMB and SMB models, pointing out the differences and limitations of the TMB model. This paper recommended employing the TMB model to estimate the operating conditions but that subsequent optimisation studies should be conducted on dynamic SMB models, which reflect the true process behaviour.

The TMB equivalent model of the SMB process is less complex to solve and thus

requires less computational time compared to the dynamic SMB model. However, given its failure to consider the process complexities in the SMB process, the TMB equivalent model is only suitable as an estimate of the operating parameters (Jupke *et al.*, 2002). This has lead much of the recent work done in the literature to focus on the dynamic SMB model.

Dünnebier discussed the modelling and simulation of the SMB process with linear isotherms in his work (Dünnebier *et al.*, 1998). Three modelling and simulation approaches are presented and compared: the ideal model, the closed-form solution of equilibrium-dispersive model and the general rate model. This paper also notes that the computational cost of the general rate model is high and thus, requires a simplification of the model without losing its generality and advantages for the use of this model to be cost-effective. A detailed simulation study for the separation fructose and glucose was considered using this approaches and concentration profiles across the columns plotted.

The work Strube and Schmidt-Traub (1998) compared different chromatographic column models used in the SMB model against experimental results to demonstrate a dynamic SMB simulation provides information to enable a better understanding of the process, especially for planning experiments *e.g.* explanation for product contamination when start-up is incorrect. The recommendations from this work are to use the Dispersed Plug Flow (DPF) model (which is a form of the general rate model) in the SMB process model, and in particular if non-linear isotherms have to be considered.

Dünnebier and Klatt (2000) employ the SMB model to compare three different modelling approaches for the SMB process. They are (1) rigorous general rate model approach, (2) an approach where the kinetic effects are lumped into a single parameter and (3) a solution approach using an ideal chromatographic model, neglecting all kinetic effects. However, due to the low efficiency of the system explored, approach (2) is not applicable and only approaches (1) and (3) were simulated. The ideal model was found to be capable of providing some insight to the complex interacting

dynamics of the process, particular for start-up. However, due to its unrealistic modelling assumptions, it lacks sufficient accuracy for quantitative predictions. The generate model approach allow for a quantitative analysis of the process, although the calculations tend to be more computationally expensive than that of the ideal model.

Two forms of the SMB model have emerged in recent years: (1) a dynamic SMB model obtained by connecting the dynamic chromatographic column models with cyclic port switching (*e.g.* Dünnebier *et al.* (1998)) and (2) a *cyclic steady-state* (CSS) model as developed by Minceva *et al.* (2003) which predicts the performance of the model *only* at steady-state conditions. The latter model came about as a result of the SMB process requiring a certain number of cycles before steady-state conditions are achieved.

The CSS model for SMB chromatography is relatively new and two methods of CSS modelling have surfaced thus far. One method is the CSS model for a single *cycle* (*i.e.* when a particular inlet/outlet stream of the SMB unit is moved periodically until it returns to its original position, as at the start of the cycle). Nilchan and Pantelides (1998) reported a method of complete discretisation for periodic adsorption processes, where the system of equations is discretised in both temporal and spatial domains and incorporating the periodicity conditions of CSS as additional boundary conditions in the model. These periodicity conditions state that the state of the system at the end of each cycle is identical to that at the start of the cycle.

The second method is the CSS model for a single *switching interval.* (Note that it may take several switching intervals to make up one cycle. In a switching interval, the inlet/outline streams move together one column in the direction of the mobile phase flow.) The periodicity conditions stating that state of the system at the end of a switching interval is identical to the state at the beginning of the interval, but shifted by exactly one column length (Kloppenburg and Gilles (1999)).

A comparison of these two approaches of calculating steady state directly has

been done by Minceva *et al.* (2003) for the separation of 1,1'-bi-2-naphthol enantiomers using a simulated moving bed (SMB) process, where the case study employed showed the method by Kloppenburg and Gilles (1999) to be computationally more efficient.

References	Model	Remarks
Storti *et al.* (1993) Mazzotti *et al.* (1997) Strube *et al.* (1997) Pröll and Küsters (1998) Migliorini *et al.* (1998, 1999) Beste *et al.* (2000) Biressi *et al.* (2000) Houwing *et al.* (2002a,b) Minceva and Rodrigues (2002)	TMB model	The SMB processes is modelled by treating it as an equivalent TMB process. Such a model neglects process dynamics, as well as the effects of the periodic changes in the flowrates on the system.
Strube *et al.* (1997) Dünnebier *et al.* (1998) Strube and Schmidt-Traub (1998) Dünnebier and Klatt (1999, 2000) Klatt *et al.* (2000) Jupke *et al.* (2002)	SMB model	The SMB model is a dynamic model in which column models models are linked to a nodal model, through which the streams are simultaneously switched periodically. Such a model gives a true representation of the ongoing changes in the SMB process and the type of chromatography model used can be varied.
Kloppenburg and Gilles (1999) Minceva *et al.* (2003)	CSS models	These models (per cycle or per switching interval) predict the steady state conditions of the SMB process directly.
Ludemann-Hombourger *et al.* (2000) Ludemann-Hombourger *et al.* (2002) Zhang *et al.* (2002, 2003a) Subramani *et al.* (2003)	Varicol model	This is a modification of the SMB process in which the inlet/outlet streams are now switched. asynchronously.
Zhang *et al.* (2003b) Zhang *et al.* (2004)	PowerFeed model	This is a modification of the Varicol process where the inlet/outlet *flowrates* are also varied during the switching interval.
Schramm *et al.* (2003)	ModiCon model	This is a modification of the Varicol process where *feed concentration* is changed periodically.

Table 2.6: A summary of the work in the literature on multi-column chromatography models

2.3.5 Discussion of the models

The microscopic and macroscopic chromatographic models have developed over the years, with the fundamental difference between the models being in the modelling approach. The microscopic model depicts chromatography at a molecular level by the random distribution of molecules along the chromatographic column, accompanied by a Poisson distribution of adsorption events. On the other hand, the macroscopic model is obtained by formulating a differential mass balance equation describing the chromatographic in the level of detail desired. The chromatographic band profiles then are obtained by integrating the mass balance equations.

Felinger *et al* (2004) demonstrated that both these models can be equivalent to one another in predicting the elution profiles for chromatography. However, this was only applicable when the microscopic model employed a particular probability structure. It is also lacking in describing the actual process dynamics, such as disturbances or changes, in the separation process, which is reflected in the macroscopic model. With large-scale processes, it is important that the process dynamics are contained in the chosen model. This leads to the focus on macroscopic models.

The focus of this work is thus on macroscopic models, in which the model is developed from the mass balance equations across the process.

The plate models were popular in 1950s due to their capability in describing the elution profile and peak shape for chromatography. This was at a time when modelling of chromatographic processes was relatively new and there were severe limitations in computational power. However, it was evident that with increasing non-linearity in the separation process, the ideal assumptions that were used to formulate the theory were not valid. This theoretical approach can therefore only be employed for the modelling of linear chromatographic separations.

The contrast to this are the rate models, which is capable of modelling both linear and non-linear chromatographic processes. The rate model is thus employed throughout this thesis for the modelling and optimisation of the chromatographic

process as it facilitates an indepth study of the contribution of the process kinetics such as eddy diffusion and axial dispersion, and their effects on the concentration of the components ove time, as these are significant in non-linear chromatography.

Generally there are three rate models which available in the literature: the ideal model, the equilibrium-dispersive model and the general rate model. These are all based on assumptions of varying complexity. Of these, the ideal model is the simplest model, assuming infinite column efficiency with no axial disperison of mass transfer effects. Whilst an analytical solution is easily obtainable for this model, it fails to accurately model non-linear chromatographic separations.

The equilibrium-dispersive model has been used to efficiently describe a high performance liquid chromatographic separation (Heuer *et al.*, 1996; Teoh *et al.*, 2001), given that the mass transfer mechanics are sufficiently fast enough. In this model, finite column efficiency and a lumped apparent dispersion coefficient to account for mass transfer kinetics are considered.

The general rate model is by far the most comprehensive of all the chromatographic models as it captures not only the variations of the component concentrations along the column but also within the macropores of the stationary phase. It is thus well suited to study chromatographic processes in which the mass transfer kinetics are slow. In the past, the application of this model was hindered by the lack of efficient computation and reliable numerical solution algorithms. However, with the advances in computational power and availability of robust algorithms, these restrictions now no longer apply, although the general rate model still requires a longer computational time compared to either the ideal or the equilibrium-dispersive model. A summary of the model types discussed in this chapter is outlined in Table 2.7.

There is very little work done comparing these models for a real separation process. Whilst some work has compared models of chromatography alongside the equilibrium-dispersive model and general rate model, much of the comparative work compare them on a theoretical basis only or examine the conditions under which these models are applicable using experimental results at an analytical scale for

Column Models	Characteristics
Martin and Synge Plate Model	The column is equivalent to a series of continuous flow mixers
Craig Plate Model	The column is represented as having discontinuous equilibrium stages
Ideal Rate Model	Column efficiency is infinite, axial dispersion is neglected and constant equilibrium of mobile and stationary phases
Equilibrium-dispersive Rate Model	All nonequilibrium effects can be lumped into a single apparent axial dispersion coefficient for each component. This coefficient is independent of component concentrations
General Rate Model	Takes into account band broadening phenomena (eddy diffusion, axial dispersion, mass transfer resistances) which may influence the band profiles

Table 2.7: The chromatography column models and their characteristics

simple systems. There is thus a need for a systematic approach to discern which of the models are appropriate for complex experimental separations, such as those found in biochemical and phamaceutical applications, and how to determine the parameters in these models from experimental data.

Traditionally, much of the mathematical modelling of SMB was done using a true-moving bed (TMB) model. Some of these optimisation studies were then conducted on the TMB models, *e.g.* Mazzotti *et al.*, 1997; Pröll and Küsters, 1998; Beste *et al.*, 2000; Biressi *et al.*, 2000; Houwing *et al.*, 2002a,b. Most of these studies deemed the TMB model to suffice for the prediction of the steady state performance of the SMB process for design purposes, provided geometric and kinematic conversion rules were fulfilled.

However, later research on modelling the SMB process which considered both the TMB model and SMB model suggested that the TMB model was inadequate in some areas (*e.g.* Beste *et al.*, 2000; Strube *et al.*, 1997). For instance, Strube

et al. (1997) attempted to optimise the SMB process by optimising the process using the TMB model, and subsequently using the operating parameters obtained as the input data for an SMB process model. The results obtained on the SMB model showed a decrease in purity relative to that predicted by the TMB model, and the optimisation criteria of maximal feed throughput, minimal desorbent requirement and dilution were not met. This work demonstrated that due to the periodic flow in SMB, the SMB process has to be described by rigorous dynamic models which consider axial dispersion and mass transfer resistance.

2.4 Comparing different operations in chromatographic processes

Over the years, the operation of the chromatographic process in these industries has developed rapidly and it is no longer limited to batch processing. In column chromatography, other operating strategies and techniques have been used to improve the throughput of the process. These include using having gradient elution in the column, the recycling and peak shaving technique and sequential injection techniques on the column. Whilst some work has been done in the literature examining these strategies and optimising them, they are not commonly used in the process industries, unless it is a familiar technique associated with the separation e.g. gradient elution in reverse phase chromatography. Table 2.8 shows at a glance the comparisons that have been made among the these different chromatographic processes.

Closed-loop recycling has been studied in the works of Heuer *et al.* (1995), Grill (1998), Grill and Miller (1998), Quiñones *et al.* (2000) and Teoh *et al.* (2001). The modelling of this technique is described and discussed in detail by Heuer *et al.* (1995) and Quiñones *et al.* (2000). Grill (1998) introduces a periodic injection in the recycle, such that the fresh sample injected does not mix with the previous

recycled chromatographic profile which is still circulating. Teoh *et al.* (2001) conducted a dynamic optimisation for a HPLC column running under this technique and demonstrated that recycling does not necessarily guarantee an increment in yield.

Whilst the single column is still popular in preparative chromatography, multi-column processes, such as simulated moving bed (SMB) chromatography, are now becoming increasingly favoured in industrial-scale chromatography. Among the multi-column chromatography operations available, the technology of the simulated moving bed (SMB) process is perhaps the most prolific and best known. In the SMB process, a fixed adsorbent bed is used, with feed and product positions are successively switched at regular timed intervals to simulate the countercurrent movement of the bed against the flow of mobile phase. More recent however, is the development of the Varicol process, a process not unlike the SMB, but instead employs the nonsynchronous switching of the inlet and outlet ports in its operation. Other variants of the SMB process include PowerFeed, where flow rates in the unit are allowed to change during the switching period (studied extensively in the works of Zhang *et al.* (2003b) and Zhang *et al.* (2004)), and ModiCon, in which the feed concentration is modified periodically (detailed studies found in the work of Schramm *et al.* (2003). Both processes demonstrate a remarkable potential for the improvement of the separation performance compared to the conventional SMB process, although the choice of operation depends on the physical properties of the specific problem being considered (Schramm *et al.*, 2003).

In recent years, some work has been done to compare the different chromatographic systems available. Nicoud *et al.* (1993) compared the eluent consumption, specific productivity and recovery ratio for liquid chromatography and the simulated moving bed chromatography for the enantioseparation of a chiral epoxide on a preparative scale. The findings showed that among the two systems, the SMB unit required less solvent and had a recovery rate of nearly 100%, compared to about 70% in liquid chromatography.

Kennedy *et al.* (2004) investigated the development and scale up of steady state recycle (SSR) technique in batch chromatography. This requires the timed events for sample fraction cuts, recycle and sample injection to be determined in order to develop a constant sample profile. This concentration becomes constant or steady state after a number of cycles. In this work, optimised batch chromatography is compared to SSR for six active pharmaceutical intermediates in terms of productivity and solvent usage. In all cases studied, solvent usage decreased and improvement in productivity was observed when SSR was employed. It is a technique worth considering when the feed sample quantities are in the range of 50g to kilograms.

Miller *et al.* (2003) and Grill *et al.* (2004) conducted comparisons of different chromatographic systems for the resolution of a racemic pharmaceutical intermediate at preparative and process scales. The work of Miller *et al.* (2003) focussed on batch and simulated moving bed (SMB) chromatography, whilst Grill *et al.* (2004) compared preparative high pressure liquid chromatography (HPLC), steady state recycle (SSR) and SMB. Both these works made the comparisons on the basis of production rate and solvent consumption; these being the most important factors in determining the operating costs. Grill *et al.* (2004) concluded that the SMB technique was the best choice for the process scale, whilst lab-scale SMB and SSR are comparable for a moderate scale separation.

Most of the work comparing single column and multi-column chromatography has been based on comparing the two processes on specific outcomes such as eluent consumption or specific productivity (Nicoud *et al.*, 1993; Grill *et al.*, 2004). Such comparisons fail to consider underlying economic issues which may be in conflict, e.g. multi-column processes are associated with a high investment cost but have reduced eluent consumption, whilst single columns have lower investment costs but lower efficiency. As a result, these comparisons, whilst useful in highlighting the advantages and disadvantages of both systems relative to each other, do not provide any useful means of choosing between these systems.

Papers considering chromatographic systems from an economic perspective are

relatively few, one of the more recent papers being Jupke *et al.* (2002) where an economic comparison is made between the optimal design of the batch and SMB chromatographic systems, and providing an idea of the contributions of the separations costs between the two systems. Jupke *et al.* (2002) considers a detailed breakdown of the costs in the separations including capital costs, investment costs, operation (including labour and maintenance) costs as well as depreciation over 4 years for the batch and SMB systems.

Thus, an economic comparison between the optimised process alternatives within single and multi-column chromatography is thus necessary to properly assess the strengths and weaknesses of each system, particularly from an industrial point of view.

Reference	Degrees of freedom	Feed mixtures	Optimisation solution method	Objective function	Systems compared			
					Column	Column with recycle	SMB	SMB Variant
Nicoud *et al.* (1993)	None	Enantiomers of chiral epoxide 1a,2,7,7a-tetrahydro-3-methoxynaphth-(2,b)-oxirene	None	None	√		√	
Grill & Miller (1998)	Collection time of component	Unnamed enantiomer mixture	Experimental modification	Production time	√	√		
Jupke *et al.* (2002)	*Batch*: flowrate, column length, injection time & cut times for fraction collection *SMB*: 4 flowrates, switching time	Potent cardiotonic drug (with Ca-sensitising activity) intermediate enantiomers	Algorithm in paper	Minimise costs	√		√	

Table 2.8: Examples of work comparing different chromatographic processes in optimisation

Reference	Degrees of freedom	Feed mixtures	Optimisation solution method	Objective function	Systems compared			
					Column	Column with recycle	SMB	SMB Variant
Zhang *et al.* (2002)	Feed flowrate, section flowrate, eluent flowrate switching time column configuration	Chiral mixture	Non-dominated sorting genetic algorithm (NSGA)	1) Maximise feed flowrate 2) Maximise extract and raffinate purities 3) Maximise feed flowrate and minimise eluent flowrate			√	√ (Varicol)
Miller *et al.* (2003)	Feed flowrate, switching time	Unknown pharmaceutical intermediate enantiomer	Experimental modification	None	√		√	
Subramani *et al.* (2003)	SMB and Varicol switching times, raffinate and extract flowrate column length, column configuration	Glucose and fructose	Non-dominated sorting genetic algorithm (NSGA)	1) Maximise production rate and purity of fructose 2) Maximise production rates of fructose and glucose			√	√ (Varicol)

Table 2.8: Examples of work comparing different chromatographic processes in optimisation (continued)

Reference	Degrees of freedom	Feed mixtures	Optimisation solution method	Objective function	Systems compared			
					Column	Column with recycle	SMB	SMB Variant
Schramm *et al.* (2003)	Flowrates	Cyclopentanone and cycloheptanone	Model based control	Product purity			√	√ (ModiCon)
Grill *et al.* (2004)	None	Proprietary pharmaceutical intermediate enantiomer	None	None	√	√	√	
Kennedy *et al.* (2004)	None	Proprietary pharmaceutical intermediate enantiomer	None	None	√	√		
Zhang *et al.* (2004)	2 feed flowrates in PowerFeed switching times	α-ionone and β-ionone	Non-denominated sorting genetic algorithm (NSGA)	Maximise extract and raffinate purity for 1)constant switching time 2)varying switching time			√	√ (PowerFeed)

Table 2.8: Examples of work comparing different chromatographic processes in optimisation (continued)

2.5 Review of optimisation of chromatography

The optimisation of the design and operation of chromatographic processes is of great economical importance as it is a crucial separation technique in many pharmaceutical and bioprocesses. However, it is difficult to optimise a separation without a clear understanding of how the thermodynamics of phase equilibria, the finite rate of mass transfer and dispersion phenomena interact to affect the band profiles of the individual components as these profiles determine the cut points and the purity, production rate and operation time. With the lack of computation power and reliable numerical algorithms in the past, optimisation on such a basis was not frequently attempted. Table 2.9 gives a brief overview of some of the optimisation work done in chromatography modelling.

In general, there are two main approaches to optimisation: (1) a semi-empirical approach where experimental work is used to verify the optimisation, (2) a theoretical approach which involves the use of chromatography column models to calculate conditions for an optimised separation.

Jacobson *et al.* (1992a) outlined a three-step procedure for the determination and verification of optimum operating conditions: (1) obtaining preliminary experimental data to describe the behaviour of the components in the separation process, (2) using an optimisation algorithm to determine the optimal operating conditions and (3) verifying these results by comparing them to the experimental profiles. Other studies employing a similar procedure include the work of Jacobson *et al.* (1992b) and Jungbauer and Kaltenbrunner (1996).

Much work has been done the optimisation of the design and operating parameters in chromatographic models. The optimisation is based on either the application of the ideal model (Knox and Pyper, 1986; Golshan-Shirazi and Guiochon, 1989a, b) or that of the equilibrium-dispersive model (Felinger and Guiochon, 1996a, b ; Teoh *et al.*, 2001). Given that real chromatography columns exhibit finite efficiencies, the equilibrium-dispersive model is a more realistic model compared to the ideal model,

which assumes these efficiencies to be infinite.

Felinger and Guiochon (1996a) studied the optimisation of design and operation of a preparative chromatographic process. An objective function was introduced in which the product of the production rate and the recovery yield is maximised. These calculations were carried out for isocratic and gradient elution, as well as displacement chromatography. It was found that the objective function leads to optimum experimental conditions where not only the production rate is maximised, but the recovery yield is also significantly improved. This hybrid objective function was also applied to the optimisation of the experimental conditions in overloaded gradient elution chromatography (Felinger and Guiochon, 1996b).

Teoh *et al.* (2001) investigated a high performance liquid chromatographic separation using an equilibrium-dispersive model. The model was used in the optimisation of a preparative chromatographic column using closed-loop recycling operation. The results confirmed that the effective column length could be increased by as much as 200% by the recycling operation. However, recycling does not necessarily gurantee an increment in yield as this depends on the component production being optimised.

In recent years, the work on optimisation in chromatography has also extended to expanded chromatography systems such as simulated moving bed chromatography (Mazzotti *et al.*, 1997; Klatt *et al.*, 2000; Jupke *et al.*, 2002; Schramm *et al.*, 2003) and Varicol processes (Toumi *et al.*, 2003; Zhang *et al.*, 2002; Zhang *et al.*, 2003a,b). This is investigated in further detail in Chapter 4.

Toumi *et al.* (2003) considered a rigourous model-based optimisation framework for the chromatographic separation of proprandol isomers (which exhibit highly non-linear behaviour) for the SMB and Varicol process, in which the throughput (or feed flowrate) was optimised. It was found that a higher production was obtained with the Varicol process compared with the SMB, with the optimisation strategy acting as a set-point generator for low-level controller. This was extended further in Toumi and Engell (2004), in the optimisation for a reactive SMB process, which com-

bined the quasi-continuous chromatographic separation with enzymatic biochemical conversion of glucose to fructose. A non-linear model predictive controller was implemented in the simulations and at a real plant of a small production scale, with experiments confirming the excellence of the developed control scheme. In addition, Engell and Toumi (2005) presented an overview of model-based techniques for the optimisation and control of batch and continuous chromatography, considering maximising the productivity of the batch process and minimising the separation costs of the SMB process. However, there is no comparison of either process in this work.

A multiobjective function optimisation, maximising both the purity of the extract and the productivity of the unit, for both the simulated moving bed (SMB) and Varicol chromatographic processes was investigated by Zhang *et al.* (2003a). This work utilised an equilibrium stage chromatography model (based on the plate model theory). The optimisation technique was based on a genetic algorithm, and allows for the performances of both SMB and Varicol separation systems to be compared under equal optimal conditions. The parameters being investigated were the size of the packing material, the total number of columns and the total amount of feed concentration.

These studies suggest that the design and operation of a successful SMB unit requires an accurate and reliable dynamic model of the process, taking into account the continuous dynamics in each column and the discrete events of port switching. Thus, a thorough optimisation of the SMB unit should be based on a dynamic SMB model.

Optimisation of a dynamic SMB model has only been investigated recently (Mazzotti *et al.*, 1997; Strube *et al.*, 1997; Klatt *et al.*, 2000; Dünnebier *et al.*, 2000; Houwing *et al.*, 2002a,b; Jupke *et al.*, 2002). Other systems closely related to the SMB include closed loop steady state recycling (CLSSR) chromatography (Grill, 1998; Grill and Miller, 1998; Grill *et al.*, 2004) and also the development of the Varicol process (Ludemann-Hombourger *et al.*, 2000 and 2002; Zhang *et al.*, 2002 and 2003; Subramani *et al.*, 2003), which is a modification of the SMB system.

These previous approaches to optimisation of the SMB process have mainly focussed on dynamic simulation until steady state (*e.g.* Dünnebier and Klatt, 1999; Klatt *et al.*, 2000; Jupke *et al.*, 2002), the use of the Triangular theory (*e.g.* Mazzotti *et al.*, 1997; Houwing *et al.*, 2002a,b) and multi-objective optimisation (*e.g.* Zhang *et al.*, 2002; Zhang *et al.*, 2003; Subramani *et al.*, 2003).

Reference	Model	Numerical solution	Remarks
Ghodbane & Guiochon (1988)	Ideal model	Godunov algorithm	Computer simulation was performed to determined the best loading factor of a chromatography column. Guidelines for predicting the best overloading extent was provided.
Wilhem & Rita (1989)	Equilibrium dispersive model	Gauss Newton method	Steady state optimisation technique to determine the cost of stationary phase subjected to purity and geometry constraints. Restricted to linear chromatography.
Jacobson *et al.* (1992a, b)	Equilibrium dispersive model	Finite difference	Traditional experimental approach with computer simulation was applied to determine the optimum production rate of an enantiomer purification by varying the sample size and the retention parameters.
Felinger & Guiochon (1994)	Equilibrium	Non simplex algorithm	A hybrid objective function was constructed to optimise the experimental conditions of a preparative chromatography system to obtain a minimum production cost for the system accordingly.
Felinger & Guiochon (1996a)	Ideal and equilibrium dispersive models	Non simplex algorithm	A novel objective function was defined to optimise the design and operating conditions of a chromatography system.

Table 2.9: Examples of optimisation work done in chromatography.

Reference	Model	Numerical solution	Remarks
Ghodbane & Guiochon (1988)	Ideal model	Godunov algorithm	Computer simulation was performed to determined the best loading factor of a chromatography column. Guidelines for predicting the best overloading extent was provided.
Wilhem & Rita (1989)	Equilibrium dispersive model	Gauss Newton method	Steady state optimisation technique to determine the cost of stationary phase subjected to purity and geometry constraints. Restricted to linear chromatography.
Jacobson *et al.* (1992a, b)	Equilibrium dispersive model	Finite difference	Traditional experimental approach with computer simulation was applied to determine the optimum production rate of an enantiomer purification by varying the sample size and the retention parameters.
Felinger & Guiochon (1994)	Equilibrium	Non simplex algorithm	A hybrid objective function was constructed to optimise the experimental conditions of a preparative chromatography system to obtain a minimum production cost for the system accordingly.
Felinger & Guiochon (1996a)	Ideal and equilibrium dispersive models	Non simplex algorithm	A novel objective function was defined to optimise the design and operating conditions of a chromatography system.

Table 2.9: Examples of optimisation work done in chromatography.

Reference	Model	Numerical solution	Remarks
Felinger & Guiochon (1996b)	Equilibrium dispersive model	Non simplex algorithm	A novel objective function was defined to optimise the experimental conditions of an overloaded gradient elution chromatography.
Jungbauer & Kaltenbrunner (1996)	Criag plate model		Traditional experimental approach with computer simulation was applied to determing the distribution coefficients in ion-exchange chromatography. Investigation of the fundamental questions in optimising ion-exchange chromatography was conducted.
Lin it et al. (1998)	Equilibrium dispersive model	Perturbation and modified collocation methods	Numerical optimisation of the column length and operating conditions was performed.
Teoh *et al.*, (2001)	Equilibrium dispersive model	Orthogonal collocation on finite elements	Optimisation for HPLC column using closed-loop recycling operation for productivity of components in a binary separation.

Table 2.9: Examples of optimisation work done in chromatography.

2.5.1 Summary

From the literature review, the approach to optimisation in chromatography has changed dramatically with the advances in computational technology and information available. Most of the initial work was based on empirical methods. Subsequently, computer simulation and optimisation techniques such as the Gauss-Newton method, non-Simplex algorithm etc. were commonly used in predicting the optimum experimental conditions given a particular objective function (usually maximising production rate).

Another area of research explored was the objective function employed in the optimisation, as the optimal experimental conditions found may be very different depending on this. It was found that hybrid objective functions, or indirectly multivariable objective functions, enable a much more satisfactory means of meeting the objective function without compromising process constraints.

Much of the work discussed confines the optimisation work done to optimising only the operating conditions, or else limited design parameters of the process. In reality, such solutions are *sub-optimal* as they do not examine all potential areas for optimisation.

2.6 Concluding remarks

Over the years, significant work has been done in the modelling and, to a lesser extent, optimisation of chromatographic processes. Section 2.2 discusses the various types of models available in the literature and also provides details to the assumptions that make up these models. The review of the work done in modelling of chromatography, particularly rate models, in Section 2.3 makes it clear that with the advances in computation, the more complex and comprehensive models may now be solved and used.

Chromatography technology itself has also advanced enormously over the years, and continuous and multi-column chromatographic processes are now being consid-

ered. Similarly, the work in developing chromatographic models have expanded into the modelling and optimisation of multi-column chromatographic processes such as the simulated moving bed (SMB) and the Varicol processes as well.

The efficient computation power available at present allows for more realistic and complex chromatography models, such as the equilibrium-dispersive model and the general rate model, to be solved and used for optimisation. In the following sections, detailed mathematical models coupled with a dynamic optimisation approach will be employed for the modelling and optimisation of both single and multi-column chromatographic processes.

Chapter 3

A systematic approach to modelling chromatographic processes

In this chapter, a systematic approach is proposed (Section 3.2), which allows the estimation of model parameters for the equilibrium-dispersive and general rate models, and to then select which is the appropriate model of the two for a given application. The approach is applied to three case studies (Section 3.3), one theoretical and two experimental. The case studies consider the suitability and range of application of the two models in describing the behaviour of complex chromatographic separations. It is found that, whilst the equilibrium-dispersive model is a good approximation in most cases, there are instances when the more detailed general rate model is required to capture the process behaviour more accurately.

3.1 Introduction

Modelling and optimisation of process-scale chromatography allows the investigation of different design and operating alternatives. However, in order to achieve this, accurate mathematical models of the chromatographic process are needed. Much of the work published on developing such models considers only analytical scale separations, and all need further experimental work needs to be done in order to obtain the model parameters. Little research is conducted on developing models for more complex separations. Thus, there is a a need for a systematic approach to determine the parameters in chromatography models and, more importantly, to select the most appropriate model for complex separations, such as those found in biochemical applications.

In this work, a novel systematic approach is proposed to obtain accurate model parameters from experimental and literature data for two commonly-used chromatography models - the equilibrium-dispersive model and the general rate model. A key feature in the approach is a procedure used to approximate the feed concentration for mixtures where the feed concentration is unknown, which is common in complex mixtures such as those used in bioprocesses.

The objectives of this approach are therefore to (1) determine the feed concentration of an unknown mixture, (2) determine or estimate the model parameters of each model and (3) select the most appropriate model for a given process using a graphical method representing the chromatographic performance in the model. The deliverable is thus a method for modelling, as well as guidelines for how to determine which model is appropriate for which application.

3.1.1 Chromatography models in literature

Several mathematical models of chromatographic processes are available and have been applied successfully for the calculation of the band profiles obtained in chromatography (Guiochon *et al.*, 1994). Models studied in the literature include the

ideal model, the equilibrium-dispersive model (ED) and the general rate (GR) model, with the latter two being most widely used.

The equilibrium-dispersive model accounts only for a finite extent of axial dispersion as it uses an apparent lumped dispersion coefficient to account for any band-broadening effects. It is accurate, provided the mass transfer in the chromatographic column is controlled only by molecular diffusion across the mobile phase flowing around the packing particles and the exchange of eluites between the stationary and mobile phases is very fast (Guiochon *et al.*, 1994). In other cases, it serves as an approximation only. It has nevertheless been used extensively and verified with experimental data by many authors (Felinger and Guiochon, 1992; Guiochon *et al.*, 1994; Heuer *et al.*, 1996; Teoh *et al.*, 2001; Antos *et al.*, 2003). Much of the work demonstrates the success in employing the equilibrium-dispersive model in modelling and optimising preparative chromatography. More details on the modelling and optimisation work on this model can be found in Section 2.3.2 and Section 2.4.

The general rate model is widely acknowledged to be the most comprehensive among the chromatography models (Guiochon *et al.*, 1994; Kaczmarski *et al.*, 2001; Teoh, 2002) as it accounts for the axial dispersion and all the mass transfer resistances *e.g.* external mass transfer of solute molecules from bulk phase to the external surface of the adsorbent, diffusion of the solute molecules through the particle pores and adsorption-desorption processes on the site of the particles. It has been successfully employed in many chromatography applications (Gu *et al.*, 1990; Li *et al.*, 1998; Kaczmarski *et al.*, 2001; Gu, 1995; Gu and Zheng, 1999; Klatt *et al.*, 2000; Piątkowski *et al.*, 2003) including complex processes such as simulated moving bed chromatography. However, the general rate model requires a relatively large number of parameters in order to characterise the axial dispersion, external mass transfer and effective diffusion through the pores, some of which are difficult to measure accurately (Kaczmarski *et al.*, 2001). It also involves two partial differential equations in its mass balances, and is therefore more computationally demanding than the

simpler chromatography models. Further details on the modelling and optimisation work on this model may be referred to in Section 2.3.2 and Section 2.4.

The equilibrium-dispersive and general rate models are the most popular in the literature of chromatography but there are trade-offs associated with each. The ED model can be solved in a short time with fairly accurate solutions, whilst the GR model captures the process dynamics more accurately as it takes into account all the mass transfer resistances in the process, but it is computationally expensive. The application of these models, however, also requires the knowledge of how to obtain the model parameters from experimental and literature data. Also, more importantly, how to select the appropriate model for a given application.

There has been some work which has compared the other available models of chromatography such as the transport-dispersive model (which uses a lumped dispersion coefficient and the lumped mass transfer coefficient) (Antos *et al.*, 2003; Piątkowski *et al.*, 2003) and the lumped pore diffusion model (a simplified form of the general rate model employing a lumped overall mass transfer coefficient) (Kaczmarski and Antos, 1996) with the equilibrium-dispersive model and general rate model. However, much of the comparative work done on these models compares them on a theoretical basis or examines the conditions under which these models are applicable using experimental results at an analytical scale for simple systems. There is thus a need for a systematic approach to discern which models are appropriate for complex separations, such as those found in biochemical and pharmaceutical applications, and how best to determine the parameters in these models.

The focus of this work on model parameter determination and model selection will be the equilibrium-dispersive model and the general rate model and complex systems will be considered to demonstrate the approach.

3.2 A systematic approach for model parameter determination and model selection

In this section, the approach proposed for determining model parameters is outlined. In the literature, there is no methodical means by which unknown model parameters, such as the feed concentration, can be estimated for a mixture which consists of many unknown components. In particular, with complex bio-mixtures, with several impurities present, it is difficult to know what is the actual composition of the feed. The proposed approach details how the feed concentration may be approximated and demonstrates that detailed information of all the components in the mixtures is not necessary in the model development. Nevertheless, some information is still needed for the accurate representation of the process, as detailed in Section 2.1.1.

Figure 3.1 shows a general flowchart of the systematic approach used in this work. The type of separation in the experimental set-up is first identified in order to develop the model. The next step of identifying the known model parameters (in both the equilibrium-dispersive and the general rate models) involves both common and distinct model parameters. The remaining unknown parameters are then estimated, followed by the selection of the most appropriate model for the separation.

Some of the parameters of the models can be determined from the experimental set-up or from the literature. The unknown parameters, in this work, the isotherm parameters, must then be estimated. Once the parameters of the candidate models have been determined, the selection of the most appropriate model then needs to be made on the basis of the performance of the models against the experimental data it represents. This is done, in this work, using a graphical method representing the chromatographic performance in the model.

3.2.1 Parameters common in both models

Some parameters are common in both the ED and GR models, and their identification is one of the key steps in the approach shown in Figure 3.1. Known common model parameters, such as column length L, column diameter D_C, particle radius R_P, and the flow-rate of the mobile phase Q, are easily found from the experimental set-up. Other common model parameters, like the feed concentration of the components and the isotherm parameters, may not be readily known, and are here termed *unknown common model parameters.* The proposed approach uses a procedure to determine the individual feed component concentrations first, if unknown, with the isotherm parameters estimated at a later stage. If the feed concentration is known, other uncertain parameters, such as the mass tranfer resistances in the general rate model, may be estimated instead.

Outline of the procedure for feed concentration determination

In most industrial chemical separations, the total concentration of the overall feed mixture is usually known. However, in complex separations, such as those in bioprocess applications, where the feed contains impurities or many unknown components, it may be difficult to identify which components should be modelled. To model all of the components, and the associated model parameters, is costly both in terms of time and computation expense. Thus a procedure to determine the feed concentration for accurate modelling is necessary, using information only from the chromatogram, and this is proposed in this section.

The procedure for feed concentration determination of a mixture containing several unknown components in the feed developed in this work assumes that:

- the identity of some of the components is known *e.g.* protein names
- chromatographic data of at least one of the components
- chromatographic data of the total mass of components eluted

Figure 3.2 outlines the procedure for determining the feed concentration from the experimental chromatograms, for which many of the feed component concentrations are unknown. In complex separations there may often be several components, which either do not bind to the column or are present in insignificant amounts. These are not present in the experimental chromatograms and are removed from the model using the procedure outlined below.

Step 1 Input parameters are identified and defined: N_T is the total number of components in the feed mixture, whilst N_{NP} is the number of peaks on the chromatogram from the column. R_C is a confidence ratio, and is employed in the procedure to determine a reasonable number of components for which the estimated parameters are likely to be statistically significant (refer to Appendix C for more information on statistics).

Step 2 Known components in the feed mixture which are likely to be retained on the column are identified. Next, the characteristic property of the chromatographic separation must be known, *e.g.* affinity for stationary phase, molecular size or hydrophobicity. The separation property determines if the components are retained. The number of *unretained* components are identified as N_R.

Step 3 The number of feed components appearing in negligible amounts, N_S, is identified. The total number of components which bind to the column and is subsequently eluted to form the chromatogram is N_C, which is defined by $N_C = N_T - N_R - N_S$. Thus, components small in quantity (N_S), and not retained on the column (N_R), are not included in the model.

Step 4 Pseudo-components may be defined by lumping components which have similar properties as they will elute in the same manner, to give N'_C, the number of components to be modelled. This reduces the number of variables which need to be considered in the model and thereby reduces the complexity of the problem.

Step 5 The ratio of the number of modelled components to the number of peaks on the chromatogram, $\frac{N'_C}{N_{NP}}$, is determined. N'_C cannot be less than N_{NP} as this would suggest that there are fewer components in the model than in the

experimental data. However, at the same time, the parameter values obtained may not be statistically significant if too many parameters are estimated simultaneously. Thus, a decision block is set up where the calculation continues to Step 6 only if $\frac{N'_C}{N_{NP}}$ fulfils the criterion of a lower bound of 1 and an upper bound of R_C. Otherwise, the process is repeated by redefining the either N_R, N_S and/or N'_C, to re-evaluate the components and reduce the number of pseudo-components.

Step 6 The components (both pseudo-components and real) from Step 5 may now be regarded as the total number of components present in the separation for the purpose of modelling the process. The magnitude of the characteristic property the separation for each of the components is used to determine the affinity of the components for the stationary phase, and thus the order in which they elute from the column.

Step 7 The feed concentration for each peak is calculated using the trapezium rule on the area under each peak on the chromatogram. Each peak is assumed to be Gaussian-shaped and symmetrical as these are not generally not explicitly shown on the total concentration chromatogram. The trapezium rule is illustrated in Figure 3.3, with the shaded section under the peak expressed as:

$$\text{Shaded section} = \frac{1}{2}h(f1 + f2) \tag{3.1}$$

The summation of the all the different segments under the peak give the total area under the peak.

Step 8 The chromatogram peaks are then identified by the order of elution of the components and the known proportions of the components present. The feed concentration of the components (pseudo and real) is thus determined.

3.2.2 Distinct model parameters

Having determined the common model parameters for the models including the feed concentrations, the distinct model parameters, which are the parameters character-

istic of each model, must be found (see Figure 3.1). These include the apparent axial dispersion coefficients in the equilibrium-dispersive model and mass transfer resistance coefficients in the GR model. In this work, these parameters were determined using literature correlations, although some values can be determined by performing experiments. The distinct model parameters used in this work, along with suitable correlations are summarised in Tables 3.1 and 3.2.

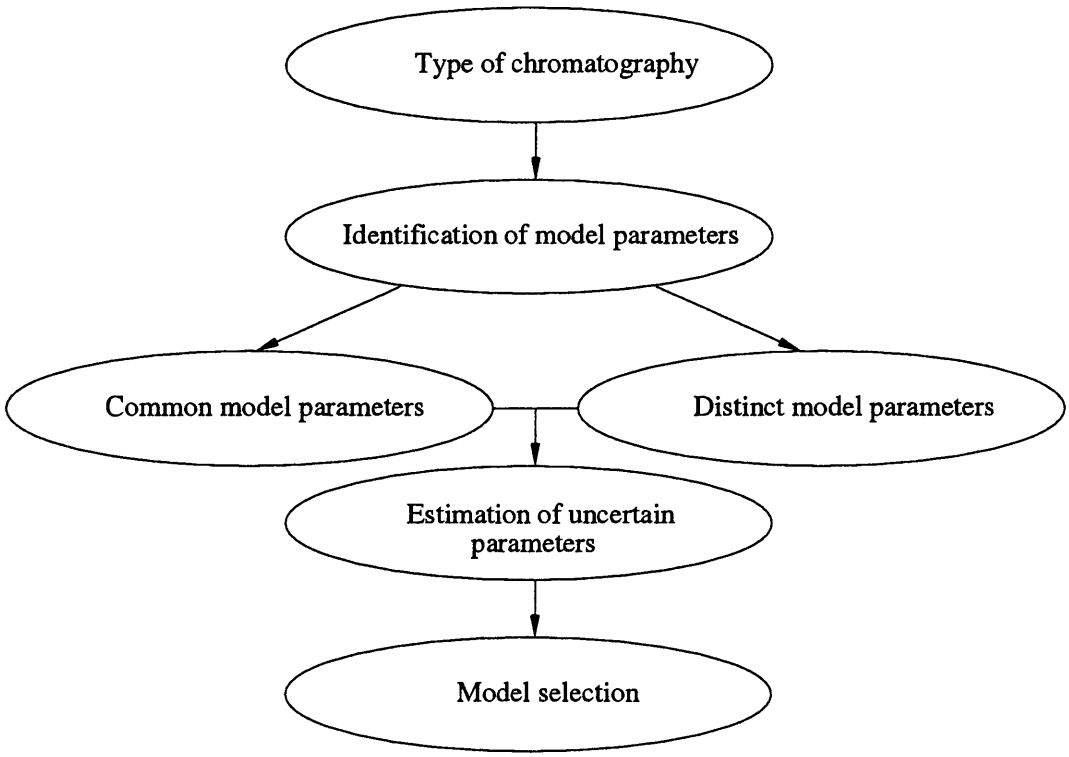

Figure 3.1: Flowchart of the approach

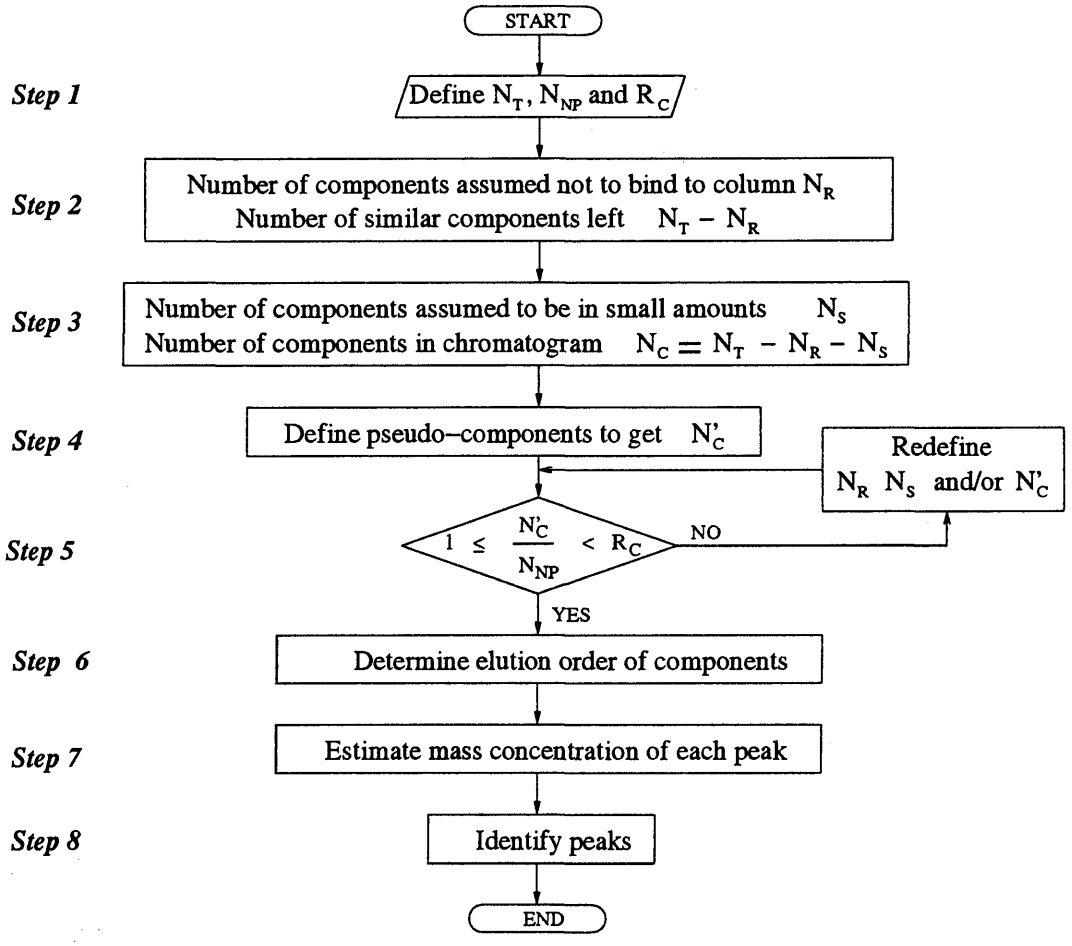

Figure 3.2: Flowchart of feed concentration determination

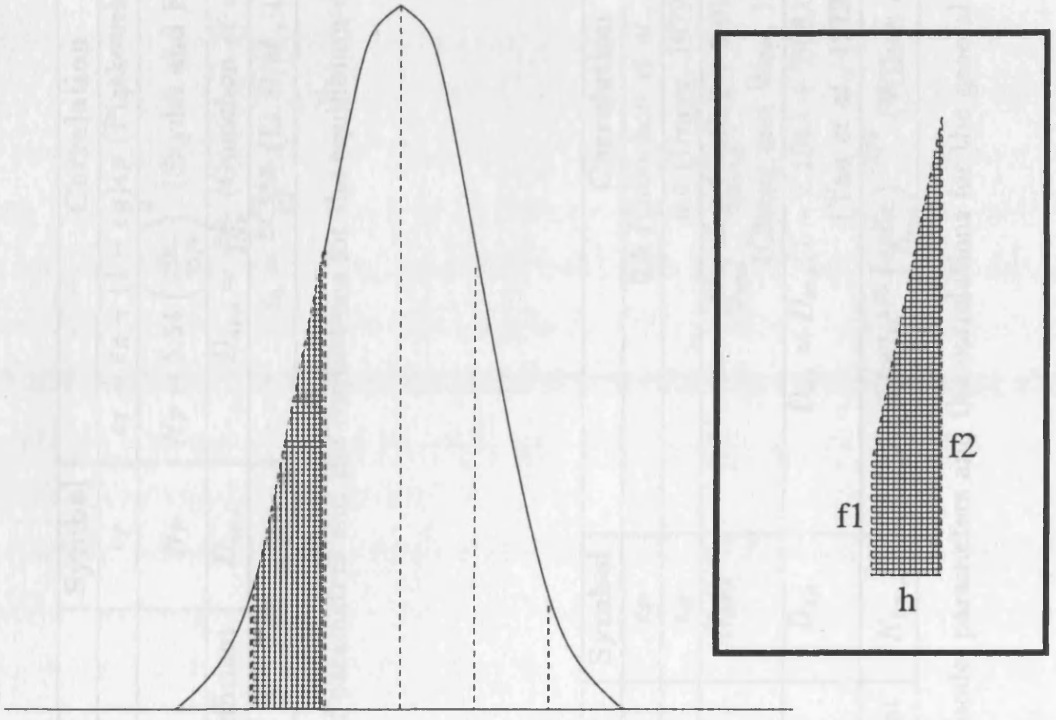

Figure 3.3: Illustration of the trapezium rule to estimate area under a peak

Parameters	Symbol	Correlation
Total porosity	ϵ_T	$\epsilon_T = \epsilon_B + (1-\epsilon_B)\epsilon_P$ (Piątkowski *et al.*, 2003)
Plate number	N_P	$N_P = 5.54\left(\frac{t_R}{w_{1/2}}\right)^2$ (Snyder and Kirkland, 1974)
Apparent dispersion coefficient	$D_{ap,i}$	$D_{ap,i} = \frac{uL}{2N_P}$ (Guiochon *et al.*, 1994)
Dead time	t_0	$t_0 = \frac{\pi d^2 L \epsilon_B}{4Q}$ (Li *et al.*, 1998)

Table 3.1: Distinct model parameters and the correlations for the equilibium-dispersive model

Parameters	Symbol	Correlation
Particle porosity	ϵ_P	0.5 (Guiochon *et al.*, 1994)
Bed porosity	ϵ_B	0.4 (Unger, 1979)
Axial dispersion coefficient	$D_{ax,i}$	$\frac{vL}{D_{ax,i}} = \frac{L}{2R_P\epsilon_B}(0.2 + 0.011Re^{0.48})$ (Chung and Wen, 1968)
Effective diffusivity coefficient	$D_{e,i}$	$D_{e,i} = D_{m,i}(1 - 2.104\lambda + 2.09\lambda^3 - 0.95\lambda^5)/\tau_{tor}$ (Yau *et al.*, 1979)
Mass transfer resistance coeffcient	$K_{pm,i}$	$K_{pm,i} = 0.687v^{1/3}\left(\frac{\epsilon_B R_P}{D_{m,i}}\right)^{-2/3}$ (Wilson and Geankopolis, 1966)

Table 3.2: Distinct model parameters and the correlations for the general rate model

3.2.3 Parameter estimation of unknown parameters

In Figure 3.1, having obtained both the common and distinct model parameters, what remains to be determined are normally the isotherm parameters. These parameters are often determined experimentally. In cases where only limited chromatographic data is available and no further experimental work can be done, parameter estimation may be used to determine the unknown isotherm parameters.

Parameter estimation refers to the process of obtaining the unknown values of the parameters by matching the model predictions to the available sets of experimental data (Englezos and Kalogerakis, 2001). In the approach proposed in this work, it is assumed that the values of the isotherm parameters are not usually known, and that these need to be determined by parameter estimation. Should the isotherm parameters already be known, parameter estimation may be used to estimate other coefficients, *e.g.* the effective diffusivities in the GR model. It is possible to estimate other parameters together with the isotherm parameters, however, estimating a large number of parameters based on little input data renders all the parameter values obtained statistically unreliable.

In this section, the procedure for estimating the unknown model parameters is outlined (see Figure 3.4). All the input blocks (trapeziums) and the action blocks (boxes) are labelled numerically, whilst the decision block (diamond-shaped figure) are labelled using Roman numerals. The *gPROMS* (Process Systems Enterprise Ltd., 2005) modelling software was used to estimate the parameters in this work and more details of this parameter estimation tool used may be referred to in Appendix C.

Trapezium 1 Compile the experimental data, usually chromatographic data of the process.

Trapezium 2 Program the model of the process using the chosen programming tool.

Box 3 Set the bounds for the parameters to be estimated. The parameters are estimated within the range imposed by these bounds.

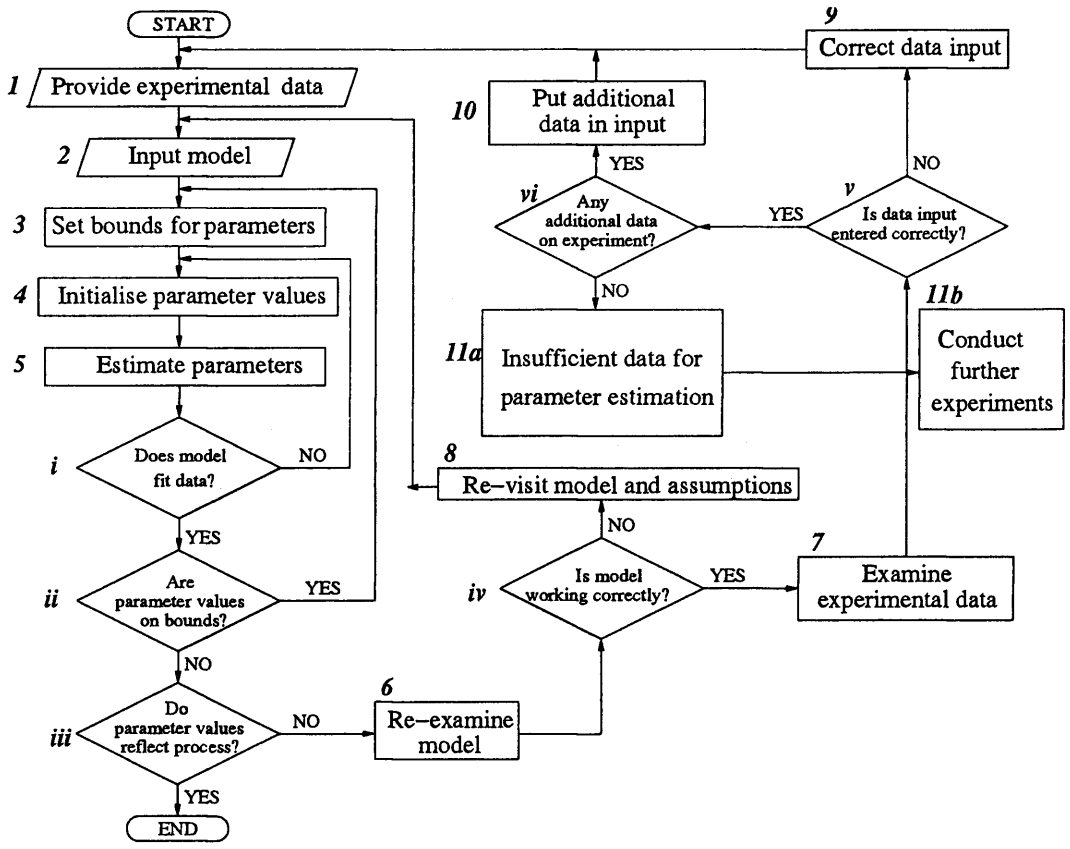

Figure 3.4: Flowchart of parameter estimation

Box 4 Initialise the values of the estimated parameters in the model. During all the test runs, the parameter estimation will initiate using these values.

Box 5 Carry out parameter estimation.

Decision i Determine if the model fits the experimental data given in Trapezium 1. If it does, proceed to the next step; otherwise return to Box 4 and change the values for initialisation. (Different initial guesses may be needed if initial values are too far from the estimated values for the model to fit the data.)

Decision ii Check that the estimated parameter values do not lie on the bounds set in Box 3. If they do, return to Box 3 to increase the bounds; if not proceed to the next step. (If values lie on the bound, it often means the parameter estimation has been constrained by the bounds on that parameter.)

Decision iii Check that the estimated parameter values obtained reflect the process accurately from previous knowledge of the process. With limited data provided for parameter estimation, the estimated parameters may not reflect certain behaviour correctly, *e.g.* the elution order or band width. If the model does reflect the process, then the parameter estimation comes to an end. However, if it does not, then proceed to Box 6.

Box 6 Examine the model equations to determine why there is a discrepancy between the model prediction and the experimental data.

Decision iv If the model is working correctly *i.e.* reflects the behaviour of a chromatographic process but the discrepancy is still present, proceed to Box 7. If the model is determined not to be working correctly, then proceed to Box 8.

Box 7 Examine that the experimental data used in the estimation is correctly entered and proceed to Decision v.

Box 8 Re-visit the modelling assumptions. Return to Trapezium 2.

Decision v If the experimental data input has been entered wrongly for the parameter estimation, proceed to Box 9. If the experimental data given is correct, proceed to Decision vi.

Box 9 Correct the experimental data input and return to Trapezium 1.

Decision vi Determine if there is any additional data available on the experiment. If there is additional data, proceed to Box 10. If there is no additional data on the experiment, proceed to Box 11.

Box 10 Add the additional experimental data to the input data and return to Trapezium 1.

Box 11a and 11b There is probably insufficient data for accurate parameter estimation. Since there is no additional data to be gathered, further experiments have to be conducted (Box 11b).

The procedure ends successfully when the parameters estimated reflect the process at Decision iii, or unsuccessfully if there is insufficient data for parameter estimation.

3.2.4 Model selection

Once the parameters of both the ED and GR models have been determined from the experimental data, the final step of the approach is to decide which of the two models is better suited for modelling the process (see Figure 3.1)). The performances of the models are compared against the experimental data to decide which is more suitable. Merely examining the goodness-of-fit of the model against the experimental data is, however, not sufficient as it is subject to perception.

Since some differences between predicted and experimental data are unavoidable, the crucial issue is which of the models will be a closer fit to the data, which may not be easily discerned by merely examining the chromatograms. What is needed is a means by which any change in the predicted data from the experimental data is accentuated to show the difference in a manner which is useful.

Fractionation and maximum purification factor diagrams are recent graphical methods used to illustrate the trade-off between purity and recovery in chromatographic performance (Ngiam *et al.*, 2001; Ngiam, 2002) and these are used in this work. They are highly sensitive to how small changes in the chromatogram affect the purity and recovery of the process. Thus, by using these diagrams on the predicted and experimental data, the closeness of the model predication to the experimental data is made much more evident in order for the user to decide which of the models is better suited to describing the process.

3.3 Case Studies

In the previous section, a systematic approach has been described where model parameters for different candidate models are estimated and the appropriate model selected for a given separation process. The approach is now illustrated in this section for three case studies. The first case study is theoretical, and is included to illustrate the steps in the approach, as well as to validate the parameter estimation technique. The second and third case studies employ experimental data

Parameter	Symbol	Units	Value
Column length	L	cm	15
Column diameter	D_C	cm	60
Particle radius	R_P	μm	45
Volumetric flowrate	Q	ml/min	5640
Load volume		ml	148,000
Total component concentration		mg/ml	15

Table 3.3: Dimensions of column in Case Study 1

from other workers (Khanom, 2003; Edwards-Parton, 2004) in two different types of chromatography to illustrate the approach.

3.3.1 Case Study 1

The first example is a theoretical case study on modelling a step elution hydrophobic interaction chromatographic separation for 12 components, of which only the concentration of one component is known, employing industrial dimensions for the column (see Table 3.3). The 'experimental data' was generated using the GR model (refer to Figure 3.5 (a) and (b)). However, the only data in the approach used is of one component and the total component concentration to reflect the limitations typically encountered in gathering industrial data. This data was used to illustrate the proposed approach in detail to obtain the parameters for both the ED and GR models. The primary purpose of this is to demonstrate the viability of the parameter estimation technique by comparing the estimated values with the actual values employed in the GR model when generating the data. The case study is fairly simple to work on, as compared to an experimental case study, as it has clearly known and defined feed components.

Determining feed concentration

Table 3.4 shows the components and their known characteristic properties which are used in separation. The value of the characteristic property is used as an indication

Component	Molecular weight (Da)	Amount present (%)	Characteristic property value
A	50 00	5	7
B	150 000	5	7
C	55 000	11	8
D	15 000	8.3	9
E	40 000	9	10
F	10 000	23	11
G	30 000	7	12
H	6 000	5	12
I	150 000	10	1
J	62 000	15	2
K	23 000	0.5	7
L	16 000	1.2	9
		$\sum = 100\%$	

Table 3.4: Known components in the mixture with characteristic property

Component	Pseudo-component	Average molecular weight	Amount present	Characteristic property	Concentration (mg/ml)
A and B	1	100 000	10	7	1.5
C	2	55 000	11	8	1.65
D	3	15 000	8.3	9	1.24
E	4	40 000	9	10	1.35
F	5	10 000	23	11	3.45
G and H	6	20 000	12	12	1.80
			$\sum = 73.3\%$ of total concentration		

Table 3.5: Feed component concentration in Case Study 1

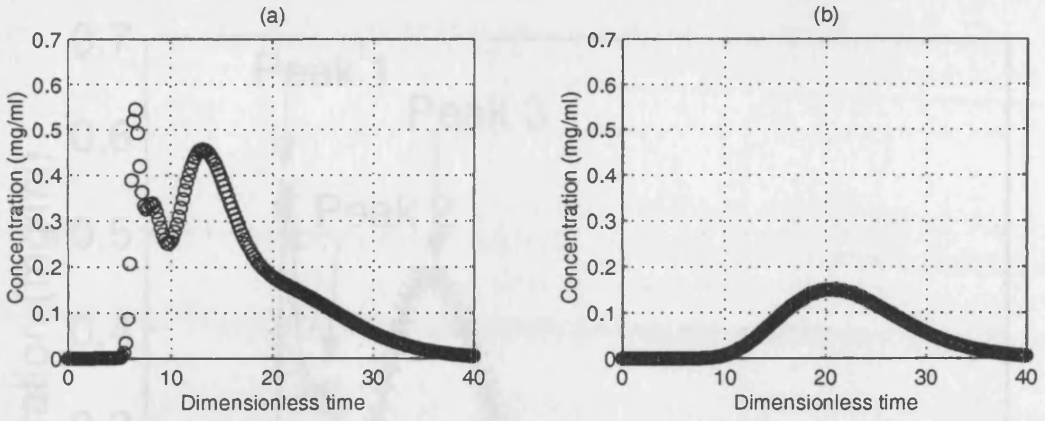

Figure 3.5: Experimental chromatograms generated using the GR model for Case Study 1

(a) Total component chromatogram, (b) Component 6 chromatogram

of the strength of the components' affinity for the stationary phase, with higher values having a stronger affinity for the stationary phase. Components with very low values do not bind to the stationary phase but rather go straight through the column. They do not appear in the chromatogram and are thus not considered in the simulation.

Figure 3.2 has shown the procedure for feed concentration determination and the steps outlined earlier are explained below for this case study to demonstrate the approach.

Step 1 N_T is the total number of components in the feed mixture, and in this example, this is defined as 12. N_{NP}, the number of peaks on the chromatogram, can be observed from Figure 3.6 as there are 4 distinguishable peaks. R_C, the confidence ratio described earlier, is defined as 2.

Step 2 From Table 3.4, components I and J have separation properties which are much lower (of values 1 and 2, respectively) than the other components and are therefore considered to go straight through the column, *i.e.* $N_R = 2$. The number of components which will bind to the column is $N_T - N_R = 12 - 2 = 10$.

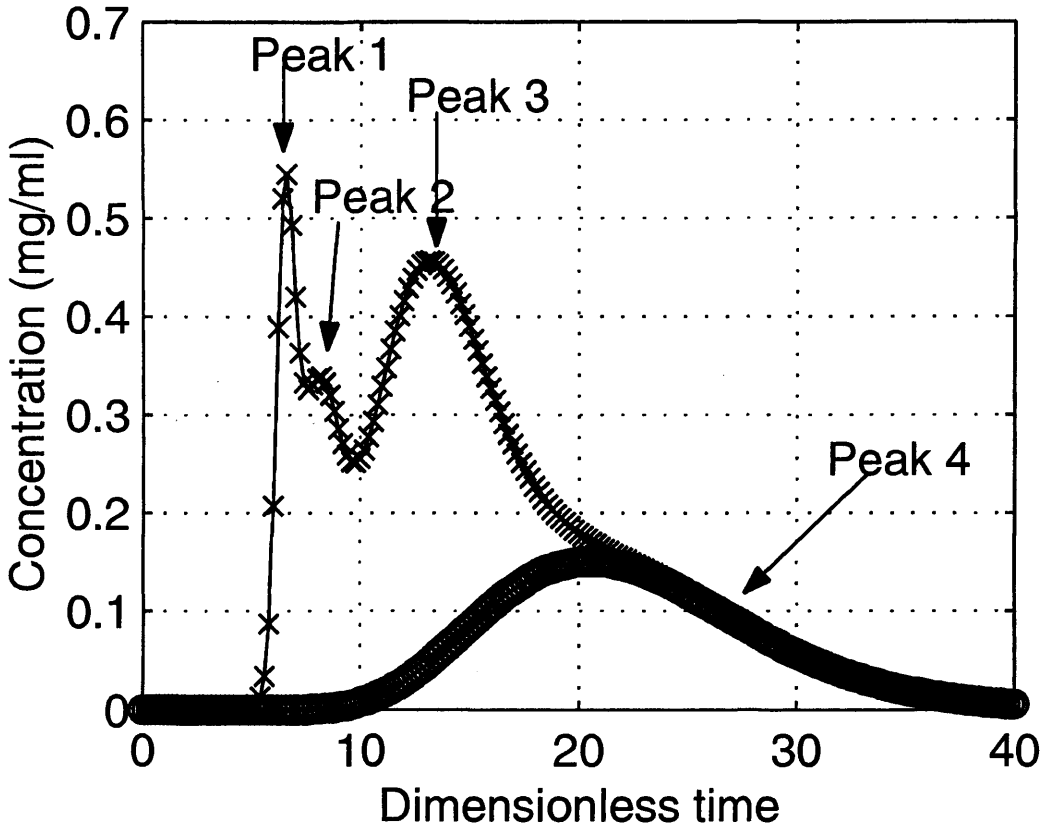

Figure 3.6: The chromatographic peaks in the experimental chromatograms in Case Study 1

Step 3 In the next step, negligible amounts of components that are present in the mixture are identified. From Table 3.4, the amount of components K and L are significantly lower compared to the rest of the mixture and these components are regarded as negligible in the process, *i.e.* $N_S = 2$. The number of components eluting from the column is N_C, where N_C is defined by $N_C = N_T - N_R - N_S = 8$. Thus, components small in quantity (N_S), and not retained on the column (N_R), are not included in the model (component I, J, K and L).

Step 4 Components with similar affinity properties are lumped to form pseudo-components at this stage. Component A and B are lumped to form Component 1, whilst G and H are lumped to form Component 6. Table 3.5 shows the list of

Peak	Concentration (Peak area) mg/ml
1	3.2
2	1.1
3	4.9
4	1.8

Table 3.6: Area under each peak in Case Study 1

pseudo-components. N'_C, the number of components used in the model, is thus 6.

Step 5 The ratio of the number of modelled components to the number of peaks on the chromatogram, $\frac{N'_C}{N_{NP}} = \frac{6}{4}$. This value is less than the confidence ratio R_C of 2, for which the parameters estimated are deemed to be statistically significant and the calculation continues to Step 6. Thus 6 modelled components have to be fitted to the data from 4 peaks.

Step 6 The components (both pseudo-components and real) from Step 5 may now be regarded as the total number of components present in the separation for the purpose of modelling the process, N'_C. The magnitude of the characteristic property of the components (which the separation is based on) in Table 3.5 is used to obtain an estimate of the order in which the components elute from the column. For this example, component 1 elutes first, followed by 2, 3 *etc.*

Step 7 The feed concentration for each peak is calculated using the trapezium rule on the area under each peak on the total component mass (Figure 3.5(a)) and Component 6 chromatogram (Figure 3.5(b)). Figure 3.7 shows 4 peaks that are estimated to be present on the redrawn total component chromatogram and Table 3.6 shows the concentration for each assumed peak.

Step 8 The chromatogram peaks are identified by the order of elution of the components and the concentration of components compared to the peak area (see Table 3.7). Peak 1 is made up of components 1 and 2; peak 2 is component 3, peak 3 is components 4 and 5 whilst peak 4 is component 6.

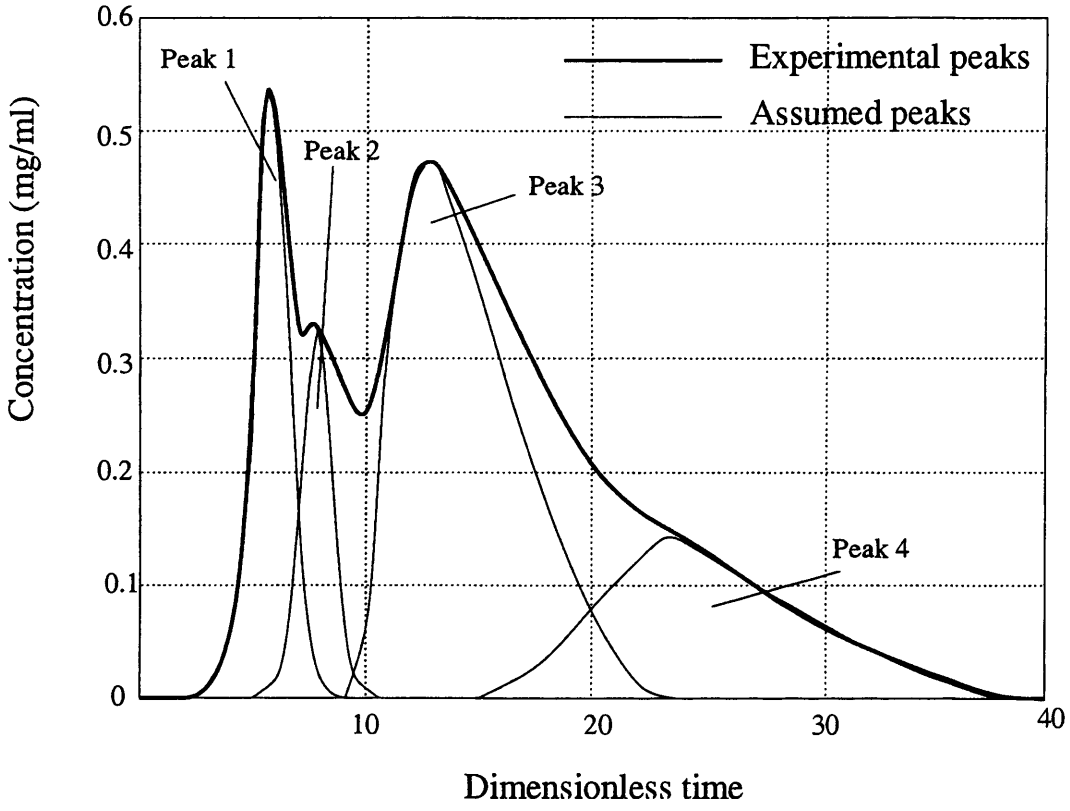

Figure 3.7: 4 assumed peaks drawn as shown against the total component chromatogram

Note: Only Peak 4 (component 6 chromatogram) known as it is given in the experimental data

In summary, the approach is as follows. From Figure 3.6, the number of peaks N_{NP} is identified as 4. The feed mixture loaded onto the column contains 12 components, for which 2 do not bind to the column and 2 are present in negligible amounts. Thus the components binding to the column, $N_C = 8$. 2 pseudo-components are formed, each consists of 2 components, to give $N'_C = 6$. $\frac{N'_C}{N_{NP}} = \frac{6}{4}$ and the criteria $1 < \frac{N'_C}{N_{NP}} < R_C$, where R_C is 2, is fulfilled. 6 components are to be modelled and the feed concentrations of these are determined from the chromatogram.

Peak	Concentration (Peak area) mg/ml	Pseudo Components	Calculated concentration mg/ml
1	3.2	1 and 2	3.15
2	1.1	3	1.24
3	4.9	4 and 5	4.8
4	1.8	6	1.8

Table 3.7: Identifying peaks to components by concentration comparison in Case Study 1

Parameter determination

The distinct parameters for both models in this case study were obtained using the correlations in Tables 3.1 and 3.2 and are shown in Table 3.8.

Isotherm parameter estimation

The common and distinct model parameters were readily determined from the experimental data and the correlations outlined earlier. The remaining parameters which to be estimated are the isotherm parameters. For the approach in this paper, any isotherm model may be employed. A linear isotherm is used here to illustrate the approach. The process uses step elution, where the mobile phase (and hence, the isotherm) is changed during the process. Thus for each component there are two isotherm parameters to be estimated, giving a total of 12 estimated parameters ($K1_i$ and $K2_i$).

It is assumed that the final component eluted, Component 6 (G and H together), is the desired product. As data on all components are usually not available in a real process, only chromatograms for Component 6 and the total protein concentration (Figures 3.5(a) and 3.5(b)) are used here for the model parameter estimation.

The ED model predicts the general trend for the total protein concentration in Figure 3.8(a) well. However, it is poorer at capturing the process dynamics for the

Equilibrium-dispersive model parameters							
Parameter	*Symbol*	*Value*					
Total porosity	ϵ_T	0.7					
Dead time (s)	t_0	315					
Plate number	N_P	12.4					
Apparent dispersion coefficient $\times 10^3$ (cm^2/s)	$D_{ap,i}$	29					
General rate model parameters							
Parameter	*Symbol*	*Value*					
Particle porosity	ϵ_P	0.5					
Bed porosity	ϵ_B	0.4					
Axial dispersion coefficient $\times 10^3(cm/s)$	$D_{ax,i}$	1.48					
Components	i	1	2	3	4	5	6
Effective diffusivity coefficient $\times 10^7$ $(cm^2/s))$	$D_{e,i}$	7.64	1.08	2.04	1.27	2.43	1.78
Mass transfer resistance coefficient $\times 10^3$ (cm^2/s)	$K_{pm,i}$	1.43	1.63	2.18	1.75	2.38	1.04

Table 3.8: Distinct model parameters determined for Case Study 1

individual elution profile of Component 6, where the start of elution is predicted to be after the actual elution process.

Table 3.9 shows the original GR model parameters (right column) used to generate the experimental data, and the GR model parameters estimated using only the data for Component 6 and the total protein *i.e.* Figures3.5(a) and 3.5(b). Different initial values for the estimated parameters were used in the estimation. Similar estimates to the original parameters are obtained for Component 6, and these were found to be statistically significant for a 95% confidence level (see Appendix D).

Table 3.10 shows the parameters of ED estimated, which are quite different from those estimated in Table 3.9 due to the different nature of the two models. However, Figure 3.8 show a relatively good fit, and the estimated parameters are deemed 95% accurate (see Appendix D).

The parameter estimations for the ED model and the GR model take 1226 and 6827 CPU seconds respectively, showing that the ED model is still useful for general

Parameter	Parameter estimation				Data generation
	Initial value	Lower bound	Upper bound	Estimation	GR Model
$K1_1$	90	65	250	87.2	100
$K1_2$	90	80	250	109	100
$K1_3$	90	80	250	104	100
$K1_4$	90	80	250	125	100
$K1_5$	90	80	250	90	100
$K1_6$*	**90**	**80**	**250**	**100**	**100**
$K2_1$	0.1	0.05	1	0.14	0.1
$K2_2$	0.1	0.05	1	0.26	0.3
$K2_3$	2	0.1	5	2.45	2.5
$K2_4$	2	0.1	30	6.45	8
$K2_5$	2	0.1	30	10.1	10
$K2_6$*	**2**	**0.05**	**30**	**22.0**	**22**

Table 3.9: Comparison of GR model parameters and estimations for isotherm parameters for Case Study 1

* Experimental data supplied

Parameter	Parameter estimation			
	Initial value	Lower bound	Upper bound	Estimation
$K1_1$	100	50	550	75
$K1_2$	100	50	550	103
$K1_3$	100	50	550	136
$K1_4$	100	50	550	550**
$K1_5$	100	50	550	125.68
$K1_6$*	**100**	**50**	**550**	**199.3**
$K2_1$	0.1	0.01	5	2.09
$K2_2$	2	0.01	5	1.82
$K2_3$	2	0.01	15	6.75
$K2_4$	2	0.01	15	6.82
$K2_5$	2	0.01	30	19.62
$K2_6$*	**5**	**0.01**	**50**	**40.54**

Table 3.10: Comparison of ED model parameters and estimations for isotherm parameters for Case Study 1

* Experimental data supplied, **estimate on bound

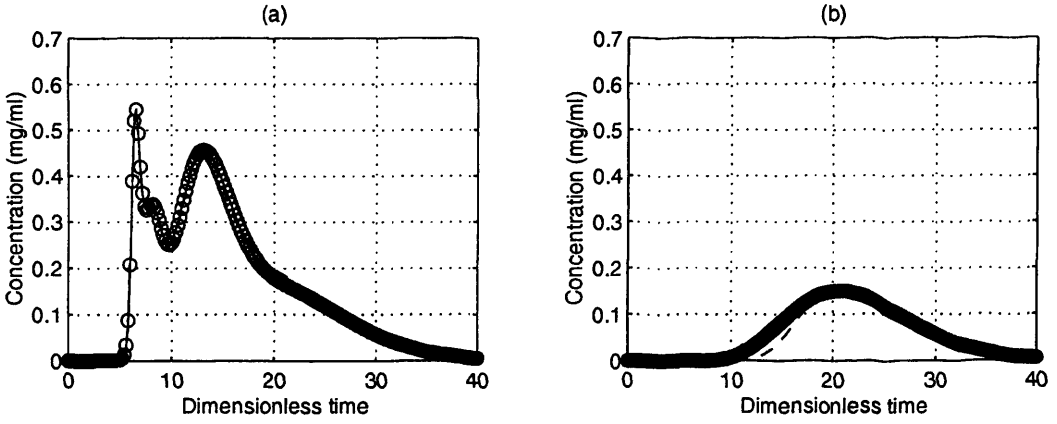

Figure 3.8: Comparison of the parameter estimation and experimental results in Case Study 1
(a) Total component chromatogram, (b) Component 6 chromatogram 'o': Experimental data (GR model), '- - -': ED model, '—': GR model

predictive purposes, as it has a faster computational time.

Distinct model parameter estimation

In some cases, the isotherm parameters have been determined during the course of the experiment and can be employed in the model. The user may then choose to estimate the distinct model parameters for the ED and GR model instead.

This will be demonstrated for this case study to demonstrate that the parameter estimation technique can be employed for any uncertain parameters the user decides on. Table 3.11 shows the parameter estimations carried out for the diffusivity coefficients for component i, $D_{e,i}$, in the GR model, whilst Table 3.12 shows the parameter estimation for the theoretical number of plates, N_P, in the ED model.

The results from these estimations (particularly those in bold) show that the models are capable also of estimating these uncertain band-broadening coefficients in the model and that the estimated values are very close to those actually used in the original model. Some of the parameters in Table 3.11 do not predict the similar values as those in the GR model but are very close. However, as the original data only contains information on the total components and component 6, such values

Parameter	Parameter estimation (10^{-7})				Data generation
	Initial value	Lower bound	Upper bound	Estimation	GR Model
$D_{e,1}$	0.2	0.1	10	0.97	0.72
$D_{e,2}$	1.0	0.1	10	0.78	1.05
$D_{e,3}$	2.0	0.1	10	1.92	2.02
$D_{e,4}$	1.0	0.1	10	1.18	1.25
$D_{e,5}$	2.0	0.1	10	2.47	2.43
$D_{e,6}$*	**2.0**	**0.1**	**10**	**1.78**	**1.77**

Table 3.11: Comparison of model parameters and estimations for general rate model diffusivity coefficients for Case Study 1

* Experimental data supplied

Parameter	Parameter estimation				
	Initial value	Lower bound	Upper bound	Estimation	ED Model
N_P	10	5	100	12.04	12.05

Table 3.12: Comparison of model parameters and estimations for equilibrium-dispersive model plate number for Case Study 1

are relatively good estimates.

Summary

Case study 1 is a theoretical case study based on hydrophobic interaction chromatography. Data provided has been limited to the total concentration and that of one component so as to replicate experimental conditions in bioprocesses where only information is limited to the component of interest. The case study illustrates in detail the methodology outlined previously (Section 3.2) for model parameter estimation, and also validates the parameter estimation technique used.

3.3.2 Case Study 2

The second case study is the purification of a labile protein, alcohol dehydrogenase (ADH) from a yeast homogenate supernatant, using step gradient hydrophobic interaction chromatography, carried out by Khanom (2003). The column is of 12.5cm

Parameter	Symbol	Units	Value
Column length	L	cm	12.5
Column diameter	D_C	cm	1.6
Particle radius	R_P	μm	45
Volumetric flowrate	Q	ml/min	2.5
Load volume		ml	250 (10CV)
Total component concentration		mg/ml	10

Table 3.13: Dimensions of column in Case Study 2

length and 1.6cm diameter, operating at a flow-rate of 2.5ml/min. Other parameters of the experimental set-up are detailed in Table 3.13. In this case study only the experimental data of the ADH and total protein chromatograms are available.

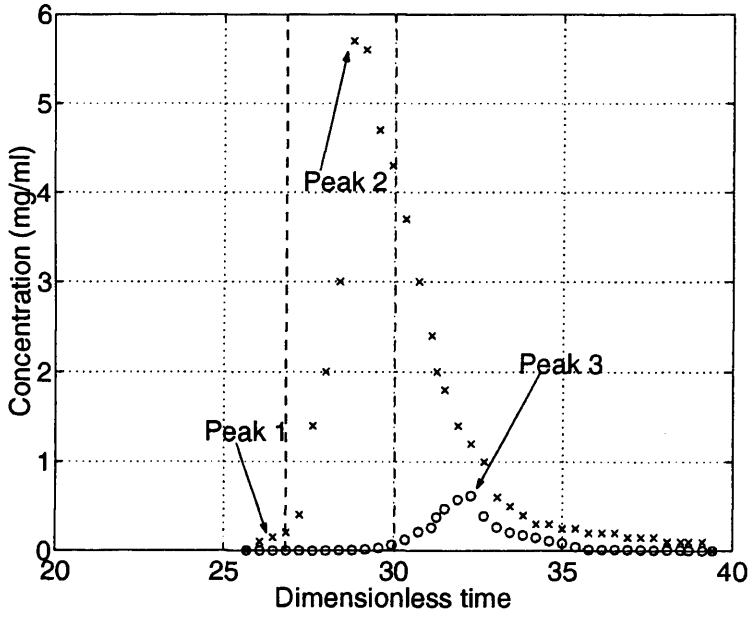

Figure 3.9: Experimental elution profiles for Case Study 2
('x': Total protein, 'o': ADH protein)

Determining feed concentration

The feed mixture loaded onto the column is yeast homogenate, and the only protein known to be present is ADH. This lack of information requires a close examination of the known make-up of yeast homogenate.

Step 1 The work of Gygi *et al.* (1999) provides an extensive list of genes of proteins found in yeast Saccharomyces cerevisiae. Using the figures from their paper, the total number of proteins, N_T is found to be 127. The number of peaks N_{NP} is identified as 3 (see Figure 3.9); one small peak in the front, a tall one the in the centre of the chromatogram and the third is mostly made up of ADH. R_C, the confidence ratio is defined as 2.

Step 2 Since it is not known which of the yeast proteins (ADH aside) will bind to the column, this is deduced from the charge on the protein, given by the GeneDB website (http://www.genedb.org/). The charge value (the charge sign may be disregarded) provides an indication of the hydrophobicity of the protein, and thus whether or not it binds to the column. ADH has a charge of 1, and charge values close to this value will bind to the column. Components with a charge greater than 4 are considered to be proteins which do not bind and are grouped to form N_R, which is 62.

Step 3 57 proteins are present in negligible amounts (N_S) based on the protein abundance per cell given by Gygi *et al.* (1999). Thus the components binding to the column,$N_C = N_T - N_R - N_S = 8$. These are listed in Table 3.15.

Step 4 3 pseudo-components are formed, each consisting of 2 components, to give the number of components used in the model, $N'_C = 5$.

Step 5 $\frac{N'_C}{N_{NP}} = \frac{5}{3}$ and the criteria $1 < \frac{N'_C}{N_{NP}} < R_C$, where R_C is 2, is fulfilled. 5 components are therefore to be modelled and the feed concentrations of these are determined from the chromatogram (Figure 3.9).

Step 6 The components (both pseudo-components and real) from Step 5 may now be regarded as the total number of components present in the separation for the purpose of modelling the process, N'_C.

Step 7 The concentrations are determined from the area under each peak using the trapezium rule, and shown in Table 3.14.

Step 8 No concentrations have been given in this case study and the make up of the yeast homogenate differs for every situation. In order to be proceed further,

Peak	Concentration (Peak area) mg/ml
1	0.03
2	0.6
3	0.06

Table 3.14: Area under each peak in Case Study 1

two assumptions are made, which are *only* applicable in this scenario as there are three peaks:

- The first assumption is that Peak 1 contains only 1 pseudo-component (Component number 1). The justification for this is that is that it contains the smallest area and that the protein abundance for Component number 1 is significantly lower than Component number 2
- The second assumption is that since Peak 3 is known to be Component number 5 (ADH), the remaining feed components make up Peak 2. Given that the individual concentrations of components are unknown for all components (aside from ADH), component numbers 2, 3 and 4 are equally divided to form the concentration of the second peak.

The chromatogram peaks are thus identified by the order of elution of the components and the proportion of components estimated to be present: The first peak contains component 1, the second peak is made up of components 2, 3 and 4, whilst component 5 (ADH) is the the third peak. The results are outlined in Table 3.15.

Component number	Feed concentration (mg/ml)	Gene name	Description	Charge value *	Protein abundance ** (10^3 copies/cell)
1	0.03	PYK1	Pyruvate kinase	4.5	225.3
		YLR109W	Alkyl hydroperoxide reductase	-4.5	94.4
2	0.2	ENO2	Enolase II	4	775
		PGK	Phosphoglycerate kinase	-4	338.9
3	0.2	PDC1	Pyruvate decaboxylase	-3	326
4	0.2	TDH2	Glyceraldehydes- 2 3-phosphate dehydrogenase 2	2	992.5
5	0.06	ADH1	Alcohol dehydrogenase	1	887.8
		PSA1	Mannose-1-phosphate guanyltransferase	-1	96.4

Table 3.15: Components deduced to be present in the chromatogram for Case Study 2
*Values taken from GeneED database, ** Values taken from Gygi *et al.* (1999)

Components	Molecular weight (Da)
1	55 000
2	69 000
3	61 000
4	35 800
5	36 800

Table 3.16: Molecular weight of the modelled components in Case Study 2

Parameter determination

The distinct parameters for both models in this case study were obtained using the correlations in Tables 3.1 and 3.2. The average molecular weights of the components (pseudo and real components) necessary for these calculations are tabulated in Table 3.16. The distinct parameters determined are shown in Table 3.17.

Parameter estimation results

The competitive Langmuir isotherm is used (Refer to Appendix B) in this case study and the estimation results for all parameters are shown in Tables 3.18. Figures 3.10(a) and 3.10(b) show the comparison of the models against the experimental chromatograms for ADH and total protein concentration. It shows similar observations to those in Case Study 1, with the ED model predicting the general trend well for the total protein concentration but showing a poorer fit for the ADH.

From the performance of the models, it is difficult to decide which model should be employed. Merely judging the "goodness-of-fit" of the models against the experimental chromatograms is subjective, especially if both models look very similar. A graphical representation of the chromatograms used by Ngiam (2002) was therefore employed to highlight differences between the models and the purity and recovery they predict.

The fractionation diagram (refer to Appendix F for further explanations of this diagram) of the ADH product against the total product for both models and the experimental data is seen in Figure 3.11(a). The figure shows the change in the

Equilibrium-dispersive model parameters						
Parameter	*Symbol*			*Value*		
Total porosity	ϵ_T			0.7		
Dead time (s)	t_0			243		
Plate number	N_P			108		
Apparent dispersion coefficient $\times 10^3$ (cm^2/s)	$D_{ap,i}$			3		
General rate model parameters						
Parameter	*Symbol*			*Value*		
Particle porosity	ϵ_P			0.5		
Bed porosity	ϵ_B			0.4		
Axial dispersion coeffcient $\times 10^3(cm/s)$	$D_{ax,i}$			0.925		
Components	i	1	2	3	4	5
Effective diffusivity coefficient $\times 10^7$ (cm^2/s)	$D_{e,i}$	1.00	2.01	0.92	1.32	1.30
Mass transfer resistance coefficient $\times 10^3$ (cm^2/s)	$K_{pm,i}$	1.02	1.32	1.00	1.12	1.12

Table 3.17: Distinct model parameters determined for Case Study 2

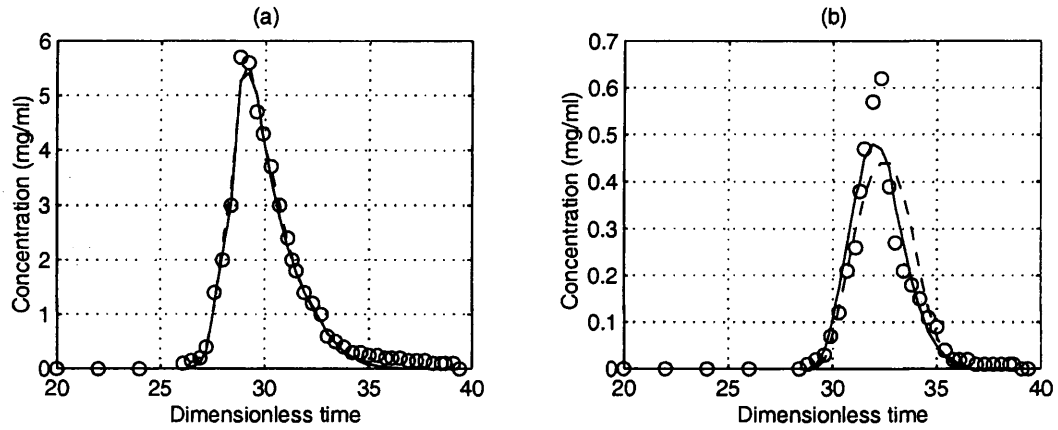

Figure 3.10: Comparison of predicted against experimental data for chromatograms in Case Study 2 (10CV load)
(a) Total protein chromatogram, (b) ADH chromatogram ('o': Experimental data, '- - -': ED model, '—' GR model)

ED	**Parameter estimation**			
Parameter	**Initial value**	**Lower bound**	**Upper bound**	**Estimation**
bl_1	5	2	50	47.9
bl_2	10	8	25	16.3
bl_3	10	8	30	16.8
bl_4	10	8	50	15.6
bl_5*	**30**	**15**	**50**	**19.3**
$b2_1$	0.5	0.3	10	0.88
$b2_2$	0.5	0.3	10	1.67
$b2_3$	0.5	0.3	10	0.98
$b2_4$	0.7	0.5	10	1.29
$b2_5$*	**1.6**	**1**	**10**	**2.27**
C^∞	8.8	4	8.8	8.46
GR	**Parameter estimation**			
Parameter	**Initial value**	**Lower bound**	**Upper bound**	**Estimation**
bl_1	45	10	100	19.58
bl_2	90	10	300	41.14
bl_3	155	20	300	280.31
bl_4	200	50	350	309.61
bl_5*	**200**	**10**	**350**	**14.61**
$b2_1$	0.071	0.03	0.2	0.042
$b2_2$	0.143	0.05	0.5	0.219
$b2_3$	0.2	0.05	0.5	0.418
$b2_4$	0.167	0.05	0.5	0.294
$b2_5$*	**0.556**	**0.2**	**1**	**0.741**
C^∞	8.8	4	8.8	7.79

Table 3.18: Values used in the parameter estimation for the equilibrium-dispersive and the general rate models in Case Study 2 (10CV load)

* Experimental data supplied

elution of product (ADH) against that of the total protein mixture eluted (Ngiam, 2002).

The maximum purification diagram (refer to Appendix F for further explanations of this diagram) seen in Figure 3.11(b) shows the trade-off between yield and purity of ADH. The GR model shows the yield/purity relationship more accurately than the ED model for the ADH protein. The area of interest in most bio-separations lies in the region where the yield fraction is $0.8 - 1$, for which both models show similar performance, but with the GR model giving a slightly better prediction. A visual judgement of Figure 3.9 shows very little difference in the chromatograms produced by the two models as they both capture the general shape of the experimental chromatogram. However, the maximum purification diagram shows that the GR model predicts the experimental data better. Thus, it may be concluded that in this case study, the GR model is a better choice for modelling the ADH chromatogram.

Validation of models

A form of validation was carried out for this case study, where the ED models developed based on 3 different data sets (of load samples 5CV, 10CV and 20CV) were used to predict the other data. It is evident from Figures 3.12 - 3.14, that the models using parameter estimations based on the same data set displays the best performance against the same data set, so the emphasis of this comparison is focussed on using one data set to predict the performance of another data set.

The prediction conducted using data set 3 (20CV) was found to be the poorest among the three. This can be seen visually from the chromatograms (Figures 3.12 - 3.14) and likewise demonstrated by the maximum purification diagrams (Figures 3.15 - 3.17). It displays particularly, poor performance when predicting the total protein concentrations, which had been a previous strength in the ED model developed from data set 2 shown in Figure 3.10(a). This in turn affects the maximum purification factor diagram generated. The differences between the predicted chromatograms are only worth highlighting using the maximum purification factor

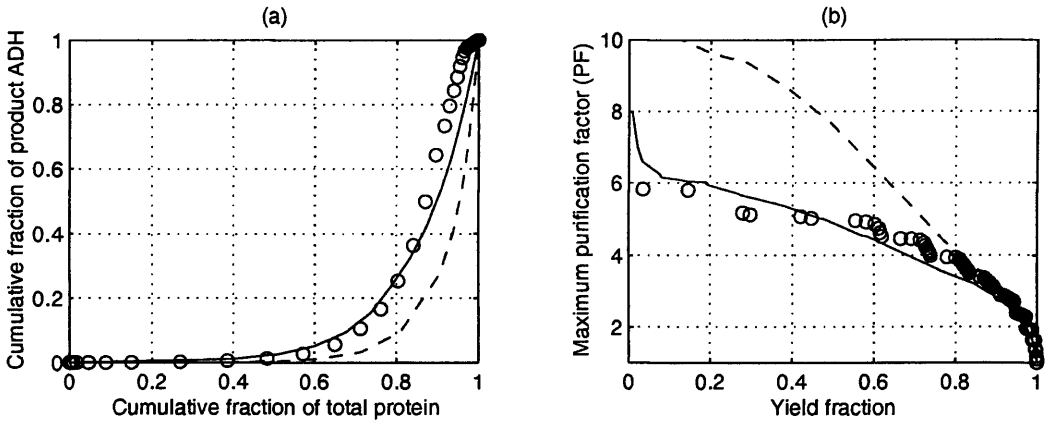

Figure 3.11: Purification diagram and maximum purification factor diagram for alcohol dehydrogenase against total protein in Case Study 2 (10CV load)
(a) Fractionation diagram, (b) Maximum purification diagram ('o': Experimental data, '- - -': ED model, '—' GR model)

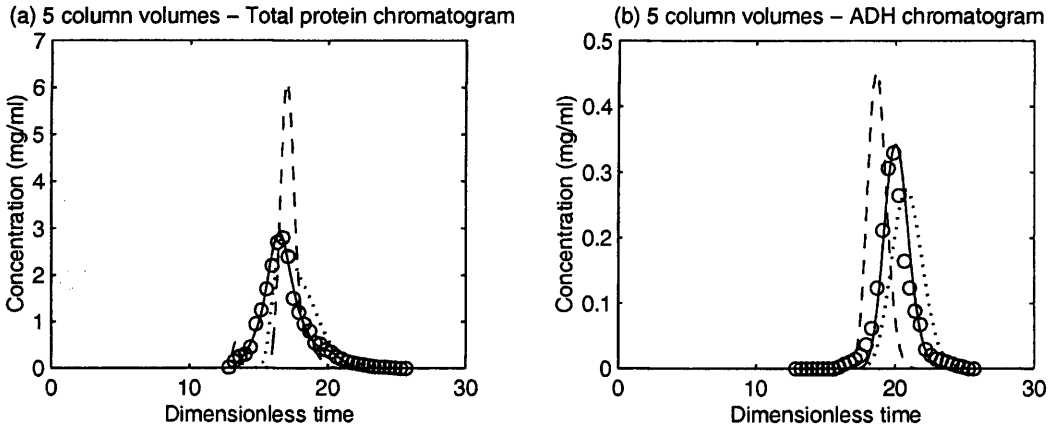

Figure 3.12: Comparison of predicted data and experimental data for chromatograms in Case Study 2, for data set 1 5CV load
('o': Experimental data, '—': Data 1, '· · ·': Data 2, '- - -': Data 3)

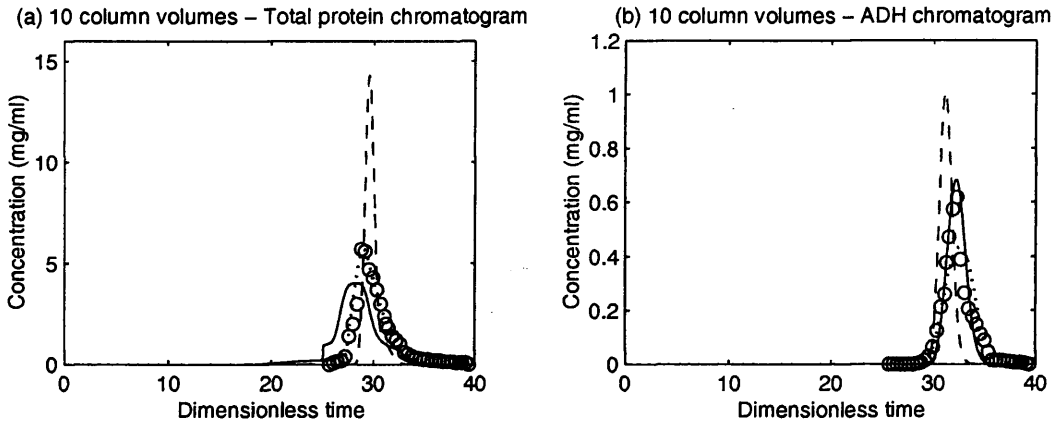

Figure 3.13: Comparison of predicted data and experimental data for chromatograms in Case Study 2, for data set 2 10CV load
('o': Experimental data, '—': Data 1, '· · ·': Data 2, '- - -': Data 3)

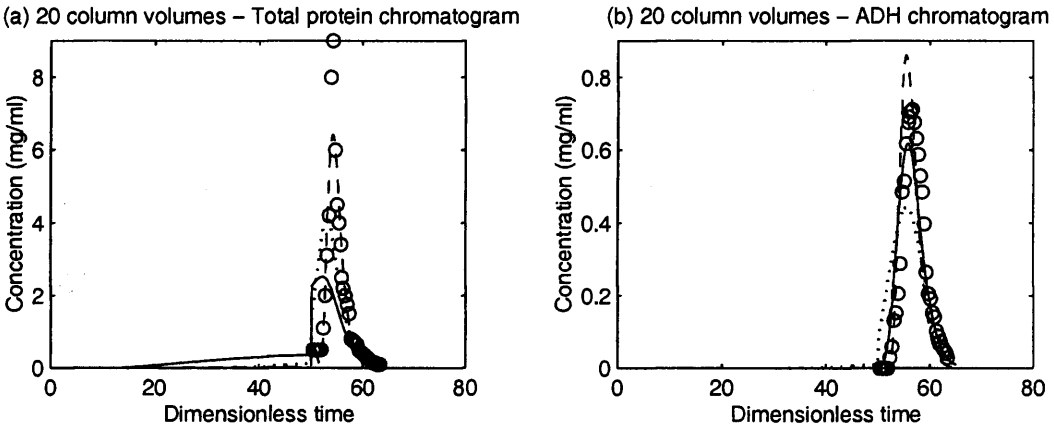

Figure 3.14: Comparison of predicted data and experimental data for chromatograms in Case Study 2, for data set 3 20CV load
('o': Experimental data, '—': Data 1, '· · ·': Data 2, '- - -': Data 3)

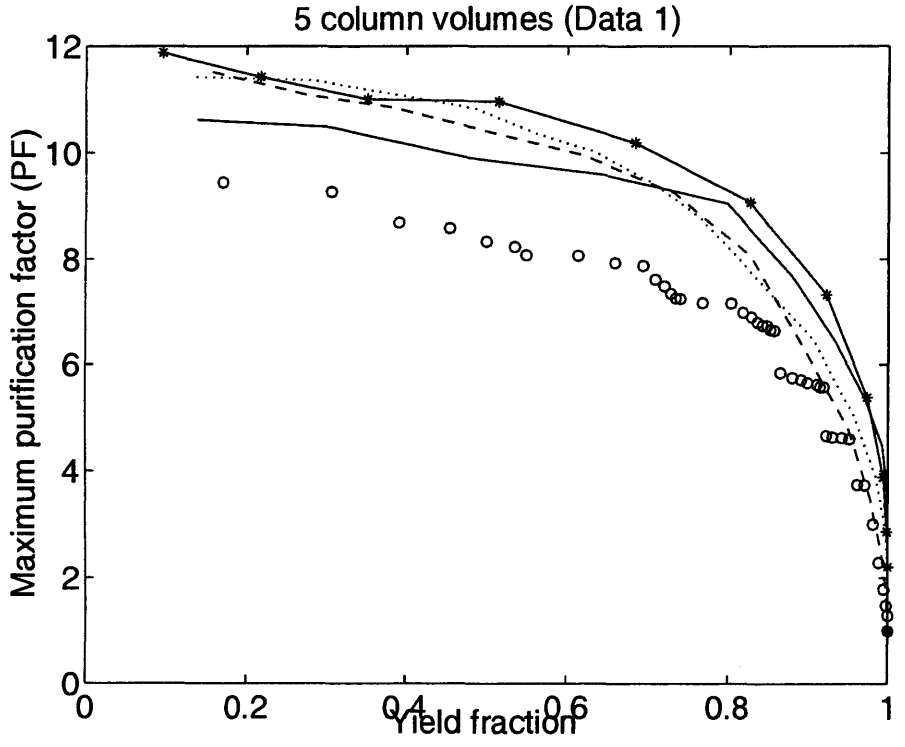

Figure 3.15: Maximum purification factor diagrams for Case Study 2 (5CV load) for all parameter estimations
('o': Experimental data, '—': Data set 1, '· · ·': Data set 2, - - -': Data set 3)

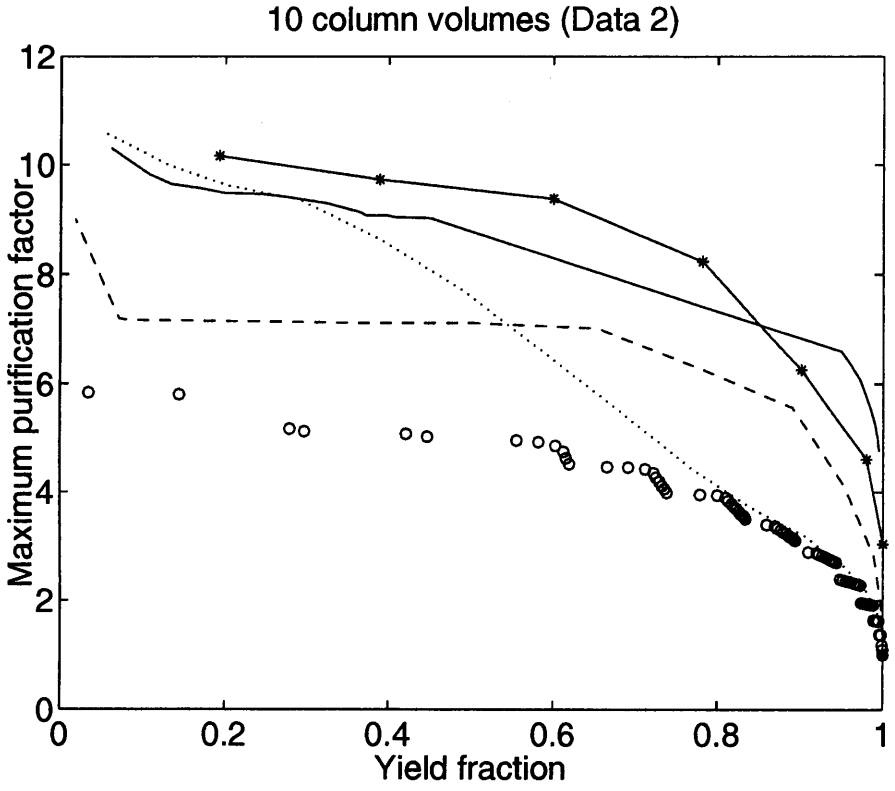

Figure 3.16: Maximum purification factor diagram for Case Study 2 (10CV load) for all parameter estimations

('o': Experimental data, '—': Data set 1, '· · ·': Data set 2, - - -': Data set 3)

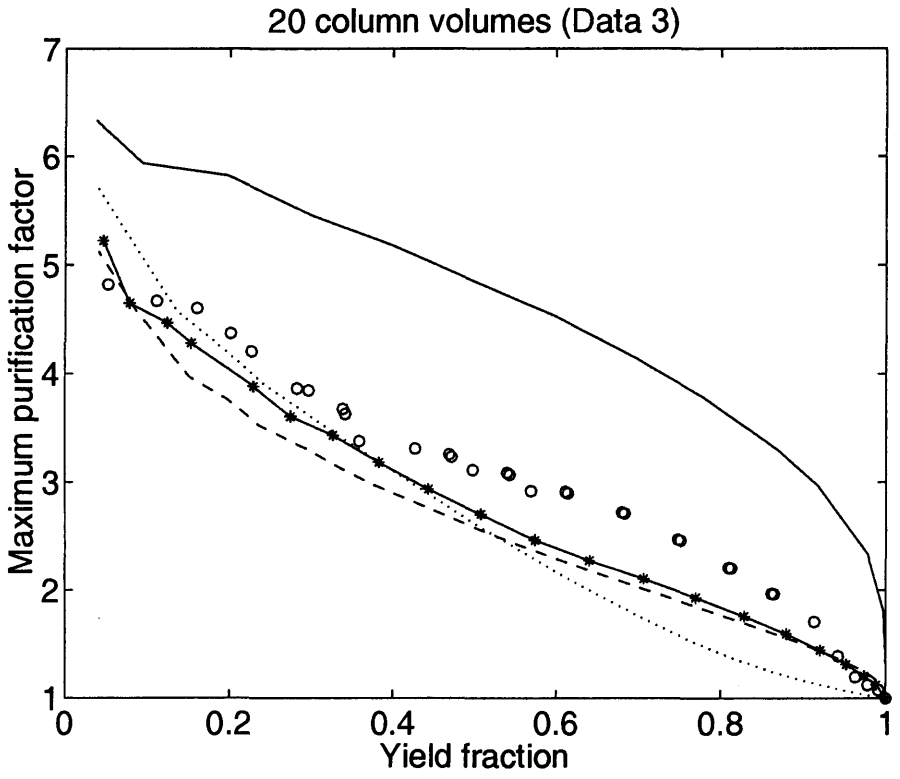

Figure 3.17: Maximum purification factor diagram for Case Study 2 (20CV load) for all parameter estimations

('o': Experimental data, '—': Data set 1, '· · ·': Data set 2, - - -': Data set3)

diagram when the total protein concentration predicted by the models are similar. Otherwise, the diagram is only showing the data of the predicted targeted protein relative to the predicted total protein, and has no comparative value.

Where possible, more data sets should be employed in the parameter estimation of the model to make the models more accurate. Given the vast differences in the amounts of sample loads used in this case study, it is unlikely that the isotherm parameters estimated in one set would be interchangeable with those of another data set. However, it is useful to determine which data set among the three would be more useful for modelling purposes. Among the three, the third data set involving 20CV sample load was found to be the poorest in terms of performance. 5CV and 10 CV show rather mixed results, looking at the maximum purification diagrams in Figures 3.15 - 3.16. Whilst data which falls in the middle range (*e.g.* 10CV for this case) is would generally assumed to be more applicable in developing a more general model, Figure 3.17 shows that Data set 2 predicts the 20CV load very poorly. It is thus recommended, that where possible, similar data sets should be used in the parameter estimation.

3.3.3 Case Study 3

Ion exchange chromatography (IEX) is one of the most powerful techniques for the purification of proteins in the biotechnology industry and is employed in the first steps of most large scale purification processes (Bonnerjea *et al.* 1986). Thus, the final case study examines gradient elution ion-exchange chromatography for a mixture of hen egg white proteins and whale myoglobin from the work of Edwards-Parton (2004). The ion exchanger is a 1ml SP Sepharose Fast Flow HiTrap column of 2.5cm length and 0.7cm internal column diameter. The buffer used was 20mM sodium phosphate, and the egg white protein was mixed in a ratio of 1:4 with the buffer and centrifuged to remove precipitate and solids. 0.5g/ml of myoglobin was then added to the mixture. The elution buffer used was a mixture of 20mM sodium phosphate and 2M sodium chloride, both of pH 5.5, and the amount of sodium

chloride is increased gradually to a maximum amount of 50% of the buffer by the end of elution. The absorption data was measured at 280 and 408nm (the egg white proteins absorbed at 280nm while the myoglobin absorbed at 480 nm).

Modification of isotherm model

In this third case study, the mode of operation is using *gradient elution*, where the concentration of a *moderator*, in this case sodium chloride (NaCl), in the buffer (mobile phase) is increased at a linear rate to facilitate the elution of the proteins. The ongoing change in the concentration in the mobile phase however, means that the isotherm model is changing constantly in the chromatographic operation. The multicomponent Langmuir isotherm model (see Appendix B.4) is given by:

$$q_i = \frac{a_i C_i^m}{1 + \sum_{j=1}^{N} b_j C_i^m} \quad \text{Equilibrium} - \text{dispersive model} \tag{3.2}$$

$$C_i^{ps} = \frac{a_i C_i^p}{1 + \sum_{j=1}^{N} b_j C_i^p} \quad \text{General rate model} \tag{3.3}$$

According to Gu and Zheng (1999), for gradient elution, the relationship between the components and the moderator is written as:

$$\log_{10} b_i = \alpha_i - \beta_i \log_{10} C_{NaCl} + \gamma_i C_{mod} \tag{3.4}$$

where α, β and γ are experimental correlation parameters for the component-moderator relationship and C_{mod} is the moderator (sodium chloride) concentration. The retention factor k (refer to Appendix A) is related to the b isotherm coefficient by the following equation (Gu and Zheng, 1999):

$$k_i = FC^{\infty} b_i \tag{3.5}$$

where F is the phase ratio ($F = \frac{(1-\epsilon_B)(1-\epsilon_P)}{[\epsilon_B + (1-\epsilon_B)\epsilon_P]}$) and C^{infty} is the adsorption saturation capacity. This can be used to rewrite Equation 3.4 in the form:

chloride is increased gradually to a maximum amount of 50% of the buffer by the end of elution. The absorption data was measured at 280 and 408nm (the egg white proteins absorbed at 280nm while the myoglobin absorbed at 480 nm).

Modification of isotherm model

In this third case study, the mode of operation is using *gradient elution*, where the concentration of a *moderator*, in this case sodium chloride (NaCl), in the buffer (mobile phase) is increased at a linear rate to facilitate the elution of the proteins. The ongoing change in the concentration in the mobile phase however, means that the isotherm model is changing constantly in the chromatographic operation. The multicomponent Langmuir isotherm model (see Appendix B.4) is given by:

$$q_i = \frac{a_i C_i^m}{1 + \sum_{j=1}^{N} b_j C_i^m} \quad \text{Equilibrium} - \text{dispersive model} \tag{3.2}$$

$$C_i^{ps} = \frac{a_i C_i^p}{1 + \sum_{j=1}^{N} b_j C_i^p} \quad \text{General rate model} \tag{3.3}$$

According to Gu and Zheng (1999), for gradient elution, the relationship between the components and the moderator is written as:

$$\log_{10} b_i = \alpha_i - \beta_i \log_{10} C_{NaCl} + \gamma_i C_{mod} \tag{3.4}$$

where α, β and γ are experimental correlation parameters for the component-moderator relationship and C_{mod} is the moderator (sodium chloride) concentration. The retention factor k (refer to Appendix A) is related to the b isotherm coefficient by the following equation (Gu and Zheng, 1999):

$$k_i = FC^{\infty} b_i \tag{3.5}$$

where F is the phase ratio ($F = \frac{(1-\epsilon_B)(1-\epsilon_P)}{[\epsilon_B + (1-\epsilon_B)\epsilon_P]}$) and C^{infty} is the adsorption saturation capacity. This can be used to rewrite Equation 3.4 in the form:

chloride is increased gradually to a maximum amount of 50% of the buffer by the end of elution. The absorption data was measured at 280 and 408nm (the egg white proteins absorbed at 280nm while the myoglobin absorbed at 480 nm).

Modification of isotherm model

In this third case study, the mode of operation is using *gradient elution*, where the concentration of a *moderator*, in this case sodium chloride (NaCl), in the buffer (mobile phase) is increased at a linear rate to facilitate the elution of the proteins. The ongoing change in the concentration in the mobile phase however, means that the isotherm model is changing constantly in the chromatographic operation. The multicomponent Langmuir isotherm model (see Appendix B.4) is given by:

$$q_i = \frac{a_i C_i^m}{1 + \sum_{j=1}^{N} b_j C_i^m} \quad \text{Equilibrium} - \text{dispersive model} \tag{3.2}$$

$$C_i^{ps} = \frac{a_i C_i^p}{1 + \sum_{j=1}^{N} b_j C_i^p} \quad \text{General rate model} \tag{3.3}$$

According to Gu and Zheng (1999), for gradient elution, the relationship between the components and the moderator is written as:

$$\log_{10} b_i = \alpha_i - \beta_i \log_{10} C_{NaCl} + \gamma_i C_{mod} \tag{3.4}$$

where α, β and γ are experimental correlation parameters for the component-moderator relationship and C_{mod} is the moderator (sodium chloride) concentration. The retention factor k (refer to Appendix A) is related to the b isotherm coefficient by the following equation (Gu and Zheng, 1999):

$$k_i = FC^{\infty} b_i \tag{3.5}$$

where F is the phase ratio ($F = \frac{(1-\epsilon_B)(1-\epsilon_P)}{[\epsilon_B + (1-\epsilon_B)\epsilon_P]}$) and C^{infty} is the adsorption saturation capacity. This can be used to rewrite Equation 3.4 in the form:

$$\log_{10} k_i = \alpha_i' - \beta_i \log_{10} C_{NaCl} + \gamma_i C_{mod} \tag{3.6}$$

where $\alpha_i' = \alpha + \log_{10} FC^{\infty}$. In the work of Gu and Zheng (1999), the term β was taken to be 0, which is also used here and Equation 3.6 is rewritten as:

$$\log_{10} b_i = \alpha_i' - \log_{10} FC^{\infty} + \gamma_i C_{mod} \tag{3.7}$$

Gu and Zheng (1999) state that C_{NaCl} can have other units aside from $molL^{-1}$, though other binding components must have units of $molL^{-1}$ to be consistent with C^{∞}. In this work, the volume fraction is adopted from the work of Gu and Zheng (1999) for C_m, and in this work the mass fraction of NaCl is used. Equation 3.7 is expressed as:

$$\log_{10} b_i = \alpha_i' - \log_{10} FC^{\infty} + \gamma_i \frac{C_{NaCl}}{C_{NaCl,Total}} \tag{3.8}$$

where C_{NaCl} is the mass concentration NaCl in the buffer and $C_{NaCl,Total}$ is the molecular mass of NaCl used (for 2M NaCl, the molecular mass is 116.88).

Determining feed concentration

From Figure 3.18, the number of peaks N_{NP} is identified as 4; three of the peaks being egg white proteins, whilst the fourth peak is the myoglobin. The feed mixture loaded onto the column is a mixture of diluted egg white proteins and myoglobin. Egg whites contains as many as 15 egg white proteins (Awadé and Efstathiou, 1999) (thus $N_T = 16$, including the myoglobin), of which one protein is determined to be non-binding to the column. This is deduced from the isoelectric points, or pI values, of the egg white proteins as given by Awadé and Efstathiou (1999). The pI value provides an indication as to the charge present on the protein, and thus how strongly the protein binds to the column. Of the remaining 15 proteins, 10 are present in negligible amounts. Thus the components binding to the column, $N_C = 5$. 1 pseudo-component is formed (ovalbumin and ovomuscoid are lumped as one pseudo-

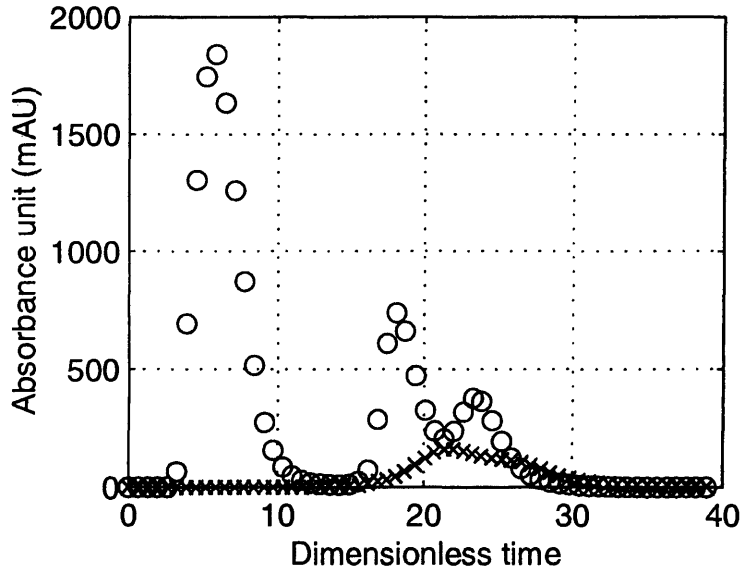

Figure 3.18: Experimental elution profiles for Case Study 3
('—': Egg white proteins, 'x': Myoglobin)

component as they have similar pI values) to give the number of components used in the model, $N'_C = 4$. $\frac{N'_C}{N_{NP}} = \frac{4}{4}$ and the criteria $1 \leq \frac{N'_C}{N_{NP}} < R_C$, where R_C is 2, is fulfilled. 4 components are to be modelled and the feed concentrations of these are determined from the chromatogram using the procedure outlined earlier and the feed concentrations determined are shown in Table 3.19 (where component values are taken from Awadé and Efstathiou (1999) and Fasman (1992)).

Component number	Feed concentration (mg/ml)	Protein	pI value	Amount of total egg white protein (%)	Average molecular weight (M_R)	Extinction coefficient (ϵ)
		Ovalbumin	4.5	54		
1	0.03	Ovomuscoid	4.1	11	40 000	32 180
2	0.2	Ovotransferrin	6.0	12-13	77 000	85 000
3	0.2	Lysozyme	10.7	3.4-3.5	14 300	36 000
4	0.2	Myoglobin	7	-	16 000	160 000

Table 3.19: Feed concentration as calculated from the chromatogram for Case Study 3
pI values and protein amounts taken from Awadé and Efstathiou (1999), M_R and ϵ values from Fasman (1992)

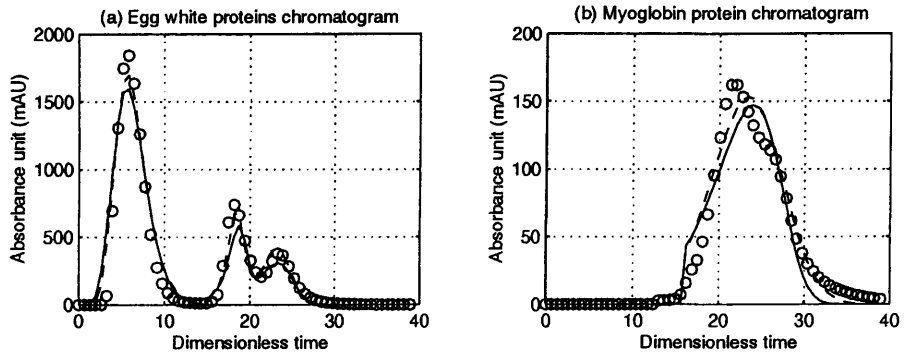

Figure 3.19: Comparison of predicted data against experimental data for chromatograms in Case Study 3
('o': Experimental data, '- - -': ED model, '—' GR model)

Parameter determination

The parameters for both models can be determined using literature correlations, which are summarised in Table 3.20.

Parameter estimation results

Earlier, the modification of the Langmuir isotherm model was discussed. The isotherm parameters estimated in this case study are thus α_i' and γ_i.

Figures 3.19(a) and 3.19(b) compare the models against the experimental data for the egg white proteins and the myoglobin, respectively. The fractionation and maximum purification diagrams are seen in Figures 3.20 and 3.21, respectively, with myoglobin as the target product. It has been difficult to estimate the parameters for the GR model, with some of the distinct parameters being modified from those found using the correlations in Table 3.2 to fit the experimental data better. This explains the poor fitting for the GR model (Figures 3.19(a) and 3.19(b)). With a gradient elution, the isotherm parameters change dynamically during the process, compounding the difficulty of the parameter estimation.

However, even though the fitting on the chromatogram appears to be poor, the fractionation diagrams and maximum purification factor diagrams in Figures

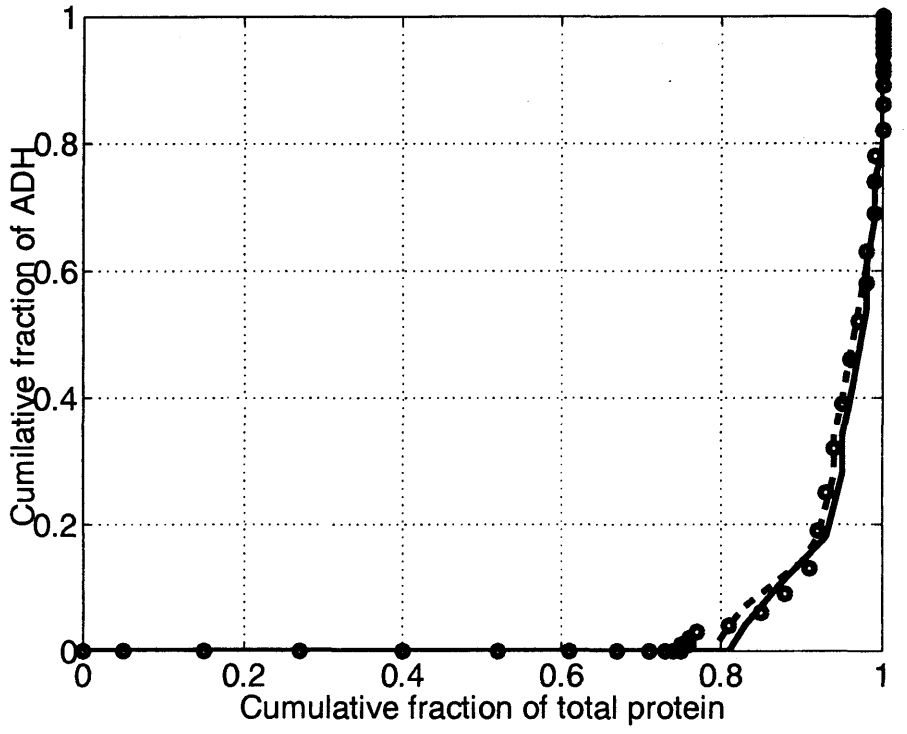

Figure 3.20: Fractionation diagram of myoglobin against total protein for Case Study 3

('o': Experimental data, '- - -': ED model, '—' GR model)

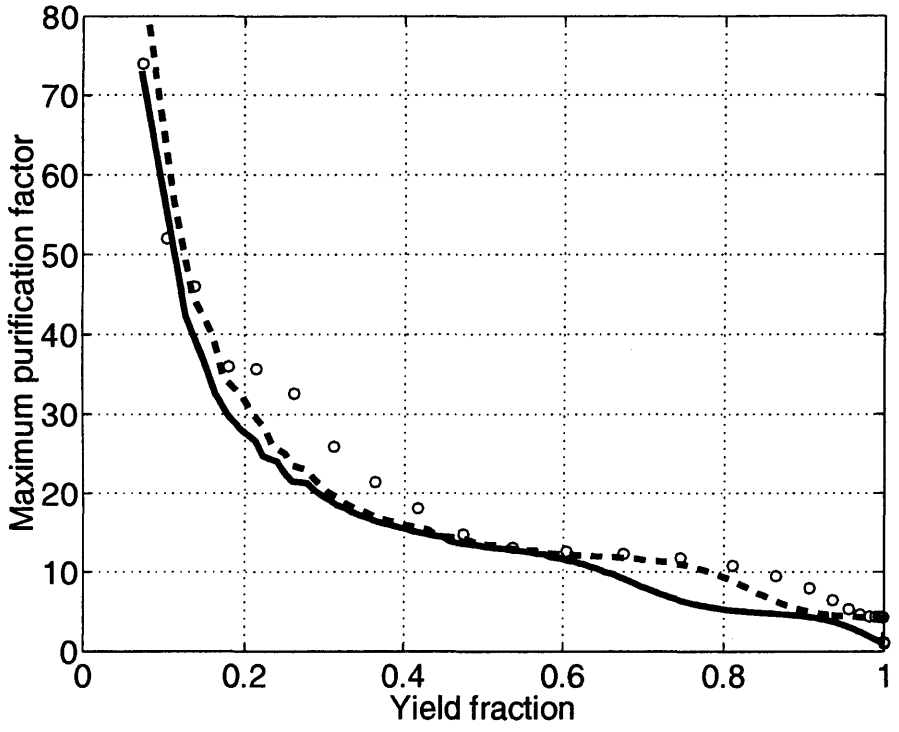

Figure 3.21: Maximum purification factor diagram for Case Study 3
('o': Experimental data, '- - -': ED model, '—' GR model)

Equilibrium-dispersive model parameters					
Parameter	*Symbol*	*Value*			
Total porosity	ϵ_T	0.7			
Dead time (s)	t_0	15.43			
Plate number	N_P	7			
Apparent dispersion coefficient $\times 10^3$ (cm^2/s)	$D_{ap,i}$	28.5			
General rate model parameters					
Parameter	*Symbol*	*Value*			
Particle porosity	ϵ_P	0.5			
Bed porosity	ϵ_B	0.4			
Axial dispersion coeffcient $\times 10^3 (cm/s)$	$D_{ax,i}$	2.86			
Components	i	1	2	3	4
Effective diffusivity coefficient $\times 10^7$ (cm^2/s)	$D_{e,i}$	2.62	1.83	4.26	4.05
Mass transfer resistance coefficient $\times 10^3$ (cm^2/s)	$K_{pm,i}$	2.19	1.89	2.75	2.68

Table 3.20: Distinct model parameters determined for Case Study 3

3.20 and 3.21, respectively, demonstrate that the performance of both models in predicting the process behaviour is reasonable for higher yields.

Often, when IEX is used in the first few processing stops, it is important that the yield is high (even if not necessarily very pure) in order that valuable product is not lost, and thus the region of interest in the maximum purification diagram for bio-separations is usually a yield fraction of $0.8 - 1$. From Figure 3.21, it is clear that both models behave similarly in this yield fraction region.

From the results, it is noted that the ED model is capable of predicting the process behaviour well for this case study. Given similar predictions for ED and GR models, the ED model is preferable as it is less complex and computationally inexpensive.

Suggestions for improving the fit of the models would be to find a more suitable isotherm, as the choice of isotherm employed in this case study is the Langmuir isotherm.

ED	**Parameter estimation**			
Parameter	**Initial value**	**Lower bound**	**Upper bound**	**Estimation**
α_1'	-0.6	-2	0.5	-0.7
α_2'	0.15	-1	0.5	0.089
α_3'	0.6	0.01	1.5	0.271
α_4	0.2	0.01	0.5	0.158
γ_1	-10	-10	-6.5	-6.5
γ_2	-10	-10	-8	-10
γ_3	-4	-8	-1	-3.67
γ_4	-2	-3	-1	-1.95
C^∞	40	20	70	46.08
GR	**Parameter estimation**			
Parameter	**Initial value**	**Lower bound**	**Upper bound**	**Estimation**
α_1'	-1.6	-2	1	-0.993
α_2'	-0.4	-0.4	-0.6	-0.191
α_3'	0.6	0.6	-0.6	0.104
α_4	0.00591	0.006	-0.1	-0.00106
γ_1	-10	-10	-6.5	-8.96
γ_2	-10	-10	-8	-12
γ_3	-6.5	-6.5	-1	-5.37
γ_4	-3.8	-3.8	-1	-3.52
C^∞	40	25	70	42.41

Table 3.21: Values used in the parameter estimation for the equilibrium-dispersive and the general rate models in Case Study 2 (10CV load)

3.4 Conclusions

This chapter has outlined an approach to modelling the process complexities of complex chromatographic separations based on a combination of experimental data, literature correlations and parameter estimation. The approach allows the user to estimate model parameters for candidate models and subsequently to select the best model for the process based on a given experimental set. The approach was then applied to three case studies of increasing complexity in terms of experimental information and process dynamics. The approach was demonstrated to be successful in determining the model parameters and model selection for the process in all cases. The general rate model is shown to perform better, but the difficulty in obtaining its model parameters means that with similar model behaviour, the equilibrium-dispersive model is preferable. The results from the equilibrium-dispersive model have shown that the model is able to predict complex separations, to a certain degree of accuracy, in particular it predicts well the total component concentration.

Chapter 4

Modelling and optimisation of SMB chromatography

The previous three chapters have focused on single column chromatography. Whilst the single column is still popular in both preparative and industrial work, its inefficient usage of the stationary phase and high solvent cost means that other processes, in particular the multi-column chromatographic alternatives such as simulated moving bed (SMB) and Varicol processes are increasingly favoured. In this chapter, the development of a dynamic model for the simulated moving bed (SMB) chromatographic process is outlined, followed by that of two cyclic steady state (CSS) models. Work demonstrating the performance of the CSS models relative to the dynamic SMB model is also presented. Finally, the operating parameters of the SMB process is dynamically optimised, with an increasing number of degrees of freedom, to demonstrate the use of the model in detailed optimisation.

4.1 Introduction

Traditionally, the single chromatographic column is deemed sufficient for most of the purposes of preparative and industrial chromatography. However, with an increase in demand for high purify products in industrial sectors such as the pharmaceutical industry, multi-column chromatographic processes, in particular, the simulated moving bed (SMB) technique are becomingly more popular, with advantages such as its low eluent consumption and high efficiency of adsorbent usage.

In the literature review in Chapter 2, it was shown that the level of detail in modelling the SMB process has undergone many changes. Previously, the mathematical modelling of the SMB process was simplified by treating the process as an equivalent true-moving system (TMB) where the solid and fluid velocities are involved and the boundary conditions of the chromatography columns are independent of time. With the advances of computational power and understanding of the complexity of the process, the *dynamics* of the SMB system can now also be considered in the mathematical model. This includes process complexities such as the various sections with a number of chromatography columns in each, and whose boundary conditions change with time (Hassan *et al.*, 1995).

The SMB system is essentially a cyclic operation, and requires a number of cycles before *cyclic steady state conditions* are achieved in the system. As SMB is also a continuous operation, the determination of the cyclic steady state (CSS) conditions are crucial in assessing the SMB performance. These conditions can be obtained by running the dynamic model until steady state, which can take up to 15-20 cycles. However, if the model is used in optimisation, a large number of runs becomes necessary and the use of a dynamic model is very inefficient. Thus, in this work, a cyclic steady state (CSS) model for the SMB process is employed, originally proposed by Minceva *et al.* (2003), where the steady state conditions are determined directly.

The work of Minceva *et al.* (2003) is extended in this chapter to consider the

optimisation of the CSS operation of SMB, which hitherto has not been done in the literature. The effect of the decision variables on the SMB performance at CSS conditions are also demonstrated in some simulation studies. Finally, an optimisation of the production rate of the extract is detailed. It is found that the CSS mode used in this work can accurately predict the cyclic steady state conditions found by the dynamic model.

4.2 Concept of the simulated moving bed (SMB) process

In chromatography, the concept of a true moving bed (TMB) involves moving the stationary phase in countercurrent direction to the mobile phase in order to increase the interaction between the two phases, and thereby increase the rate of separation between the components in the mixture fed to the system. However, with a TMB, the mechanical complexities of moving the stationary phase deem it economically unfavourable. In its place, a *simulated* moving bed (SMB) process, in which the inlet and outlet lines are switched in such a manner as to simulate, or imitate, the action of an TMB, is used.

Figure 4.1 illustrates the concept of SMB. The unit can be divided into four sections, normally with an equal number of columns in each. The number of columns in each section can be varied but for simplicity, the number of columns is often kept equal.

The operation of the SMB unit can be described as follows:

Feed The feed is a mixture of A and B, where A has a stronger affinity for the adsorbent. Feed enters section III where the less retained component B elutes faster than A towards section III and IV. At an appropriate switching time, the feed is switched one column downstream in the direction of the flow of the fluid. As such, the more retained component A has a higher concentration in Section I and II.

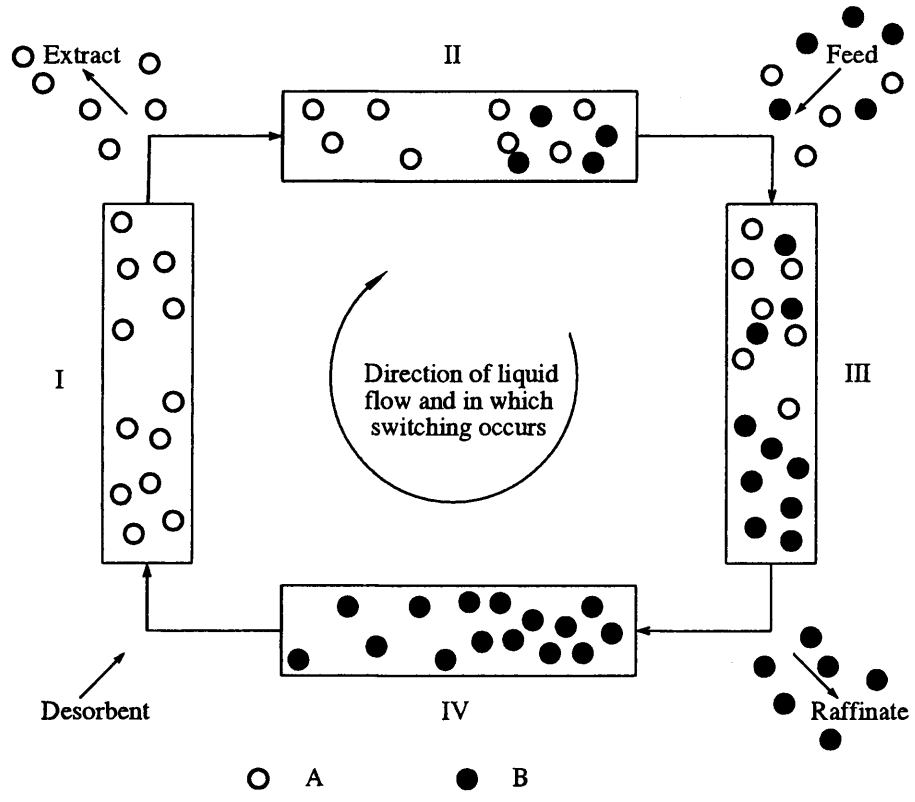

Figure 4.1: Illustration of the SMB principle, with equal number of columns in each section

Desorbent Desorbent entering Section I desorbs the more retained component A, which then elutes towards the extract port, whilst B is desorbed in Section II and III. Component B is adsorbed in Section IV to regenerate the desorbent.

Raffinate The raffinate port is located after the feed port at the end of Section III, where the less retained component B is desorbed and eluted first and leaves the SMB system through this port.

Extract The extract port is located at the end of Section I where the more retained component A is desorbed by the desorbent at the beginning of this section and A thus leaves the SMB system through this port.

4.3 Modelling of SMB Systems

4.3.1 TMB or SMB?

The mathematical modelling of the SMB system has been handled by two main approaches in the literature: (1) as an equivalent true-moving bed (TMB) system, where solid and fluid velocities are involved and the boundary conditions of the chromatography columns are independent of time and (2) as a countercurrent simulated moving bed (SMB) system where there are various sections with a number of columns in each, and whose boundary conditions change with time (Hassan *et al.*, 1995).

The TMB equivalent model of the SMB process is less complex to solve and thus requires less computational time compared to the dynamic SMB model. However, given its failure to consider the process complexities in the SMB process, the TMB equivalent model is only suitable as an estimate of the operating parameters (Jupke *et al.*, 2002). Thus, in the following only a detailed SMB model will be considered in order to carry out an accurate modelling of the process.

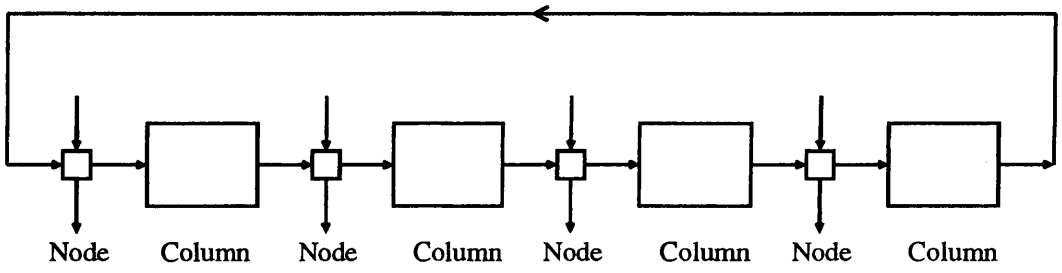

Figure 4.2: Illustration of the SMB model, where inlet and outlet lines can be switched by changing the values of the external streams at the nodes

4.3.2 Dynamic or Steady-state?

Having decided on the use of an SMB model, the next decision to consider is the *type* of SMB model to employ. The literature review in Chapter 2 has shown that two kinds of SMB model have emerged in recent years: (1) a dynamic SMB model obtained by connecting the dynamic chromatographic column models with cyclic port switching (*e.g.* Dünnebier *et al.* (1998)) and (2) a cyclic steady-state model as developed by Minceva *et al.* (2003) which predicts the performance of the model *only* at steady-state conditions. The latter model came about as a result the SMB process requiring a certain number of cycles before steady-state conditions are achieved.

The literature review in Chapter 2 may be referred to for more details on the works of dynamic modelling of SMB chromatographic systems, *e.g.* Dünnebier *et al.* (1998), Strube and Schmidt-Traub (1998), Strube *et al.* (1997) *etc.*. The dynamic model of an SMB system can be obtained by connecting the dynamic chromatographic column models of single columns with models of cyclic port switching (Dünnebier *et al.* (1998).

4.3.3 Details of the SMB Model

The simulated moving bed unit can be modelled dynamically by connecting the dynamic models of single chromatographic columns into sections, with a node model, which will consider cyclic valve switching for the inlet (feed, desorbent) or outlet streams (extract, raffinate) between each, as illustrated in Figure 4.2.

Due to the complexity of the system, assumptions have been made to simplify the model and thus make calculations easier:

- No backmixing at the nodes
- No dead-volumes in pipes, columns and connections
- Isothermal operation
- Isocratic elution
- No concentration gradient in the radial direction
- No local equilibrium between the macropore and stagnant liquid phase within
- Dispersion described by a lumped axial dispersion coefficient

Further improvements to the model can also be made if necessary to take these factors into account if the assumptions are invalid due to changes in operating conditions. Assumptions are also made for the mass balances in the column model chosen and more details about these assumptions, including their justification, can be found in Guiochon *et al.* (1994).

The Chromatography Column Model

In this work, each of the chromatographic columns are modelled based on a dispersed plug flow (DPF) model, assuming a plug flow of the solid and axially dispersed plug flow of the fluid. This is essentially a simplified general rate model, neglecting the mass transfer resistance (refer to Appendix B). The basic differential equation of the fluid mass balance including mass transfer resistance is:

$$\frac{\partial C_i(z,t))}{\partial t} = D_{ax}(t)\frac{\partial^2 C_i(z,t)}{\partial z^2} - v(t)\frac{\partial C_i(z,t)}{\partial z} - \frac{1-\epsilon}{\epsilon}\frac{\partial q_i(z,t)}{\partial t} \tag{4.1}$$

The axial dispersion coefficient D_{ax} is calculated using the correlations employed by Dünnebier *et al.* (1998) , which are

$$D_{ax} = \frac{uL}{Pe} \tag{4.2}$$

$$Pe = \frac{0.2}{\epsilon_T} + 0.011\epsilon_T \left[\frac{Re}{\epsilon_T}\right]^{0.48} \tag{4.3}$$

$$Re = \frac{2\epsilon_T u R_p \rho}{\eta} \tag{4.4}$$

The particle mass balance, including the effective diffusivity, is adopted from the work of Strube *et al.* (1997):

$$\frac{\partial q_i(z,t)}{\partial t} = \frac{3k_{eff,i}}{R_p}(C_i(z,t) - C_{P_i}(z,t)) \tag{4.5}$$

Isotherms The integration of the differential mass balances of the components in chromatography requires prior knowledge of their equilibrium isotherm, which describes the distribution of the solute between the two phases of the chromatographic system. The most general isotherm can be given in the form:

$$q_i = f(C_{P_i}(z), ..., C_{P_n}(z)) \quad with \quad i = 1, 2, ..., n \tag{4.6}$$

where n is the number of components.

In accordance with the parameters given in Dünnebier *et al.* (1998), a linear isotherm is employed in the following work:

$$q_i = K_i C_{P_i} \tag{4.7}$$

Note that other isotherm models such as the Langmuir isotherm or the Bi-Langmuir isotherm (refer to Appendix B) can also be employed.

Boundary and initial conditions The Danckwerts boundary conditions at the column inlet and outlet are employed here, modified according to those used in

Dünnebier *et al.* (1998).

At the column inlet:

$$C_i(z = 0, t) = Cin_i \tag{4.8}$$

At the column outlet:

$$C_i(z = L, t) = Cout_i \tag{4.9}$$

$$\frac{\partial C_i(z = L, t)}{\partial z} = 0 \tag{4.10}$$

The initial conditions describe the state of the column when the experiment or operation begins. These are:

$$C_i(z, t = 0) = 0 \quad \text{at } t = 0 \tag{4.11}$$

$$\frac{\partial q_i(z, t = 0)}{\partial t} = 0 \quad \text{at } t = 0 \tag{4.12}$$

The Node Model

The node model represents what happens at the points of switching, and is illustrated by Figure 4.3. The assumptions of the node model are:

- No holdup in the nodes
- No backmixing at the nodes
- No loss of fluid (or mass) at the nodes, *e.g.* leaks

Across each node, the key mass balances that define it are:

Total material balance:

$$Qin + QNin = Qout + QNout \tag{4.13}$$

Component material balance:

$$QinCin_i + QNinCNin_i = QoutCout_i + QNoutCNout_i \tag{4.14}$$

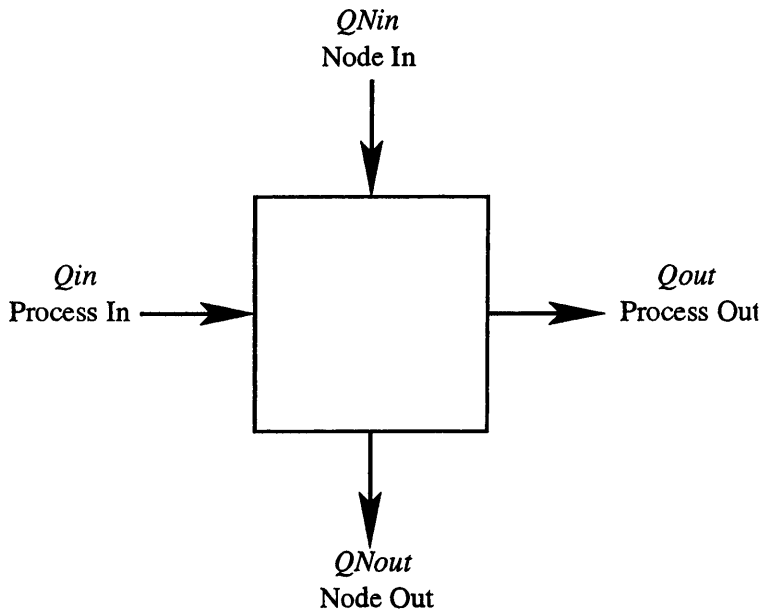

Figure 4.3: Illustration of the node model

Since there are four main nodes, the nodes can be named after their respective inlet and outlet streams at the point - feed, desorbent, extract and raffinate. For these four nodes in the system, the overall mass balance over the system is:

$$Q_{Feed} + Q_{Desorbent} = Q_{Extract} + Q_{Raffinate} \tag{4.15}$$

The same nodal model can be changed to an inlet (feed, desorbent) or outlet (extract, raffinate) stream depending by assigning appropriate values to the concentrations and flowrates at the nodes.

Node at feed point:

$$QNout = 0 \tag{4.16}$$

$$QNin = QFeed \tag{4.17}$$

$$CNin_i = C_{Feed} \tag{4.18}$$

Node at desorbent point:

$$QNout = 0 \tag{4.19}$$

$$QNin = Q_{Desorbent} \tag{4.20}$$

$$CNin_i = 0 \tag{4.21}$$

Node at extract point:

$$QNout = Q_{Extract} \tag{4.22}$$

$$QNin = 0 \tag{4.23}$$

$$CNout = C_{Extract} \tag{4.24}$$

Node at raffinate point:

$$QNout = Q_{Raffinate} \tag{4.25}$$

$$QNin = 0 \tag{4.26}$$

$$CNout = C_{Raffinate} \tag{4.27}$$

4.4 Direct determination of cyclic steady state for the SMB process

SMB processes typically require a number of cycles before steady state conditions are achieved, as there are constant changes to the states in the processes. This will be further illustrated in the case study discussed in Section 4.6. The dynamic nature of these processes make direct steady state modelling a useful feature in order to predict the performance of the model at *steady state*, instead of running a simulation via several cycles.

Two slightly different approaches have been presented in the literature:

- **Method 1**: Nilchan and Pantelides (1998) reported a method of complete discretisation for periodic adsorption processes, where the system of equations is discretised in both temporal and spatial domains and incorporating the periodicity conditions of *cyclic steady state* (CSS) as additional boundary conditions in the model. These periodicity conditions state that the state of the system at the end of each cycle is identical to that at the start of the cycle.

- **Method 2**: A similar means of direct computation of periodic SMB states is discussed by Kloppenburg and Gilles (1999), with a periodic state being identified as the spatially distributed state of the SMB process at the end of a switching interval which is identical to the state at the beginning of the interval, only shifted exactly one column length.

A comparison of these two approaches of calculating steady state directly has been done by Minceva *et al.* (2003) for the separation of 1,1'-bi-2-naphthol enantiomers using a simulated moving bed (SMB) process, where the case study employed showed the method by Kloppenburg and Gilles (1999) to be computationally more efficient.

The work on direct determination of CSS in the SMB process is covered in this section, based on the methods proposed by Nilchan and Pantelides (1998) and by Kloppenburg and Gilles (1999). The former is termed Method 1 (CSS Cycle) and the latter Method 2 (CSS Switch). The discretisation of the spatial and temporal domains in CSS models are described in Section 4.4.1, followed by the mathematical formulation of both CSS models in Section 4.4.2.

4.4.1 Normalisation of spatial and temporal domains

The lengths of the spatial and temporal domains are often used as decision variables in the optimisation *e.g.* length of the column or cycle period. These variables are mostly implicit in the models and are used to define the domains (*e.g.* $z \in [0, L]$, $t \in [0, T_{switch}]$), there is therefore a need to normalise these variables within the domain.

The normalised spatial variable can be defined as $\zeta \in [0,1]$ and the normalised temporary variable can be expressed as $\theta \in [0,1]$, where:

$$\zeta \equiv \frac{z}{L} \quad ; \quad \theta \equiv \frac{t}{T_{switch}} \tag{4.28}$$

More details on the approach of normalising the spatial and temporal domains can be found in Nilchan and Pantelides (1998), *e.g.* how the partial derivatives and integrals can be expressed in terms of these new variables. The normalisations means that the model equations, Equations 4.1 and 4.5, can be rewritten as:

$$\begin{aligned} \frac{1}{T_{switch}}\frac{\partial C_i(\zeta,\theta)}{\partial \theta} &= D_{ax}(\theta)\left(\frac{1}{L^2}\right)\frac{\partial^2 C_i(\zeta,\theta)}{\partial \zeta^2} - v(\theta)\left(\frac{1}{L}\right)\frac{\partial C_i(\zeta,\theta)}{\partial \zeta} \\ &- \frac{1-\epsilon}{\epsilon}\left(\frac{1}{T_{switch}}\right)\frac{\partial q_i(\zeta,\theta)}{\partial \theta} \end{aligned} \tag{4.29}$$

$$\left(\frac{1}{T_{switch}}\right)\frac{\partial q_i(\zeta,\theta)}{\partial \theta} = k_{eff_i}\frac{3}{R_p}(C_i(\zeta,\theta) - C_{P_i}(\zeta,\theta)) \tag{4.30}$$

The boundary condition, Equation 4.10, is also rewritten as

$$\left(\frac{1}{L}\right)\frac{\partial C_i(\zeta=1,\theta)}{\partial \zeta} = 0 \tag{4.31}$$

4.4.2 Mathematical formulation of the CSS models

In the CSS chromatography models, the mass balances employed are exactly the same as those in the dynamic models. The dynamic model is transformed into a CSS model simply by replacing its initial conditions with *periodicity conditions* (which are the steady state conditions expected at the column's axial and spatial boundaries). A simulation of the CSS model is thus able to reproduce the performance of the dynamic model at steady state conditions *directly.*

Method 1 (CSS Cycle model)

The first method, based on the work by Nilchan and Pantelides (1998), is based on the fact that when the system is at steady state, the conditions in both the stationary and mobile phases at the end of the cycle are identical to the conditions at the beginning of the cycle, Here, the term *cycle* refers to the inlet and outlet lines of desorbent, extract, feed and raffinate returning to the *original positions* after the time when they begun to move.

The intial conditions outlined in Section 4.3.3 (Equations 4.11 and 4.12), are those of a dynamic model and thus, no longer apply. They are replaced with the following periodicity conditions:

$$C_{i,z}(t=0) = C_{i,z}(t=T_{cycle}) \tag{4.32}$$

$$q_{i,z}(t=0) = q_{i,z}(t=T_{cycle}) \tag{4.33}$$

In dimensionless form, these conditions may be rewritten as:

$$C_{i,\zeta}(\theta=0) = C_{i,\zeta}(\theta=1) \tag{4.34}$$

$$q_{i,\zeta}(\theta=0) = q_{i,\zeta}(\theta=1) \tag{4.35}$$

Method 2 (CSS Switch model)

The second method, based on the work by Kloppenburg and Gilles (1999), is based on the fact that when the system is at steady state, the state of column $j+1$ at the end of a switching period is identical to the state of column j (the preceding column) at the beginning of the switching period. In this case, the periodicity conditions are expressed as:

$$C_{i,z}(j,t=0) = C_{i,z}(j+1,t=T_{switch}) \tag{4.36}$$

$$q_{i,z}(j, t = 0) = q_{i,z}(j + 1, t = T_{switch}) \quad (4.37)$$

where the dimensionless forms are:

$$C_{i,\zeta}(j, \theta = 0) = C_{i,\zeta}(j + 1, \theta = 1) \quad (4.38)$$

$$q_{i,\zeta}(j, \theta = 0) = q_{i,\zeta}(j + 1, \theta = 1) \quad (4.39)$$

4.5 Optimisation of SMB Operation

Optimisation of the SMB unit is relatively new in the literature, as it is a difficult process to model, let alone optimise. In addition, SMB has only recently been favoured for industrial separations due to earlier patent constraints and lack of understanding about the process. With its rising popularity, however, research has expanded to the modelling of this process and its optimisation.

4.5.1 Review of optimisation work

Traditionally, much of the mathematical modelling of SMB was done using a true-moving bed (TMB) model. Some of these optimisation studies were then conducted on the TMB models, *e.g.* Mazzotti *et al.*, 1997; Pröll and Küsters, 1998; Beste *et al.*, 2000; Biressi *et al.*, 2000; Houwing *et al.*, 2002a,b. Most of these studies deemed the TMB model to suffice for the prediction of the steady state performance of the SMB process for design purposes, provided geometric and kinematic conversion rules were fulfilled.

However, later research on modelling the SMB process which considered both the TMB model and SMB model suggested that the TMB model was inadequate in some areas (*e.g.* Beste *et al.*, 2000; Strube *et al.*, 1997). For instance, Strube *et al.* (1997) attempted to optimise the SMB process by optimising the process using the TMB model, and subsequently using the operating parameters obtained as the

input data for an SMB process model. The results obtained on the SMB model showed a decrease in purity relative to that predicted by the TMB model, and the optimisation criteria of maximal feed throughput, minimal desorbent requirement and dilution were not met. This work demonstrated that due to the periodic flow in SMB, the SMB process has to be described by rigorous dynamic models which consider axial dispersion and mass transfer resistance.

In this work, an approach is described hitherto not employed for simulated moving bed processes. Past optimisation work on the SMB process has been based on either the less complex TMB model or the dynamic SMB model. The latter has been shown to be superior to the TMB model in representing the SMB process more accurately. However, these models require a number of cycles before steady state conditions of the process are achieved. This is where the advantage of employing the CSS models outlined in Section 4.4.2 is critical, as solving these models determines the steady state conditions of the process directly.

In this work, the CSS (Switch) model (Section 4.4.2) is considered for optimisation of the SMB process at its *steady state conditions*, which has not been done previously. The optimisation approach employed is a direct approach of *control vector parameterisation*, where the infinite dimensional problem is converted to a finite dimensional non-linear programming (NLP) problem. This approach has been demonstrated to be an efficient approach for optimisating problems involving ordinary differential equations as equality constraints (Vassiliadis, 1993; Vassiliadis *et al.*, 1999; Balsa-Canto *et al.*, 2001 and 2002).

4.5.2 Decision variables

As this work is investigating the optimisation of the operation of the SMB process, the decision variables chosen for the optimisation will focus primarily on *operating variables*, such as flowrates and switching time. Column sizes are generally standardised, and is thus not considered here. However, a simultaneous optimisation of

the design and operation of the SMB system will be considered in Chapter 5.

Decision variables available when operating the SMB process are as follows:

- Recycle flowrate - the internal flowrate of the process in section I between the desorbent and raffinate nodes
- Feed flowrate - the flowrate of the feed entering the SMB system
- Desorbent flowrate - the flowrate of the desorbent entering the SMB system
- Extract flowrate - the flowrate of the extract leaving the system, containing the component which has the higher affinity for the stationary phase (component A in Figure 4.1)
- Switching time - the time interval between the switching action of the inlet and outlet lines

Note that the SMB operation actually consists of 5 flowrates: recycle, feed, desorbent, extract and raffinate. However, the overall mass balance in the SMB node (Equation 4.15) means that when the extract, the desorbent and the feed flowrates are determined or optimised, the raffinate flowrate is immediately determined from the overall mass balance.

4.5.3 Summary

In this chapter, an approach for the modelling and optimisation of the SMB process is presented, including a discussion on the types of SMB models available *e.g.* TMB equivalent model, dynamic SBM model, CSS models. The work done in the literature on optimisation of the SMB process is also examined and hitherto, the optimisation of the CSS model for chromatography has not been done before.

In the following section, a case study is presented to compare the performance of the CSS models formulated with the dynamic SMB model, and some simulation and optimisation studies are then carried out on the CSS models.

Number of columns in each section	2
Number of components	2
Length, L	47.5 cm
Diameter, D_c	1.4 cm
Total porosity, ϵ_T	0.45
Fluid density, ρ	1 g/cm^3
Fluid viscosity, η	8 $\times 10^{-3} g/(cms)$
Particle radius, R_p	0.0011 cm
Henry's coefficient, K_A	0.56
Henry's coefficient, K_B	0.23
Effective overall mass transfer coefficient, $k_{eff,A}$	$2.09 \times 10^{-5} cm/min$
Effective overall mass transfer coefficient, $k_{eff,B}$	$1.72 \times 10^{-5} cm/min$

Table 4.1: Model parameters of the SMB unit (Dünnebier *et al.*, 1998)

Feed flowrate, Q_{Feed}	0.0166 cm^3/s
Desorbent flowrate, $Q_{Desorbent}$	0.0266 cm^3/s
Extract flowrate, $Q_{Extract}$	0.0233 cm^3/s
Recycle flowrate, $Q_{Recycle}$	0.0665 cm^3/s
Concentration of feed, C_{Feed}	0.05 g/cm^3
Switching time, T_{switch}	618 seconds

Table 4.2: Operating parameters of the SMB unit (Dünnebier *et al.*, 1998)

4.6 Case study: verification and optimisation of the CSS model

A case study is used to verify both the CSS models developed earlier in Section 4.4.2 by comparing their results with those obtained using the dynamic model. The criteria for the verification of the CSS models will be the goodness-of-fit of the concentration profiles along the length of the SMB units (*i.e.* the length of all columns in the unit) generated by these models, against the concentration profiles generated by the equivalent dynamic SMB model at steady state.

The detailed case study parameters used are those presented by Dünnebier *et al.* (1998) and are given in (Tables 4.1 and 4.2).

In this section, simulations are conducted on the dynamic SMB model, to demon-

strate the presence of cyclic steady state conditions after a number of switching periods. Subsequently, the CSS models formulated in Section 4.4.2 are verified by comparison with the dynamic steady state model in terms of their accuracy and reliability. Finally, the effects of the decision variables on the production rate and purity of products is demonstrated. These decision variables are later to be considered in the optimisation studies (Sections 4.6.3 and 4.6.4) of this chapter.

4.6.1 Simulation results of the dynamic SMB model

Simulations of the case study described above were conducted at the same conditions throughout to establish the concentration profiles at various time periods in order to understand the behaviour of the components over time. The numerical solution employed was orthogonal collocation finite element method (OCFEM), which is covered in greater detail in Appendix C.2. A fourth-order OCFEM with ten collocation points was used.

The results from the model shown are of the concentration profiles *inside* the SMB unit over time as well as the values of the resulting production rate, purity and recovery yield for the extract and raffinate.

Figure 4.4 shows the system at start-up with the feed entering at column five, and it is observed that the fifth column is saturated with the feed by the end of the first switching period. Component B is eluting faster than component A, as it has a lower affinity for the stationary phase. Hence, more of component B is present in the sixth column.

At the first nodal switch, the nodes are switched one column in the direction of the mobile phase flow (*i.e.* it appears as though the columns are moving in the opposite direction to the mobile phase). At the end of the second switching time (see Figure 4.5), the fifth column, which was saturated with feed at the beginning of the second switching period, now has only very little of component B, since it elutes faster. In addition, the concentrations of both components in the sixth column

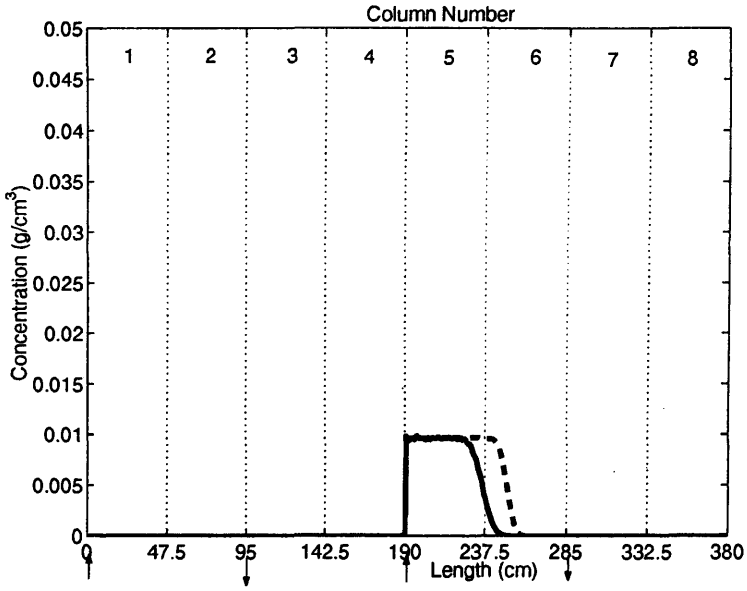

Figure 4.4: Profile along the SMB after the 1st switching period (618 seconds)
('—' : Component A and '- -' : Component B)
Arrows at columns denote: desorbent enters 1, extract leaves 2, feed enters 5, raffinate leaves 6

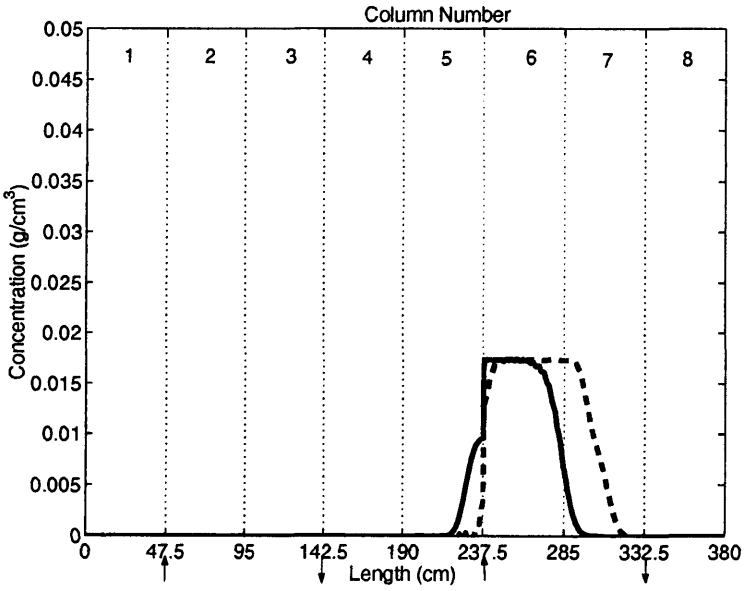

Figure 4.5: Profile along the SMB after the 2nd switching period (1236 seconds)
('—' : Component A and '- -' : Component B)
Arrows at columns denote: desorbent enters 2, extract leaves 3, feed enters 6, raffinate leaves 7

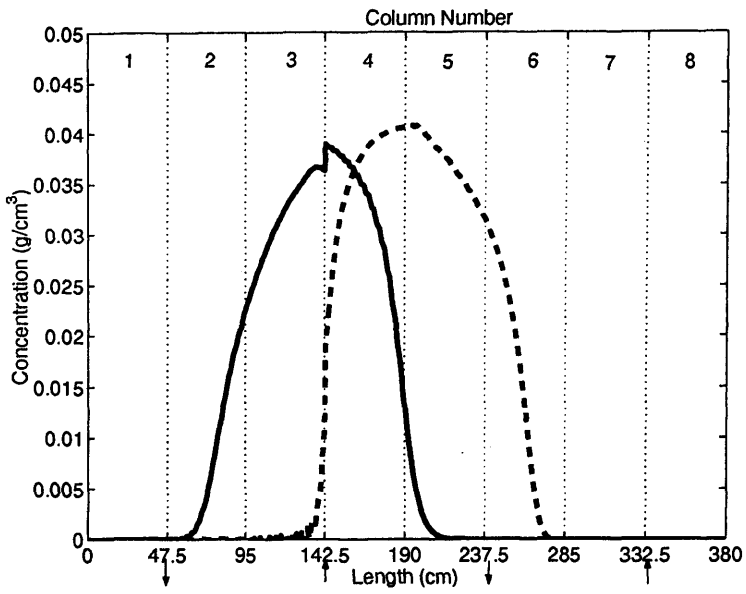

Figure 4.6: Profile along the SMB after the 8th switching period (4944 seconds)
('—' : Component A and '- -' : Component B)
Arrows at columns denote: desorbent enters 8, extract leaves 1, feed enters 4, raffinate leaves 5

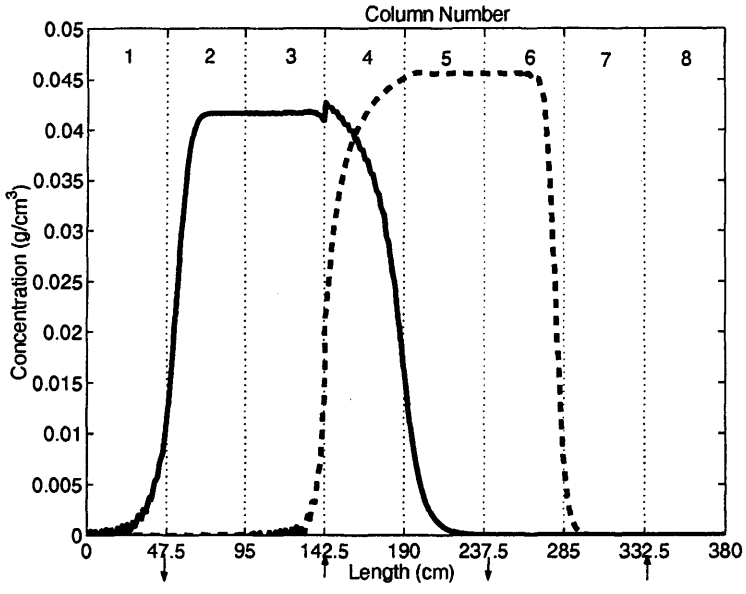

Figure 4.7: Profile along the SMB after the 40th switching period, at steady state conditions

('—' : Component A and '- -' : Component B)
Arrows at columns denote: desorbent enters 8, extract leaves 1, feed enters 4, raffinate leaves 5

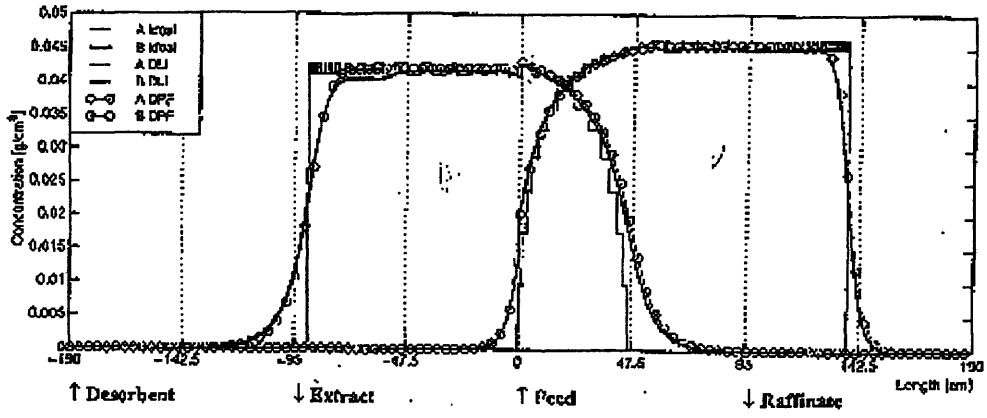

Figure 4.8: Profile along the SMB at the end of a switching period at steady state (Dünnebier *et al.* (1998))

increases as feed enters the column.

By the eighth switching period, the classic appearance of the concentration profile in the SMB is apparent in Figure 4.6, and it can be observed that most of component A leaves the SMB system via the extract port, whilst most of component B leaves through the raffinate node. At the end of the 40th switching period, Figure 4.7 shows the two concentration plateaus which are characteristic of the SMB concentration profiles in the literature (Dünnebier *et al.*, 1998; Strube *et al.*, 1997). Furthermore, the results demonstrate a very good agreement with the work done by Dünnebier *et al.*(1998), whose work is reproduced in Figure 4.8.

From these simulations, it can be seen how the start-up operation of the SMB unit proceeds. It is also demonstrated that as a cyclic operation, the SMB unit requires several cycles before steady state conditions are achieved. The contrast in Figure 4.6 at 8 switching periods (1 cycle) to Figure 4.7 at 40 switching periods (5 cycles) is evident.

As it is the steady state conditions of the SMB operation that are of interest, the rest of this section will employ a cyclic steady state (CSS) model to investigate the optimal operating parameters. The CSS models to be used in the optimisation are first verified in the next section to affirm that they are equivalent to the dynamic

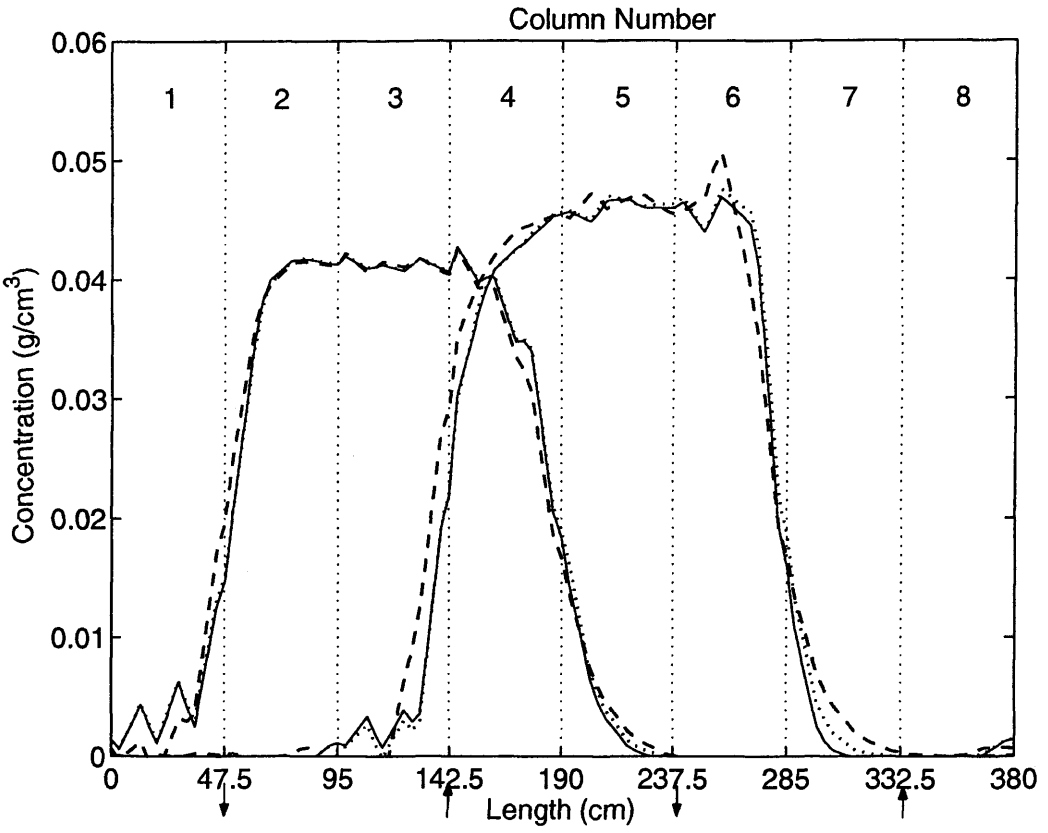

Figure 4.9: Profile along the columns for the dynamic and CSS models for 3 finite elements across the axial domain

('—' : Dynamic model, '- -' : CSS (Cycle) Model, '· · ·' : CSS (Switch) Model)

Arrows at columns denote: desorbent enters 8, extract leaves 1, feed enters 4, raffinate leaves 5

SMB model.

4.6.2 Verification of the CSS models

Both the CSS models developed earlier (Section 4.4.2) were verified by comparing their results for the concentration profiles along the length of the SMB unit with the dynamic SMB model at steady state.

It is crucial that the CSS models not only produce accurate results compared to that of the dynamic model at steady state, but that they should also accurately reflect the behaviour of the dynamic model. The graphs in Figure 4.9 show a comparison of the concentration profiles across the axial domain of the dynamic model

Model Type	CPU Time (seconds)
Dynamic	43.77
CSS (Cycle)	624.01
CSS (Switch)	58.00

Table 4.3: Comparison of the computational times for each model in Case I

at steady state and the CSS models. The oscillations in the dynamic SMB model are present in the diagram due to the numerical calculations arising from the spatial discretisation. This will not significantly affect the output values (such purities and recovery yields) as the general shape of the profiles are well captured. Whilst the kinks in the graph bear evidence to the inaccuracies that arise from discretising the temporal domain, both CSS models do reflect the dynamics of the SMB process very well.

Minceva *et al.* (2003) has done a similar comparison between the two CSS models. They noted that with the same time step, the CSS (Cycle) model would have n times more ordinary differential equations compared to the CSS (Switch) model, where n is the number of switching periods. This is because the former simulates the entire cycle (with n switching periods), whilst the latter simulates a single switching period.

It is also evident that of the two CSS models, the CSS (Switch) model shows better agreement with the dynamic model visually in the case study presented in Figure 4.9. This is because of the difference in the complexity of the two models and also the different time step, since CSS (Cycle) used 120 finite elements (time step 41.2 seconds) and CSS (Switch) used 40 finite elements (time step 15.45 seconds). The difference in the number of finite elements used was due to computational memory limits for each model, but the work done by Minceva *et al.* (2003) also suggests that the CSS (Switch) model is the more efficient computationally, of the

two CSS models.

Simple relative error calculations on the concentration profiles generated by the CSS (Cycle) and CSS (Switch) models compared to the dynamic model was done (Refer to Appendix G) by comparing the differences in the values of the concentration profiles predicted by the CSS models against the dynamic model. 44% of the plotted points in the CSS (Switch) model had relative errors (compared to the dynamic model) less than 5%, whilst the CSS (Cycle) model had 28% of the plotted points meeting this criteria. This thus confirms that the CSS (switch) model is the better of the two models in representing the SMB process.

4.6.3 Effects of decision variables on SMB operation

Having verified that the CSS Switch model is a suitable candidate for optimisation purposes, it is now used in a number of simulation studies to ascertain the effects of the decision variables used in the optimisation (Refer to Section 4.5.2 for these) on the operation. In particular, the effects of these variables on the purity and production rate of the products will be examined, and the focus will be on the extract as it generally contains the more valuable product *i.e.* the extract contains the more retained component A.

Recycle flowrate

Figures 4.10(a) and 4.10(b) show the effects of a change in the recycle flowrate on the extract production rate and purity, respectively. As the recycle flowrate, *i.e.* the internal flowrate in the SMB system, increases, the production rate gradually increases, up until $0.07cm^3/s$, then it falls sharply. However, the purity of the extract remains very low except for one flowrate examined. These studies imply that there is only a narrow range for which the recycle flowrate exhibits optimal performance for this case study. Changing the recycle flowrate affects the flowrates in every section of the SMB system, and thus affects the separation of the components largely.

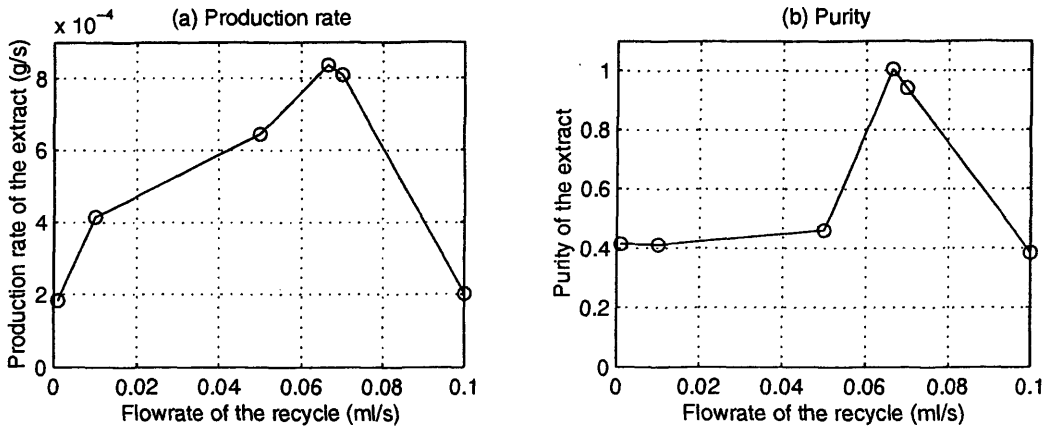

Figure 4.10: Effect on system performance by varying the recycle flowrate

Feed flowrate

Figures 4.11(a) and 4.11(b) show that there is not a significant change in the performance of the system beyond a certain feed flowrate. As the flowrate is increased, the production rate gradually increases but after a flowrate of $0.03cm^3/s$, there appears to be no further increase. There is hardly any change in the purity despite the variation in the flowrate. This is likely to be because this flowrate contributes the most to the amount of feed entering the system, although not necessarily affecting the separation of the products. As the size of the column is fixed, it is likely that saturation occurs in the columns with high feed flowrates, and the performance will level off. Higher feed flowrates thus do not necessarily lead to better performances.

Desorbent flowrate

The desorbent desorbs component A which has a higher affinity for the stationary phase. Figures 4.12(a) and 4.12(b) show that the performance of the SMB can vary quite significantly with changes in the desorbent flowrate. The production rate decreases as the flowrate of the desorbent increases, as does the purity. However, at the highest flowrate examined ($0.03cm^3/s$), the purity suddenly peaks again. Among all the variables present, the desorbent flowrate is found to have the most narrow range for variation within the case study, since at higher flowrates it produces

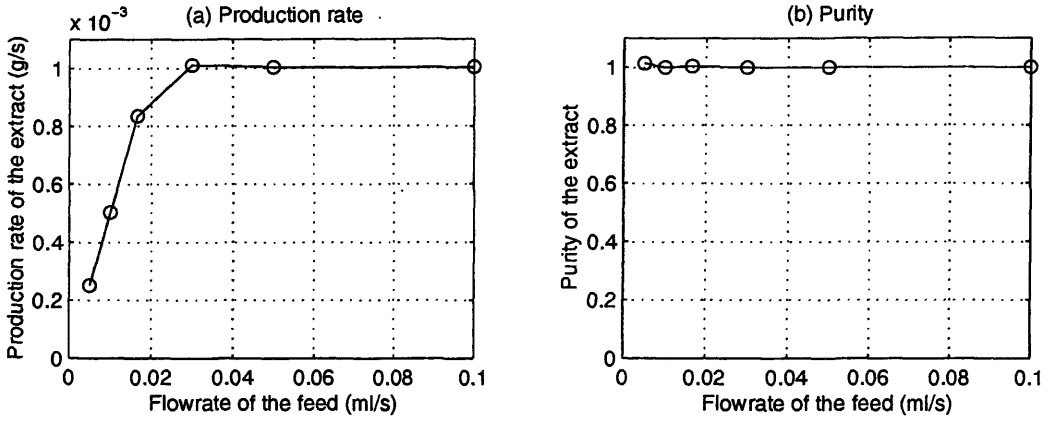

Figure 4.11: Effect on system performance by varying the feed flowrate

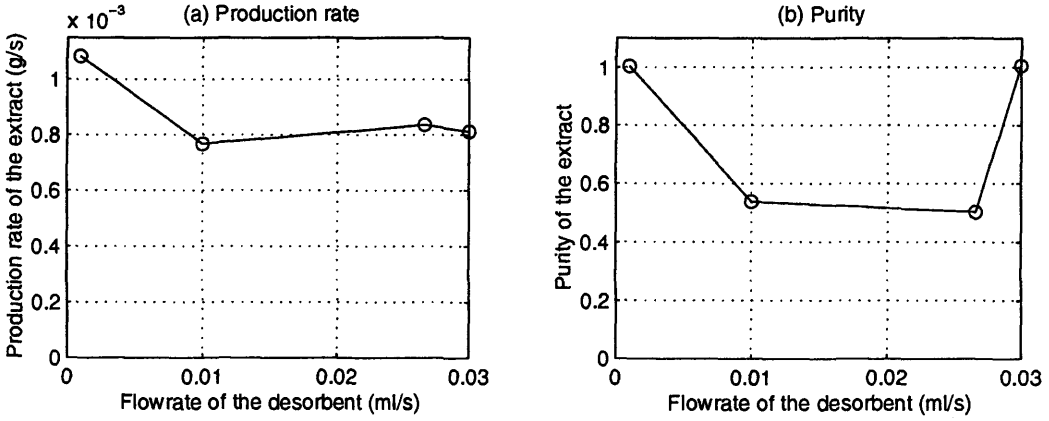

Figure 4.12: Effect on system performance by varying the desorbent flowrate

infeasible calculations.

Extract flowrate

The production rate of the extract is generally expected to increase with the increase in the extract flowrate, which is demonstrated in Figure 4.13(a). However, Figure 4.13(b) shows that whilst increasing the extract flowrate improves the production rate of the extract generally, the quality of this improved production is poorer (*i.e.* the production rate increases, whilst the purity decreases). This again suggests an optimal flowrate needs to be located, where the objective of higher production rate can be met without compromising the quality of the product.

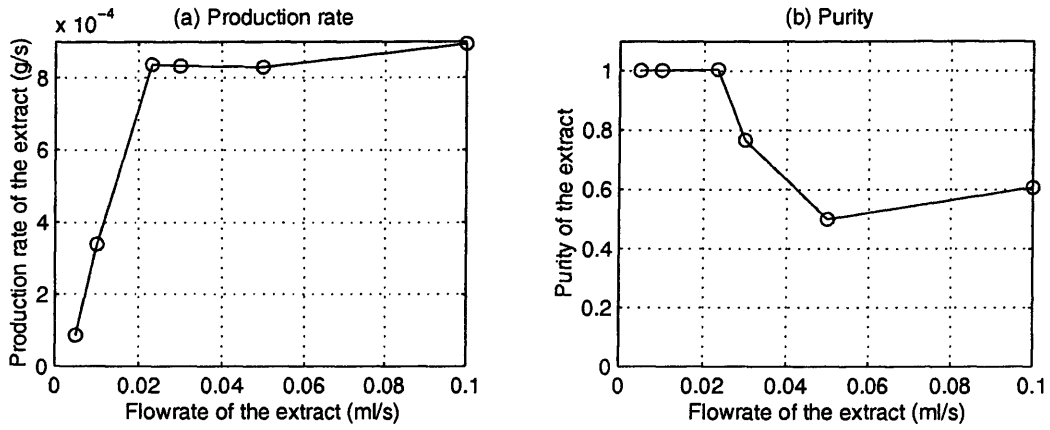

Figure 4.13: Effect on system performance by varying the extract flowrate

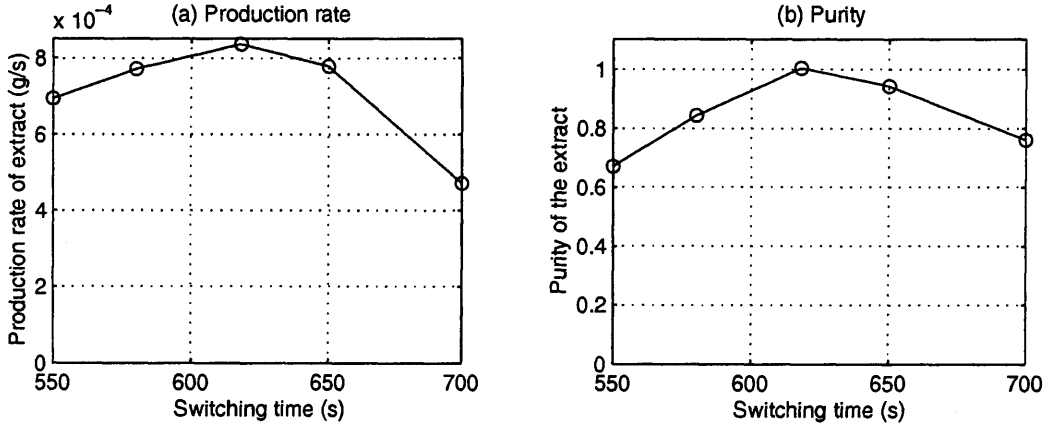

Figure 4.14: Effect on system performance by varying the switching time

Switching time

Choosing sub-optimal switching times can result not only in very poor separation, but also wasted time, labour and effort. Figures 4.14(a) and 4.14(b) demonstrate the effects on the performance with changes in the switching time. It is clear that an optimal switching time can be located for the switching time, and that away from this optimum, the performance of the unit deteriorates rapidly.

Summary

Each decision variable was investigated on its own in Section 4.6.3, and changing even one of these variables can affect the performance of the SMB unit greatly,

and not necessarily in the desired fashion (*e.g.* high production but of low purity extract). To manually change each of these variables to locate the optimum operating conditions would not only take a very long time, but also produce sub-optimal results. Thus, in order to locate the optimal operating parameters, computational optimisation is the only feasible solution whereby all the decision variables are determined simultaneously as demonstrated in the next section.

4.6.4 Optimisation studies on the SMB operation

In these studies, the optimisation was carried out on the CSS (Switch) model outlined in Section 4.4.2. The optimisation problem was formulated to maximise the production rate of the extract (the more retained component A), as this is typically the more valuable or desired product in most separations. Subsequently, the effect of increasing the number of decision variables (discussed in Section 4.6.3) on the optimisation of the process was demonstrated.

Formulating the optimisation problem

The objective function of the optimisation is to maximise the production rate of the extract (Pr_A) for the separation of a binary feed mixture containing components A and B (refer to Table 4.1 for the model parameters of the separation), where the extract contains the more retained component A:

$$\max_{\theta, P(\zeta,\theta)} Pr_A \tag{4.40}$$

subject to

$$Pu_i^{min} \leq Pu_i \leq 1 \tag{4.41}$$

where Pu_i is the purity of the component i and Pu_i^{min} is set at 0.985.
where θ is the dimensionless time horizon for 1 switching period and $P(\theta)$ is the vector of decision variables, discretised along the spatial and time domains, z and t,

Time invariant parameter	Lower bound	Upper bound	Units
Feed flowrate, Q_{Feed}	0.001	0.18	ml/s
Desorbent flowrate, $Q_{Desorbent}$	0.001	0.18	ml/s
Extract flowrate, $Q_{Extract}$	0.001	0.18	ml/s
Recycle flowrate, $Q_{Recycle}$	0.001	0.2	ml/s
Switching time, T_{switch}	200	700	s

Table 4.4: Bounds on the degrees of freedom

respectively (Refer to Section 4.4.1 for more details on the discretisation of the spatial and time domains). The decision variables considered are the switching time of the inlet and outlet lines and their flowrates over the SMB unit. The full definitions of these system performance parameters for optimisation, which was solved using *gPROMS* (Process Systems Enterprise Ltd., 2005), are given in Appendix C.

Effects of the decision variables on the optimistion

The effect on the system performance of gradually removing the degrees of freedom (time invariant parameters) available when designing the SMB chromatographic process will also be examined. Table 4.4 shows the decision variables considered in this optimisation problem with the upper and lower bounds, respectively.

A number of optimisation runs are conducted, in which the number of decision variables used in each optimisation is increased after each run to investigate the effects on the optimisation. Table 4.5 records these optimisation cases. In Case A, only the switching time is optimised and in Case E, all the decision variables are optimised.

Optimisation results

Figures 4.10-4.14 demonstrated the effect on the performance of the SMB process when each of the degrees of freedom are varied, one at a time, with respect to the production rate and the purity of the extract. It was difficult to optimise the process merely by using one degree of freedom, as evidenced by Case A in Table 4.5 when only the switching time is optimised. This is due to the tight constraints on the

Case	Decision variables					Pr_A $\times 10^{-4}$ g/s	Pu_A %	CPU time s
	T_{switch} s	Q_{Feed} ml/s	$Q_{Desorbent}$ ml/s	$Q_{Extract}$ ml/s	$Q_{Recycle}$ s			
A	618	0.0166†	0.0266†	0.0233†	0.0665†	8.362	99.98	146.9
B	611	0.0193	0.0266†	0.0233†	0.0665†	9.623	99.98	1084.5
C	630	0.0195	0.0237	0.0233†	0.0665†	9.746	98.5	1181.2
D	249	0.0444	0.1740	0.0703	0.0665 †	22.174	98.5	5912.6
E	200 ‡	0.0462	0.1750	0.1508	0.1872	23.09	98.5	9634.2

Table 4.5: Optimisation results of the case study

† : Fixed value for decision variable

‡ : Lower bound value of decision variable

purity and recovery yield of the extract that is used in the optimisation problem, which is necessary to yield an effective separation in the SMB chromatographic process. It is clear that to consider a true optimisation of the whole SMB process, all the operating parameters must be optimised. Note that the only parameter which is not considered in this study is the concentration of the feed, as in most cases, the feed composition is fixed.

From Cases B to E, the number of decision variables varied was increased. It is observed that as the number of decision variables that is allowed to vary increased, the performance of the system improved. In addition, with each increase in the number of degrees of freedom, the optimisation took a progressively longer time. This shows the advantage in employing the CSS model to handle the optimisation as it means that optimisation is conducted at steady-state conditions directly, instead of simulating many switches to reach steady-state conditions, for each step of the optimisation. The more complex optimisation runs require 100-160 CPU minutes.

With Cases D and E in particular, there is a marked increase in the flowrates of the feed and the desorbent when the flowrate of the extract is included as a decision variable. The dimensions of the column were examined, and were able to accommodate the increased flowrates. These 3 flowrates are linked by the mass balance across the node (Equation 4.15). Having the extract flowrate as a decision

variable means that Q_{Feed} and $Q_{Desorbent}$ can vary to give higher productivity.

It is noted that for Cases D and E, the flowrate of the desorbent is increased considerately in value is the flowrate of the desorbent. This is of interest as the optimisations seems to suggest that a higher flowrate of desorbent, accompanied by a shorter switching time improves the production rate. The flowrates within each section of the SMB system are consequently adjusted with these changes to improve the separation. In Case E, a higher flowrate is observed in the extract for nearly the same production rate, which implies that the concentration of component 1 in the extract is much lower than that of Case D.

By using all the flowrates and switching period as degrees of freedom in this optimisation, the performance of the system, the production rate of the process, is improved significantly by as much as 280% in some optimisations for the production rate of the process.

4.7 Conclusions

This work outlines a new optimisation approach for the SMB chromatographic process using a cyclic steady state (CSS) model for one switching period. The CSS (Switch) model is verified in terms of its accuracy and compared to a detailed dynamic SMB model. It is found to be highly accurate in modelling the process. The performance of the CSS (Switch) model is also compared with the CSS (Cycle) model and was found to be more computationally efficient and accurate in predicting the dynamic behaviour of the system. The CSS (Switch) model is then used for an new optimisation approach. It is found to be an efficient method in locating the optimal process parameters with a short computational time. The study also highlighted the important of establishing all relevant degrees of freedom and showed that optimising the system for a single degree of freedom does not give the optimal operation performance achievable by the system.

Chapter 5

A systematic approach to optimising chromatographic processes

In this chapter, the optimisation of the design and operation of different chromatographic alternatives are considered. These fall into two main categories: single column and multi-column processes, and both processes are used extensively in industry. However, the procedure for selecting the most appropriate process for a given separation, as well as the best operating policy alternative associated with it, is still largely unclear. An approach for how this selection should be made is thus needed and will be presented in this chapter. Given the trade-offs of each process, it is imperative that an economic objective function is used. The approach involves optimising both single and multi-column processes together their operating alternatives. The final choice is then made based on the most profitable process.

5.1 Introduction

Over the years, the operation of the chromatographic process in pharmaceutical industries has developed rapidly and it is no longer limited to batch processing. Whilst the single column is still popular in preparative chromatography, multi-column processes, such as simulated moving bed (SMB) chromatography, are now becoming increasingly favoured in industrial-scale chromatography as a continuous alternative, producing large amounts of highly purified products. As such, the decision of whether to use a single column or a multi-column process for a given separation is a largely ambiguous one. As the configurations and process operations of the two modes are vastly different, economics form an integral part of any comparison. This work considers optimisation of the design and operation of both single and multi-column chromatographic processes, taking into account both capital and operating costs. Such a detailed comparison has not been examined so far in the open literature.

Previous work comparing single column and multi-column chromatography has mainly been based on comparing the two processes on specific outcomes such as eluent consumption or specific productivity (Nicoud *et al.*, 1993; Grill *et al.*, 2004). Such comparisons fail to consider underlying economic issues which may be in conflict, *e.g.* multi-column processes are associated with a high investment cost but have reduced eluent consumption, whilst single columns have lower investment costs but lower efficiency. As a result, these comparisons, whilst useful in highlighting the advantages and disadvantages of both systems relative to each other, do not provide any useful means of choosing between these systems. An economic comparison between the optimised process alternatives is thus necessary to properly assess the strengths and weaknesses of each system, particularly from an industrial point of view.

In this work, reliable and accurate chromatography models are used to describe single and multi-column chromatography processes whose design and operation are

optimised simultaneously for each process to maximise their individual annual profit. Thus, the decision variables considered include not only the configuration, but also the design of the columns used, as well as the operating policy employed. For single column configuration, a single column, as well as a single column with recycle and peak shaving operations, are considered, whilst for the multi-column alternative, the SMB process and its variations (Varicol, PowerFeed etc.) are examined. In addition, the effects of employing different objective functions (*e.g.* maximum productivity or minimum separation costs) in the optimisation are assessed.

A detailed economic appraisal is performed of all process options. The case study employed in Chapter 4 is used to illustrate the approach. The simplified general rate model is used to model the columns. The effects of considering different objective functions are highlighted and demonstrate the importance of making the correct function choice depending on the purpose of the optimisation.

Jupke *et al.* (2002) has compared batch and SMB chromatography using a comprehensive cost objective function to optimise the designs of the processes for an enantiomeric separation. In this work, this work will be taken a step further to also include batch chromatography with recycle and the Varicol processes when considering column design, configuration and operating policy.

5.2 Principles of the chromatographic alternatives

In this section, the operating principles of the single and multi-column processes, and their operational alternatives are discussed, *i.e.* single column, single column with recycle, SMB and Varicol processes.

5.2.1 Column (batch) chromatography

Conventional batch column chromatography is a well-established technique for efficient separation for preparative purposes and this is reviewed in detail by Guiochon (2002). However, the eluent costs involved can be high and the use of the matrix

(stationary phase) of the column is usually not very efficient. In addition, for difficult separations, the recovery yields obtained can be low for products with high purity constraints. In such cases, other operating policies for the column have to be examined.

5.2.2 Column chromatography with recycling

Employing a recycling operation strategy has been found in the literature to be effective in increasing the recovery yield of the separation and enhance column efficiency (Seidel-Morgenstern and Guiochon, 1993; Heuer *et al.*, 1995; Teoh *et al.*, 2001).

Conventional recycling column chromatography

In conventional (closed-loop) recycling operation, the product from the column is usually recycled back to the column up to several times, with the purified products collected at the end of the last cycle. This combination of increased recovery yields whilst reducing the matrix cost makes this an attractive option for high value product(s) purification. However, for products which are difficult to separate and have a vast overlapping band area between components as a result, this technique is infeasible as recycling actually makes the separation more difficult. This is because the elution peaks become progressively broader and flatter with each recycle, thereby increasing the band overlap area.

Figure 5.1 is a schematic diagram of the closed-loop recycling chromatographic system with a HPLC unit, a high pressure pump, a six-port sample injection valve and an UV detector. An additional four-port valve installed between the detector outlet and the pump inlet allows the operation to be in either conventional elution mode or closed-loop recycling mode.

Recycling The four-port valve is closed and purified samples are pumped back into the column again.

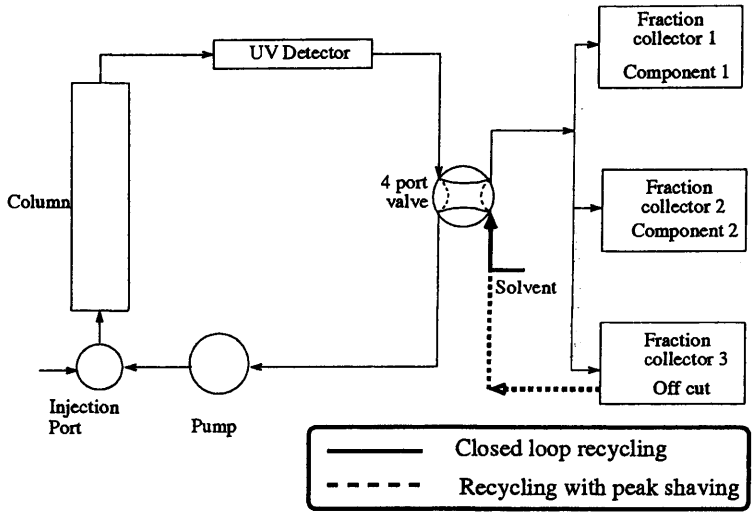

Figure 5.1: Schematic diagram of a chromatographic unit with recycling operation.

Elution The four-port valve is opened and solvent enters the system. The purified samples are collected in the fraction collectors.

Note that one of the effects of closed loop recycling is that with each cycle, the elution profiles of the separated components become progressively flatter, broader and more asymmetrical (Teoh *et al.*, 2001).

Recycling with peak shaving chromatography

With conventional recycle operation in chromatography, the material is usually recycled back to the column several times, with the purified products collected at the end of the last cycle. In contrast, when using a peak shaving technique, the volume of eluent containing sufficiently purified products is collected after each cycle, leaving only the off-specification fractions to be recycled. This accounts for the higher recovery yields achieved when a peak shaving technique is applied.

Implenting a peak shaving technique to conventional recycling chromatography is found to be best suited to difficult separation processes (Teoh, 2002). The main benefit from peak shaving is that the overlapping of peaks stemming from consecutive cycles is averted, as the overall mass being recycled is reduced due to the product collection.

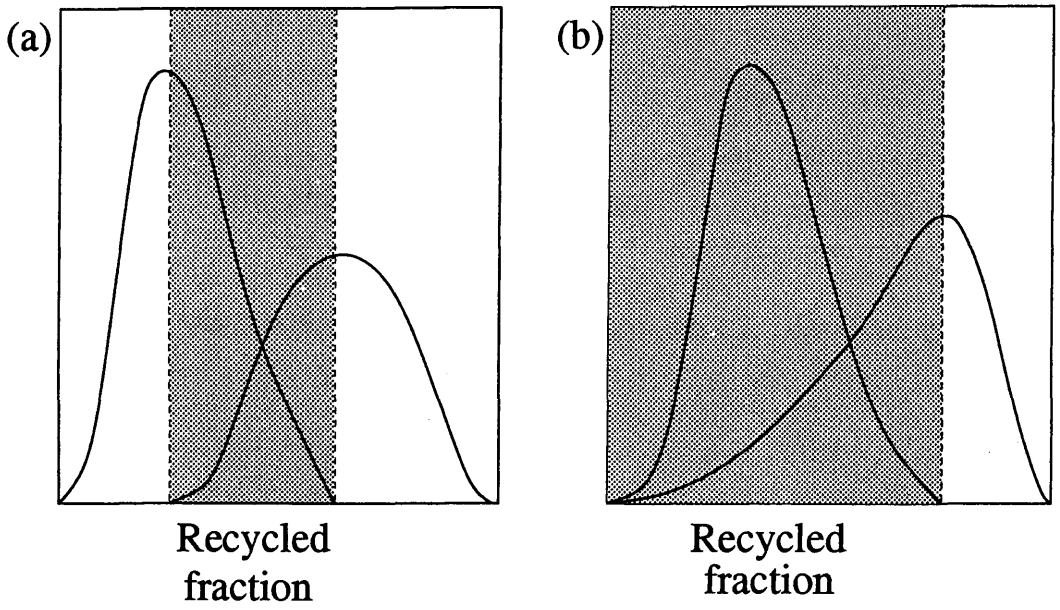

Figure 5.2: Illustration of the different peak shaving modes. The shaded areas show the recycled fractions.

Figure 5.1 shows the alternative recycle path that is followed when a peak shaving technique is implemented.

Two different modes for the peak shaving technique will be considered in this work for a general binary mixture (see Figure 5.2):

1. Fractions of both components that fulfill the purity requirements are collected and only the off-specification fractions are recycled.

2. Only one of the sufficiently purified components is collected and the remainder recycled. (In Figure 5.2, the second component is collected.)

5.2.3 Simulated moving bed chromatography

The main characteristic of a simulated moving bed (SMB) process is its ability to produce large amounts of highly purified products using less eluent as the matrix is more efficiently used. However, the implementation of this process often requires new investment of equipment, *i.e.* existing chromatographic batch columns are usually not applicable, due to the highly automated nature of the SMB process.

5.2.4 Varicol chromatography

The Varicol process is a recent variant form of the simulated moving bed process, where the switching action of the flowrates takes place *asynchronously*. The Varicol process is based on non-simultaneous and unequal shifts of the inlet and outlet ports (Ludemann-Hombourger *et al.*, 2002). An operational schematic of the Varicol process is compared to that of a SMB process in Figure 5.3. Figure 5.3 shows that in a single switching period belonging to the SMB process, the column configuration for Varicol has changed in succession: 1/2/2/1, 2/1/2/1, 2/2/1/1, 1/2/1/2 and finally back to the original configuration of 1/2/2/1 (where each number indicates the number of columns in that section).

Both experimental and computational work has demonstrated that the Varicol can achieve better performances than the SMB, in terms of both increased specific productivity and reduced eluent consumption but at the cost of greater complexity (Ludemann-Hombourger *et al.*, 2002; Zhang *et al.*, 2002; Zhang *et al.*, 2003a).

5.3 Systematic approach

Whilst much work in the literature has focussed on the modelling and optimisation of chromatographic processes, there remains, however, a lack of a methodical procedure to compare the performance of different chromatographic processes for the same separation. In this section, a methodology used to select an appropriate chromatographic processes for a given separation is outlined. Figure 5.4 shows the flowchart to the approach which is detailed in the subsequent sections. The separation problem is formulated such that each process alternative produces the same amount of products at the same product constraints. The model parameters for each process alternative are identified from the literature and/or experimental set-ups, including the determination of any unknown parameters. A scale-up procedure may be necessary for some of the processes to separate the required quantity of products. This is followed by optimisation of all the single and multi-column process

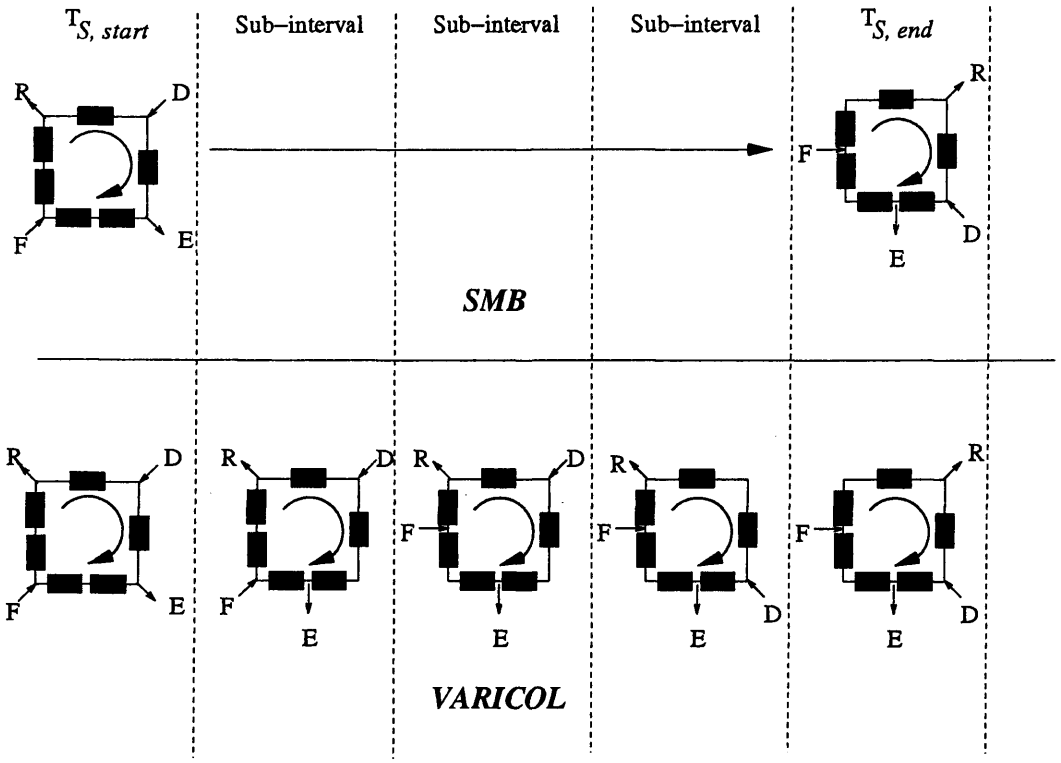

Figure 5.3: Schematic comparison of the operations of the SMB and the Varicol process (Zhang *et al.*, 2003a).
$T_{S,start}$: Start of switching period for SMB, $T_{S,end}$: End of switching period for SMB

alternatives using an economic objective function. Finally, the performances of each process are compared to select the most appropriate one for the given separation.

5.3.1 Separation specification

The action in step I of *separation specification* in Figure 5.4 refers to formulating the separation that is undertaken in all the chromatographic alternatives. There are three main steps in specifying the requirements of the separation, outlined as follows:

- **Step 1** The required *production amount for a single year* is specified.
- **Step 2** The *total number of operating hours for a single year* is specified (which cannot exceed 8760 hours, the maximum number of hours in a year).

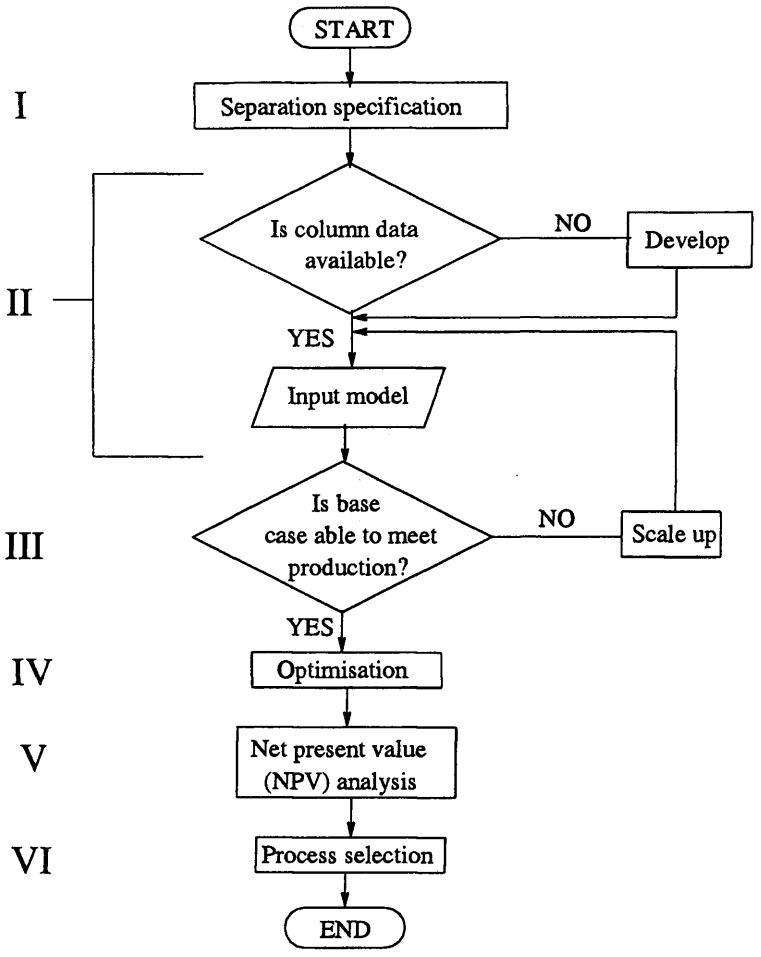

Figure 5.4: Flowchart of the approach for comparing different chromatographic alternatives

- **Step 3** A breakdown of the plant schedule is established *e.g.* for start-up, shut-down, maintenance *etc.* to determine the *actual* number of operating hours for production.

5.3.2 Availability of data

Step II in Figure 5.4 is a decision box where column data for modelling is identified. If no data is available, either from the literature or experimental set-up (which is very rare these days), then the design for each chromatographic unit is necessary. Design of chromatographic processes has been covered extensively in research (*e.g.* Guiochon *et al.*, 1994; Storti *et al.*, 1993). The separation data that is available is

Chromatographic process	Flowrate/Time
Single column	
and	Eluent flowrate
Single column with recycle	
	Recycle flowrate
SMB process	Extract flowrate
and	Desorbent flowrate
Varicol process	Feed flowrate
	Raffinate flowrate
	Switching time(s)

Table 5.1: Model parameters for single and multi-column chromatographic processes

then used in the chromatographic model.

Model parameters

Some model parameters are common in all the different chromatographic processes although they may have different values for each. These include model parameters such as column length L, column diameter D_C, and particle radius R_P. Other common model parameters, like the feed concentration of the components and the isotherm parameters, may not be readily known. For these, the proposed approach outlined in Chapter 3 for the determination of individual feed component concentrations, as well as the estimation of isotherm parameters, can be used.

Other model parameters are the different flowrates and operating policies and/or schedules in each chromatographic process. Table 5.1 tabulates these parameters across the single and multi-column processes.

5.3.3 Scale-up of operation

Given the specified production amount and the available production time for a year, a process able to produce the requisite amount has to be designed or scaled-up from existing designs. In this approach, dimensions from a case study have been employed and scaled up suitably to achieve this production. This can be similarly done for an

Maintain	Bed height
	Eluent velocity
	Sample concentration
	Gradient slope/bed volume (gradient elution)
	Sample residence time
Increase	Column diameter
	Sample volume in proportion to column cross-sectional area
	Volumetric flow rate in proportion to column cross-sectional area
	Gradient volume in proportion to column cross-sectional area
Check	Reduction in supportive wall effects (increased pressure drop)
	Sample distribution (band broadening)
	Piping and system dead volumes

Table 5.2: Guidelines for scale-up of chromatography (Sofer and Hagel, 1997)

existing experimental set-up to determine an industrial scale-up.

In this work, some general recommendations based on work in the literature (Sofer and Hagel, 1997; Li *et al.*, 1998) is used. Sofer and Hagel (1997) recommended the guidelines tabulated in Table 5.2 for scale-up of chromatographic purification. In the process of scale-up, scale factors are used according to some of the guidelines listed in Table 5.2, particularly maintaining the bed height and increasing the column diameter, sample volume and volumetric flowrate. (Refer to the case study in Section 5.4.1 for examples of the calculation details.)

For cases where the model meets the production specified in step I of the approach (see Figure 5.4), the optimisation of the alternatives can then begin.

For a scale up factor used, the following equations are employed:

$$\text{Scaled} - \text{up flowrate} = \text{Base case flowrate} \times \text{Scale up factor}^2 \tag{5.1}$$

$$\text{Scaled} - \text{up diameter} = \text{Base case diameter} \times \text{Scale up factor} \tag{5.2}$$

The injection time (t_{inj}) from the base case is fixed. This means that with

the increased volumetric flowrate, the injected volume increases. To calculate the production in each batch, the following calculations are carried out:

$$\text{Production (g) in 1 batch} = \text{Flowrate} \times t_{inj} \times C_{Feed} \tag{5.3}$$

where C_{Feed} is the feed concentration.

Finally, the annual total production in a year may be calculated using the following equation:

$$\text{Production (kg) per year} = \text{Batch production (kg)} \times \text{Number of batches per year} \tag{5.4}$$

5.3.4 Optimisation

In the following sections, the terms involved in formulating the optimisation problem are outlined: the different aspects of costing that make up the *production cost* and *annual net profit* are defined, followed by the objective functions and the companying optimisation constraints.

Formulating the optimisation problem

A crucial aspect in optimisation is the choice of objective function. In Chapter 2, the wide range of work done in the literature on optimisation of chromatography was reviewed, for single and multi-column chromatographic processes and their various operating policies (Section 2.4). Several objective functions have been proposed in the literature, *e.g.* Guiochon *et al.* (1994), Felinger and Guiochon (1996a, b); Teoh *et al.* (2001), Jupke *et al.* (2002), Zhang *et al.* (2003a) *etc.*. Amongst these, however, only the work of Jupke *et al.* (2002) has considered the economic implications in the optimisation to provide a real comparison of the process economy for batch (column) and SMB chromatography. The work of Jupke *et al.* is extended in this work to include a recycling policy for the single column and also to consider

the Varicol process. In the following sections, the costs involved in the chromatographic process are outlined, and the objective function and process constraints of the problem are highlighted.

Production costs

In this section, the *production costs* and the definition of the *net profit* for each chromatographic unit are outlined, as they are terms used in the objective function.

Labour and maintenance (operation) costs The labour and maintenance (operation) costs are assumed to be a cost factor of a certain plant size, and dependent on the operating time. The total annual operating costs may be written as:

$$C_{op}^{annual} = C_{op}^{h} t_{op} \tag{5.5}$$

where C_{op}^{annual} is the total operating cost, C_{op}^{h} is the operating costs per hour and t_{op} is the annual operation time of the plant.

Eluent cost A popular comparison between single and multi-column processes is in terms of the amount of eluent used. Thus, the cost of the eluent is an important factor to be considered in the objective function. The annual eluent costs, C_{el}^{annual} may be written as:

$$C_{el}^{annual} = \frac{E_c}{t_{cycle}} t_{op} C_{el} \tag{5.6}$$

where E_c is the eluent consumption over one cycle, t_{cycle} the time taken to complete one cycle (of the column/column with recycle/SMB/Varicol process), t_{op} is the annual operation time of the plant and C_{el} is the cost per kilogram of eluent.

Adsorbent cost The cost of the adsorbent, or matrix, in a chromatographic column is normally high. Often, these are highly specific to the separation involved, *i.e.* the cost is fixed. However, adsorbents also have a finite lifetime in which they

can be used for chromatographic separations. Hence, the cost of the adsorbent is an important factor:

$$C_{ads}^{annual} = \frac{t_{op}}{t_{life}} V_c \rho_{app} C_{ads} \tag{5.7}$$

where C_{ads}^{annual} is the annual cost of the adsorbent, t_{op} is the annual operation time of the plant, t_{life} is the lifetime of the adsorbent, V_c is the volume of the column, ρ_{app} is the apparent density of the adsorbent and C_{ads} is the cost per kilogram of adsorbent. The adsorbent cost used is also assume to take into account the capital costs for the column size (as both depend on the column volume, V_c).

Cost of waste In all separations, there will inevitably be some waste products arising from the separation. These include impurities in the feed mixture or off-specification products where it is no longer economically viable to further purify them. The cost of this waste generated needs to be accounted for, and the cost of the crude loss of product defined in Jupke *et al.* (2002) is used as an estimate.

$$C_{waste}^{annual} = \frac{M_{waste}}{t_{cycle}} t_{op} C_{waste} \tag{5.8}$$

where C_{waste}^{annual} is the total annual cost of the waste products generated, M_{waste} is the mass of waste products generated over one cycle, t_{cycle} the time taken to complete one cycle (of the column/column with recycle/SMB/Varicol processes), t_{op} is the annual operation time of the plant and C_{waste} is the cost per kilogram of waste generated.

Total production cost The total annual cost for each chromatographic process may be written as follows:

$$C_{Total}^{annual} = C_{op}^{annual} + C_{el}^{annual} + C_{ads}^{annual} + C_{waste}^{annual} \tag{5.9}$$

The overhead costs (*e.g.* utility, facility costs *etc.*) are considered to be negligible in comparison to the rest of these other costs and are thus disregarded in this cost

function.

Sales income The sales income, also viewed as the net profit, is the difference between the amount of money made from the sales of the product and the cost of processing the product. The latter includes not only the production costs outlined earlier in this section, but also the costs of the raw material used to make the product.

Net profit The annual net profit for each chromatographic process may be written as follows:

$$P^{annual} = S_{income}^{annual} - C_{Total} - C_{RM} \tag{5.10}$$

where P^{annual} is the net annual profit, S_{income} is the annual sales income from selling the purified products produced, C_{Total}^{annual} is the annual total production costs and C_{RM} is the cost of the raw material.

Outline of optimisation problem

The optimisation is conducted using three objective functions (1) maximising the recovery yield and productivity, (2) minimising annual production costs and (3) maximising annual net profit.

The following definitions are used in the optimisations conducted:

$$Pr_i = \frac{\text{Mass of i produced}}{\text{Batch time} \times \text{Column volume}} \tag{5.11}$$

$$Pu_i = \frac{\text{Mass of i produced}}{\text{Mass of total mixtureproduced}} \tag{5.12}$$

$$Y_i = \frac{\text{Mass of i produced}}{\text{Mass of i fed to column}} \tag{5.13}$$

where Pr_i, Pu_i and Y_i are the productivity, purity and recovery yield of component i, respectively.

Recovery yield and production rate The recovery yield and production rate can be maximised simultaneously using a hybrid objective function, proposed by Felinger and Guiochon (1996b), which is a product of the productivity and recovery yield.

$$\max_{\tau,u(t)} \Phi(Y_A \times Pr_A) \tag{5.14}$$

subject to the constraints given by:

$$Pu_i^{min} \leq Pu_i \leq 1 \tag{5.15}$$

$$Y_i^{min} \leq Y_i \leq 1 \tag{5.16}$$

$$\Delta P_j^{min} \leq \Delta P_j \leq \Delta P_j^{max} \tag{5.17}$$

Generally, the single column processes have a lower recovery yield compared to the multi-column processes. Jupke *et al.* (2002) demonstrated recovery yields of 96% and 100% for the optimised batch and SMB chromatographic processes, respectively. As the scaled-up case shows the SMB/Varicol processes to have high recovery yields already, this optimisation will focus on the single column processes.

Annual production cost If the objective function in the optimisation is to minimise the production costs (C_{Total}) for the separation of a *fixed* feed amount in all the chromatographic processes, subject to the purity and recovery yield constraints, then the following equations apply:

$$\min_{\tau,u(t)} \Phi(C_{Total}^{annual}) \tag{5.18}$$

where C_{Total}^{annual} is the annual net profit, and the optimisation is subject to the constraints as given in Equations 5.15, 5.16 and 5.17.

where τ is the total time horizon and $u(t)$ is the vector of control variables. Pu_i and Y_i are the purity and recovery yield of component i, respectively, whilst ΔP_j is the pressure drop across column j. (Other constraints can, of course, be used instead of these if purity and recovery are not of major concern.)

In the chromatographic processes considered here, the control variables are the valve switching actions (*e.g.* during product collection in column chromatography, or flowrate switching in the SMB/Varicol process). The full definitions of these system performance parameters for optimisation are given in Appendix C.2.

Annual net profit For the scenario where the objective is the annual profit made is maximised, the following objective function is used:

$$\max_{\tau,u(t)} \Phi(P^{annual}) \tag{5.19}$$

where P^{annual} is the annual net profit, and the optimisation is subject to the constraints as given in Equations 5.15, 5.16 and 5.17.

The choice of the objective function depends largely on the aim of the optimisation. Minimising the production cost (Equation 5.14) should be used when seeking to lower the production cost of the process (say for eluent and adsorbent costs) *and* when the profit margin is not a constraint. Otherwise, the net profit objective function (Equation 5.19) should be used, as it incorporates aim the minimisation of the production costs as well and maximising the sales income to do this.

5.3.5 Costing and project evaluation

An economic appraisal is carried out on each of the optimised chromatographic alternatives, where the cashflow of implementing each process in a plant over a number of years is considered.

Investment breakdown estimation

The *fixed capital investment* (FCI) is the total amount of money needed to supply the necessary plant and manufacturing facilities, in addition to the finances required as working capital for operation of the facilities (Peters *et al.*, 2003). One way of estimating the cost components in the capital investment is to assume each component as a percentage of the equipment delivery cost. The calculations of the capital cost for single and multi-column processes can be found in Appendix H.

Table 5.3 shows a plant unit whose delivered purchase cost is US $10,000 and the estimation of its capital cost using the percentage breakdown in Peters *et al.* (2003).

Direct costs are costs which are directly related to the plant unit purchased and other equipment/facilities that are necessary for operation and accommodation of the unit. *Indirect costs* refer to costs which are also necessary to the completion of the installation of the unit but more of non-manufacturing nature. The *working capital* is the capital that is necessary for the operation of the plant initially, such as the raw materials or finished products in stock and cash on hand for any payments.

Economic appraisal

Having thus obtained a full costing of each process for a full operating year from the preceding sections, the economic performance of these different chromatographic processes are examined using economic evaluation tools (refer to I for full details on these) in step V of the approach in Figure 5.4.

The capital costs of each chromatographic unit is estimated at this stage (and this work uses the delivered equipment costing method in Peters *et al.* (1999)). Subsequently, a basic Net Present Value (NPV) analysis of the chromatographic units over a fixed number of years is done (for more details, see Sinott (1999)) and the discounted cash flow diagram is drawn up to view the economic performance of the different separation units over time. As different forms of economic appraisals exist and may vary according to the institutions/companies using these, any of these

Components	**Percentage of delivered equipment cost**	**Estimated cost (US $)**
Direct costs		
Purchased equipment delivered (including fabricated equipment, process machinery, pumps and compressors)		10, 000
Purchased-equipment installation	0.39	3,900
Instrumentation (installed)	0.26	2,600
Piping (installed)	0.31	3,100
Electrical (installed)	0.1	1,000
Buildings (including services)	0.29	2,900
Yard improvements	0.12	1,200
Service facilities (installed)	0.55	5,500
Indirect costs		
Engineering and supervision	0.32	3,200
Construction expense	0.34	3,400
Legal expense	0.04	400
Contractor's fee	0.19	1,900
Contingency	0.37	3,700
Total (FCI)		42,800
Working capital*	0.75	7,500
Total capital investment		**50, 300**

Table 5.3: Estimated capital costs based on percentage of delivered-equipment cost method for a plant unit costing US $10,000(Peters *et al.*, 2003)
(*or approximately 15% of total capital investment)

appraisals may be used at this stage.

5.3.6 Process selection

The analysis for the process selection is done by comparing the cash flow diagrams across the different chromatographic alternatives. The performances of each unit varies over time and these must also be compared.

5.3.7 Summary

In this section, based on the previous research done in the area of optimisation of chromatographic processes, the necessity for formulating an optimisation based on *economic principles* is emphasised. Some of the economic terms used as a basis for the objective functions are also detailed, and the optimisation problem is defined along with its constraints. Thus, the single and multi-column processes are optimised using the objective function (Equations 5.14 or 5.18) and subject to the constraints (Equations 5.15, 5.16 and 5.17).

5.4 Case study

A case study will be used to illustrate the approach proposed in this chapter. The case study is based on the parameters and operating conditions presented by Dünnebier *et al.* (1998). Their work originally examined the separation of a binary mixture for an SMB process. This is now extended to single column processes. The components of the binary mixture are labelled A and B for the purposes of this work.

5.4.1 Employing the systematic approach

The systematic approach outlined in Section 5.3 and in Figure 5.4 is employed in this case study, with each step explained.

I Separation specification

The procedure for specifying the separation is outlined as follows:

- **Step 1** The *production amount for a single year* is a *minimum* of 2000 kg of product (1000 kg each of A and B).
- **Step 2** The *total number of operating hours for a single year* is 8000 hours.
- **Step 3** The start-up/shutdown/maintenance time is assumed to be about 20% of the production time.

II Availability of data

The column dimensions, the feed concentrations and isotherms are known and tabulated in Table 5.4. In addition, Table 5.4 summarises the model parameters across the single and multi-column processes used in this case study, adapted from the work of Dünnebier *et al.* (1998).

The work of Dünnebier *et al.* (1998) provides the dimensions for columns in the SMB unit *only*. As there is no information available on single columns for a similar separation, the column dimensions (Table 5.4) of the SMB unit are used for single column process in order to calculate its annual production . $10ml$ of the feed is loaded onto the single column, and takes approximately 100 minutes to elute from the column. Thus, in one year, the single column produces 4800 batches. Table 5.5 shows a summary of similar calculations for the annual production in other chromatographic processes.

In this work, the subintervals of switching for the Varicol process are made equal *i.e.* $0.25T_{Switch}$, $0.5T_{Switch}$, $0.75T_{Switch}$ and T_{Switch}, at which the flowrates of extract, feed, desorbent and raffinate are changed, respectively (refer to Figure 5.3 for an illustration). This is because with a dimensionless time unit, θ, as used in the model, the time interval for each switching action must be specified *a priori*.

	Column length (cm) 47.5 **Column diameter (cm)** 1.4 **Feed concentration** A = 0.05, B = 0.05 **Isotherm coefficients** $K_A = 0.56$, $K_B = 0.23$
Chromatographic process	**Flowrate** (cm^3/s)
Single column and Single column with recycle	Eluent flowrate 0.0166
Recycle flowrate 0.0665	
SMB process and Varicol process	Extract flowrate 0.0233 Desorbent flowrate 0.0266 Feed flowrate 0.0166 Raffinate flowrate 0.0199
SMB process	Switching time 618 seconds
Varicol process	4 equal subintervals adding up to 618 seconds

Table 5.4: Model parameters from Dünnebier *et al.* (1998) for single and multi-column chromatographic processes

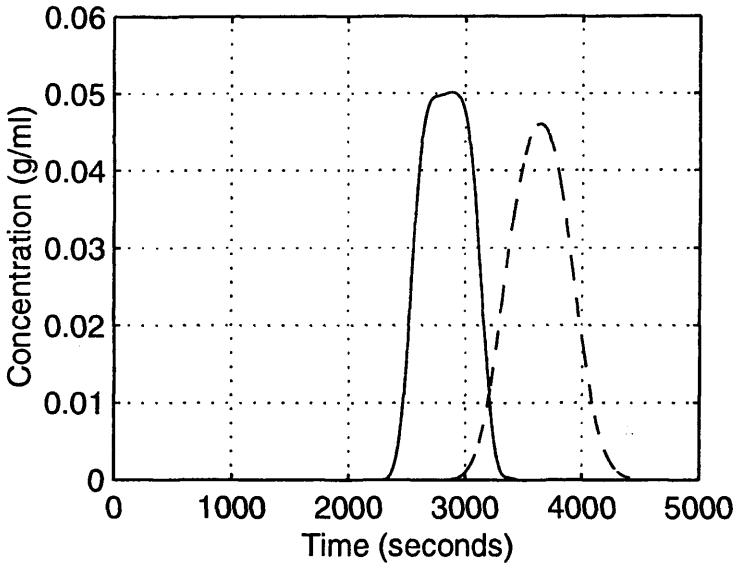

Figure 5.5: Elution profile for single column using the column dimensions in Dünnebier *et al.* (1998)
('- - -': Component A, '—': Component B)

III Scale-up of operation

The guidelines recommended earlier (Table 5.2) are used to scale up the parameters from the work of Dünnebier *et al.* (1998) from their production amounts in Table 5.5 to producing 1000kg *each* of component A and B annually. (These scale up calculations may be found in Appendix H.) Table 5.7 summarises all the scaled-up parameters from the *base case* (Table 5.4). The parameters which are increased are the diameter(s) and flowrates. In the multi-column processes, the same switching period is retained to maintain the elution profiles from the case study and only the flowrates and column diameters are scaled up. Likewise, the single column retains the same elution profile when its diameter and eluent flowrate are scaled up. Table 5.7 shows the flowrates and diameters that have been scaled up using the scale up factors in Table 5.6. For more details on the scale up calculations, refer to Appendix H.

Chromatographic process	Production per batch (g)	Batch time (min)	Number of batches in 1 year	Amount produced (kg/year)
Single column	0.50	100	4800	2.40
Single column with recycle	0.50	170	2880	1.44
SMB and Varicol	0.13	10.3	5820	23.88

Table 5.5: Estimates for base case production calculation, using the model parameters in Dünnebier *et al.* (1998)

Chromatographic process	Scaled-up case annual production (kg)	Scale up factor	Scaled-up annual production (kg)
Single column	2.40	21	1060
Single column with recycle	1.44	37.8	1050
SMB and Varicol	23.88	6.5	1010

Table 5.6: The scaled-up chromatographic units

Chromatographic process	**Flowrate** (cm^3/s)	**Diameter** (cm)
Single column	Eluent 8.03	30.8
Single column with recycle	Eluent 14.94	42
SMB process and Varicol process	Recycle flowrate 3.740 Extract flowrate 1.3106 Desorbent flowrate 1.496 Feed flowrate 0.9338 Raffinate flowrate 1.1192	10.5

Table 5.7: Model parameters in the scaled up case for single and multi-column chromatographic processes

Parameter	**Cost (US $)**
Adsorbent cost C_{ads} (US $/g)	13.45
Eluent cost C_{el} (US $/ml)	4.7×10^{-4}
Operation cost C_{op}^{h} (US $/h)	22.4
Raw material cost (US $/g)	7.17
Waste cost* C_{waste}(US $/g)	1.5

Table 5.8: Estimated costs factors used to establish production cost and net annual profit, from Jupke *et al.* (2002) except *
(* estimated)

IV Optimisation

Table 5.8 shows the different cost factors that make up the production costs, and these are employed in the economic evaluation. The purities and recovery yields of the products for each of the chromatographic processes of the scaled up case are summarised in Table 5.9.

Three scenarios are explored in the optimisation studies carried out. In Scenario I, the single column processes are optimised for a hybrid function of production rate and recovery yield for each of the components A and B. In Scenario II, the annual production costs across the single column and multi-column processes are minimised. Finally, in Scenario III, the annual net profit of all the processes are maximised.

	Component 1	Component 2
Single column		
Purity	0.997	0.995
Recovery yield	0.913	0.837
Function($Pr_i \times Y_i$)	9.49×10^{-7}	7.989×10^{-7}
Single column with recycle		
Purity	0.997	0.995
Recovery yield	0.930	0.867
Function($Pr_i \times Y_i$)	5.78×10^{-7}	5.04×10^{-7}
SMB unit		
Purity	0.9956	1
Recovery yield	1	0.99
Varicol unit		
Purity	0.9997	0.9965
Recovery yield	0.9998	0.997

Table 5.9: Scaled-up case results for purities and recovery yields

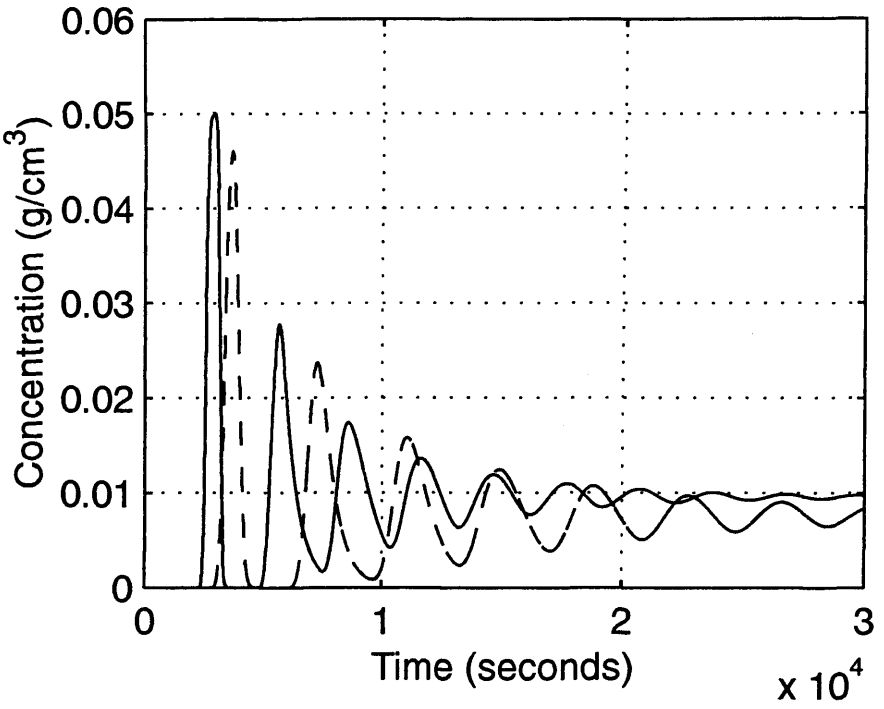

Figure 5.6: Elution profile for case study employed under a closed-loop recycling scheme

('- - -': Component A, '—': Component B)

Recycling policy in single column chromatography Section 5.2.2 has briefly outlined a few of the recycling policies employed in chromatography for single columns. The operating policies for closed-loop recycling chromatography with and without a peak shaving technique are demonstrated for this case study to determine which of these two policies will should be implemented in the single recycle column. Figure 5.6 shows the outcome for the conventional closed-loop recycling policy employed, and it is evident that this policy is unsuitable for this separation as the recycled profiles overlap too closely with the previous profiles. A peak shaving technique is thus implemented in the recycling policy to improve the separation.

Scenario I: Maximising recovery yield and production rate Single column processes generally have a lower recovery yield compared to the multi-column processes. In this scenario, both the design and operation of the single column and

single column with recycle is optimised to maximise their recovery yield and productivity. The hybrid objective function proposed by Felinger and Guiochon (1996b), *i.e.* a product of the productivity and recovery yield, is used. These functions are maximised for components A and B and discussed in the following sections.

Maximising recovery yield function of extract (component A) The yield and production rate of the extract is improved for the single column and single column with recycle using the objective function:

$$\max_{\tau,u(t)} \Phi(Y_A \times Pr_A) \tag{5.20}$$

subject to constraints

$$0.995 \leq Pu_A \leq 1 \qquad 0.995 \leq Pu_B \leq 1 \tag{5.21}$$

$$0.80 \leq Y_A \leq 1 \qquad 0.80 \leq Y_B \leq 1 \tag{5.22}$$

$$13\text{bar} \leq \Delta P \leq 100\text{bar} \tag{5.23}$$

The results of the optimisation carried out is tabulated in Table 5.10. The column with a recycling policy collapses to a single column without recycle, as the optimised number of cycles was 1, and gave the same optimised model parameters as the single column optimisation. The recovery yield of component A was improved using the optimised results from 0.913 to 0.916 for the single column, whilst in the column model with a recycling policy, the recovery yield of component A decreased from 0.930 to 0.916. This is likely as a result of the significant increase in the productivity from 9.49 $\times 10^6 gs^{-1}cm^{-3}$ to 15.08 $\times 10^6 gs^{-1}cm^{-3}$ (nearly 60% increase) for a single column without recycle, and the slight drop in recovery yield does not compromise the large increase in productivity in the hybrid function. In both cases, however, the recovery yields of component B dropped marginally as the objective function was based on A only.

Single column		
	Scaled- up case	*Optimised case*
Diameter (cm)	30.8	15.76
Length (cm)	47.5	100*
Eluent flowrate (ml/s)	8.03	4.68
Pu_A	0.997	0.995
Pu_B	0.995	0.995
Y_A	0.913	0.916
Y_B	0.837	0.8*
Pr_A $(\times 10^{-7})$	10.39	16.47
Function $Pr_A \times Y_A$ $(\times 10^{-7})$	9.49	15.08
C_{Total}^{annual}	1, 078, 000	813, 000
$P^{annual} \times 10^6$	3.49	2.02
Single column with recycle		
	Scaled-up case	*Optimised case*
Diameter (cm)	42	15.76
Length (cm)	47.5	100*
Eluent flowrate (ml/s)	14.94	4.68
Cycle	2	1
Pu_A	0.997	0.995
Pu_B	0.995	0.995
Y_A	0.930	0.916
Y_B	0.867	0.8*
Pr_A $(\times 10^{-7})$	5.29	16.47
Function $Pr_A \times Y_A$ $(\times 10^{-7})$	4.92	15.08
C_{Total}^{annual}	1,037,000	813, 000
$P^{annual} \times 10^6$	3.37	2.02

Table 5.10: Optimisation results for Scenario I: maximising the hybrid function for component A

(*optimised result on bound)

There was also a slight decrease in the total annual production cost and the annual net profit in carrying out this optimisation. This is probably because of the decrease in the recovery yield of component B.

Maximising recovery yield function of raffinate (component B) The recovery yield of the raffinate is improved for the single column and single column with recycle using the objective function:

$$\max_{\tau,u(t)} \Phi(Y_B \times Pr_B) \tag{5.24}$$

subject to constraints in Equations 5.21, 5.22 and 5.23.

The results of the optimisation carried out is tabulated in Table 5.11. Similarly, the optimal number of cycles for the single column with recycle is 1 and it thus produced identical optimised parameters as the single column. From these results, the recovery yield of the raffinate was significantly improved upon using the optimised results from 0.837 to 0.895 in the single column (though slightly less for the single column with recycle from 0.867 to 0.895). The productivity of the single column doubled from 7.99 $\times 10^6 gs^{-1}cm^{-3}$ to 12.85 $\times 10^6 gs^{-1}cm^{-3}$, whilst for the single column with recycle, it increased nearly threefold (similar to the previous optimisation).

This suggests that the single column with recycle is likely to collapse to a single column when the productivity of the process is involved, as a single column operation has a much greater productivity. There was a significant decrease in the total annual production cost and the annual net profit in carrying out this optimisation. This is probably because of the large decrease in the recovery yield of component A from 0.913 to 0.800 for the single column.

Scenario II: Minimising total production cost Table 5.12 outlines the decision variables of each process in the optimisations done in Scenarios II and III. The single column has an extra decision variable as compared to the single column: the optimal number of cycles in the operation. The production amount is fixed in

Single column		
	Scaled-up case	*Optimised case*
Diameter (cm)	30.8	16.69
Length (cm)	47.5	100*
Eluent flowrate (ml/s)	8.03	4.73
Pu_A	0.997	0.995
Pu_B	0.995	0.995
Y_A	0.913	0.800*
Y_B	0.837	0.895
Pr_B ($\times 10^{-7}$)	9.55	14.36
Function $Pr_B \times Y_B$ ($\times 10^{-7}$)	7.99	12.85
C_{Total}^{annual}	1,078,000	642, 000
$P^{annual} \times 10^6$	3.49	1.94
Single column with recycle		
	Scaled-up case	*Optimised case*
Diameter (cm)	42	16.69
Length (cm)	47.5	100*
Eluent flowrate (ml/s)	14.94	4.73
Cycle	2	1
Pu_A	0.997	0.995
Pu_B	0.995	0.995
Y_A	0.930	0.800*
Y_B	0.867	0.895
Pr_B ($\times 10^{-7}$)	4.94	14.36
Function $Pr_B \times Y_B$ ($\times 10^{-7}$)	4.29	12.85
C_{Total}^{annual}	1, 037, 000	642, 000
$P^{annual} \times 10^6$	3.37	1.94

Table 5.11: Optimisation results for Scenario I: maximising the hybrid function for component B

(*optimised result on bound)

Single column	**Single column with recycle**	**Simulated moving bed process**	**Varicol process**
- Column length	- Column length	- Column length	- Column length
- Column diameter	- Column diameter	- Column diameter	- Column diameter
- Eluent flowrate	- Eluent flowrate	- Eluent flowrate	- Eluent flowrate
- Fraction cut times	- Fraction cut times	- Switching time	- Switching times
	- Number of cycles	- Raffinate flowrate	- Raffinate flowrate
		- Extract flowrate	- Extract flowrate
		- Desorbent flowrate	- Desorbent flowrate
		- Recycle flowrate	- Recycle flowrate

Table 5.12: Decision variables in optimising all four chromatographic processes

all optimisation at 1010 kg *each* of component A and B, to fulfill the separation specifications stated earlier. Thus, in the SMB/Varicol processes, the feed flowrate is a fixed value.

$$\text{Production amount} = \text{Feed flowrate} \times \text{Feed concentration} \times t_{op} \tag{5.25}$$

where t_{op} is the annual operating time.

In this optimisation, the total annual production cost is examined for all four chromatographic alternatives: single column, single column with recycle, simulated moving bed and Varicol processes. In this scenario, the objective function is the minimisation of the *total operating costs* of each process, as defined in Equation 5.9:

$$\max_{\tau, u(t)} \Phi(C_{Total}) \tag{5.26}$$

subject to the constraints in Equations 5.21, 5.22 and 5.23.

Table 5.13 show the optimisation results for all the different processes when minimising the total production cost. The optimal number of cycles in the single column with recycles is 1, *i.e.* it collapses to a single column. Both models thus produce the same optimised design and operation parameters in the optimisation.

	Single column	**Single column with recycle**	**Simulated moving bed process**	**Varicol process**
Diameter (cm)	19.45	19.45	8.43	7.86
Length (cm)	100	100	20	35.43
Flowrate (ml/s)	5.45	5.45	Recycle: 2.641 Extract: 1.100 Desorbent: 1.230	Recycle: 2.82 Extract: 1.011 Desorbent: 1.063
Number of cycles	-	1	-	-
Switching time (s)	-	-	234	87 each subinter
Pu_A	0.995	0.995	0.995	0.995
Pu_B	0.995	0.995	0.995	0.995
Y_A	0.80	0.80	0.995	0.995
Y_B	0.98	0.98	0.995	0.995
C_{Total}^{annual} (US \$)	536, 000	536, 000	268, 000	309, 000
P^{annual} (US \$) $\times 10^6$	3.00	3.00	5.37	5.36

Table 5.13: Optimisation results for Scenario II

The annual net profit for the single column process falls from US \$ 3.49 $\times 10^6$ to US \$3.00 $\times 10^6$, although the annual production cost is lowered to US \$536, 000 from US \$1, 078,000. The lowered annual net profit suggests that the sales income is lower in the optimised case. The single column shows a much higher total production cost, just over twice that of the SMB process.

The multi-column processes have higher annual net profits than the single column processes as the recovery yields are maintained at a high value of 0.995. The high recovery yields are characteristic of the SMB/Varicol processes and show that even at lower costs, these cannot be reduced or the separation is compromised in the unit.

Scenario III: Maximising annual profit In this scenario, another economic objective function, the *annual profit* of all the processes is subject to scrutiny. In the previous section, the minimisation of the production costs was conducted and was used in the work of Jupke *et al.* (2002). However, the productivity of the process is not included in the objective function and may be compromised to achieve lower costs. This idea is further explored by including the annual profit explicitly in the

	Single column	**Single column with recycle**	**Simulated moving bed process**	**Varicol process**
Diameter (cm)	22.34	22.34	7.03	8.95
Length (cm)	100	100	29.57	22.46
Flowrate (ml/s)	6.59	6.59	Recycle: 3.096 Extract: 1.509 Desorbent: 1.751	Recycle: 1.72 Extract: 1.45 Desorbent: 1.72
Number of cycles	-	1	-	-
Switch time (s)	-	-	200	218
C_{Total} (US \$)	607, 000	607, 000	278, 000	296, 000
P^{annual} (US \$) $\times 10^6$	5.02	5.02	5.43	5.38

Table 5.14: Optimisation results for Scenario III

objective function:

$$\max_{\tau, u(t)} \Phi(P^{annual}) \tag{5.27}$$

subject to the constraints in Equations 5.21, 5.22 and 5.23.

The profit values in Table 5.14 differ slightly from those obtained in Table 5.13. In this scenario, the profit is employed in the objective function and in this manner, the productivity of the process is also considered, alongside the production costs. It is evident that minimising the production costs (see Table 5.13) does not necessarily lead to maximum profit for the process.

This scenario repeats the previous scenario, where the optimal number of cycles in the single column with recycle collapses to a single column and produces the same optimised results. Notably, the net profit of the single column is markedly increased, compared to those obtained with the optimisations in Scenarios I and II. Whilst the increment in the net profit is marginal for the SMB/Varicol process from the previous scenario, the annual net profit of the SMB process is about 8% higher than that of the single column when both are optimised.

Chromatographic process	**Estimated cost US $**
Single column and Single column with recycle	754, 500
SMB process and Varicol process	1, 630, 000

Table 5.15: Estimated capital costs based on percentage of delivered-equipment cost for all chromatographic processes considered

V Economic appraisal of the separation

An economic appraisal of the separation is conducted, based on Scenario III, to determine the most profitable separation process after a plant life period of 15 years.

Capital costs of units Table 5.15 shows the capital cost of the chromatographic units based on the delivered-equipment cost (Peters *et al.*, 2003). The breakdown of the cost and its calculations are detailed in Appendix H. The capital costs of the units are taken into account in the Net Present Value (NPV) calculations.

Cash flow diagram In this section, the maximum annual profit operation of all the four chromatographic processes are subjected to an economic analysis where the cash flows for each process area evaluated over 15 years to demonstrate the value of their investment to a project. (Appendix I may be referred to for more details on the terms commonly used in such appraisals.) It is assumed that the maximised net profit in Table 5.14 is made each year of the plant life.

The cumulative discounted cash flow (DCF) diagrams, using a 15% discount, for all processes are shown together in Figure 5.7. The cumulative DCF diagram reflects the value of the profits made over the present time, hence the cash flows appear to level off with time, despite a fixed annual net profit assumed each year. The single

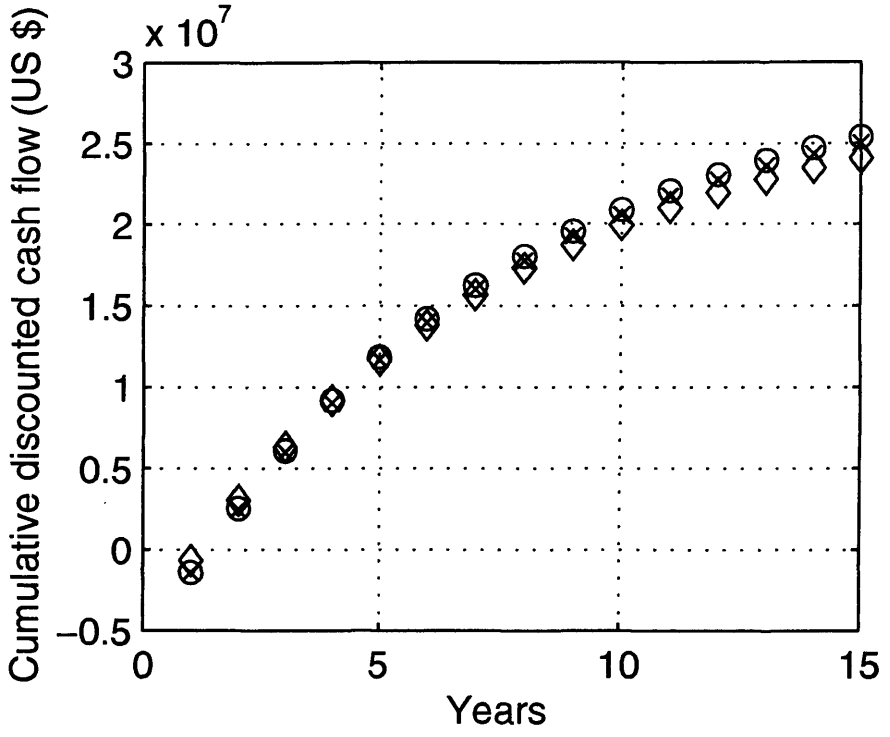

Figure 5.7: Discounted cumulative cash flow figure for all chromatographic alternatives
◇: Single column, ○: SMB unit and ×: Varicol unit

column with recycle is shown to have an optimum value of 1 cycle *i.e.* collapsing to a single column without recycle. Thus, in Figure 5.7, the three processes shown are the single column, SMB and Varicol processes.

Initially, the single column has the best economic performance among all the processes, which is expected, given its capital cost is half that of the multi-column processes. This also means that the single column has a shorter payback time, as compared to the multi-column processes, although this is only a difference of a few months. However, by the fifth year, all three processes show the same cumulative DCF value, and the multi-column processes are more profitable than the single column. The SMB process is the strongest performer at the end of 15 years, with the Varicol process second and the single column last, although it was initially first.

Thus, an important consideration for investment of a process is the time of the

plant life. For this case study, for a long term (more than 5 years) investment, the SMB/Varicol process is a better option. The cumulative DCF also shows that whilst the net profit of the SMB process is only slightly higher than that of the Varicol process (US $\$5.43 \times 10^6$ and US $\$5.33 \times 10^6$, respectively), this difference is significant over time.

VI Process selction

Amongst the processes explored, the single column is demonstrated to be the least cost-efficient over time, even though its capital cost is not the highest. Initially (time 0 to 5 years), it has a greater cash flow than either SMB/Varicol units but this is only up to the first 3 years. This is largely due to the high production costs associated with this process because of the size of the single column (and hence the amount of absorbent) and the eluent consumption. Table 5.14 shows that at the optimum, the annual production cost of the single column is more than twice that of the SMB unit.

The economic performances of the multi-column processes appear to be very similar to each other over the first 8 years, although after this, the SMB process has a markedly higher cumulative DCF. This suggest that there is little difference in using either of the processes over the first 8 years and that SMB should evidently be the first choice for selection as it is the most profitable process at the end of the plant life.

However, the optimisation has been limited for the multi-column processes in two aspects:

1. The column configuration of the multi-column processes has not been optimised in this case study, *i.e.* the column configuration of 2/2/2/2 is fixed, due to the difficulties encountered in optimising such a complex model. Literature has suggested that the Varicol processes save on adsorbent cost (by using less columns) and are hence more attractive than the SMB unit.

2. The Varicol process is limited to equal sub-intervals of switching times, as a limitation of the CSS model implemented. This means that the other potential degrees of freedom in unequal switching times has not yet been explored.

Even with these limitations, however, the multi-column chromatographic processes are evidently the best choice for this case study.

5.5 Concluding remarks

In this chapter, a systematic approach for the optimisation of single and multi-column processes has been demonstrated. A case study is used to demonstrate the approach and each process is scaled-up to produced a specific amount of products of a required purity. Subsequently, the processes are optimised for three different scenarios.

Scenario I only involved the single column processes to demonstrate that optimisation can improve the design of the column such that its results are comparable with the multi-column processes. Using a hybrid objective function including the productivity and recovery yield of one of the products, can greatly improve the recovery yield of the single column processes. Scenario II and III were optimisations conducted for all single and multi-column processes, and show that the minimisation of the production costs of the process did not necessarily lead to the maximum profit, although the results were not far off.

All three scenarios showed the single column with recycle collapsing to a single column, with an optimal number of cycles at 1. Figure 5.6 shows that the overlap increases with the number of recycles for the conventional closed-loop recycling policy, and thus a peak shaving technique is implemented for the mixed fractions in the overlap area. However, as the retention times for the components are long, a single column operation is able to handle the separation when it is optimised. The need for the recycling policy in the optimisation may vary with the objective function used as well, since the objective functions examined in the three scenarios

favour high productivity, which the single column without recycle is predisposed to.

Some interesting results were shown in the economical appraisal, which was conducted for the maximum profit results found in Scenario III. It was demonstrated that whilst the single column initially showed a strong economic performance against its multi-column counterparts, this gradually deteriorated with time due to its operating costs being twice as much as the multicolumn-processes. The SMB process proved to be the best choice for this case study.

In other situations, such as where the comparison is made between an existing single column process and the new implementation of a multi-column process, or the separation requirements are different, this appraisal will change. For example, if a single column is already implemented in the plant, its capital cost will be lower and may thus be more profitable than a multi-column process. In another instance, if the investment is a short-term one, the single column may be a economically more viable one with its low capital cost. The single column with a recycling policy may also be more feasible optimally in other separations to lower production costs for the single column operation.

Chapter 6

Conclusions and recommendations for future work

This chapter summarises the main findings of this research into systematic approaches for the modelling and optimisation of chromatographic processes (Section 6.1). Directions for future work are also outlined (Section 6.2).

6.1 Conclusions

The primary objectives in this research were to resolve the issues of 1) the choice of mathematical models employed for a chromatographic separation and 2) to compare the different chromatographic configurations applied to the same separation. In addressing these issues, it was deemed necessary to establish systematic approaches to develop dynamic mathematical models for complex bio-separations and subsequently to optimised such separations using the models.

The literature review in Chapter 2 showed that whilst much has been achieved in the mathematical modelling of chromatography, comparative studies of the different models used in chromatography were relatively few. In addition, much of the

research in these focused on theoretical model comparisons, and were rarely experimentally verified. Such studies, whilst highlighting the merits of the models and providing information on the applicability of the models, failed to direct a user to any particular model for a given experimental process.

The review also showed that over time, whilst the single column chromatographic process was still popular, the interest in multi-column chromatographic processes for large-scale industry have led to an increase in the research being conducted in this area. However, little work has been done in comparing the design and operating policy involved of both the single and multi-column chromatographic processes.

The equilibrium-dispersive model and the general rate model are amongst the more popular models employed in the modelling of chromatographic processes in the literature and are reported to accurately describe the dynamic behaviour in chromatography (Chapter 2). Whilst there are also other mathematical models used in chromatography such as the ideal model, transport-dispersive model and lumped kinetic models, these are generally simplifications of the two models. As such, the focus of this research is on these two models (details of these models are given in Appendix B).

Generally, the equilibrium-dispersive model is adequate for the modelling of chromatographic processes, *i.e.* the different design and operating policies considered in this thesis, *e.g.* single column, single column with recycling, simulated moving bed chromatography *etc.*. The general rate model accounts for effects of dispersion, diffusion and mass transfer resistance on the band profiles, which can be significant in large-scale chromatographic processes. However, this is at the expense of longer computational time. The different trade-offs of these models lead to the need for an approach to select the most appropriate model for a given process. Some general conclusions on the usage of these models will be drawn in Section 6.1.1.

In recent years, the simulated moving bed (SMB) chromatographic process has gained popularity with its ability to generate large quantities of highly purified products. The SMB process is a dynamic process which may require many cycles

to achieve steady state. A dynamic cyclic steady state (CSS) model is therefore proposed for modelling and optimisation and verified using a dynamic SMB model (Chapter 4). The CSS model is then employed in the optimisation of the operating conditions for an industrial case study taken from the literature, and the findings from this work is summarised in Section 6.1.2.

With the large number of different alternatives available in chromatography today as a result of the advancements in technology, it is increasingly more difficult to identify an appropriate separation process for a given separation (Chapter 2). Whilst batch (or column) chromatography is still widely used, multi-column processes (*e.g.* SMB, Varicol *etc.*) are becoming progressively popular for the efficient large scale production of highly purified products. Processes such as SMB are typically employed when a large production (in terms of tonnes per year) is required, but at lower production levels, it is not clear if other chromatographic alternatives are more economically viable. Some conclusions drawn from a study of these alternatives will be summarised in Section 6.1.3.

6.1.1 A systematic approach to model parameter estimation and model selection of chromatographic processes

With the trade-offs associated with the equilibrium-dispersive and the general rate models, it is difficult to select an appropriate model for a given separation. The systematic approach proposed in this work details the effort to determine the parameters for both models and to subsequently select an appropriate model based on the performances of the models. Dimensionless versions of both models have been employed in this work to render a fair and straightforward comparison of the performances across the models (Appendix B), and these models are coupled with a robust parameter estimation technique (Appendix D) to determine the uncertain parameters (in this work, these were the isotherm parameters).

The approach was first illustrated by obtaining the parameters for the equilibrium-dispersive model using simulation data generated by the general rate model for which

the number of components was known. The estimated equilibrium-dispersive model parameters were found to be statistically significant for the data used, thus verifying the parameter estimation technique used.

In handling data from the bio-processes, there are often many unknowns that make up the feed mixture. To compound this difficulty, the data obtained is often limited to only knowledge of the concentration of a few known components present and the total concentration. The systematic approach proposed in this work also included a detailed procedure of the feed concentration determination for modelling from experimental data. The approach was demonstrated using two experimental case studies.

A visual assessment of the "goodness-of-fit" of the models' performance was found to be inadequate, especially when the models produced very similar band profiles. A recent graphical method was used to highlight the significance of any changes in the band elution profiles between the models and experimental data. Such a tool can show at a glance which of the models follow the experimental band profile at significant yield fractions. This is highly valued in bio-processes, which demand a high yield fraction for the later downstream processing steps.

6.1.2 Modelling and optimisation of simulated moving bed chromatographic processes

The rising popularity of multi-column processes, particularly the simulated moving bed (SMB) chromatographic process has prompted much research into the modelling and optimisation of the process. With the advances in computation power and increased understanding of the complex process over the years, more accurate models such as the dynamic SMB model can now be used, as opposed to the simplified true moving bed (TMB) equivalent model used in previous years.

As the SMB process is a cyclic one, it requires many cycles before it achieves steady state conditions. Cyclic steady state (CSS) models for the SMB process are relatively new and have not previously been optimised in the literature. In this work,

an outline for a new optimisation approach for the SMB chromatographic process using the CSS model over one switching period (CSS (Switch) model).

The CSS (Switch) model is verified in terms of its accuracy and compared to a detailed dynamic SMB model. It is found to be highly accurate in representing the process. The performance of the CSS (Switch) model is also compared with that of the CSS (Cycle) model and was found to be more computationally efficient and accurate in predicting the dynamic behaviour of the system.

The CSS (Switch) model is then used to optimise the operating parameters of a case study. It is found to be an efficient method in locating the optimal process parameters in a short computational time. The study also highlighted the important of establishing all relevant degrees of freedom and showed that optimising the system for a single degree of freedom does not give the optimal operation performance achievable by the system.

6.1.3 A systematic approach to the model optimisation for single and multi-column chromatographic processes

Different chromatographic alternatives involving single column and multi-column processes were investigated in Chapter 5 using a variety of objective functions for a given separation on an industrial scale. The optimal solution for these chromatographic alternatives is determined using a simplified general rate model (Appendix B), coupled with a dynamic optimisation technique (Appendix H). The following sections summaries the main findings of each process.

Batch (column) chromatography

Conventional batch chromatography is a well-established technique for efficient separation. However, eluent costs can also run high unless some form of recycle is employed in the process. In addition, for difficult separations, the recovery yields obtained can be low for products meeting high purity constraints. In such cases, other operating policies for the column have to be examined.

Batch chromatography and recycling strategies

Employing a recycling operation strategy has been demonstrated in the literature to be effective in increasing the recovery yield of the separation. This combination of increased recovery yields whilst reducing the matrix cost makes this an attractive option for high value product(s) purification. However, for products which are difficult to separate and have vast overlapping band area between components as a result, this technique is demonstrated to be infeasible. Recycling the feed from such a separation actually makes the separation more difficult as the elution peaks become progressively broader and flatter with each recycle, increasing the band overlap area.

Implementing a peak shaving technique to conventional recycling chromatography is demonstrated to be better-suited to difficult separation processes. The main benefit from peak shaving is that the overlapping of peaks stemming from consecutive cycles is averted, as the overall mass being recycled is reduced due to product collection.

Simulated moving bed chromatography

The singular characteristic of the simulated moving bed (SMB) process is its ability to produce large amounts of highly purified products. The employment of a recycle stream in this process means that much less eluent is used, and the matrix is more efficiently used, with greater amounts of product generated. However, the implentation of this process often requires new investment of equipment, *i.e.* existing chromatographic batch columns are usually not applicable, due to the highly automated nature of the process. This also entails some additional investment for the process design prior to installation.

Varicol chromatography

The Varicol process is really a variant form of the simulated moving bed process. However, there are a greater number of degrees of freedom associated with this

process arising from the multiple sub-interval switching periods which characterise it. Whilst it has been demonstrated in the open literature to perform better than the traditional SMB process, the asynchronous switching period can cause some difficulty in process design and operation automation.

Economic comparison of all processes

The single column and multi-column processes outlined were all optimised simultaneously for design and operation for the same case study, where the single column with recycle operation collapsed to a single column for one cycle. The discounted cash flow diagram for the case study investigated showed the multi-column processes performing the best at the end of 15 years. The single column was last, although it had the best economic performance initially. Depending on the plant life and costs involved in the separation, these economic comparison results may differ.

6.2 Directions for future work

In this section, some of the limitations of this work are discussed and recommendations for future work are outlined.

6.2.1 Modelling detail

In order to increase the flexibility of the mathematical model used in this work, the following aspects should be considered:

Heat balances

The chromatographic separations considered in this work are of an isothermal nature or are temperature controlled, as is the case of bioprocesses. As such, the heat balances in these systems can be safely neglected. However, in cases where the heat of adsorption is high, heat balances are necessary to describe the separation system completely. Heat balances should also be considered in future work, as a means to improve the accuracy of the model.

6.2.2 Experimental measurements

Much of the experimental data used in this thesis was obtained from other sources, *i.e.* done by persons other than the author. In order to be able to make the best use of such data in modelling, it is important to obtain as much information as possible on the experimental system. Therefore, some suggestions have been put forward for necessary experimental measurements to aid the modelling process.

Dead volume Dead-volume in the chromatographic system is unavoidable, and its presence contributes to the band-broadening of the elution profiles. The effects of dead-volume on the chromatographic process have been assumed using literature correlations in this work. However, this detail can be easily measured and recorded during the course of the experiment to render more accurate modelling.

Isotherms Isothermal relationships of the separated components form the primary basis for the chromatographic process. In this work, the isotherm coefficients have been estimated using parameter estimation, whilst band-broadening effects (*i.e.* axial dispersion, diffusion and mass transfer resistances) have been estimated using literature correlations. In experimental work, it is easier (and more accurate) to evaluate the isothermal relationships, than to determine the individual band-broadening effects. As such, where possible, experimental measurements of the isotherms should be done, allowing for the band-broadening effects to be estimated instead.

6.2.3 Modelling and optimisation work

Here, the recommendations for further modelling and optimisation work are summarised:

Microscopic modelling

In this work, the modelling work for chromatography has been focussed on macroscopic modelling. Recent work in the literature has demonstrated the viability of

equivalence between microscopic (which considers the molecular chromatography on a molecular level using statistics) and macroscopic (which considers the mass balances of chromatography) models under certain circumstances (Felinger *et al.*, 2004). The development of a microscopic model of chromatography for a given separation can be examined, in order to compare this with work done in this thesis with the macroscopic models.

Other operating policies

Other variants of the Varicol process, such as PowerFeed and ModiCon, are up and coming techniques which have recently been developed as discussed in the literature review (Chapter 2). Such techniques have demonstrated a further improvement upon the performance of the Varicol processes. Such processes can also be modelled for consideration in future work when examining the performances of chromatographic processes.

Optimisation of the full general rate model

The optimisation work done in this thesis was conducted using a simplified version of the general rate model which was able to capture the main elution profiles used, and took much less computational time. However, more thorough optimisation work should be done using the full general rate model, which considers the other band-broadening effects such as mass transfer resistance on the separation (this has been neglected in the simplified model), to consider the process design in detail.

Other optimisation alternatives

The optimisation solutions presented in this thesis have been obtained employing a local optimisation technique. A range of initial guesses have been applied to ensure a global optimum, other, and better solutions (global optimum) may exist. Other optimisation techniques such as genetic algorithms, should also be compared to the findings of this work for validation.

6.3 Summary and main contributions

This thesis has developed and presented a number of systematic approaches to modelling and optimisation of both single and multi-column chromatographic processes. Experimental case studies have been used to verify the approaches where possible, and in others, verified literature data has been used as case studies.

The main contributions from this thesis are:

- a systematic approach to estimating model parameters and model selection for chromatographic processes using experimental data, literature correlations and parameter estimation
- verification and optimisation of a cyclic steady state (CSS) model for the simulated moving bed process
- a systematic approach to model scale-up and economic optimisation to compare single and multi-column chromatographic processes

List of publications

1. S. H. M. Chan, E. Sørensen and N. Titchener-Hooker, Optimal operation of simulated moving bed chromatographic processes, European Congress of Chemical Engineering 4, (Granada) Spain, September 2003.

2. S. H. M. Chan, E. Sørensen, N. Titchener-Hooker and D. Bracewell, A systematic procedure for model selection and model parameter estimation for chromatographic processes, American Institute of Chemical Engineers Annual Meeting, (Austin, Texas) United States of America, November 2004.

3. S. H. M. Chan, E. Sørensen, N. Titchener-Hooker and D. Bracewell, Modelling chromatographic processes - the good, the bad and the ugly, World Congress of Chemical Engineering, (Glasgow) United Kingdom, July 2005.

4. S. H. M. Chan, E. Sørensen, N. Titchener-Hooker and D. Bracewell, A systematic procedure for model selection and model parameter estimation for chromatographic processes, *in preparation*

5. S. H. M. Chan, E. Sørensen, N. Titchener-Hooker and D. Bracewell, Optimal economic design and operation of single and multi-column chromatographic processes, *in preparation*

Bibliography

[1] D. Antos, K. Kaczmarski, P. Wojciech, and A.Seidel-Morgenstern. Concentration dependence of lumped mass transfer coefficients: Linear versus nonlinear chromatography and isocratic versus gradient operation. *Journal of Chromatography A*, 1006:61–76, 2003.

[2] A. C. Awadé and Théo Efstathiou. Comparison of three liquid chromatographic methods for egg-white protein analysis. *Journal Chromatography B*, 723:69–74, 1999.

[3] E. Balsa-Canto, J. R. Banga, A. A. Alonso, and V. S. Vassiliadis. Dynamic optimisation of chemical and biochemical processes using restricted second-order information. *Computers and Chemical Engineering*, 25:539–546, 2001.

[4] E. Balsa-Canto, J. R. Banga, A. A. Alonso, and V. S. Vassiliadis. Restricted second order information for the solution of optimal control problems using control vector parameterization. *Journal of Process Control*, 12:243–255, 2002.

[5] Y. Bard. *Nonlinear parameter estimation.* Academic Press, Inc, 1974.

[6] J. C. Bellot and J. S. Condoret. Liquid chromatography modelling: a review. *Process Biochemistry*, 26:363–376, 1991.

[7] J. C. Bellot and J. S. Condoret. Selection of competitive adsorption model for modelling displacement chromatography. *Journal of Chromatography A*, 657:305–326, 1993a.

[8] J. C. Bellot and J. S. Condoret. Review: Modelling of liquid chromatography equilibria. *Process Biochemistry*, 28:365–376, 1993b.

[9] Y. A. Beste, M. Lisso, G. Wozny, and W. Arlt. Optimization of simulated moving bed plants with low efficient stationary phases: separation of fructose and glucose. *Journal of Chromatography A*, 868:169–188, 2000.

[10] G. Biressi, O. Ludemann-Hornbourger, M. Mazzotti, R.-M. Nicoud, and M. Morbidelli. Design and optimisation of a simulated moving bed unit: role of deviations from equilibrium theory. *Journal of Chromatography A*, 876:3–15, 2000.

[11] J. Bonnerjea, S. Oh, M. Hoare, and P. Dunnill. Protein purification: The right step at the right time. *Biotechnology*, 4:954–958, 1986.

[12] P. H. Boyer and J. T. Hsu. Experimental studies of restricted protein diffusion in an agarose matrix. *American Institue of Chemical Engineering*, 38:259–272, 1992.

[13] E. Cavoy, M.-F. Deltent, S. Lehoucq, and D. Miggiano. Laboratory-developed simulated moving bed for chiral drug separations. design of the system and separation of tramadol enantiomers. *Journal of Chromatography A*, 769:49–57, 1997.

[14] F. Charton, M. Bailly, and G. Guiochon. Recycling in preparative chromatography. *Journal of Chromatography A*, 1994.

[15] F. Charton, S. C. Jacobson, and G. Guiochon. Modelling of adsorption behaviour and the chromatographic band profiles of enantiomers: Behaviour of methyl mandelate on immobilised cellulose. *Journal of Chromatography A*, 630:21–35, 1993.

[16] F. Charton and R.-M. Nicoud. Complete design of a simulated moving bed. *Journal of Chromatography A*, 702:97–112, 1995.

[17] T. C. E. Cheng and K. L. Teo. Further extension of student-related optimal control problem. *Mathematical Modelling*, 9:499–506, 1987.

[18] J. M. Coulson and J. F. Richardson, editors. *Chemical Engineering Volume 2: Particle Technology and Separation Processes.* Butterworth-Heinemann, 4th edition, 1991.

[19] G. B. Cox, L. R. Synder, and J. W. Dolan. Preparative high-performance liquid chromatography under gradient conditions : I. band broadening in gradient elution as a function of sample size. *Journal of Chromatography A*, 484:409–423, 1989.

[20] P. V. Danckwerts. Continuous flow systems - distribution of residence times. *Chemical Engineering Science*, 2:1–13, 1953.

[21] F. Dondi, A. Cavazzini, M. Remelli, A. Felinger, and M. Martin. Stochastic theory of size exclusion chromatography by the characteristic function approach. *Journal of Chromatography A*, 943:185–207, 2002.

[22] F. Dondi and M. Remelli. Statistical mechanics and thermodynamics. *Journal of Physical Chemistry*, 90:1885–1891, 1986.

[23] G. Dünnebier, J. Fricke, and K.-U. Klatt. Optimal design and operation of simulated moving bed chromatographic reactors. *Industrial and Engineering Chemistry Research*, 39:2290–2304, 2000.

[24] G. Dünnebier and K.-U. Klatt. Optimal operation of simulated moving bed chromatographic processes. *Computer and Chemical Engineering Supplement*, 23, 1999.

[25] G. Dünnebier, I. Weirich, and K.-U. Klatt. Computationally efficient dynamic modelling and simulation of simulated moving bed chromatographic processes with linear isotherms. *Chemical Engineering Science*, 53(14):2537–2546, 1998.

[26] T. F. Edgar and D. M. Himmelblau. *Optimization of Chemical Processes.* McGraw-Hill International Editions, 1988.

[27] S. Edwards-Parton. Internal report. University College London, 2004.

[28] S. Engell and A. Toumi. Optimisation and control of chromatography. *Computers and Chemical Engineering*, 29:1243–1252, 2005.

[29] P. Englezos and N. Kalogerakis. *Applied parameter estimation for chemical engineers.* Marcel Dekker, Inc., 2001.

[30] D. G. Fasman, editor. *Practical handbook biochemistry and molecular biology.* CRC Press, 1992.

[31] A. Felinger, A. Cavazzini, and F. Dondi. Equivalence of the microscopic and macroscopic models of chromatography: stochasticdispersive versus lumped kinetic model. *Journal of Chromatography A*, 1043:149–157, 2004.

[32] A. Felinger and G. Guiochon. Optimization of the experimental conditions and the column design parameters in displacement chromatography. *Journal of Chromatography A*, 609:35–47, 1992.

[33] A. Felinger and G. Guiochon. Computer simulations in non-linear chromatography. *Trends in analytical chromatography*, 14(1):6–10, 1995.

[34] A. Felinger and G. Guiochon. Optimizing experimental conditions in overloaded gradient elution chromatography. *Biotechnology Progress*, 12:638–644, 1996a.

[35] A. Felinger and G. Guiochon. Optimizing preparative separations at high recovery yield. *Journal of Chromatography A*, 752:31–40, 1996b.

[36] A. Felinger and G. Guiochon. Comparing the optimum performance of different modes of preparative liquid chromatography. *Journal of Chromatography A*, 796:59–74, 1998.

[37] E. R. Francotte and P. Richert. Application of simulated moving-bed chromatography to the separation of the enantiomers of chiral drugs. *Journal of Chromatography A*, 769:101–107, 1997.

[38] S. R. Gallant, S. Vannum, and S. M. Cramer. Modelling gradient elution of proteins in ion-exchange chromatography. *American Institute of Chemical Engineering*, 42:2511–2520, 1996.

[39] S. Ghodbane and G. Guiochon. Optimisation of concentration overloaded in preparative liquid chromatography. *Analytical Chemistry*, Journal of Chromatography A:275–291, 1988.

[40] J. C. Giddings and H. Eyring. A molecular dynamic theory of chromatography. *Journal of Physical Chemistry*, 59:416–421, 1955.

[41] S. Golshan-Shirazi and G. Guiochon. Theory of optimisation of the experimental conditions of preparative elution using the ideal model of liquid chromatography. *Analytical Chemistry*, 61:1276–1287, 1989a.

[42] S. Golshan-Shirazi and G. Guiochon. Theory of optimisation of the experimental conditions of preparative elution chromatography: Optimisation of the column efficiency. *Analytical Chemistry*, 61:1368–1382, 1989b.

[43] C. M. Grill. Closed-loop recycling with periodic intra-profile injection: a new binary preparative chromatographic technique. *Journal of Chromatography A*, 796:101–113, 1998.

[44] C. M. Grill and L. Miller. Separation of a racemic pharmaceutical intermediate using closed-loop steady state recycling. *Journal of Chromatography A*, 1998.

[45] C. M. Grill, L. Miller, and T. Q. Yan. Resolution of a racemic pharmaceutical intermediate. a comparison of preparative hplc, steady state recycling, and simulated moving bed. *Journal of Chromatography A*, 2004.

[46] F. Gritti, A. Felinger, and G. Guiochon. Overloaded gradient elution chromatography on heterogeneous adsorbents in reversed-phase liquid chromatography. *Journal of Chromatography A*, 1017:45–61, 2003.

[47] T. Gu. *Mathematical modelling and scale-up of liquid chromatography.* Springer, 1995.

[48] T. Gu, G. Tsai, and G. T. Tsao. Some considerations for optimisation of desorption chromatography. *Biotechnology and Bioengineering*, 37:65–70, 1991.

[49] T. Gu, G. T. Tsao, G. J. Tsai, and M. R. Ladish. Displacement effect in multicomponent chromatography. *American Institute of Chemical Engineering*, 36:1156–1162, 1990.

[50] T. Gu and Y. Zheng. A study of the scale-up of reversed-phase liquid chromatography. *Separation and Purification Technology*, 15:41–58, 1999.

[51] G. Guiochon. Preparative liquid chromatography. *Journal of Chromatography A*, 965:129–161, 2002.

[52] G. Guiochon, S. Golshan Shirazi, and A. M. Katti. *Fundamentals of Preparative and Nonlinear Chromatography.* Academic Press, Inc., 1994.

[53] S. P. Gygi, Y. Rochon, B. R. Franza, and R. Aebersold. Correlation between protein and mrna abundance in yeast. *Molecular and Cellular Biology*, 19(3):1720–1730, 1999.

[54] I. Hägglund and J. Ståhlberg. Ideal model of chromatography applied to charged solutes in reversed-phase liquid chromatography. *Journal of Chromatography A*, 761:3–11, 1997.

[55] M. M. Hassan, A. K. M. S. Rahman, and K. F. Loughlin. Modelling of simulated moving bed adsorption systems: a more precise approach. *Separations Technology*, 5:77–89, 1995.

[56] L.-Z. He, H. Helmholz, B. Niemeyer, and X. Luo. A diffusion model for affinity adsorption of glycoprotein on immobilized lectin. In *First MIT Conference on Computational Fluid and Solid Mechanics*, pages 1232–1235, 2001.

[57] C. Heuer, P. Hugo, G. Mann, and A. Seidel-Morgenstern. Scale up in preparative chromatography. *Journal of Chromatography A*, 752:19–29, 1996.

[58] C. Heuer, P. Hugo, and A. Seidel-Morgenstern. Experimental and theoretical study of recycling in preparative chromatography. *Separation Science and Technology*, 34:173–199, 1999.

[59] C. Heuer, E. Kuster, T. Plattner, and A. Seidel-Morgenstern. Design of the simulated moving bed process based on adsorption isotherm measurements using a perturbation method. *Journal of Chromatography A*, 827:175–191, 1998.

[60] C. Heuer, A. Seidel-Morgenstern, and P. Hugo. Experimental invetigation and modelling of closed-loop recycling in preparative chromatography. *Chemical Engineering Science*, 50:1115–1127, 1995.

[61] C. D. Holland and A. I. Liapis. *Computater Methods for Solving Dynamic Separation Problems.* McGraw-Hill Inc., 1983.

[62] J. Houwing, H. A. H. Billiet, and L. A. M. van der Wielen. Optimization of azeotropic protein separations in gradient and isocratic ion-exchange simulated moving bed chromatography. *Journal of Chromatography A*, 944:189–201, 2002a.

[63] J. Houwing, S. H. van Hateren, H. A. H. Billiet, and L. A. M. van der Wielen. Effect of salt gradients on the separation of dilute mixtures of proteins by ion-exchange in simulated moving beds. *Journal of Chromatography A*, 952:85–98, 2002b.

[64] U. Huber and R. E. Majors. *Principles in preparative HPLC.* Agilent Technologies, 2004.

[65] S. C. Jacobson, A. Felinger, and G. Guiochon. Optimizing the sample size and the reduced velocity to achieve maximum production rates of enantiomers. *Biotechnology Progress*, 8:533–539, 1992a.

[66] S. C. Jacobson, A. Felinger, and G. Guiochon. Optimizing the sample size and the retention parameters to achieve maximum production rates for enantiomers in chiral chromatography. *Biotechnology and Bioengineering*, 40:1210–1217, 1992b.

[67] A. T. James and A. J. P. Martin. The analysis of fatty acids and amines by gas chromatography. *Biochemical Journal*, 50:679 – 690, 1952.

[68] T. B. Jensen, T. G. P. Reijns, H. A. H. Billiet, and L. A. M. van der Wielen. Novel simulated moving-bed method for reduced solvent consumption. *Journal of Chromatography A*, 873:149–162, 2000.

[69] R. R. Johnson. *Elementary statistics.* Duxbury Press, 7th edition, 1996.

[70] A. Jungbauer. Insights into the chromatography of proteins provided by mathematical modeling. *Current Opinion in Biotechnology*, 7:210–218, 1996.

[71] A. Jungbauer and O. Kaltenbrunner. Fundamental questions in optimizing ion-exchange chromatography of proteins using computer-aided process design. *Biotechnology and Bioengineering*, 52:223–236, 1996.

[72] A. Jupke, A. Epping, and H. Schmidt-Traub. Optimal design of batch and simulated moving bed chromatographic separation processes. *Journal of Chromatography A*, 944:93–117, 2002.

[73] M. Juza. Development of an high-performance liquid chromatographic simulated moving bed separation from an industrial perspective. *Journal of Chromatography A*, 1999.

[74] M. Juza, M. Mazzotti, and M. Morbidelli. Simulated moving-bed chromatography and its application to chirotechnology. *Tibtech*, 18:108–118, March 2000.

[75] K. Kaczmarski, D. Antos, H. Sajonz, P. Sajonz, and G. Guiochon. Comparative modeling of breakthrough curves of bovine serum albumin in anion-exchange chromatography. *Journal of Chromatography A*, 925:1–17, 2001.

[76] B. L. Karger, L. R. Snyder, and C. Horvath. *An introduction to separation science.* Wiley, 1973.

[77] P. J. Karol. A different perspective on the theoretical plate in equilibrium chromatography. *Analytical Chemistry*, 61:1937–1941, 1989.

[78] J. H. Kennedy, M. D. Belvo, V. S. Sharp, and J. D. Williams. Comparison of separation efficiency of early phase active pharmaceutical intermediates by steady state recycle and batch chromatographic techniques. *Journal of Chromatography A*, 1046:55–60, 2004.

[79] R. Khanom. Purification of alcohol dehydrogenase using hydrophobic interation chromatography and gel filtration chromatography for evaluation of chromatographic performance and the trade-off between purity and recovery. Master's thesis, University College London, University of London, United Kingdom, 2003.

[80] Kirk-Othmer. *Enclyclopedia of Chemical Technology*, volume 6. John Wiley and Sons, Inc., 4th edition, 1993.

[81] K.Kaczmarski and D. Antos. Modified rouchon and rouchon-like algorithms for solving different models of multicomponent preparative chromatography. *Journal of Chromatography A*, 756:73–87, 1996.

[82] K.-U. Klatt, F. Hanisch, G. Dünnebier, and S. Engell. Model-based optimization and control of chromatographic processes. *Computers and Chemical Engineering*, 24:1119–1126, 2000.

[83] E. Kloppenburg and E. Dieter Gilles. A new concept for operating simulated moving-bed processes. *Chemical Engineering Technology*, 22:813–817, 1999.

[84] J. H. Knox and H. M. Pyper. Framework for maximizing throughput in preparative liquid chromatography. *Journal of Chromatography A*, 363:1–30, 1986.

[85] M. R. Ladisch. *Bioseparations Engineering - Principles, Practice and Economics.* John Wiley and Sons, Inc., 2001.

[86] Z. Li, Y. Gu, and T. Gu. Mathematical modelling and scale-up of size-exclusion chromatography. *Biochemical Engineering Journal*, 2:145–155, 1998.

[87] W.-B. Lin, F.-S. Wang, and W.-C. Lee. Model simulation and optimization in preparative liquid chromatography using a combination of perturbation and modified collocation methods. *Industrial Engineering Chemical Research*, 37:4399–4407, 1998.

[88] K. B. Lipkowitz. Review: Theoretical studies of type ii-v chiral stationary phases. *Journal of Chromatography A*, 694:15–37, 1995.

[89] K. B. Lipkowitz. Review: Atomistic modeling of enantioselection in chromatography. *Journal of Chromatography A*, 906:417–442, 2001.

[90] O. Ludemann-Hombourger, R. M. Nicoud, and M. Bailly. The varicol process: A new multicolumn continuous chromatographic process. *Separation Science and Technology*, 35:1829–1862, 2000.

[91] O. Ludemann-Hombourger, G. Pigorini, R. M. Nicoud, D. S. Ross, and G. Terfloth. Application of the "varicol" process to the separation of the isomers of

the sb-553261 racemate. *Journal of Chromatography A, 947 (2002) 59-68*, 947:59–68, 2002.

[92] R. Luus. Optimal control of batch reactors by iterative dynamic programming. *Journal of Process Control*, 1994.

[93] Z. Ma, R. D. Whitley, and N. H. L. Wang. Pore and surface diffusion in multicomponent adsorption and liquid chromatography systems. *American Institute of Chemical Engineering*, 42:1244–1262, 1996.

[94] A. J. P. Martin and R. L. M. Synge. A new form of chromatogram employing two liquid phases 1. a heory of chromatograph 2. application to the micro-determination of the higher monoamine-acids in proteins. *Biochemical Journal*, 35:1358 – 1368, 1941.

[95] M. Mazzotti, G. Storti, and M. Morbidelli. Optimal operation of simulated moving bed units for nonlinear chromatographic separations. *Journal of Chromatography A*, 769:3–24, 1997.

[96] J. J. McKetta. *Encyclopedia of Chemical Processing and Design*, volume 8. Marcel Dekker, Inc., 1979.

[97] H. M. McNair and J. M. Miller. *Basic Gas Chromatography*. John Wiley and Sons, Inc., 1998.

[98] C. Migliorini, M. Mazzotti, and M. Morbidelli. Continuous chromatographic separation through simulated moving beds under linear and nonlinear conditions. *Journal of Chromatography A*, 827:161–173, 1998.

[99] C. Migliorini, M. Mazzotti, and M. Morbidelli. Simulated moving-beds units with extra-column dead volume. *American Institute of Chemical Engineering*, 45:1411–1421, 1999.

[100] K. Mihlbachler, J. Fricke, T. Yun, A. Seidel-Morgenstern, H. Schmidt-Traub, and G. Guiochon. Effect of homogeneity of the column set on the performance of a simulated moving bed i. theory. *Journal of Chromatography A*, 908:49–70, 2001.

[101] L. Miller, C. M. Grill, T. Yan, O. Dapremont, E. Huthmann, and M. Juza. Batch and simulated moving bed chromatographic resolution of a pharmaceutical racemate. *Journal of Chromatography A*, 2003.

[102] M. Minceva, L. S. Pais, and A. E. Rodrigues. Cyclic steady state of simulated moving bed processes for enantiomers separation. *Chemical Engineering and Processing*, 42:93–104, 2003.

[103] M. Minceva and A. E. Rodrigues. Mideling and simulation of a simulated moving bed for the separation of *p*-xylene. *Industrial and Engineering Chemical Research*, 41:3454–3461, 2002.

[104] S. H. Ngiam. *Graphical frameworks for facilitating the study of chromatographic separations.* PhD thesis, University College London, University of London, United Kingdom, 2002.

[105] S. H. Ngiam, Y. H. Zhou, M. K. Turner, and N. J. Titchener-Hooker. Graphical method for the calculation of chromatographic performance in representing the trade-off between purity and recovery. *Journal of Chromatography A*, 2001.

[106] R.-M. Nicoud, G. Fuchs, P. Adam, M. Bailly, R. Küsters, F. D. Antia, R. Reuille, and E. Schmid. Preparative scale enantioseparation of a chiral epoxide: Comparison of liquid chromatography and simulated moving bed adsorption technology. *Chirality*, 5:267–271, 1993.

[107] S. Nilchan and C. C. Pantelides. On the optimisation of periodic adsorption processes. *Adsorption*, 4:113–147, 1998.

[108] R. Ouellet and R. T. Bui. A new tool for solving industrial continuous optimal problems. *Applied Mathematical Modelling*, 17:298–310, 1993.

[109] M. Pedeferri, G. Zenoni, M. Mazzotti, and M. Marbidelli. Experimental analysis of a chiral separation through simulated moving bed chromatography. *Chemical Engineering Science*, 1999.

[110] S. G. Perry, R. Amos, and P. I. Brewer. *Practical Liquid Chromatography.* Plenium Press, 1972.

[111] M. S. Peters, K. D. Timmerhaus, and R. E. West. *Plant design and economics for chemical engineers.* McGraw-Hill, 5th edition, 2003.

[112] Pharmacia Bioprocess Technology. *Hydrophobic interaction chromatography: Principles and methods*, 1993.

[113] W. Piątkowski, D. Antos, and K. Kaczmarski. Modeling of preparative chromatography processes with slow intraparticle mass transport kinetics. *Journal of Chromatography A*, 988:219–231, 2003.

[114] T. Pröll and E. Küsters. Optimization strategy for simulated moving bed systems. *Journal of Chromatography A*, 800:135–150, 1998.

[115] I. Quiñones, C. M. Grill, L. Miller, and G. Guiochon. Modelling of separations by closed-loop steady-state recycling chromatography of a racemic pharmaceutical intermediate. *Journal of Chromatography A*, 867:1–21, 2000.

[116] H. Schmidt-Traub and J. Strube. Dynamic simulation of simulated-moving-bed chromatographic processes. *Computers and Chemical Engineering*, 20:S641–S646, 1996.

[117] H. Schramm, M. Kaspereit, A. Kienle, and A. Seidel-Morgenstern. Simulated moving bed process with cyclic modulation of the feed concentration. *Journal of Chromatography A*, 1006:77–86, 2003.

[118] P. A. Schweitzer. *Handbook of Separation Techniques for Chemical Engineers.* McGraw-Hill, Inc, 3rd edition, 1996.

[119] R. P. W. Scott. *Contemporary Liquid Chromatography.* John Wiley and Sons, Inc., 1976.

[120] A. Seidel-Morgenstern and G. Guiochon. Theoretical study of recycling in preparative chromatography. *American Institute of Chemical Engineering*, 39:809–819, 1993.

[121] R. K. Sinnott. *Coulson and Richardson's Chemical Engineering Volume 6 - Chemical Engineering Design*, volume 2. Butterworth-Heinemann, 3rd edition, 2001.

[122] D. A. Skoog, D. M. West, F. J. Holler, and S. R. Crouch. *Fundamentals of Analytical Chemistry.* Brooks/Cole-Thomson Learning, eighth edition, 2004.

[123] L. R. Snyder and G. B. Cox. Preparative high performance under isocratic conditions: Ii. the role of column variables. *Journal of Chromatography A*, 483:85–94, 1989.

[124] L. R. Snyder, J. W. Dolan, , D. C. Lommen, and G. B. Cox. Preparative high-performance liquid chromatography under gradient conditions : Ii. a computer program for the design of reversed-phase gradient-elution separations of peptide and protein samples. *Journal of Chromatography A*, 484:425–435, 1989b.

[125] L. R. Snyder, J. W. Dolan, and G. B. Cox. Preparative high performance under isocratic conditions: I. craig similations for heavily overloaded separations. *Journal of Chromatography A*, 483:63–84, 1989a.

[126] L. R. Snyder, J. W. Dolan, and G. B. Cox. Preparative high-performance liquid chromatography under gradient conditions : Iii. craig simulations for heavily overloaded separations. *Journal of Chromatography A*, 484:437–450, 1989c.

[127] L. R. Snyder and J. J. Kirkland. *Introduction to Modern Liquid Chromatography.* John Wiley and Sons, Inc., 1974.

[128] G. Sofer and L. Hagel. *Handbook of process chromatography: a guide to optimization, scale up and validation.* Academic Press, 1997.

[129] G. Storti, M. Mazzotti, M. Morbidelli, and S. Carrà. Robust design of binary countercurrent adsorption separation processes. *American Institute of Chemical Engineering Journal*, 39:471 – 492, 1993.

[130] J. Strube, U. Altenhöner, M. Meurer, H. Schmidt-Traub, and M. Schulte. Dynamic simulation of simulated moving-bed chromatographic processes for the optimization of chiral separations. *Journal of Chromatography A*, 769:81–92, 1997.

[131] J. Strube and H. Schmidt-Traub. Dynamic simulation of simulated-moving-bed chromatographic processes. *Computers and Chemical Engineering*, 22:1309–1317, 1998.

[132] H. J. Subramani, K. Hidajat, and A. K. Ray. Optimisation of simulated moving bed and varicol processes for glucose-fructose separation. *Transactions of Institution of Chemical Engineers*, 81:549–567, 2003.

[133] G. Subramanian, editor. *Process scale liquid chromatography.* Wiley-VCH, 1995.

[134] G. Subramanian, editor. *Chiral separation techniques - a practical approach.* Wiley-VCH, 2nd edition, 2001.

[135] H. K. Teoh. *Optimal Design and Operation of High Performance Liquid Chromatographic Processes.* PhD thesis, University College London, University of London, United Kingdom, 2002.

[136] H. K. Teoh, M. Turner, N. Titchener-Hooker, and E. Sørensen. Experimental verification and optimisation of a detailed dynamic high performance liquid chromatographic column model. *Computers and Chemical Engineering*, 2001.

[137] A. Toumi and S. Engell. Optimisation-based control of a reactive simulating moving bed process for glucose isomerisation. *Chemical Engineering Science*, 59:3777–3792, 2004.

[138] A. Toumi, S. Engell, O. Ludemann-Hombourger, R. M. Nicoud, and M. Bailly. Optimization of simulated moving bed and varicol processes. *Journal of Chromatography A*, 1006:15–31, 2003.

[139] R. E. Treybal. *Mass-transfer operations.* McGraw-Hill Book Company, third edition, 1981.

[140] V. S. Vassiliadis. *Computational solution of dynamic optimization problems with general differential-algebraic constraints.* PhD thesis, Imperial College, University of London, UK, 1993.

[141] V. S. Vassiliadis, E. Balsa Canto, and J. R. Banga. Second-order sensitivities of general dynamic systems with application to optimal control problem. *Chemical Engineering Science*, 54:3851–3860, 1999.

[142] G. Wang. Optimal control problem governed by non well-posed semilinear elliptic equation. *Nonlinear Analysis*, 49:315–333, 2002.

[143] S. Weinstein, L. Leiserowitz, and E. Gil-Av. Chiral secondary amides. 2. molecular packing and chiral recognition. *Journal of American Chemical Society*, pages 2768–2772, 1980.

[144] S. M. Wheelwright. *Protein purification: Design and scale up of downstream processing.* Hanser, 1991.

[145] T. H. Wonnacott and R. J. Wonnacott. *Introductory statistics.* John Wiley and Sons, 5th edition, 1990.

[146] M. E. Young and P. A. Carroad. Estimation of diffusion coefficients of proteins. *Biotechnology and Bioengineering*, 22:947–955, 1980.

[147] T. Yun, Z. Bensetiti, G. Zhong, and G. Guiochon. Effects of column efficiency on internal concentration profiles and the performance of a simulated moving-bed unit in the case of a linear isotherm. *Journal of Chromatography A*, 1997.

[148] Z. Zhang, K. Hidajat, A. K. Ray, and M. Morbidelli. Multiobjective optimisation of smb and varicol process for chiral separation. *American Institute for Chemical Engineering Journal*, 48:2800–2816, 2002.

[149] Z. Zhang, M. Mazzotti, and M. Morbidelli. Multiobjective optimisation of simulated moving bed and varicol processes using a genetic algorithm. *Journal of Chromatography A*, 989:95–108, 2003a.

[150] Z. Zhang, M. Mazzotti, and M. Morbidelli. Powerfeed operation of simulated moving bed units: changing flow-rates during the switching interval. *Journal of Chromatography A*, 1006:87–99, 2003b.

[151] Z. Zhang, M. Morbidelli, and M. Mazzotti. Experimental assessment of powerfeed chromatography. *American Institute for Chemical Engineering Journal*, 50:625–632, 2004.

[152] G. Zhong and G. Guiochon. Simulated moving bed chromatography: effects of axial dispersion and mass transfer under linear conditions. *Chemical Engineering Science*, 1997a.

[153] G. Zhong and G. Guiochon. Simulated moving bed chromatography: Comparison between the behaviours under linear and non-linear conditions. *Chemical Engineering Science*, 1997b.

[154] G. Zhong and G. Guiochon. Steady-state analysis of simulated moving-bed chromatography using linear, ideal model. *Chemical Engineering Science*, 53(6):1121–1130, 1998.

Nomenclature

A	Term in the *Van Deemter's equation* representing eddy diffusion
Abs	Measure absorbance (AU)
a	First coefficient of the Langmuir isotherm
B	Term in the *Van Deemter's equation* representing longitudinal molecular diffusion
Bi	Biot number
b	Second coefficient of the Langmuir isotherm ratio of rates of adsorption and desorption $\frac{k_a}{k_d}$
C, C_m	Term in the *Van Deemter's equation* representing mass transfer in the stationary and mobile phase respectively
C^{∞}	Adsorption saturation capacity
C_{ads}	Cost per kilogram of adsorbent (US \$)
C_{ads}^{annual}	Cost of the adsorbent per year (US \$)
C_{el}	Cost per kilogram of eluent (US \$)
C_{el}^{annual}	Cost of the eluent per year (US \$)
C_{feed}	Cost per kilogram of feed (US \$)
C_{waste}	Capital cost of the equipment (US \$)
C_{waste}^{annual}	Cost of the waste per year (US \$)
C_i	Concentration of component i in the mobile phase
C_i^m	Concentration of component i in the mobile phase
C_i^p	Concentration of component i in the stagnant mobile phase (heterogenous particles)
C_i^{ps}	Concentration of component i adsorbed on the stationary phase
C_i^{sp}	Concentration of component i adsorbed on the outer layer of the stationary phase (homogenous particles)
C_{mod}	Mass fraction of the moderator in the buffer (used in isotherms)
C_{op}^{annual}	Operation cost per year (US \$)
C_{op}^{h}	Operation cost per hour (US \$)
C_{Pi}	Equilibrium concentration of component i in the mobile phase
C_{RM}	Cost price of the raw material (US\$)
C_{Total}^{annual}	Total production costs per year (US \$)
Cin_i	Concentration of component i in the main process entering in the node
$Cout_i$	Concentration of component i in the main process leaving

	in the node
D	Diameter of the column
$D_{a,i}$	Apparent dispersion coefficient
D_{ax}	Axial dispersion coefficient
$D_{eff,i}^{sp}$	Pseudo diffusivity of component i in the adsorbed layer (homogenous particles)
$D_{f,i}^{p}$	Pseudo diffusivity of component i in the macropores (heterogenous particles)
D_p	Diffusion coefficient in particle
D_AB	Diffusion coefficient for A in B
D_L	Axial diffusion coefficient
d	Distance between peak maxima
d_p	Particle size
E_c	Eluent consumption over one cycle
$f1$, $f2$	Lengths of the parallel sides of the trapezium (Trapezium rule)
F	Phase ratio $\frac{V_s}{V_m}$ and $\frac{1-\epsilon}{\epsilon}$
F_c	Column flowrate
h	Width of trapezium, between the the parallel sides (Trapezium rule)
H	Height equivalent to a theoretical plate (HETP)
k	Retention factor
k_a	Rate constant of adsorption
k_d	Rate constant of desorption
$k_{eff,i}$	Effective mass transfer resistance of component i
k_f	Film mass transfer coefficient
k_L	Liquid mass transfer coefficient
K_i	Linear isotherm coefficient for component i
$K_{pm,i}$	Mass transfer coefficient of the mobile phase towards the particle outer area for component i
K_C	Equilibrium constant
L	Length of the column
$M_{m,i}$	Amount of material for interval i [m= product P, or impurities A/B]
M_{waste}	Mass of waste products generated over one cycle
$M_{R,i}$	Molecular mass of component i
$M_{T,i}$	Total amount of material for interval i
N	Plate number (related to column efficiency)
N_A	Flux of component A in solution in B (Fick's law)
p	path length used in absorbance calculations
P	Finite vector of decision variables for parameter estimation
P^{annual}	Net profit earned in one year
Pe	Axial Peclet number
Pe_p	Particle Peclet number
Pr_i	Production rate of component i
Pu_i	Purity of component i

Pu_i^{min}	Minimum purity of component i
$Pr(x)$	Probablity distribution of random variable X
q_i	Concentration of component i in the stationary phase
$q_{i,s}$	Saturation capacity of the adsorbent
$Q_{Desorbent}$	Volumetric flowrate of the desorbent
$Q_{Extract}$	Volumetric flowrate of the extract
Q_{Feed}	Volumetric flowrate of the feed
$Q_{Raffinate}$	Volumetric flowrate of the raffinate
Qin_i	Volumetric flowrate of the main process entering in the node
$Qout_i$	Volumetric flowrate of the main process leaving in the node
$QNin_i$	Volumetric flowrate of the inlet stream entering in the node
$QNout_i$	Volumetric flowrate of the outlet stream leaving in the node
R	Retardation factor
R_p	Particle radius
R_s	Resolution
S_{income}^{annual}	Sales income for one year (US $)
S_p	Particle geometric cross-sectional area
t_{cycle}	Time to complete one cycle
t_{inj}	Time taken to inject the sample load onto the column
t_{life}	Lifetime of adsorbent
t_m	Time between the upper and lower limit of the interval i
t_{op}	Time to operate the process for one year
t_M	Retention time of a nonretained component
t_R	Retention time of a component
t'_R	Adjusted retention time
T_{cycle}	Time taken for the inlet and outlet lines to return to the original positions after they are first moved in SMB/Varicol process
T_{switch}	Switching time period of the SMB/Varicol process
u	Velocity of the mobile phase
$\bar{u}$	Average velocity of mobile phase
v	Interstitial velocity of the mobile phase
V_c	Volume of the column
V_o	Column void volume
V_M	Volume of the mobile phase
V_R	Retention volume
V'_R	Adjusted retention volume
V_S	Volume of the stationary phase (adsorbent)
w_b	Peak width at the base of the peak
w_h	Peak width at half the peak height
W_i	Amount/weight of component i (g)
x	Values of a random variable X
X	Random variable with values x
$\bar{X}$	Sample mean of random variable X

Y_i	Recovery yield of component i
z	Axial coordinate
t	Time coordinate

Greek letters

α, α'	parameter for component-moderator(salt) relationship in isotherm
β	parameter for component-moderator(salt) relationship in isotherm
ϵ	Molar absorptivity coefficient ($Lmol^{-1}cm^{-1}$)
ϵ_B	Porosity factor of the adsorbent
ϵ_P	Internal porosity
ϵ_T	Total porosity
η	Viscosity of the mobile phase
γ	parameter for component-moderator(salt) relationship in isotherm
μ	Velocity of solute through the column
ρ	Density of the mobile phase
ρ_{app}	Apparent density of the adsorbent
ΔC	Change in concentration across the fluid phase interface
ΔP	Pressure across the column (bar)
ΔP^{max}	Maximum pressure across the column (bar)
ΔP^{min}	Minimum pressure across the column (bar)
Φ	Objective function
σ	One quarter of the peak width w_b at the base
σ^2	Variance of a random variable X
ζ	Dimensionless axial coordinate
θ	Dimensionless time coordinate

Appendix A

Common terms in chromatography

A.1 The Chromatogram

Figure A.1 is a normal chromatogram showing two resolved substances. The terms below describe the various parts of the chromatogram.

Adjusted retention time The time between the dead point and the peak maximum, t'_R

Adjusted retention volume The volume of material that passed through the column between the dead point and the peak maximum, V'_R

Baseline The part of the chromatogram recorded when only the mobile phase is emerging from the column.

Dead point The first small peak in the early part of the chromatogram represents a component that is not retained in the system. The point at which this unretained component is eluted is called the dead point.

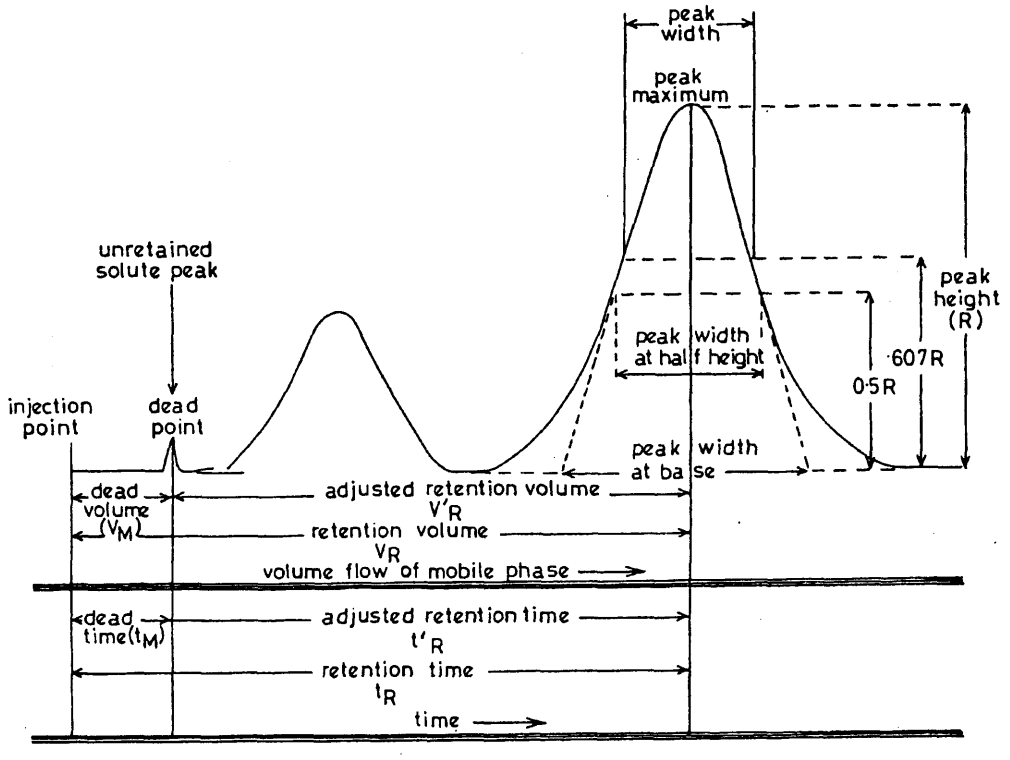

Figure A.1: A typical chromatogram (Scott, 1976)

Dead time The time between the injection point and the peak maximum for the unretained component, t_M

Dead volume/Hold-up volume The volume of the mobile phase that passes through the column between the injection point and the dead point, V_M

Injection point A mark is made on the chromatogram when the sample is injected into the chromatographic system.

Peak maximum The point at which the maximum concentration of any peak eluted.

Peak height The distance between the peak maximum and a line joining the base of the peak (an extrapolation of the baseline).

Peak width The distance between the tangents to the points of inflection at the base of the peak

Retention time The time between the injection point and the peak maximum of any peak, t_R

Retention volume The volume of material that passed through the column between the injection point and the peak maximum of any peak, V_R

A.2 Chromatographic Terms and Symbols

The basic theory of chromatography and the equations employed to describe the process are explained here. Since the physical processes in gas chromatography and liquid chromatography are identical, the use of these symbols and nomenclature is the same (Scott, 1976).

The following terms and their associated symbols will be defined:

- Column overloading

- Distribution constant
- Retention factor
- Retardation factor
- Band broadening
- Peak shapes
- Plate height
- Resolution

Column overloading

Overloaded chromatography is a name given to the process when a large sample is used so that the column is operated under nonlinear isocratic conditions. Column overloading can be done in two ways - concentration or volume overloading. In concentration overloading, the concentration of the sample is increased, but the sample volume injected remains the same. In volume overloading, the sample concentration remains the same, whilst the volume of the sample injected is increased.

Concentration overloading is only possible when the sample feed has good solubility in the mobile phase; otherwise, volume overloading must be used (Huber and Majors, 2004).

Distribution Constant

The distribution constant is a thermodynamic equilibrium constant, K_C. For a solute or component A:

$$K_C = \frac{[A]_S}{[A]_M} \tag{A.1}$$

where the square brackets denote molar concentrations and the subscripts S and M refer to stationary and mobile phases, respectively. The larger the value of K_c,

the greater the affinity of the solute or component for the stationary phase and the longer it is retained in the column.

There are two assumptions associated with this constant. The first assumption is that chromatography is an equilibrium process, although it is clearly not as the mobile phase is constantly moving component molecules down the column. However, the system operates close to equilibrium when the mass transfer kinetics are fast. The second assumption is that the components do not interact with one another. This is reasonable because of the low concentrations generally present in the column and also because the components are increasingly being separated from each other as they pass through the column. Interaction between the components are detected when the chromatographic results deviate from this theory, *i.e.* the peak shapes become flatter or broader (band-broadening).

Retention Factor

The distribution constant K_C can be broken down into two terms:

$$K_C = k \times F \tag{A.2}$$

where F is the phase volume ratio and k is the retention factor.
The phase volume ratio is defined as

$$F = \frac{V_M}{V_S} \tag{A.3}$$

where V_M is the dead volume, and V_S is the stationary phase volume.
The retention factor, k, is the ratio of the *amount* (g, grams) of component in the stationary phase, $(W_A)_S$, to the *amount* (g, grams) the mobile phase $(W_A)_M$:

$$k = \frac{(W_A)_S}{(W_A)_M} \tag{A.4}$$

The relationship between the concentration, volume and weight of component A, in the mobile/stationary phase is as follows:

$$[A] = \frac{W_A}{V} \quad \text{Units} \frac{g}{cm^3} \tag{A.5}$$

The larger the value of k, the greater the amount of the component in the stationary phase and the longer it will be retained on the column and k thus measures the extent to which a component is retained.

Equations A.2 and A.3 can be rearranged to yield a more useful working definition

$$k = \frac{K_C}{F} = \frac{K_C V_S}{V_M} \tag{A.6}$$

$$V_R = V_M + K_C V_S \tag{A.7}$$

where V_R is the retention volume, V_M is the retention volume for the retained component (dead volume), K_C is the distribution constant and V_S is the volume of the stationary phase.

Rearranging A.7 produces a new term, V'_R, the *adjusted* retention volume:

$$V_R - V_M = V'_R = K_C V_S \tag{A.8}$$

The *adjusted retention volume*, V'_R, is directly proportional to the thermodynamic distribution constant, K_C, and corrects the retention volumes of the components.

Rearranging Equation A.8 and substituting it yields a useful working equation for k:

$$k = \frac{V'_R}{V_M} = (\frac{V_R}{V_M}) - 1 \tag{A.9}$$

Both the retention volume V'_R and V_M can be measured directly from a chromatogram, such as the one in Figure A.1 so it is simple to determine the retention factor, k for any component.

Retardation Factor

The retention behaviour of a component can also be expressed using the *retardation factor* R which compares the velocity of the component through the column, μ, and the average velocity of the mobile phase, ū:

$$R = \frac{\mu}{\bar{u}} \tag{A.10}$$

where μ and ū can be obtained from:

$$\mu = \frac{L}{t_R} \tag{A.11}$$

$$\bar{u} = \frac{L}{t_M} \tag{A.12}$$

where L is the column length, t_R is the retention time of a component, and t_M is the retention time of a nonretained component defined in Section A.1.

The relationship between the retention volume, V_R and retention time, t_R, is given by:

$$V_R = t_R \times F_c \tag{A.13}$$

where F_c is the flowrate of the mobile phase in the column, which is usually assumed to be constant.

Combining Equations A.10, A.11, A.12 and A.13, the following definition of R is obtained:

$$R = \frac{\mu}{\bar{u}} = \frac{L/t_R}{L/t_M} = \frac{t_R}{t_M} = \frac{V_R/F_c}{V_M/F_c} = \frac{V_M}{V_R} \tag{A.14}$$

Equation A.14 can be rearranged to obtain a relationship between k and R using Equation A.9:

$$k = (\frac{V_R}{V_M}) - 1 = \frac{1}{R} - 1R = \frac{1}{(1+k)} \tag{A.15}$$

Plate Height

The rate at which the band in the chromatogram broadens depends on the "inefficiency" of the column which is more precisely defined as the *height equivalent to a theoretical plate (HETP)*. Martin and Synge defined the HETP, or H, as: *a unit of column length sufficient to bring the solute in the mobile phase into equilibrium with the solute in the stationary phase* (Coulson and Richardson, 1991). Plate models using this concept show H as:

$$H = \frac{L}{N} \tag{A.16}$$

where L is the column length and N is the plate number.

The plate number N is defined by McNair and Miller (1998) as a measure of the efficiency of the chromatographic system:

$$N = (\frac{t_R}{\sigma})^2 = 5.54(\frac{t_R}{w_h})^2 \tag{A.17}$$

Figures A.2 and A.3 show the measurements required for the calculation of N (in Equation A.17) from the chromatogram, where t_R is the time between the start of the chromatogram to the component peak, and w_h is the width of the peak at half the peak height.

Band Broadening

Band broadening refers to the gradual increasing width in the chromatographic zone as time increases and occurs in all forms of chromatography. Ban broadening results from the various kinetic processes taking place in the column as the separation progresses.

In most chromatographic separations, the components spread along the column as they are being separated. The molecules of a constituent begin as a narrow band at the top of the column. As the molecules move through the column, the narrow band gradually broadens, until towards the end of the column, the molecules are

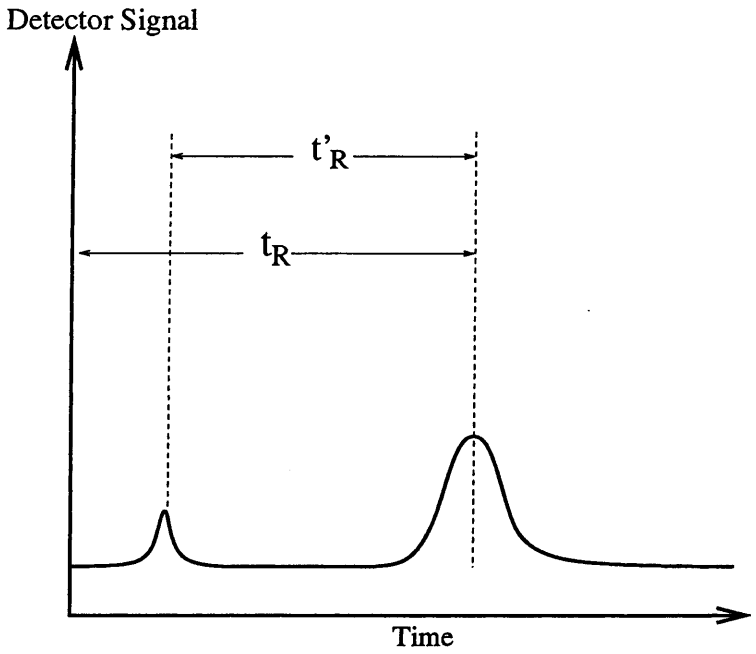

Figure A.2: Parameters which define the plate number

spread over a much wider portion of the column. From this, it can be deduced that the average migration rate for individual molecules of the constituent are not the same (Snyder and Kirkland, 1974).

This spreading of molecules is caused by the physical processes of eddy diffusion, longitudinal molecular diffusion and mass transfer kinetics taking place during chromatography and is known as *band spreading.* These physical processes are taken into account using the *van Deemter Equation.* A modern version of this equation is (Coulson and Richardson, 1991):

$$H = A + \frac{B}{\bar{u}} + C\bar{u} + C_m\bar{u} \tag{A.18}$$

which is related to $\bar{u}$, the average velocity of the mobile phase. Equation A.18 takes into account the three main effects that contribute to band broadening in packed columns; eddy diffusion (A-term), longitudinal molecular diffusion (B-term) and mass transfer in the stationary liquid phase and mobile phase (terms C and C_m

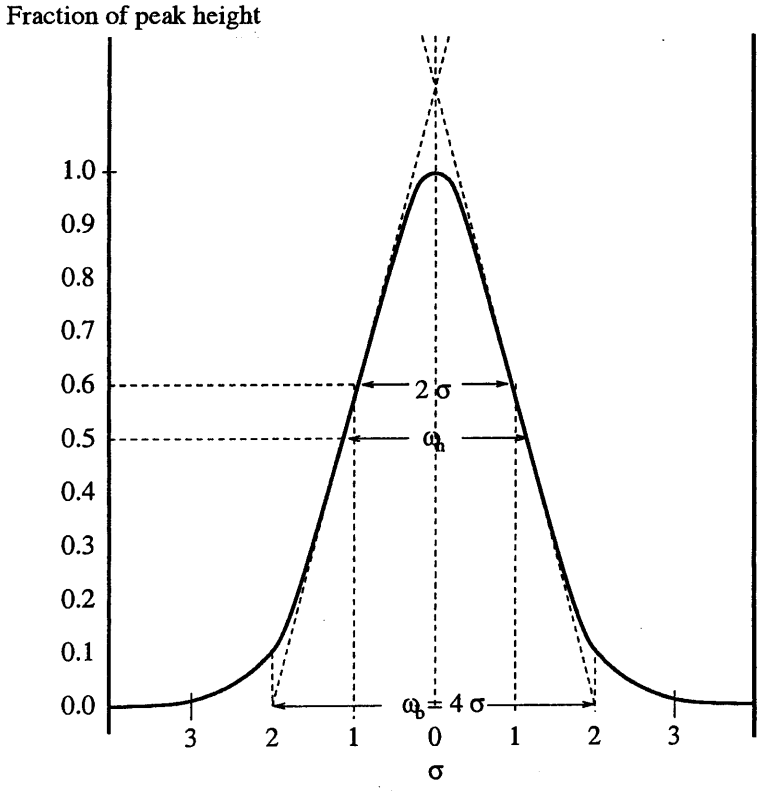

Figure A.3: Normal Gaussian distribution

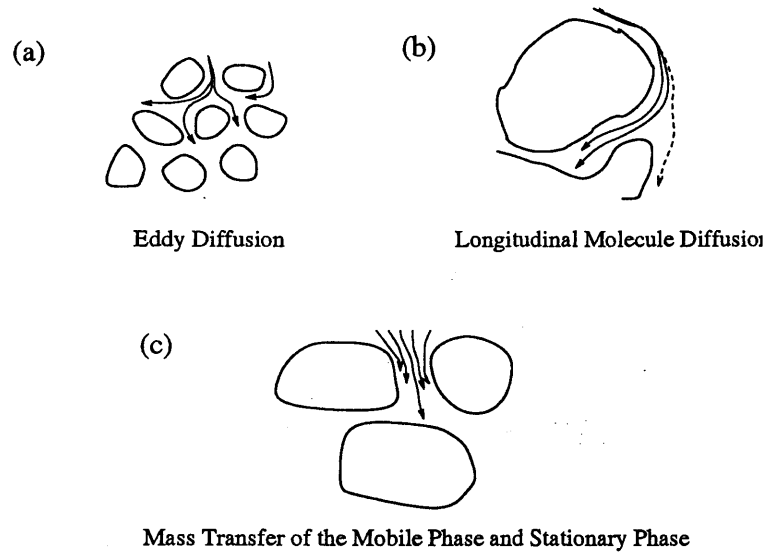

Figure A.4: Band Broadening in Chromatography

respectively).

Eddy diffusion in Figure A.4(a) describes the fact that the flow of liquid through a packed bed is irregular and these different flow paths vary in length and thus the flow velocities are different for each flow path.

Longitudinal molecular diffusion is the random movement of the molecules towards areas of lower component concentration. The longer the sample is in the column or the slower the flowrate, the wider the zone broadens. In Figure A.4(b), the dotted line illustrates the normal flow path otherwise.

The C term describes the lack of equilibrium between component in the two phases due to slow mass transfer in the stationary phase film. Figure A.4(c) shows this with the two flow paths penetrating the stationary phase, spending a longer time in the particle. C_m describes the slow mass transfer of component in the mobile phase during the passage of the component to and from the interface with the stationary phase. This is illustrated with the five flow paths in Figure A.4(c), with the flow path in the middle being the fastest, while those closer to the stationary phase particles being slower.

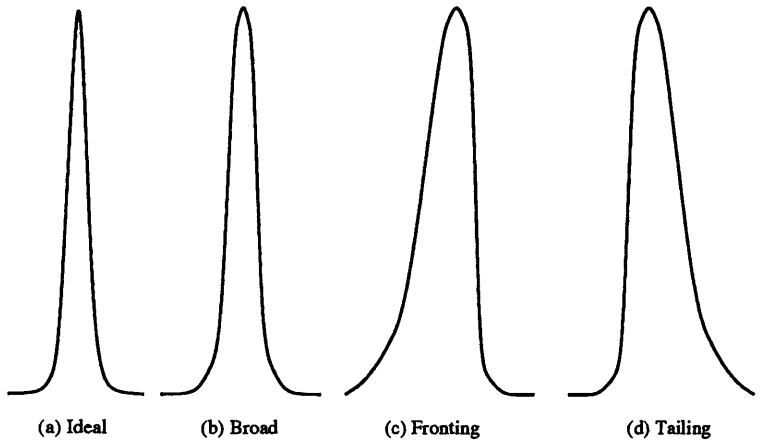

Figure A.5: Peak shapes of the chromatogram

Peak Shapes

Earlier, it has been noted that the component molecules act independently of one another during the chromatographic process. As such, a randomised aggregation of retention times are produced after repeated sorptions and desorptions. A component usually produces a distribution, or peak, which can be approximated as being *normal* or *Gaussian* and this peak shape represents the ideal.

Nonsymmetrical peaks are usually an indication of undesirable interaction between the constituents and the phases used in the process.Broad peaks are an indication that mass transfer kinetics are too slow. Asymmetric peaks are described as *fronting* (the front is less steep that the rear) or *tailing* (the rear is less steep than the front) depending on the location of the asymmetry. These are generally related to the shape of the adsorption isotherm in the separation system. Figure A.5 shows the appearance of these peak shapes.

Resolution

The *resolution* between two components achieved by a column depend on the opposed effects of the increasing separation of band centres and the increasing band width as bands migrate along the column (Coulson and Richardson, 1991). The

term *resolution* refers to the degree to which adjacent peaks are separated and the resolution R_s is defined by McNair and Miller (1998):

$$R_s = \frac{(t_R)_B - (t_R)_A}{\frac{(w_b)_A + (w_b)_B}{2}} = \frac{2d}{(w_b)_A + (w_b)_B} \tag{A.19}$$

where d is the distance between the peak maxima for the two components A and B, and w_b is the peak width at the base of A and B as denoted by the subscripts. Refer to Figure A.1 for an example of two component peaks in a chromatogram.

Appendix B

The mass balances of chromatography

The mass balances of chromatography that define the rate models used in this thesis are examined here and are derived from first principles using the law of conservation of mass with appropriate assumptions. The models being examined are the equilibrium-dispersive model and the general rate model, which commonly used in the open literature to describe chromatographic processes.

B.1 Derivation of the rate model

The following describe the assumptions on which the derivation of the differential mass balances of the components are based on:

- The column is assumed to be radially homogeneous.
- The compressibility of the mobile phase is negligible. Thus the mobile phase velocity is considered constant along the column and is proportional to the

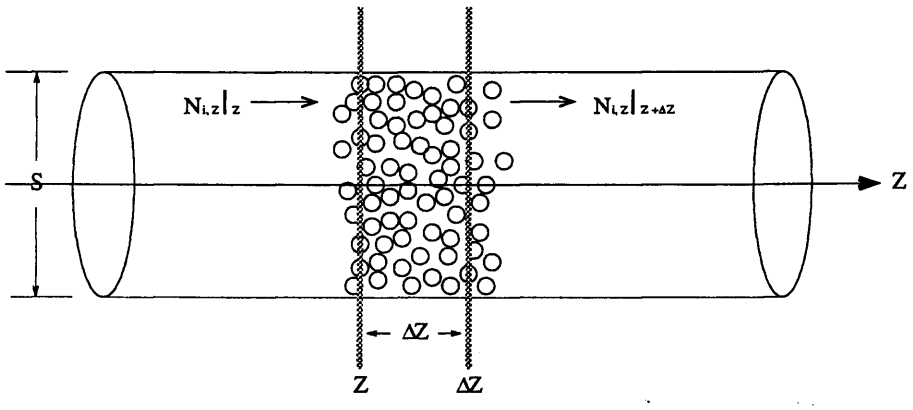

Figure B.1: Cross sectional profile of the chromatography column

pressure gradient which is itself constant. Similarly, the coefficients of the isotherm can be regarded as being independent of the pressure and constant along the column.

- The axial dispersion coefficient is assumed to be constant. It includes the contributions to the axial dispersion of the band due to molecular diffusion and eddy diffusion.

- The partial molar volumes of the sample components are the same in both phases. Thus, we can consider that the mass transfers taking place during the adsorption process are made at constant volume.

- The mobile phase is not adsorbed on the stationary phase.

- It is assumed that there are no thermal effects and the influence of the heat of adsorption on the band profile is neglected.

The principle of conservation of mass states that the differential mass balance in the bulk mobile phase is described as the difference between the amount of component i which enters a slice of column of thickness Δz during the time Δt and the amount of the same component which exits that slice in the same time is equal to

the amount accumulated in the slice:

$$Amount_{IN} - Amount_{OUT} = Amount_{ACCUMULATION} \tag{B.1}$$

The flux, $N_{i,z}$, of component i which enters the slice is

$$N_{i,z}\mid_{z,t} \quad = \quad \epsilon_T S(uC_i^m - D_{L,i}\frac{\partial C_i^m}{\partial z})\mid_{z,t} \tag{B.2}$$

where ϵ_T is the total porosity of the column packing, S the column geometric cross-sectional area, u the local average mobile phase velocity, C_i^m the local solute concentration in the mobile phase, $D_{L,i}$, the axial dispersion coefficient of component i in the mobile phase of component i, and z the distance along the column. The first term in the parentheses in Equation B.2 is the convection term and the second term is the axial dispersion term.

The flux of solute which exits from the slice is equivalently

$$N_{i,z}\mid_{z+\Delta z,t} \quad = \quad \epsilon_T S(uC_i^m - D_{L,i}\frac{\partial C_i^m}{\partial z})\mid_{z+\Delta z,t} \tag{B.3}$$

The rate of accumulation in the slice of volume $S\Delta z$ is

$$S\Delta z(\epsilon_T\frac{\partial C_i^m}{\partial t} + (1-\epsilon_T)\frac{\partial q_i}{\partial t})\mid_{\bar{z},t} \tag{B.4}$$

where $\bar{z}$ is the average value of z for the slice. The first and seconds terms in the parentheses in Equation B.4 correspond to the accumulation of the solutes in the mobile and stationary phases, respectively.

Thus the differential mass balance for component i in the mobile phase is

$$\frac{\partial C_i^m}{\partial t}\mid_{\bar{z}} + \frac{1-\epsilon_T}{\epsilon_T}\frac{\partial q_i}{\partial t}\mid_{\bar{z}} \quad = \quad \frac{D_{L,i}\frac{\partial C_i^m}{\partial z}\mid_{z+\Delta z,t} - D_{L,i}\frac{\partial C_i^m}{\partial z}\mid_{z,t}}{\Delta z} - \frac{uC_i^m\mid_{z+\Delta z,t} - uC_i^m\mid_{z,t}}{\Delta z} \tag{B.5}$$

Assuming that u and $D_{L,i}$ are constant along the column, and Δz tending towards 0, the mass balance may be reduced to:

$$\frac{\partial C_i^m}{\partial t} + F\frac{\partial q_i}{\partial t} + u\frac{\partial C_i^m}{\partial z} = D_{L,i}\frac{\partial^2 C_i^m}{\partial z^2} \tag{B.6}$$

where F is the phase ratio $F = \frac{1-\epsilon_T}{\epsilon_T} = \frac{V_S}{V_M}$ and V_S and V_M are the volumes of the stationary and mobile phases, respectively. Equation B.6 is a partial differential equation of the second order. The first two terms on the left hand side are the accumulation terms in the mobile and stationary phases, respectively. The third term is the convection term, whilst the term on the right hand side of the equation is the diffusion term.

B.1.1 Simplification of rate models

The rate model derived earlier is complex but can be simplified when different assumptions are employed. The following sections outline the three most common rate models used in modelling chromatographic processes according to their assumptions:

Ideal model

The ideal model assumes that the column efficiency is infinite, there is no axial dispersion and that both the mobile and the stationary phase are constantly at equilibrium (Guiochon *et al.*, 1994). As such, the axial dispersion term on the right-hand side of Equation B.6 may be neglected.

The influences of mass transfer kinetics and axial dispersion on the band profiles are completely neglected in this model. It focuses on the influence of the thermodynamics of phase equilibrium on the band profiles. Work done using this model include that of Hägglund and Ståhlberg (1997), Zhong and Guiochon (1998) and Golshan-Shirazi and Guiochon (1989a,b).

Equilibrium-dispersive model

The equilibrium-dispersive model assumes that all contributions due to nonequilibrium can be lumped into an apparent axial dispersion term, $D_{a,i}$, when the mass transfer kinetics are fast but not infinitely fast (Guiochon *et al.*, 1994). $D_{a,i}$ then replaces the term $D_{L,i}$ in Equation B.6. The model is described in more detail in

Section B.2.

This model is widely employed in the literature for modelling chromatographic processes, *e.g* Bellot and Condoret (1993a), Seidel-Morgenstern and Guiochon (1993), Charton *et al.* (1994), Heuer *et al.* (1995), Heuer *et al.* (1999), Quiñones *et al.* (2000), Mihlbachler *et al.* (2001), Teoh *et al.* (2001) etc.

General rate model

The general rate model takes into account all the phenomena which may have an influence on the band profiles, and these are described in more detail in Section B.3. The mass balances in the model is expressed by two partial differential equations for each component; one for the mobile phase flowing between the packing particles (Equation B.6 with $D_{ax,i}$ replacing $D_{L,i}$) and the another for the fluid contained inside the particles. This model is normally expressed in dimensionless form (Bellot and Condoret, 1991; Guiochon *et al.*, 1994; Gu, 1995).

Recent examples of modelling work using this model in the literature include work done by Gu and Zheng (1999), Klatt *et al.* (2000) and Kaczmarski *et al.* (2001).

B.2 Equilibrium-dispersive model

The equilibrium-dispersive model can be obtained by simplifying the rate model derived earlier, based on the following assumptions:

- The concentration of the solutes in the mobile and stationary phases are considered to be always in equilibrium in the whole column. This assumption is valid as long as the column efficiency is greated than a few hundred theoretical plates (Guiochon *et al.*, 1994)

- The contributions of all the nonequilibrium effects (such as axial dispersion and mass transfer resistance) can be lumped into an apparent axial dispersion

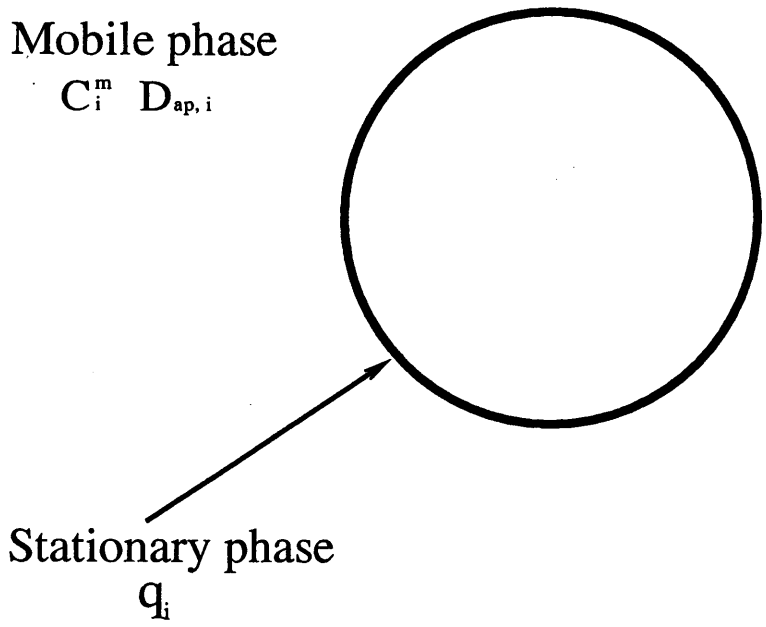

Figure B.2: Schematic of the particle flow in the equilibrium-dispersive model

coefficient, $D_{ap,i}$.

Figure B.2 shows the relationship described by the assumptions. The model thus essentially considers only two phases: the mobile phase and the stationary phase.

B.2.1 Dimensional equilibrium-dispersive model

The differential mass balance for component i can be described by the following mathematical form, in which $D_{L,i}$ in Equation B.6 is replaced by $D_{a,i}$:

$$\frac{\partial C_i^m}{\partial t} + F\frac{\partial q_i}{\partial t} + u\frac{\partial C_i^m}{\partial z} = D_{a,i}\frac{\partial^2 C_i^m}{\partial z^2}, \quad i = 1, 2, ..., N \tag{B.7}$$

Isotherms are used to describe the relationship between the solute concentration in the stationary and mobile phases as:

$$q_i \quad = \quad f(C_1^m, C_2^m, ..., C_N^m), \quad i = 1, 2, ..., N \tag{B.8}$$

where q_i and C_i^m are the solute concentrations in the stationary and mobile phases of component i, respectively.

The interstitial velocity of the mobile phase, u, can be expressed in terms of the column length, L, and the retention time of a non-retained component, t_0:

$$u = \frac{L}{t_0} \tag{B.9}$$

The phase ratio, F, is defined as the ratio of the volume of the stationary phase (V_S) to the liquid phase (V_M) in the column. It is normally expressed as a function of the total porosity, ϵ_T:

$$F = \frac{V_S}{V_M} = \frac{1-\epsilon_T}{\epsilon_T} \tag{B.10}$$

The total column porosity, ϵ_T, is defined as the ratio between the void volume, V_o, and the column volume, V_c:

$$\epsilon_T = \frac{V_o}{V_c} \tag{B.11}$$

The apparent dispersion coefficient, $D_{ap,i}$, can be estimated from the number of theoretical plates of the column, $N_{ap,i}$ as in the following:

$$D_{ap,i} = \frac{uL}{2N_{p,i}} \tag{B.12}$$

This stems from the relationship which gives the variance (in length units), σ_l^2, of a Gaussian peak (see Figure B.3 obtained over the length of the column under linear conditions for a Dirac pulse injection, where $\sigma_l^2 = HL = 2D_{ap}t_0$. The Dirac pulse injection is the typical condition often used in the theory of linear chromatography, where the injection width is 0, rendering the concentration of a small size injection to be abnormally high (Guiochon *et al.*, 1994).

The plate number, $N_{p,i}$ can be determined from either (a) the experimental elution profile or (b) using a modern form of the *van Deemter* equation: (a) Experimental elution profile (Synder and Kirkland, 1974):

The variance of the peak shown in Figure B.3 has units of time squared as the abscissa is in time. This time-based variance is designated as τ^2. The two standard

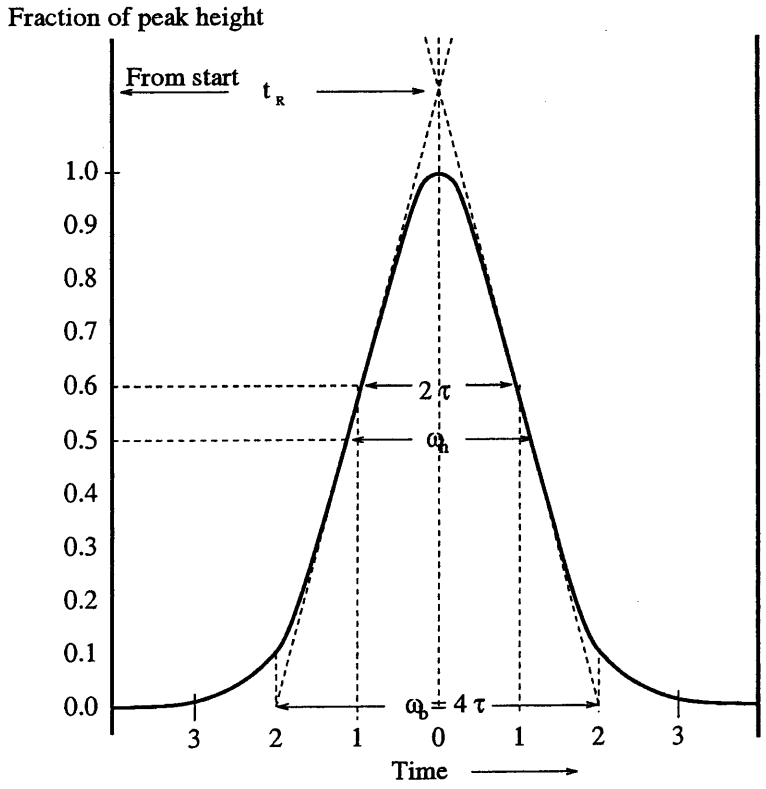

Figure B.3: Determination of the number of plates

deviations τ and σ are related by :

$$\tau = \frac{\tau}{L/t_R} \tag{B.13}$$

where L/t_R is the average linear velocity of the solute.

From Figure B.3, tangents at the inflection points on the two sides of the chromatographic peak are extended to form a triangle with the baseline. The area of this triangle can be shown to be approximately 96% of the total area under the peak (Skoog *et al.*, 2004). 96% of the area under a Gaussian peak is included within plus or minus two standard deviations of its maximum. Thus, the intercepts shown in Figure B.3 occur at approximately $\pm 2\tau$ from the maximum, and $w_b = 4\tau$, where W_b is the magnitude at the base of the triangle. Using this relationship in Equation B.13 and rearranging yields:

$$\tau = \frac{LW_b}{4t_R} \tag{B.14}$$

Since the column efficiency is defined as $H = \frac{\sigma^2}{L}$, substituting the equation for σ into it yields:

$$H = \frac{LW_b^2}{16t_R^2} \tag{B.15}$$

To obtain N, this is substituted into $N = \frac{L}{H}$ and then rearranged to obtain:

$$N = 16(\frac{t_R}{W_b})^2 \tag{B.16}$$

which may also be rewritten as

$$N_{p,i}^{exp} = 5.54(\frac{t_{R,i}}{\omega_{h,i}})^2 \tag{B.17}$$

where $N_{p,i}^{exp}$ is the experimental number of theoretical plates, $t_{R,i}$ is the retention time of the component i and $\omega_{h,i}$ is the peak width of the component i at half its peak height.

The plate number, $N_{p,i}$ can also be determined from

(b) Modern form of the *van Deemter* equation (Coulson and Richardson, 1994):

$$H_{p,i}^{mod} = A_i + \frac{B_i}{u} + C_{s,i}u + C_{m,i}u \tag{B.18}$$

where $H_{p,i}^{mod}$ is the theoretical plate height for component i. A_i, B_i, $C_{s,i}$ and $C_{m,i}$ are the van Deemter coefficients for component i, representing eddy diffusion (A_i), longitudinal diffusion (B_i), mobile phase mass transfer ($C_{m,i}$ and stationary phase mass transfer, including stagnant mobile phase in macropores ($C_{s,i}$, respectively. The parameters may also be obtained through parameter estimation, although the A and C terms tend to be dominant in liquid chromatography (Coulson and Richardson, 1994). The number of theoretical plates for component i, $N_{p,i}^{mod}$, can then be calculated from:

$$N_{p,i}^{mod} = \frac{L}{H_{p,i}^{mod}} \tag{B.19}$$

The column efficiency can be characterised by the reduced plate height, $h_{p,i}$, according to the following relationship:

$$h_{p,i} = \frac{H_{p,i}}{d_p} \tag{B.20}$$

where d_p is the diameter of the particle in the stationary phase. As a rule of thumb, the reduced plate height, $h_{p,i}$ for a component i is $2 \leq h_{p,i} \leq 4$ for an efficient column (Teoh *et al.*, 2001).

B.2.2 Dimensionless equilibrium-dispersive model

Given that the equilibrium-dispersive model is a fairly simple model, there is no real need to employ a dimensionless form for this model while doing calculations. However, as the dimensionless form of the general rate model is employed to simplify the calculations, having the equilibrium-dispersive model in a dimensionless form would be useful for any comparisons between the two models.

Model equations

In order to transform the model equations discussed in the previous section into the corresponding dimensionless forms, the following relationships apply:

$$c_i^m = \frac{C_i^m}{C_i^0} \tag{B.21}$$

$$q_i' = \frac{q_i}{C_i^0} \tag{B.22}$$

$$\zeta = \frac{z}{L} \tag{B.23}$$

$$\tau = \frac{ut}{L} \tag{B.24}$$

where C_i^0 is the sample concentration of component i, and is used to render the concentration dimensionless $[C_i^0(\tau)]$.

The Peclet number employed in the equilibrium-dispersive model equations may be expressed as:

$$Pe_i = \frac{uL}{D_{app,i}} \tag{B.25}$$

Equation B.7 may thus be rewritten as:

$$\frac{\partial c_i^m}{\partial \tau} + F\frac{\partial q_i'}{\partial \tau} + \frac{\partial c_i^m}{\partial \zeta} = \frac{1}{Pe}\frac{\partial^2 c_i^m}{\partial \zeta^2}, \quad i = 1, 2, ..., N \tag{B.26}$$

B.3 General rate model

The general model is the most comprehensive model of chromatography published in the literature, as it takes into account all the main phenomena which may have an influence on the band profiles such as axial dispersion, external mass transfer, intra-particle diffusion and the kinetics of adsorption-desorption (Guiochon *et al.*, 1994).

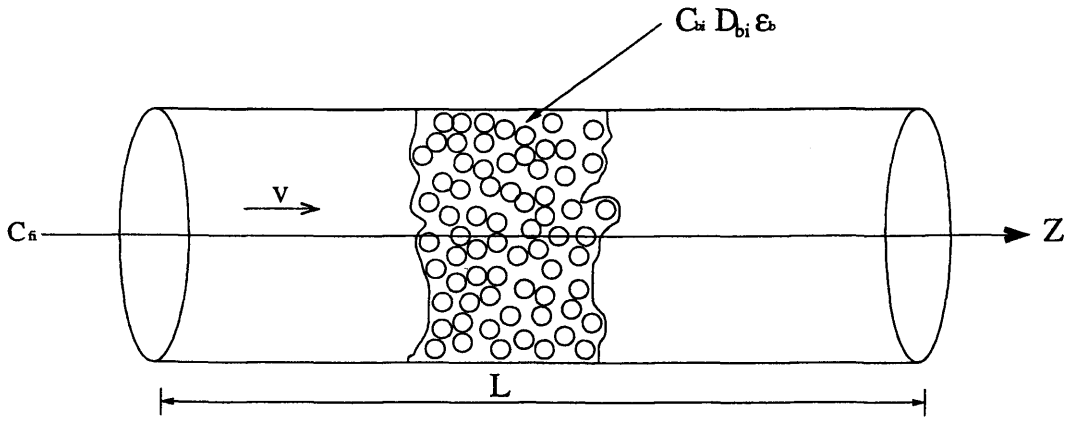

Figure B.4: Schematic of the bulk flow in the general rate model

However, as its use requires the independent determination of many parameters, it is computationally expensive, as compared to the ideal or equilibrium-dispersive model.

The general rate model considers three phases of separation. These include the mobile phase flowing in the space between the particles (the bulk liquid phase), the stagnant film of the mobile phase immobilised in the macropores (pore liquid phase) and the microporous stationary phase (adsorbed phase) where adsorption takes place. Thus, the model is able to account for the diffusional and mass transfer effects which are important in preparative and large-scale chromatography. The following assumptions are employed in a general non-linear rate model (Guiochon *et al.*, 1994):

- The compressibility of the fluid is neglected and isothermal operation is assumed.
- The column is a homogenous packed bed consisting of spherical porous particles with constant bed porosity. Hence the radial concentration gradient can be neglected.
- Local equilibrium exists for each component between the pore surface and the stagnant liquid phase in the macropores in the particle phase.

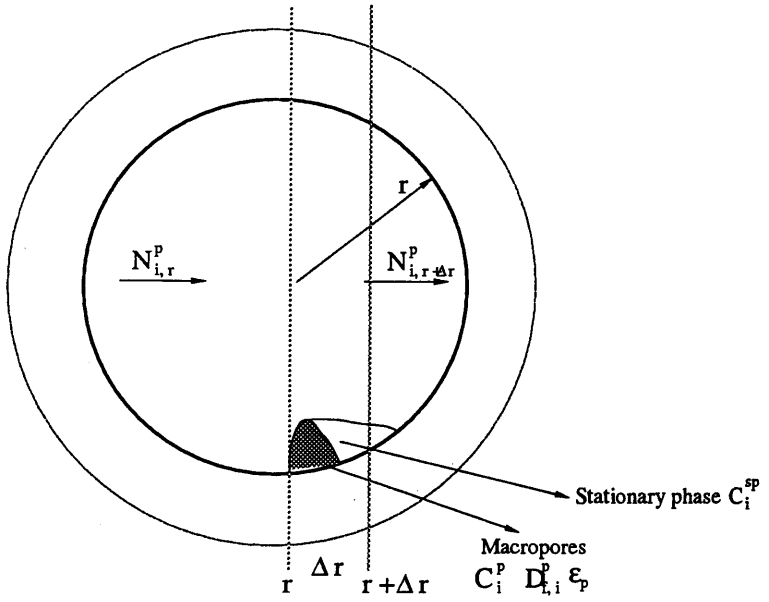

Figure B.5: Schematic of the flow across the particle in the general rate model

- Constant diffusional and mass transfer parameters are assumed.
- The mobile phase is not adsorbed on the stationary phase.

Derivation of the mass balance in the macropores

The general rate model has an additional mass balance across the macropores of the particles, as shown in Figure B.5.

$$Amount_{IN} - Amount_{OUT} = Amount_{ACCUMULATION} \tag{B.27}$$

The flux, $N^p_{i,r}$, of component i which enters the slice of the particle is

$$N^p_{i,r}\,|_{r,t} \quad = \quad \epsilon_P S_p (0 - D^p_{f,i} \frac{\partial C^p_i}{\partial r})\,|_{r,t} \tag{B.28}$$

where ϵ_P is the particle porosity, S_p the particle geometric cross-sectional area, C^p_i the solute concentration of the stagnant mobile phase in the particles, $D^p_{f,i}$, the pseudo diffusivity of component i in the macropores, and r the radial distance of the particle.

The flux of solute which exits from the slice is

$$N^p_{i,r+\Delta r}\mid_{r,t} \quad = \quad \epsilon_P S_p(0 - D^p_{f,i}\frac{\partial C^p_i}{\partial r})\mid_{r+\Delta r,t} \tag{B.29}$$

The rate of accumulation in the slice of volume $S_p\Delta r$ is

$$S^p\Delta r(\epsilon_P\frac{\partial C^p_i}{\partial t} + (1-\epsilon_P)\frac{\partial C^{sp}_i}{\partial t})\mid_{\bar{r},t} \tag{B.30}$$

where $\bar{r}$ is the average value of r for the slice, and C^{sp}_i is the concentration of the solute in the microporous stationary phase.

Thus the differential mass balance for component i in the macropores is

$$\frac{(\epsilon_P S_p D^p_{f,i}\frac{\partial Cp}{\partial r}\mid_{r+\Delta r,t} - \epsilon_P S_p D^p_{f,i}\frac{\partial Cp}{\partial r}\mid_{r,t})}{\Delta r} = S_p(\epsilon_P\frac{\partial C^p_i}{\partial t} + (1-\epsilon_P)\frac{\partial C^{sp}_i}{\partial t}) \tag{B.31}$$

With Δr tending towards 0, the mass balance may be reduced to:

$$\epsilon_P\frac{\partial C^p_i}{\partial t} + (1-\epsilon_P)\frac{\partial C^{sp}_i}{\partial t} - \epsilon_P D^p_{f,i}\frac{1}{r^2}(\frac{\partial}{\partial r}r^2\frac{\partial C^p_i}{\partial r}) = 0 \tag{B.32}$$

Equation B.32 is relevant as the diffusion in the macropores, whether coupled or not with external mass resistances, is usually a significant limiting step for the overall mass transfer rate. This mass balance accounts for:

- accumulation in the macropores ($\epsilon_P\frac{\partial C^p_i}{\partial t}$)
- accumulation in the microporous stationary phase ($(1-\epsilon_P)\frac{\partial C^{sp}_i}{\partial t}$)
- radial diffusion inside the porous particle ($\epsilon_P D^p_{f,i}\frac{1}{r^2}(\frac{\partial}{\partial r}r^2\frac{\partial C^p_i}{\partial r}$)

B.3.1 Dimensional general rate model

The model equations for the dimensional form for heterogeneous and homogenous particles given below are summarised from the works of Bellot and Condoret (1991), Gu *et al.* (1991) and Guiochon *et al.* (1994).

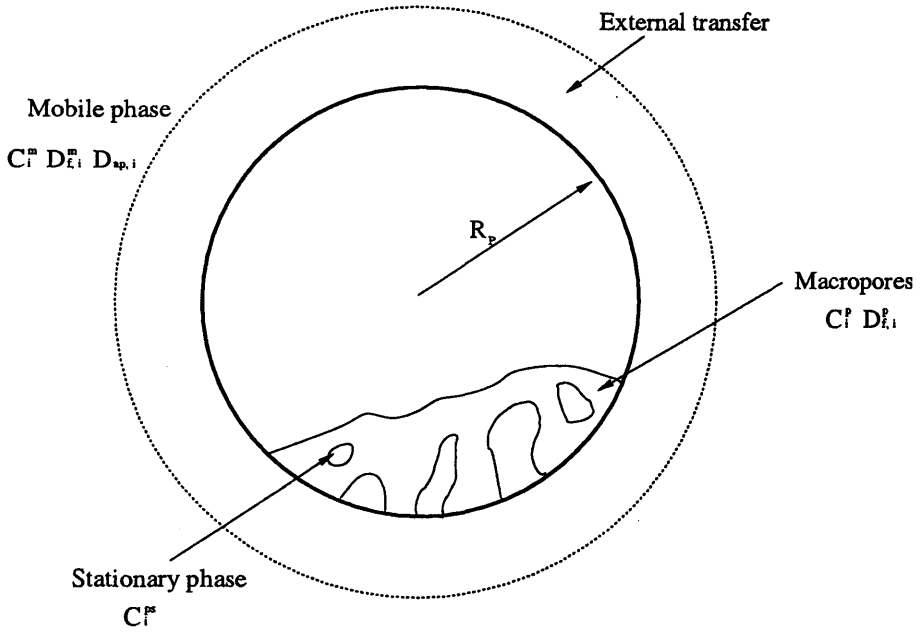

Figure B.6: Schematic of a heterogenous particle

Heterogenous particles

The continuity equation in the flowing mobile phase is

$$\frac{\partial C_i^m}{\partial t} + \frac{(1-\epsilon_B)}{\epsilon_B}\frac{\partial q_i}{\partial t} + v\frac{\partial C_i^m}{\partial z} = D_{ax,i}\frac{\partial^2 C_i^m}{\partial z^2}, \quad \forall i = 1,2,...,N, \quad z \in (0,L) \quad \text{(B.33)}$$

where C_i^m is the solute concentration in the mobile phase, q_i is the solute concentration in the stationary phase, ϵ_B is the bed voidage, v is the interstitial mobile phase velocity and $D_{ax,i}$ is the axial dispersion coefficient. The terms in the continuity equation may be described by the following phenomena:

- accumulation in the mobile phase $(\frac{\partial C_i^m}{\partial t})$
- accumulation in the stationary phase $(\frac{(1-\epsilon_B)}{\epsilon_B}\frac{\partial q_i}{\partial t})$
- convective transport in the mobile phase $(v\frac{\partial C_i^m}{\partial z})$
- transport by axial dispersion in the mobile phase $(D_{ax,i}\frac{\partial^2 C_i^m}{\partial z^2})$

Derivation of internal stagnant film diffusion equation The mass transfer rate of component i from the mobile phase towards the particle may be obtained by considering the mass balance across the internal stagnant film and across the intraparticle region.

Fick's law for the diffusion in fluids in the z direction is given by (Treybal, 1981):

$$N_A = -D_{AB}\frac{\partial C_A}{\partial z} \tag{B.34}$$

where N_A is the flux of a component A in solution in B, and D_{AB} is the diffusion coefficient for A in B. The negative sign emphasizes that diffusion occurs in the direction of a drop in concentration.

From this, the mass balance on the internal stagnant film over the particle (Figure B.6 can be derived in the form of the mass flux in the direction of radius R:

$$N_i = D^p_{f,i}\epsilon_P \left(\frac{\partial C^p_i}{\partial R}\right)_{R=R_p} \tag{B.35}$$

Since N_i describes the mass per unit surface area in unit time, to convert N_i into the form $\frac{\partial q}{\partial t}$, Equation B.35 is multiplied by the ratio $\frac{surface\ \ area\ \ of\ \ particle}{volume\ \ of\ \ particle}$. The particle is assumed to be spherical and the ratio is thus $\frac{4\pi R_p^2}{\frac{4}{4}\pi R_p^3} = \frac{3}{R_p}$. The diffusion in the internal stagnant film is accounted for by:

$$\frac{\partial q_i}{\partial t} = \frac{3D^p_{f,i}\epsilon_P}{R_p}\left(\frac{\partial C^p_i}{\partial R}\right)_{R=R_p} \quad \forall i = 1,2,...,N, \quad R \in [0, R_p] \tag{B.36}$$

where C^p_i is the solute concentration of the stagnant mobile phase in the particles, R_p is the particle radius, ϵ_P is the particle porosity and $D^p_{f,i}$ is the pseudo diffusivity of the component i in the macropores (this is usually lower than the molecular diffusion in the mobile phase).

Derivation of the intraparticle (external) diffusion equation The mass transfer rate equation for a general component A at the fluid phase interphase, or boundary, may be written as (Treybal, 1981):

$$N_A = k_L \Delta C_A \tag{B.37}$$

where k_L is the liquid mass transfer coefficient and ΔC_A is the change in concentration across the interphase.

The mass balance at the boundary of the particle may thus be described by:

$$N_i = K_{pm,i}(C_i^m - C_i^p \mid_{R=R_p}) \tag{B.38}$$

where $K_{pm,i}$ is the mass transfer coefficient of the mobile phase towards the particle outer area and is equivalent to k_L in Equation B.37
and using the conversion factor of $\frac{3}{R_p}$ to multiply Equation B.38, the external diffusion is described by:

$$\frac{\partial q_i}{\partial t} = \frac{3K_{pm,i}}{R_p}(C_i^m - C_i^p \mid_{R=R_p}) \tag{B.39}$$

The interstitial velocity, v, depends on the eluent flow rate, F_c, and the column diameter, D:

$$v = \frac{4F_c}{\epsilon_B \pi D^2} \tag{B.40}$$

Homogenous particles

For homogenous particles, each particle is considered as a pseudo-homogenous matrix where adsorption occurs at the outer area, followed by diffusion of the adsorbed components through the matrix via the macropores (Bellot and Condoret, 1991). As such, the second term in Equation B.32, expressing the accumulation in the microporous stationary phase, may be neglected to produce the following mass balance across the homogenous particle:

$$\frac{\partial C_i^{ps}}{\partial t} = D_{eff,i}^{sp}[\frac{1}{R^2}\frac{\partial}{\partial R}(R^2\frac{\partial C_i^{ps}}{\partial R})] \quad \forall i = 1,...,N \quad z \in [0,L] \quad R \in (0,R_p) \tag{B.41}$$

where $\frac{\partial C_i^{ps}}{\partial t}$ is the accumulation term in the adsorbed layer and the term on the right hand side of the equation accounts for the effective diffusion mechanism in the adsorbed layer. C_i^{ps} is the concentration of component i adsorbed on the outer layer

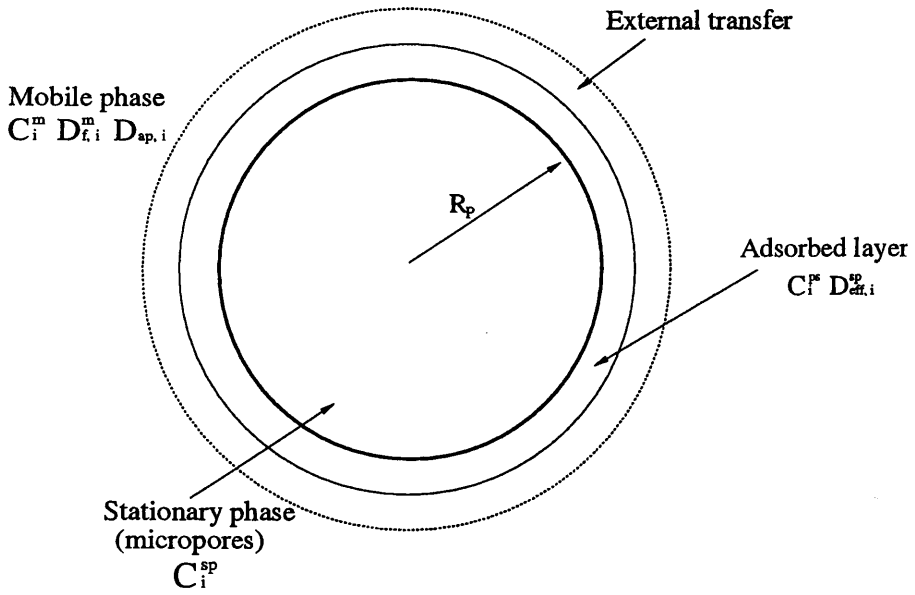

Figure B.7: Schematic of a homogenous particle

of the stationary phase, and $D_{eff,i}^{sp}$ is the effective diffusion coefficient of component i in the stationary phase, considered as pseudo-homogenous. This diffusivity is normally concentration dependent and therefore constant within the particle, but in the case of large concentration steps, this effective diffusivity should be considered a function of sorbate concentration (Bellot and Condoret, 1991).

The continuity equation in the mobile phase is similar to that of the heterogeneous particles (Equation B.33, except for the bed voidage, ϵ_B, which is replaced by the total column porosity, ϵ_T (which is related to ϵ_B and ϵ_P by $\epsilon_T = \epsilon_B + (1-\epsilon_B)\epsilon_P$), to produce the following expression:

$$\frac{\partial C_i^m}{\partial t} + \frac{(1-\epsilon_T)}{\epsilon_T}\frac{\partial q_i}{\partial t} + v\frac{\partial C_i^m}{\partial z} = D_{ax,i}\frac{\partial^2 C_i^m}{\partial z^2}, \quad \forall i = 1,2,...,N, \quad z \in (0,L) \quad \text{(B.42)}$$

The mass transferred from the mobile phase towards the adsorbed layer on the particle is similarly to Equation B.35:

$$N_i = D_{f,i}^p \epsilon_P \left(\frac{\partial C_i^{ps}}{\partial r}\right)_{R=R_p} \quad \text{(B.43)}$$

which is multiplied by the ratio $\frac{3}{R_p}$ to express the mass transfer in the homogenous particle as:

$$\frac{\partial q_i}{\partial t} = \frac{3D^p_{f,i}\epsilon_P}{R_p}\left(\frac{\partial C^p_i}{\partial R}\right)_{R=R_p} \quad \forall i = 1,2,...,N, \quad R \in [0, R_p] \tag{B.44}$$

$$\frac{\partial q_i}{\partial t} = \frac{3D^{sp}_{eff,i}}{R_p}\left(\frac{\partial C^{sp}_i}{\partial R}\right)|_{R=R_p} \quad \forall i = 1,...,N \quad z \in [0, L] \tag{B.45}$$

In this case, the equilibrium relationship links the concentration of the components adsorbed at the outer surface (C^{ps}_i at $R = R_p$) with the concentration in the mobile phase, close to the interface (C^{ms}_i):

$$C^{ps}_i = f(C^{ms}_i) \tag{B.46}$$

When considering intraparticle limiting diffusion, it may be written (Bellot and Condoret, 1991):

$$\frac{\partial q_i}{\partial t} = \frac{3K^{ms}_{pm,i}}{R_p}(f(C^m_i) - q_i) \quad \forall i = 1,...,N \quad z \in [0, L] \tag{B.47}$$

where $K^{ms}_{pm,i}$ is the mass transfer coefficient between the flowing mobile phase and the stationary phase. The external transfer is rarely a limiting step (Bellot and Condoret, 1991; Gu *et al.*, 1991).

B.3.2 Dimensionless general rate model

Due to the large number of parameters and variables involved in the dimensional general rate model, a systematic approach to identify these parameters and variables is required. The appropriate parameters and variables may be grouped together in dimensionless groups, which can then be employed to simplify the model equations accordingly, as it is usually difficult to quantify these parameters individually. The dimensionless model equation, coupled with the appropriate dimensionless equilibrium relationship and the corresponding initial and boundary conditions required to

model the system completely, are discussed in the following sections and are summarised from the works of Gu *et al.*, 1991; Ma *et al.*, 1996 and Gu and Zheng, 1999.

Model equations In order to transform the model equations discussed in the previous section into corresponding dimensionless forms, the following relationships are defined:

$$c_i^m = \frac{C_i^m}{C_i^0} \tag{B.48}$$

$$c_i^p = \frac{C_i^p}{C_i^0} \quad (Heterogenous) \tag{B.49}$$

$$c_i^{sp} = \frac{C_i^{sp}}{C_i^0} \quad (Homogenous) \tag{B.50}$$

$$c_i^{ps} = \frac{C_i^{ps}}{C_i^0} \tag{B.51}$$

$$z = \frac{z}{L} \tag{B.52}$$

$$r = \frac{R}{R_p} \tag{B.53}$$

$$\tau = \frac{ut}{L} \tag{B.54}$$

where C_i^0 is the sample concentration of component i, and is used to render the concentration dimensionless $[C_i^0(\tau)]$.

The dimensionless groups employed to simplify the model equations in this work included:

$$Bi_i = \frac{K_{pm,i}R_p}{\epsilon_P D_{f,i}^p} \quad (heterogenous) \quad \text{or} \quad \frac{K_{pm,i}R_p}{\epsilon_T D_{eff,i}^{sp}} \quad (homogenous) \tag{B.55}$$

$$Pe_i = \frac{vL}{D_{ax,i}} \tag{B.56}$$

$$\eta_i = \frac{\epsilon_P D^p_{f,i} L}{R_p^2 v} \quad (heterogenous) \quad \text{or} \quad \frac{\epsilon_T D^{sp}_{eff,i} L}{R^2 pv} \quad (homogenous) \tag{B.57}$$

$$\xi_i = \frac{3Bi_i\eta_i(1-\epsilon_B)}{\epsilon_B} \quad (heterogenous) \quad \text{or} \quad \frac{3Bi_i\eta_i(1-\epsilon_T)}{\epsilon_T} \quad (homogenous) \tag{B.58}$$

The dimensionless differential mass balance in the bulk liquid phase based on Equations B.33 and B.42 is then:

$$-\frac{1}{Pe_i}\frac{\partial^2 c_i^m}{\partial \zeta^2} + \frac{\partial c_i^m}{\partial \zeta} + \frac{\partial c_i^m}{\partial \tau} + \xi_i(c_i^m - c_i^p \mid_{r=1}) = 0 \quad \forall i = 1,...,N \quad \zeta \in (0,1) \tag{B.59}$$

The dimensionless differential mass balance in the pore phase for a heterogenous particle is:

$$\frac{\partial}{\partial \tau}[(1-\epsilon_B)c_i^{ps} + \epsilon_P c_i^p] - \eta_i[\frac{1}{r^2}\frac{\partial}{\partial r}(r^2\frac{\partial c_i^p}{\partial r})] = 0 \quad \forall i = 1,...,N, \quad \zeta \in [0,1] \quad r \in (0,1) \tag{B.60}$$

The continuity equation in the homogenous particle is transformed into its dimensionless form as:

$$\frac{\partial c_i^{sp}}{\partial \tau} = \eta_i[\frac{1}{r^2}\frac{\partial}{\partial r}(r^2\frac{\partial c_i^p}{\partial r})] \quad \forall i = 1,...,N \quad \zeta \in [0,1] \quad r \in (0,1) \tag{B.61}$$

B.4 Isotherm model

The isotherm model describes the interaction between the solute molecules in the mobile phase and the stationary phase. In most cases, under isocratic conditions *i.e.* no change in the mobile phase conditions, this relationship remains the same throughout the column However, for conditions where gradient elution is conducted,

this relationship changes across the stationary phase and with the change in the concentration of the mobile phase.

In this work, the same isotherm model is employed for both the equilibrium-dispersive and the general rate models. When the dimensionless form of the models are used, the isotherm similarly needs to be transformed, which is detailed in Section B.4.2.

B.4.1 Dimensional form

Since there is more than one component involved, a *multi-component competitive Langmuir isotherm* is employed in the models.

Isotherm for equilibrium-dispersive model

The equilibrium relationship of the solute concentration in the stationary and mobile phase is described by:

$$q_i = \frac{a_i C_i^m}{1 + \sum_{j=1}^{N} b_j C_i^m} \tag{B.62}$$

Isotherm for general rate model

The equilibrium relationship of the solute concentration inside the macropores and pore surface (stationary phase) is also described by the Langmuir isotherm:

$$C_i^{ps} = \frac{a_i C_i^p}{1 + \sum_{j=1}^{N} b_j C_i^p} \tag{B.63}$$

B.4.2 Dimensionless form

The following sections describe how the isotherms for both models are transformed to be used in the dimensionless models.

Dimensionless isotherm for equilibrium-dispersive model

The competitive Langmuir isotherm in Equation B.62 is rewritten in its dimensionless form as

$$q_i' = \frac{a_i c_i^m}{1 + \sum_{j=1}^{N} (b_j C_j^0) c_i^m} \tag{B.64}$$

where c_i^m and q_i' are the dimensionless concentrations in the mobile and stationary phases, respectively.

Dimensionless isotherm for general rate model

The competitive Langmuir isotherm in Equation B.63 is rewritten in its dimensionless form as

$$c_i^{ps} = \frac{a_i c_i^p}{1 + \sum_{j=1}^{N} b_j c_i^p} \tag{B.65}$$

where c_i^{ps} and c_i^p are the dimensionless concentrations in the microporous stationary phase and macropores, respectively.

B.5 Summary

The main equations governing the equilibrium-dispersive model and the general rate model are summarised in Table B.1.

Equilibrium-dispersive model

Dimensional $\frac{\partial C_i^m}{\partial t} + F\frac{\partial q_i}{\partial t} + u\frac{\partial C_i^m}{\partial z} = D_{a,i}\frac{\partial^2 C_i^m}{\partial z^2} \quad i = 1,2,...,N$

Dimensionless $\frac{\partial c_i^m}{\partial \tau} + F\frac{\partial q_i'}{\partial \tau} + \frac{\partial c_i^m}{\partial \zeta} = \frac{1}{Pe}\frac{\partial^2 c_i^m}{\partial \zeta^2} \quad i = 1,2,...,N$

$Pe_i = \frac{uL}{D_{app,i}}$

General rate model - Heterogenous particles

Dimensional $\frac{\partial C_i^m}{\partial t} + \frac{(1-\epsilon_B)}{\epsilon_B}\frac{\partial q_i}{\partial t} + v\frac{\partial C_i^m}{\partial z} = D_{ax,i}\frac{\partial^2 C_i^m}{\partial z^2} \quad \forall i = 1,2,...,N, \quad z \in (0,L)$

$\epsilon_P\frac{\partial C_i^p}{\partial t} + (1-\epsilon_P)\frac{\partial C_i^{sp}}{\partial t} - \epsilon_P D_{f,i}^p\frac{1}{r^2}(\frac{\partial}{\partial r}r^2\frac{\partial C_i^p}{\partial r}) = 0$

Dimensionless $-\frac{1}{Pe_i}\frac{\partial^2 c_i^m}{\partial \zeta^2} + \frac{\partial c_i^m}{\partial \zeta} + \frac{\partial c_i^m}{\partial \tau} + \xi_i(c_i^m - c_i^p\,|_{r=1}) = 0 \quad \forall i = 1,2,...,N \quad \zeta \in (0,1)$

$\frac{\partial}{\partial \tau}[(1-\epsilon_B)c_i^{ps} + \epsilon_P c_i^p] - \eta_i[\frac{1}{r^2}\frac{\partial}{\partial r}(r^2\frac{\partial c_i^p}{\partial r})] = 0 \quad \forall i = 1,2,...,N, \quad \zeta \in [0,1] \quad r \in (0,1)$

$Bi_i = \frac{K_{pm,i}R_p}{\epsilon_P D_{f,i}^p} \qquad Pe_i = \frac{vL}{D_{ax,i}}$

$\eta_i = \frac{\epsilon_P D_{f,i}^p L}{R_p^2 v} \qquad \xi_i = \frac{3Bi_i\eta_i(1-\epsilon_B)}{\epsilon_B}$

General rate model - Homogenous particles

Dimensional $\frac{\partial C_i^m}{\partial t} + \frac{(1-\epsilon_T)}{\epsilon_T}\frac{\partial q_i}{\partial t} + v\frac{\partial C_i^m}{\partial z} = D_{ax,i}\frac{\partial^2 C_i^m}{\partial z^2} \quad \forall i = 1,2,...,N, \quad z \in (0,L)$

$\frac{\partial C_i^{ps}}{\partial t} = D_{eff,i}^{sp}[\frac{1}{R^2}\frac{\partial}{\partial R}(R^2\frac{\partial C_i^{ps}}{\partial R})] \quad \forall i = 1,2,...,N \quad z \in [0,L] \quad R \in (0,R_p)$

Dimensionless $-\frac{1}{Pe_i}\frac{\partial^2 c_i^m}{\partial z^2} + \frac{\partial c_i^m}{\partial \zeta} + \frac{\partial c_i^m}{\partial \tau} + \xi_i(c_i^m - c_i^p\,|_{r=1}) = 0 \quad \forall i = 1,2,...,N \quad \zeta \in (0,1)$

$\frac{\partial c_i^{sp}}{\partial \tau} = \eta_i[\frac{1}{r^2}\frac{\partial}{\partial r}(r^2\frac{\partial c_i^p}{\partial r})] \quad \forall i = 1,2,...,N \quad \zeta \in [0,1] \quad r \in (0,1)$

$Bi_i = \frac{K_{pm,i}R_p}{\epsilon_T D_{eff,i}^{sp}} \qquad Pe_i = \frac{vL}{D_{ax,i}}$

$\eta_i = \frac{\epsilon_T D_{eff,i}^{sp} L}{R^2 pv} \qquad \xi_i = \frac{3Bi_i\eta_i(1-\epsilon_T)}{\epsilon_T}$

Table B.1: Principal equations governing the separation in the equilibrium-dispersive and the general rate model

Appendix C

Numerical solution techniques

The dynamic models outlined in Appendix B are in this work solved using gPROMS (general PROcess Modelling System) software (Process Systems Enterprise, 2005). In the following, a brief description is given of the numerical methods used by gPROMS for simulation, parameter estimation and optimisation.

C.1 Numerical methods

The mathematical models of chromatographic processes derived in Appendix B are made up of a system of partial differential algebraic equations (PDAEs), which can only be solved numerically. In this section, the numerical solution techniques for simulation in the *gPROMS* software (Process Systems Enterprise) are discussed.

C.1.1 Orthogonal collocation method

Orthogonal collocation is an efficient numerical method which can be used to solve partial differential and algebraic equations. In orthogonal collocation, the normalised space coordinate z in the interval [0,1] is divided into N elements, with

$N-1$ sub-domain boundaries as illustrated by Figure C.1 for orthogonal collocation of the fourth order.

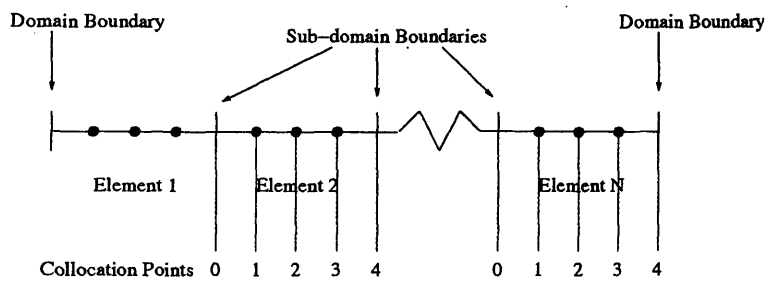

Figure C.1: Grid number for fourth order orthogonal collocation

The solution to the mathematical model is approximated in each element by a polynomial (*e.g.* Lagrange polynomial). The element is further subdivided into collocation points, with a local normalised space variable defined in each element. The model equations are fulfilled at the collocation points and the normalised positions of the collocation points are chosen as the roots of an orthogonal polynomial (*e.g.* Jacobian). Continuity of solution variables and the first order space derivatives are fulfilled at the element boundaries, whilst boundary conditions of the model equation are fulfilled at the domain boundaries.

C.1.2 Finite difference approximation of partial derivatives

The following derivations for the finite difference methods come from Holland and Liapis (1983).

Take $u(x,t)$ as a continuous function of distance and time with continuous partial derivatives over time and distance, x and t, respectively . The quantities Δx and Δt are defined such that they are always positive, with the subscripts j and n denoting small step changes in x and t, respectively.

$$\Delta x = x_{j+1} - x_j > 0 \tag{C.1}$$

and

$$\Delta t = t_{n+1} - t_n > 0 \tag{C.2}$$

The first few terms of a Taylor's series expansion of the function $u(x,t)$ about the point (x_j, t_n) and in the direction $x_{j+1}, t_n)$ are:

$$u_{j+1,n} \cong u_{j,n} + \Delta x u_x + \frac{(\Delta x)^2}{2!} u_{xx} + \frac{\Delta x)^3}{3!} u_{xxx} + \cdots \tag{C.3}$$

where the derivatives

$$u_x = \frac{\partial u}{\partial x} \tag{C.4}$$

$$u_{xx} = \frac{\partial^2 u}{\partial x^2} \tag{C.5}$$

are to be evaluated at the point (x_j, t_n)

Similarly, the function $u(x,t)$ about the point (x_j, t_n) and in the direction (x_j, t_{n+1}) is given by

$$u_{j,n+1} \cong u_{j,n} + \Delta t u_t + \frac{(\Delta t)^2}{2!} u_{tt} + \frac{\Delta x)^3}{3!} u_{ttt} + ... \tag{C.6}$$

with

$$u_t = \frac{\partial u}{\partial t} \tag{C.7}$$

$$u_{tt} = \frac{\partial^2 u}{\partial t^2}, ... \tag{C.8}$$

Forward difference formula

The *forward difference* formula with respect to x at a fixed t is obtained by solving Equation C.3 for u_x and rearranging to obtain

$$u_x = \frac{\partial u}{\partial x}\Big|_{x_j,t_n} = \frac{u_{j+1,n} - u_{j,n}}{\Delta x} + O(\Delta x) \tag{C.9}$$

Backward difference formula

When *u(x,t)* is expanded in the backward direction with respect to x from (x_j, t_n) to (x_{j-1}, t_n), the following is obtained:

$$u_{j-1,n} \cong u_{j,n} - \Delta x u_x + \frac{(\Delta x)^2}{2!} u_{xx} - \frac{(\Delta x)^3}{3!} u_{xxx} + ... \tag{C.10}$$

where

$$\Delta x = x_j - x_{j-1} \tag{C.11}$$

The *backward difference* formula with respect to x at a fixed t is obtained by solving C.10 for u_x and rearranging to obtain

$$u_x = \frac{\partial u}{\partial x}\Big|_{x_j,t_n} = \frac{u_{j+1,n} - u_{j-1,n}}{\Delta x} + O(\Delta x) \tag{C.12}$$

Central difference formula

The *central difference* formula for the expression u_x is (Holland and Liapis, 1983):

$$\frac{\partial^2 u}{\partial x^2}\Big|_{x_j,t_n} = \frac{u_{j+1,n} - 2u_{j,n} + u_{j-1,n}}{(\Delta x)^2} + O[(\Delta x)] \tag{C.13}$$

C.2 Optimisation background

Optimisation involves locating the best solution to a problem. Mathematically speaking, this means finding a minimum or maximum of a function or a model. In this section, optimisation and its terminology are introduced, followed by the optimisation methods employed in the *gPROMS* software (Process Systems Enterprise, 2005).

C.2.1 General optimisation problem formulation

The following sections outlines the general form for the optimisation problem for the chromatographic process, introducing the terms commonly encountered in the optimisation field.

Model

The mathematical model describing the chromatographic process has the general form:

$$f(x(t), \dot{x}(t), y(t), u(t), v, t) = 0 \quad \forall t \in [0, t_f] \tag{C.14}$$

where

- $x(t)$: differential variables (*e.g.* concentrations in the mobile phase and the stationary phase)
- $y(t)$: algebraic variables (*e.g.* mobile phase flowrate, velocity)
- $u(t)$: time-dependent (control) variables (*e.g.* feed injection, product withdrawal)
- v : time-invariant parameters (*e.g.* length and diameter of column, particle size)
- t : time

Initial conditions

The *initial conditions* required for the initialisation of the PDAE system can have the general form:

$$I(x(0), \dot{x}(0), y(0), u(0), v) = 0 \tag{C.15}$$

The values of the initial concentrations, holdups (*e.g.* in fraction collectors) throughout the chromatographic system may represent suitable conditions.

Constraints

Constraints refer to restrictions placed upon certain variables in order to ensure that the result of the optimisation will meet a certain criteria. There are usually different constraints which need to be considered in an optimisation problem.

Path constraints refer to those which hold at all times and may be represented as:

$$h(x(t), \dot{x}(t), y(t), u(t), v, t) \leq 0 \quad \forall t \in [0, t_f] \tag{C.16}$$

For instance, the pressure drop across the column must not exceed the maximum pressure drop at *any* time during the operation, otherwise the equipment will be damaged.

Point constraints refer to constraints which hold at a particular instant in time, t_λ, and have the general form:

$$g(x(t_\lambda), \dot{x}(t_\lambda), y(t_\lambda), u(t_\lambda), v, t_\lambda) \leq 0 \quad \lambda = 1, 2, \cdots \tag{C.17}$$

Of particular interest, are the constraints maintained at the end of the operation for the final point in time, t_f (*end-point constraints*), which usually impose the process specifications of purities and quantities of the products:

$$k(x(t_f), \dot{x}(t_f), y(t_f), u(t_f), v, t_f) \leq 0 \tag{C.18}$$

Bounds

There are also bounds imposed on the control variables and on the time-invariant parameters, which define the optimisation search space:

$$u^{min} \leq u(t) \leq u^{max} \quad \forall t \in [0, t_f] \tag{C.19}$$

$$v^{min} \leq v \leq v^{max} \quad \forall t \in [0, t_f] \tag{C.20}$$

Objective Function

The *objective function* is generally of the form:

$$\min \Phi(x(t_f), \dot{x}(t_f), y(t_f), u(t_f), v, t_f) \tag{C.21}$$

General Optimisation Problem Statement

The general dynamic optimisation problem formulation for the chromatographic process may summarised as follows:

$$\min\Phi(x(t_f), \dot{x}(t_f), y(t_f), u(t_f), v, t_f) \tag{C.22}$$

subject to

$$f(x(t), \dot{x}(t), y(t), u(t), v, t) = 0 \quad \forall t \in [0, t_f] \tag{C.23}$$

$$I(x(0), \dot{x}(0), y(0), u(0), v) = 0 \tag{C.24}$$

$$h(x(t), \dot{x}(t), y(t), u(t), v, t) \leq 0 \quad \forall t \in [0, t_f] \tag{C.25}$$

$$g(x(t_\lambda), \dot{x}(t_\lambda), y(t_\lambda), u(t_\lambda), v, t_\lambda) \leq 0 \quad \lambda = 1, 2, \cdots \tag{C.26}$$

$$k(x(t_f), \dot{x}(t_f), y(t_f), u(t_f), v, t_f) \leq 0 \tag{C.27}$$

$$u^{min} \leq u(t) \leq u^{max} \quad \forall t \in [0, t_f] \tag{C.28}$$

$$v^{min} \leq v \leq v^{max} \quad \forall t \in [0, t_f] \tag{C.29}$$

C.2.2 Optimisation methods

A class of optimisation problems exists where the equality constraints are ordinary differential equations (ODEs) and this class of problems is generally referred to as an *optimal-control* problem (OCP). There are three main methods to solving OCPs, grouped by:

1. indirect
2. direct
3. dynamic programming approaches

Indirect approach This refers to the OCP as an infinite dimensional problem where the control variable is a function of time and the solution of the OCP is thus taken from the solution of the necessary conditions derived from the Lagrange multiplier theory, leading to Pontryagin's maximum/minimum principle (Edgar and Himmelblau, 1988). In the literature a number of OCPs have been solved using this method although it is usually very difficult to solve (Cheng and Teo, 1987; Ouellet and Bui, 1993; Wang, 2002).

Dynamic programming Dynamic programming techniques can also be used to derive the optimal conditions for the OCP such as the iterative dynamic programming method employed by Luus (1994).

Direct approach In the direct approach, the original problem is transformed into a non-linear programming (NLP) problem. This is known as *control vector parameterisation*, which research has shown to be an efficient approach to solve OCPs (Vassiliadis, 1993; Vassiliadis *et al.*, 1999; Balsa-Canto *et al.*, 2001, 2002). Consider the true optimal control in a problem with the control variable $u(t)$ being approximately represented by

- a set of piecewise constant (discrete) values of u: $u(0), u(1), ..., u(n-1)$, where n is the number of time intervals. The computer optimum solution approximates the optimal control as shown by Figure C.2.
- a set of piecewise functional form of controls such as a linear or quadratic form

This resulting NLP may be solved using a standard optimisation method such as sequential quadratic programming (SQP).

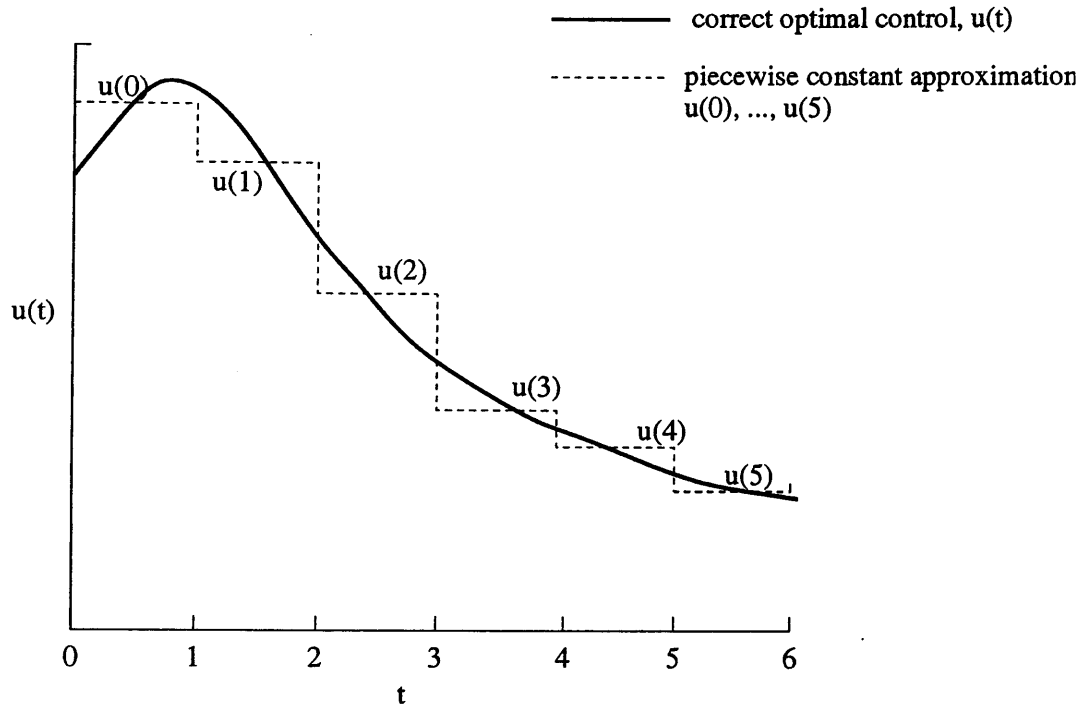

Figure C.2: Piecewise constant approximation of an optimal control

C.2.3 Dynamic optimisation

Optimisation problems considered in this work are carried out using *gPROMS* (Process Systems Enterprise, 2005). A knowledge of the approach undertaken is necessary to facilitate a complete understanding of the solution of dynamic optimisation problems within *gPROMS*.

gPROMS undertakes a *feasible path* approach, such that the solution obtained satisfies the model equation at all iterations. It employs the direct approach of *control vector parameterisation* to solving optimal control problems. All the control variables use the same control intervals, *i.e.*, they have the same number of time intervals.

A finite vector P consisting of the following decision variables solves the problem:

- Time horizon, or the total time for the operation, t_f
- Control interval durations, $\delta_k, k = 1...$number of intervals

- Parameters α_{uk} used to parameterise each control variable u in each control interval k *e.g.* injection volume, flowrates (switching action)
- Time-invariant parameters, v *e.g.* diameter and length of column, particle diameter

The approach is as follows:

1. Provide initial guesses for P
2. Iterate on P to improve the objective function (*e.g.* minimising total process costs in Chapter 5) while satisfying end point and interior point constraints (*e.g.* purities and recovery yields in fraction collectors for batch chromatography) and using the integrator to evaluate the objective function and the constraints derivatives with respect to P
3. Produce locally optimal values for P

In this manner, the infinite dimensional problem is converted to a finite dimensional non-linear programming (NLP) problem, which is solved using a sequential quadratic programming algorithm in *gPROMS*.

C.3 Parameter estimation background

In the following sections, the background to parameter estimation is outlined, including how parameter values are obtained, and background information on the statistics used in parameter estimation.

C.3.1 Introduction to parameter estimation

There are two principal methods by which unknown parameter values in mathematical models may be established (Bard, 1974):

- Calculating the value of a parameter by applying correlations that are already known.

- Measure the values of the model variables that occur in actual physical situations, and then fit the parameter values so that the model predictions of the physical situation matches the actual as closely as possible.

Parameter estimation refers to the implementation of the second procedure; the process of obtaining the unknown values of the parameters by matching the model predictions to the available sets of experimental data (Englezos and Kalogerakis, 2001). A parameter estimation problem employs the data gathered from one or more sets of experiments, which is characterised by the conditions under which they are performed, and attempts to determine the values for the unknown parameters, θ, in order to maximise the *probability* that the mathematical model will predict the values obtained from the experiment.

A parameter estimation problem is actually an optimisation problem. Thus some of the aspects of the problem formulation for parameter estimation is similar to that outlined in Section C.2.1 for an optimisation *i.e.* model(s), bounds, objective function. It involves the minimisation of the objective function (Φ), *i.e.* the difference between the experimental data (y_{exp}) and the predicted values (y_{pred}) computed using the estimated parameters in the models

$$\min\Phi(\|y_{exp} - y_{pred}\|) \tag{C.30}$$

Figure C.3 shows how the principle behind model parameter estimation in *gPROMS* (Process Systems Enterprise, 2005) works. The chromatographic process model $f(t)$ (as defined in Equation C.14) and experimental data ($y_{exp}(t)$) (chromatographic elution profiles are used in this work) is used in the estimator to estimate the vector set of unknown parameters, θ (in this thesis, unknown isotherm parameters were estimated). The estimator sets to maximise the probability that the mathematical model will predict the values obtained from the experiments, and estimate the

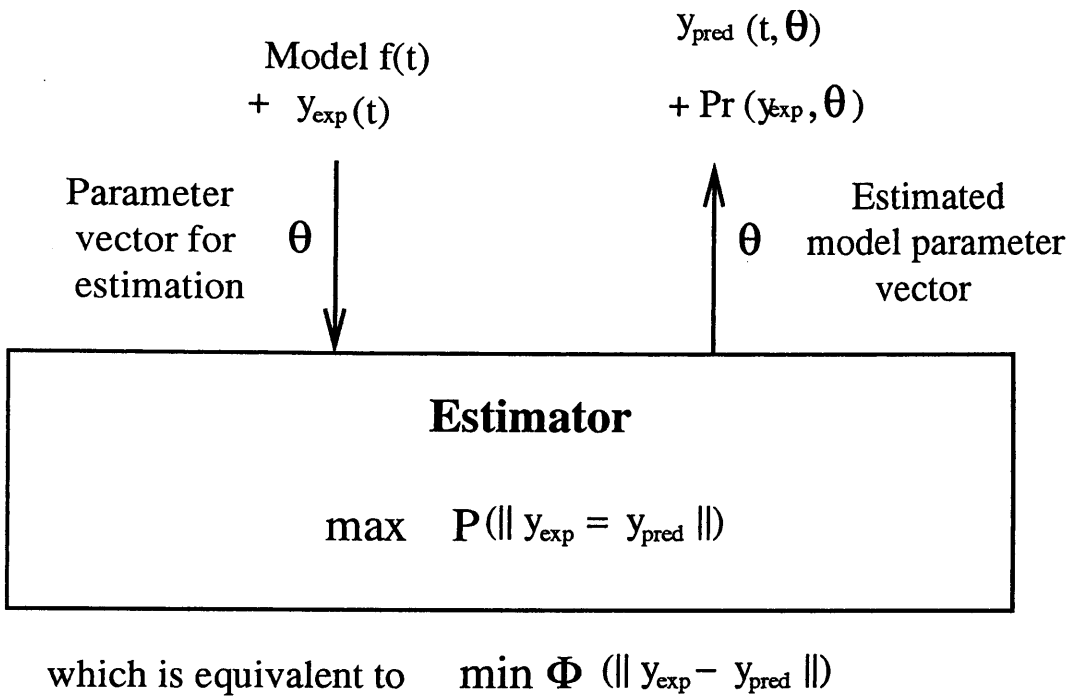

Figure C.3: Illustration of the principle of parameter estimation

specified unknown model parameters (θ) to do so. In addition, the set of inferential statistics ($Pr(y_{exp}, \theta)$) involved in the estimation procedure is generated. From this information, the values for the estimated parameters θ can be evaluated to determine if they are statistically significant.

C.4 Experimental data used for parameter estimation

Parameter estimation is based on experimental data provided to the estimator consisting of observed or measured values of the model variables. The conditions and method by which the data is obtained is not considered here, although further details on what experiments should be performed for estimating a given model may be found in Bard (1974).

In practice, the exact value of the variables are not known because:

1. Measurement techniques have limited accuracy
2. Conditions under which the model was derived are not quite attainable
3. Disturbances occur

A complete model should be able to describe these random elements of the situation, and an appropriate description of random phenomena can be done through probability statements. Thus, an understanding of the statistics involved in parameter estimation is necessary.

C.5 Introduction to statistics

Statistics is the branch of mathematics that deals with data-based decision making. In having only a sample of the population in which a decision has to be made, uncertainty arises. For instance, if the probability that the parameters estimated will give model elution profiles predicting the experimental data used is 95%, one may decide such an estimation is sufficient. Some of the terminology used in evaluating the statistics in this thesis will be outlined in the following sections.

C.5.1 Probability distributions

Probability distributions are relative frequency distributions used to describe the data of a sample, and they predict the distribution of the outcomes when the experiment is performed many times. Depending on the form of the variable, the probability distribution will be either discrete or continuous.

Discrete probability distribution

Each possible outcome of a discrete measurement has a probability. A discrete probability distribution is a data set that specifies the probability associated with each possible outcome or measurement. Examples of discrete random variables include

the number of collectors in a chromatographic separation, number of chromatographic columns *etc.*. Discrete random variable X defined on a sample space and each of its values represents an outcome or event - thus can determine the probability $P(x)$ for it.

Continuous probability distribution

A continuous random variable is one which takes an infinite number of possible values. Continuous random variables are usually measurements *e.g.* concentration, flowrate, the process operation time. Continuous probability distribution is defined as follows: the probability of a continuous random variable X assuming any particular value x is 0. The probability the continuous variable X assuming a value of x for a particular *interval* of values of X is determined by the the area under the probability density function curve (or probability distribution) for this interval.

C.5.2 Population mean

The population *mean* of a random variable indicates its average or central value. It is a useful summary value (a number) of the variable's distribution. For a random value of X with values x, the mean is defined by:

$$Mean\ \mu = \sum xP(x) \tag{C.31}$$

where $P(x)$ is the probability distribution of X.

C.5.3 Population variance

The (population) *variance* of a random variable is a non-negative number which gives an idea of how widely spread the values of the random variable are likely to be; the larger the variance, the more scattered the observations on average. Stating the variance gives an impression of how closely concentrated round the expected

value the distribution is; it is a measure of the "spread" of a distribution about its average value. The variance is symbolised by σ^2.

$$Variance\ \sigma^2 = \sum (x - \mu)^2 P(x) \tag{C.32}$$

C.5.4 Confidence intervals

A *confidence interval* provides an estimated range of values which is likely to include an unknown population parameter, with the estimated range being calculated from a given set of sample data.

If independent samples are taken repeatedly from the same population, and a confidence interval calculated for each sample, then a certain percentage (confidence level) of the intervals will include the unknown population parameter. Confidence intervals are usually calculated so that this percentage is 95%, but we can produce 90%, 99%, 99.9% (or whatever) confidence intervals for the unknown parameter.

Figure C.4 shows a probability distribution for a sample mean $\bar{X}$ around the unknown population mean μ for a confidence level of 95%. Thus 2.5% probability is each excluded in the tail ends of the distribution. Statistical tables in Wonnacott and Wonnacott (1990) show the sampling error to be $\pm$ 1.96SE, where SE is the standard error. This may be expressed as

$$\Pr(\mu - 1.96SE \leq \bar{X} \leq \mu + 1.96SE) = 95\% \tag{C.33}$$

which is equivalent to saying, "There is a 95% chance that $\bar{X}$ will be close to μ, within 1.96SE."

The width of the confidence interval gives us some idea about how uncertain we are about the unknown parameter. A very wide interval may indicate that more data should be collected before anything very definite can be said about the parameter.

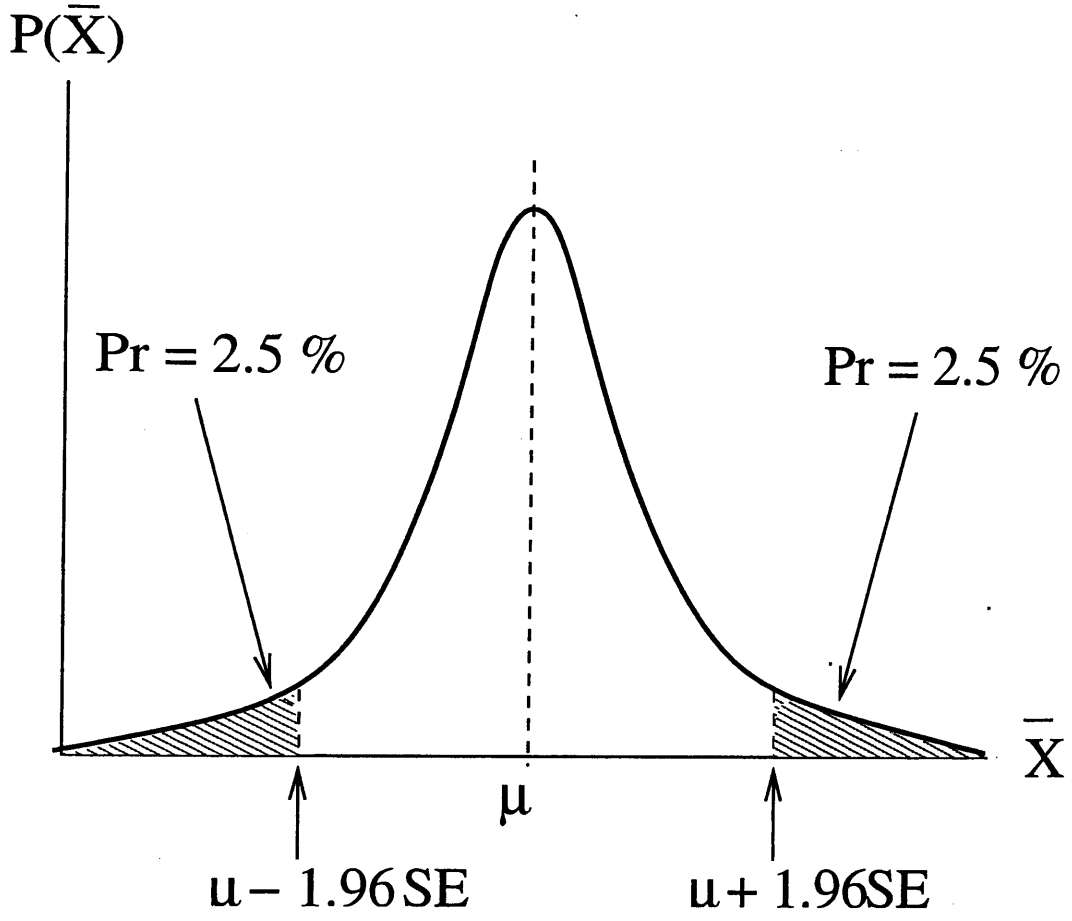

Figure C.4:

C.5.5 Estimator

An estimator is any quantity calculated from the sample data which is used to give information about an unknown quantity in the population. For example, the sample mean $\bar{X}$ is an estimator of the population mean μ:

The usual estimator of the population mean is

$$\bar{X} = \frac{\sum x_i}{n} \quad \forall i = 1, 2, \cdots, n \tag{C.34}$$

where n is the size of the sample and x_1,x_2, x_3,...,x_n are the values of the sample. If the value of the estimator in a particular sample is found to be 5, then 5 is the estimate of the population mean μ.

In *gPROMS*, the *maximum likelihood estimator* is used and more information about this and other estimators may be found in Section C.6.

C.6 Estimators

Some of the more common estimation methods are discussed in the following section.

C.6.1 Least squares

The least squares (LS) estimation method obtains its estimate of θ by minimizing the sum of squares (SSQ) where:

$$SSQ = \sum_{i=1}^{n}(z_i - f(x_i, \theta))^2 \tag{C.35}$$

where z_i is the ith observed value, and $f(x_i, \theta)$ is the outcome of the ith observation for the model. In the linear case, SSQ is minimised by the solution of a set of linear equations and does, in fact, have a unique answer of the design matrix is not singular, where one or more linear combinations of the data are identically zero. There is no exact solution for the nonlinear case, and therefore we use various nonlinear optimisation schemes that use the sum of squares as the objective function being minimised.

C.6.2 Maximum likelihood

A maximum likelihood estimate is that estimate of θ that maximises the likelihood function $L(\theta)$, where

$$L(\theta) = \prod_{i=1}^{n} f(x_i, ; \theta) \tag{C.36}$$

The likelihood function is defined as a joint probability distribution function generally based on the distribution of the error terms.

Sampling experiments have shown that the maximum likelihood method produces acceptable estimates in many situations and its generality and relative ease of application make it a strong candidate for parameter estimation (Bard, 1974). It is for these reasons, that this estimation method that is employed in the parameter estimation studies done in this research.

C.6.3 Bayes

In this approach, it is necessary to describe the parameter values before seeing the data in the form of a distribution of subjective probability, called a *prior distribution.* In Bayesian estimation, this prior density makes the estimation problem formulation more tractable mathematically.

C.6.4 Method of moments

Moments of the probability distribution of a random variable are defined in terms of expectations in that we let μ'_r denote the rth moment aout 0, $\mu'_r = E[x^r]$. $E[x^r]$ is the expected value of the rth moment, and we define the expected value to be

$$E[X] = \int_{-\infty}^{\infty} x f(x;\theta) dx \tag{C.37}$$

$E[X]$ is the average of the values of the random variable X. These values are weighted by the probability that the random variable is equal to that value, thus the integral.

C.6.5 Sampling distributions

Inferential statistics is concerned with making decisions about populations based on information obtained from random samples. In most problems, the decision ultimately becomes a choice among one of several alternatives. Whether the decision is selection from several competing hypotheses or choice of an estimate, the chal-

lenge is to make a decision with a low probability of error, but without being so conservative that useful choices cannot be made.

There are two forms of statistical inferences: confidence intervals and hypothesis testing (Johnson, 1996). Inferences about the population mean μ are based on the sample mean $\bar{X}$ and information obtained from the sampling distribution of sample means. The sampling distribution of sample means has a mean μ and a standard error of $\frac{\sigma}{\sqrt{n}}$ for all samples of size n and is normally distributed when the sampled population has a normal distribution or when the sample size is sufficiently large.

For an ideal situation, where σ is known, the test statistic z, which has standard normal distribution may be used, where $z = (\bar{X} - \mu)/(\frac{\sigma}{\sqrt{n}})$. However, when σ is unknown, the standard error $\frac{\sigma}{\sqrt{n}}$ is also unknown. Therefore, the sample standard deviation s is used as a point estimate for σ, where $\frac{s}{\sqrt{n}}$ gives the standard error of the mean.

C.6.6 Student t distribution

W. S. Gosset published a paper about this t-distribution under the pseudonym "Student" in 1908, hence its name. In deriving the t-distribution, Gosset assumed that the samples were taken from a normal population. Although this appears restrictive, it was found that satisfactory results are obtained when selecting large samples from many non-normal populations.

The Student t distribution is a family of probability distributions, where σ is unknown and has to be estimated with the *sample standard deviation* s. Then the statistic is called t instead of z. When s is used to make an inferences about the mean μ, the sample provides the value of the sample mean $\bar{X}$ and the estimated standard error $\frac{s}{\sqrt{n}}$, thus replacing the z-statistic with a new statistic which accounts for the use of an estimated standard error. This new statistic is known as the **Student's t-statistic**. Thus by using the t-statistic, we can determine both the values of $\bar{X}$ and estimated standard error $\frac{s}{\sqrt{n}}$. The Student t-distribution assumes

that the sampled population is normally distributed.

This is the sampling distribution employed in *gPROMS* (Process Systems Enterprise, 2005), to establish if the parameters estimated are statistically significant.

C.6.7 χ^2 distribution

Inferences about the variance of a normally distributed population use the **chi-square**, χ^2 distribution. The χ^2 distributions, like the Student t-distributions, are a family of probability distributions, each one being identified by the parameter, number of degrees of freedom (Johnson, 1996).

The t procedures for inferences about the mean were based on ther assumption of normality, but they are general useful even for sampled nonnormal populations, provided the the sample number is large. However, the statistical procedures for standard deviation are very sensitive to nonnormal distributions (skewness especially), and this makes it difficult to determine whether an apparent significant result is the result of the sample evidence or a violation of the assumptions (Johnson, 1996). Thus, the inference procedure of hypothesis test is usually used for the standard deviation of a normal population.

C.6.8 F distribution

The F distribution is a family of probability distributions, similar to the t distribution and χ^2 distribution. Each F distribution is identified by two numbers of $(df-1)$ for each of two samples involved. Inferences can thus be made about the ratio of variances for two normally distributed populations using the F distribution. The distribution of this ratio was first investigated by Sir Ronald Fisher (1890-1962) and it is called the Fisher (or F) distribution in his honour.

When comparing the standard deviation of two populations, the sampling distribution dealing with the sample standard deviation is sensitive to slight departures from assumptions (Johnson, 1996). Therefore, the inference procedure used is that

of the hypothesis test for the equality of the standard deviation for two normal populations.

C.7 Summary

The need for parameter estimation to obtain unknown values has been discussed and the nature of statistics behind the estimation process has been briefly introduced. A few common parameter estimator tools used have also been outlined, with the maximum likelihood estimator employed for the parameter estimation studies in this research work.

Appendix D

Statistics of parameter estimation in Chapter 3

The case studies in Chapter 3 are in this work use gPROMS (general PROcess Modelling System) software (Process Systems Enterprise, 2005) for parameter estimation. In the following, the results of the statistics of the parameter estimation generated by gPROMS are summaried.

D.1 Case study 1

Case study 1 is a theoretical separation, using data generated by the general rate model. The equilibrium-dispersive model parameters estimated using this data are tabulated in Table D.1:

The parameters with the *t-values* in bold have values higher than the reference t-value (here 1.65) and are thus regarded to be 95% accurate. In Tables D.1 and D.2, most of the data is shown to be insufficient to estimate the parameters for most of the components, apart from Component 6. This is expected, as Component 6

Parameters estimated	**Estimate**	**95% t-value**
$K1_1$	74.77	0.0677
$K1_2$	103.67	0.0563
$K1_3$	136.29	0.348
$K1_4$	550**	-
$K1_5$	125.68	**7.45**
$K1_6$*	199.3	**6.5**
$K2_1$	2.09	0.0913
$K2_2$	1.82	0.102
$K2_3$	6.75	0.171
$K2_4$	6.82	0.027
$K2_5$	19.62	**14.8**
$K2_6$*	40.54	**15.7**
Reference t-value (95%): 1.65		

Table D.1: Statistics of the isotherm parameter estimation for the equilibrium-dispersive model in Case Study 1

* Experimental data supplied, **estimate on bound

Parameters estimated	**Estimate**	**95% t-value**
$K1_1$	87.2	0.185
$K1_2$	109	0.199
$K1_3$	104	0.41
$K1_4$	125	0.0472
$K1_5$	90	0.15
$K1_6$*	100	**5.82**
$K2_1$	0.14	0.0505
$K2_2$	0.26	0.122
$K2_3$	2.45	1.1
$K2_4$	6.45	0.0667
$K2_5$	10.1	**4.91**
$K2_6$*	22.0	**12.5**
Reference t-value (95%): 1.65		

Table D.2: Statistics of the isotherm parameter estimation of for the general rate model in Case Study 1

* Experimental data supplied

Parameter estimation	Estimation	95% t-value
$b1_1$	47.9	0.00345
$b1_2$	16.3	0.00347
$b1_3$	16.8	0.00348
$b1_4$	15.6	0.00348
$b1_5$*	**19.3**	0.00348
$b2_1$	0.88	0.00346
$b2_2$	1.67	0.0035
$b2_3$	0.98	0.00351
$b2_4$	1.29	0.00351
$b2_5$*	**2.27**	0.0035
C^{∞}	8.46	0.0035
Reference t-value (95%): 1.66		

Table D.3: Statistics of the isotherm parameter estimation for the equilibrium-dispersive model in Case Study 2 (10CV load)

* Experimental data supplied

was the only experimental data supplied for the parameter estimation, in addition to the total concentration.

D.2 Case study 2

Parameters with the *t-values* values lower than the reference t-value (here 1.66) are thus regarded to have insufficient information to accurately predict the parameters. In Tables D.3 and D.4, the data is shown to be insufficient to estimate the parameters for most of the components, even with the information of Component 5 (ADH) supplied. Employing additional data sets 2 and 3 also do not render 95% t-values higher than the reference 95% t-value, suggesting that the data employed is insuf-

Parameter estimation	**Estimation**	**95% t-value**
$b1_1$	19.58	0.00151
$b1_2$	41.14	0.00148
$b1_3$	280.31	0.00113
$b1_4$	309.61	0.00113
$b1_5$*	**14.61**	0.00147
$b2_1$	0.042	0.00155
$b2_2$	0.219	0.00153
$b2_3$	0.418	0.00153
$b2_4$	0.294	0.00153
$b2_5$*	**0.741**	0.00153
C^{∞}	7.79	0.00153
Reference t-value (95%): 1.66		

Table D.4: Values used in the isotherm parameter estimation for the general rate model in Case Study 2 (10CV load)

* Experimental data supplied

Parameter	Estimate	95% t-value
α'_1	-0.7	**210**
α'_2	0.089	**26.6**
α'_3	0.271	**80.4**
α_4	0.158	**46.8**
γ_1	-6.5**	-
γ_2	-10**	-
γ_3	-3.67	**5840**
γ_4	-1.95	**2590**
C^∞	46.08	**131**
Reference t-value (95%): 1.66		

Table D.5: Statistics of the parameter estimation for the equilibrium-dispersive model in Case Study 3

** estimate on bound

ficient to estimate these parameters accurately. It is thus decided to adopt these parameters for the estimation, based on the best fit of the curve, with the lack of further information.

D.3 Case study 3

Most of the isotherm parameters estimated have *t-values* values higher than the reference t-value (here 1.66) are thus regarded to be 95% accurate in Tables D.5 and D.6. The α_4 parameter (for myoglobin) in the GR model is lower than the reference t-value, suggesting that it is less accurate, and this is reflected in the poorer fitting seen in Figure 3.19(b) in Chapter 3.

Parameter estimation	**Estimation**	**95% t-value**
α_1'	-0.993	**65.9**
α_2'	-0.191	**12.6**
α_3'	0.104	**6.84**
α_4	-0.00106	0.0698
γ_1	-8.96	**39.5**
γ_2	-12**	-
γ_3	-5.37	**4210**
γ_4	-3.52	**2850**
C^∞	42.41	**28.9**
Reference t-value (95%): 1.66		

Table D.6: Statistics of the parameter estimation for the general rate model in Case Study 3

** estimate on bound

D.4 Summary

In this chapter, the grounds for employing these parameters in the modelling are justified, based on the t-statistic, generated by *gPROMS* (Process Systems Engineering Ltd, 2005) when the parameter estimation is carried out. For further details on the background of statistics, refer to Appendix C.

Appendix E

Experimental data

In Chapter 3, the systematic approach was verified using two experimental case studies. The original form of the raw data used in these case studies are summarised in this appendix, along with the conversion factors used to modify the information from these works to the form shown and used in Chapter 3.

E.1 Case Study 2: yeast homogenate experiment

Khanom (2003) used hydrophobic interation chromatography in order to purify protein alcohol dehydrogenase (ADH) from a yeast homogenate mixture. Bakers' yeast was suspended in buffer and then disrupted by high pressure homogenisation and clarified by centrifugation. Subsequently, the mixture (supernatant) was removed by pipetting and diluted to approximately $10mg/ml$ protein before being loaded onto the chromatography column.

The hydrophobic interaction column was 12.5cm in length and 1.6 internal column diameter. The column was equilibriated with 10 column volumes (CV) buffer and then the diluted supernatant was loaded at $2.5ml/ml$ for three different column

loads: 5CV, 10CV and 20CV. After loading, the column was washed with the same equilibriating buffer. Finally, a step change in salt concentration using a different buffer was used to elute the ADH at $2.5ml/min$. The product collected was then assayed for total protein concentration and ADH activity. The experimental results are given in Figures E.1 - E.6.

The $x-axis$ of the following plots are in terms of the *cumulative elution volume*, in which the volume eluted from the column is accumulated, in the experiment. As the flowrate of the elution is known to be $2.5ml/min$, the elution time can easily be found:

$$\text{Elution time} = \frac{\text{Cumulative elution volume}}{\text{Flowrate}} \tag{E.1}$$

Subsequently, as the *dimensionless* time domain is used in both the equilibrium-dispersive and general rate model, real time in these experiments have to be re-written in dimensionless form using the following:

$$\text{Dimensionless time} = \frac{\text{Velocity} \cdot \text{Realtime}}{\text{Length of column}} \tag{E.2}$$

Finally, the activity value for ADH is converted to a more understandable *concentration* value:

$$\text{Concentration [mg/ml]} = \frac{\text{Activity unit [U/ml]}}{\text{Conversion factor [U/mg]}} \tag{E.3}$$

where the conversion factor for ADH is 340 U/mg.

E.2 Case Study 3: egg white proteins and myoglobin experiment

Edwards-Parton (2005) conducted a gradient elution ion-exchange chromatographic separation using a mixture of egg white proteins and myglobin. The ion exchanger is a 1ml *SP Sepharose Fast Flow HiTrap* column of 2.5cm length and 0.7cm internal

Component	Average molecular weight (M_R)	Extinction coefficient (ϵ)
Ovalbumin & Ovomuscoid	40 000	32 180
Ovotransferrin	77 000	85 000
Lysozyme	14 300	36 000
Myoglobin	16 000	160 000

Table E.1: Feed concentration calculations for the chromatograms in Case Study 3
M_R and ϵ values from Fasman (1992)

column diameter. 20mM sodium phosphate buffer was used. The egg white protein was mixed in a ratio of 1:4 with the buffer and centrifuged to remove precipitate and solids. A small amount of myoglobin was then added. The elution buffer used was a mixture of 20mM sodium phosphate and 2M sodium chloride both of pH 5.5, and the sodium chloride is increased gradually from 0% to a maximum amount of 50% of the buffer by the end of elution. The absorption data was measured at 280 and 408nm, with the egg white proteins being absorbed at 280nm while the myoglobin absorbed at 480 nm. The experimental results are given in Figure E.7.

The Beer-Lambert law (or Beer's law) is the linear relationship between absorbance and concentration of an absorbing species. The general Beer-Lambert law is written as:

$$Abs = \epsilon p C_i \tag{E.4}$$

where Abs is the measured absorbance, ϵ is a wavelength-dependent absorptivity coefficient, p is the path length and C_i is the concentration of component i.

Table E.1 summarises the necessary values for converting the absorbance unit values to mass values for each component.

The absorbance unit in Figure E.7 is in mAU absorbance units for a path length of 0.2cm. This is converted for a path length of 1cm:

$$mAU(0.2cm) * 5 = mAU(1cm) \tag{E.5}$$

mAU is then converted to AU:

$$\frac{mAU}{1000} = AU \tag{E.6}$$

Equation E.4 can now be used to convert the absorbance unit to give the molecular concentration of the component i:

$$C_i(\text{molL}^{-1}) = \frac{Abs(\text{AU at 1cm path length})}{\epsilon} \tag{E.7}$$

which can be converted to the mass concentration:

$$C_i(\text{gL}^{-1}) = C_i(\text{molL}^{-1}) \times M_{R,i} \tag{E.8}$$

A sample calculation for ovalbumin is shown:

$$C_{Ovalbumin} = \left(\frac{\frac{mAU(1cm)}{1000}}{32180} \right) \times 40000 \tag{E.9}$$

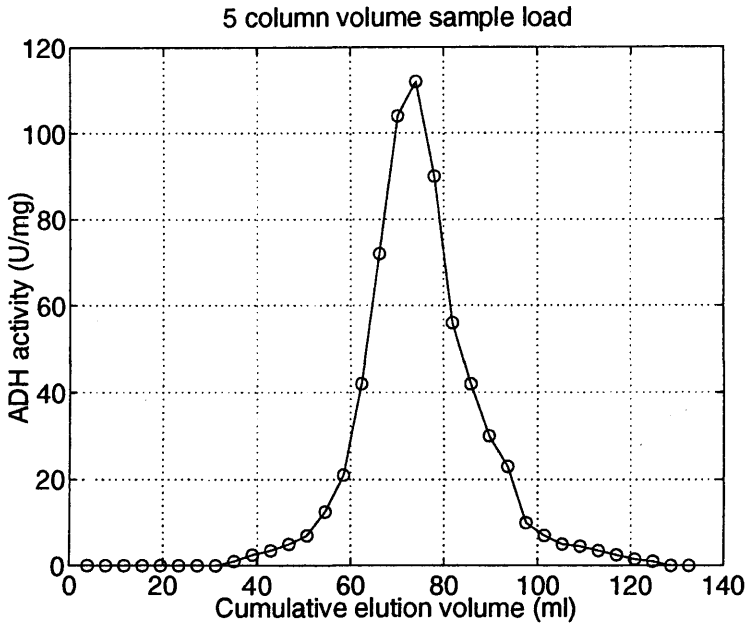

Figure E.1: ADH activity for 5CV load

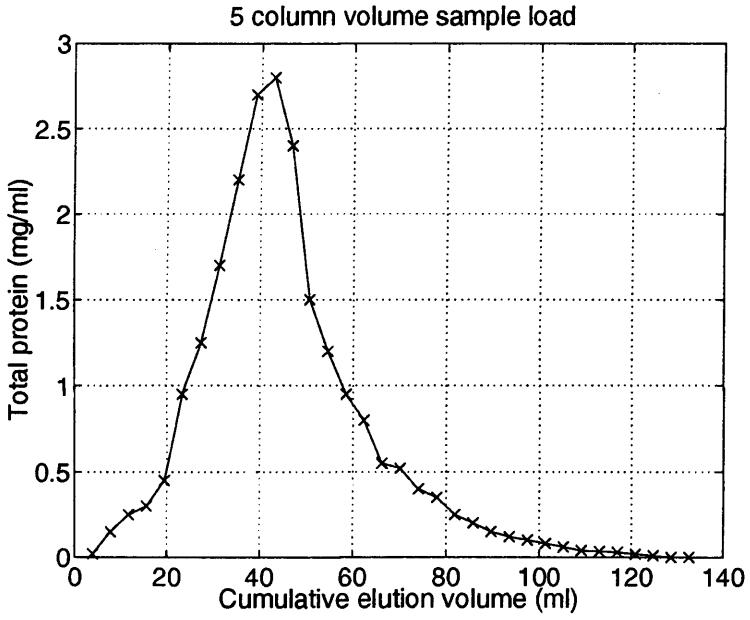

Figure E.2: Total protein concentration for 5CV load

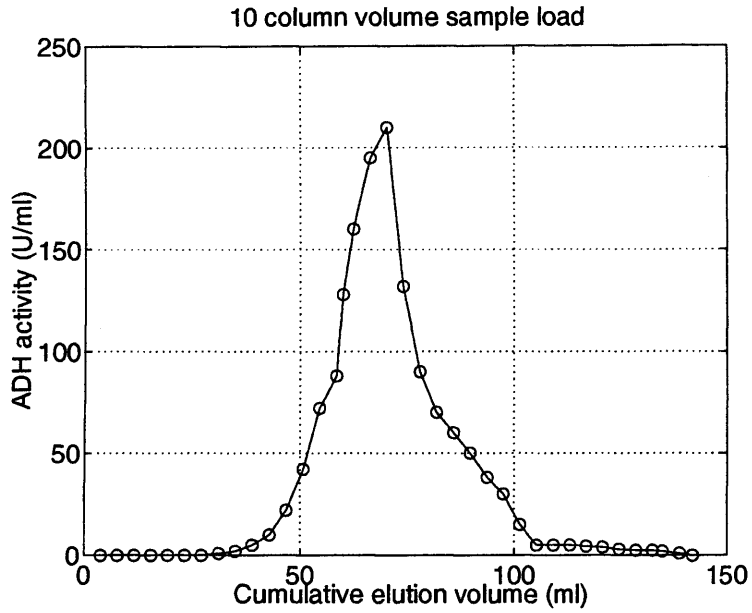

Figure E.3: ADH activity for 10CV load

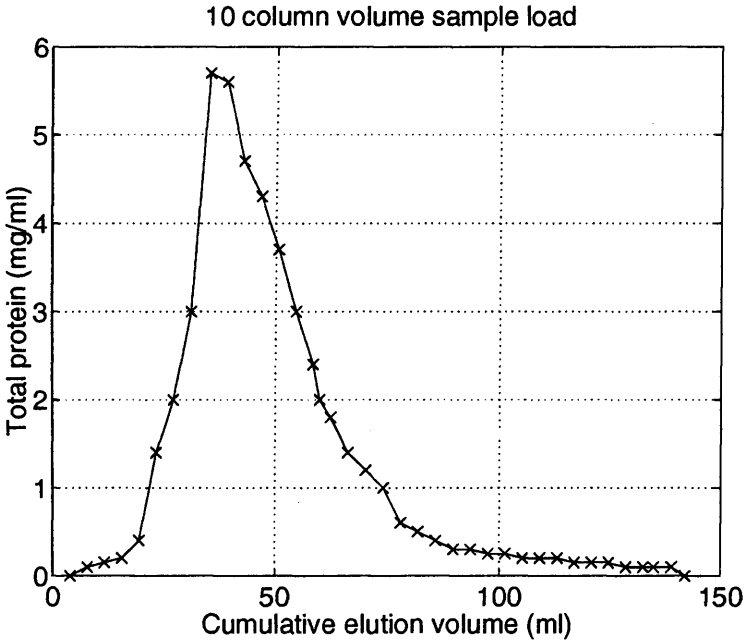

Figure E.4: Total protein concentration for 10CV load

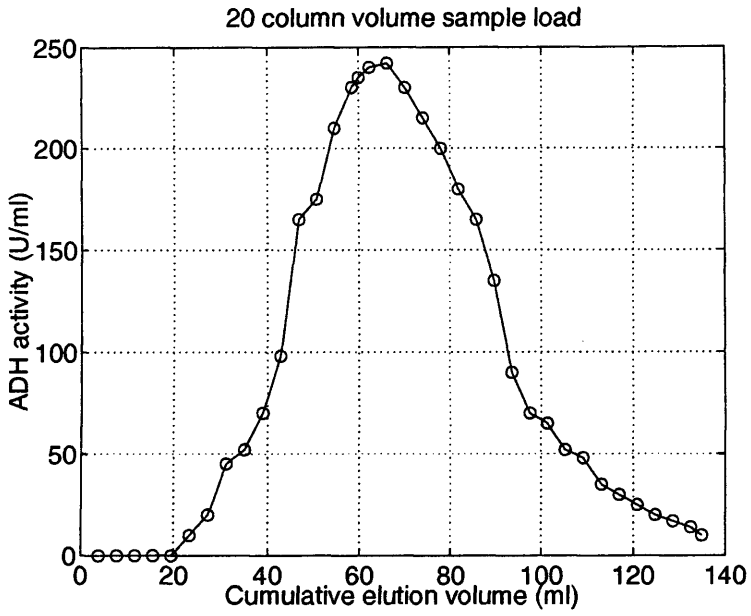

Figure E.5: ADH activity for 20CV load

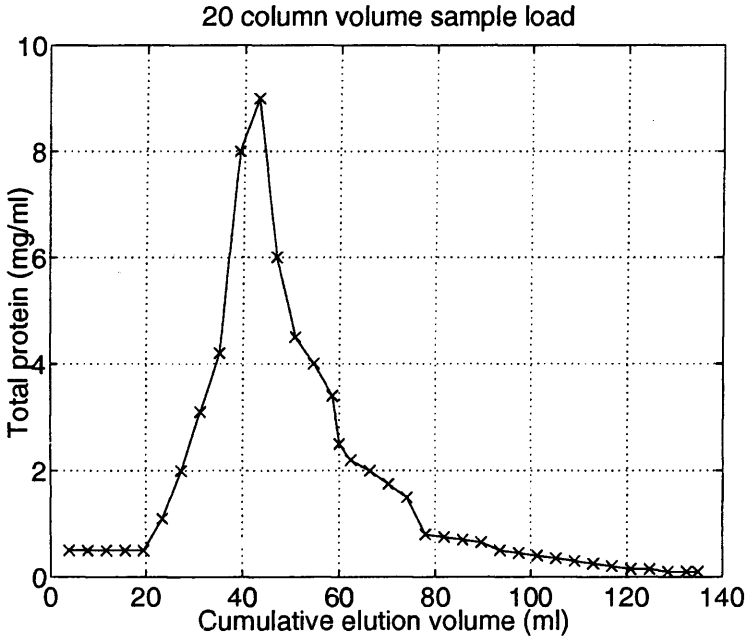

Figure E.6: Total protein concentration for 20CV load

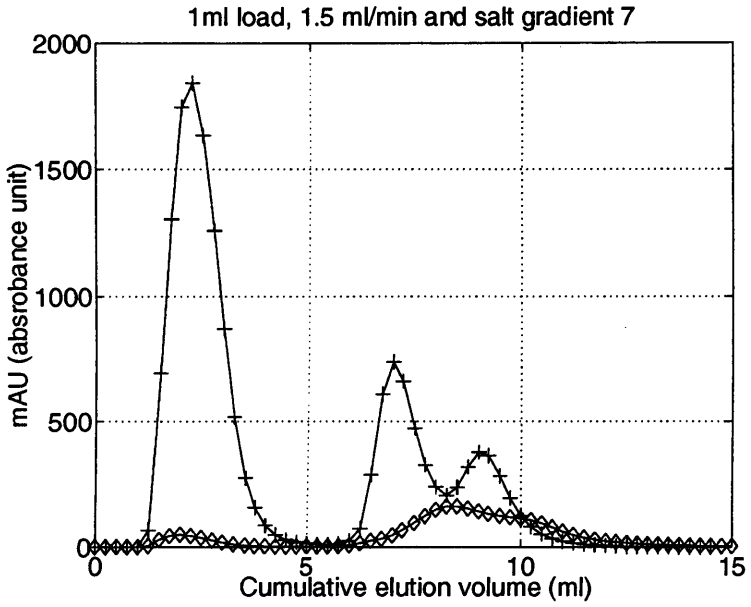

Figure E.7: Chromatogram for mixture of egg white proteins and myoglobin

'+' : Egg white proteins, '◇' : Myoglobin

Appendix F

Maximum purification diagram approach

In this appendix, the definition and methodology for developing the maximum purification diagram employed in the model selection in Chapter 3 is outlined in detail. In Section F.1, the procedure to generate the fractionation digram from a chromatogram is summarised, followed by the calculations for the purification factors from the fractionation diagram in Section F.2 and finally, how the maximum purification factor versus yield diagram is plotted in Section F.3.

F.1 Fractionation diagram

The fractionation diagram for a hypothetical feed mixture consisting of three components: product P and impurities A and B, is considered. The chromatogram generated by this separation is shown in Figure F.1(a). To obtain the area under the elution profiles, the Trapezoidal rule is used. The approximate area under the concentration curve for the interval between t_1 and t_2 is thus given by:

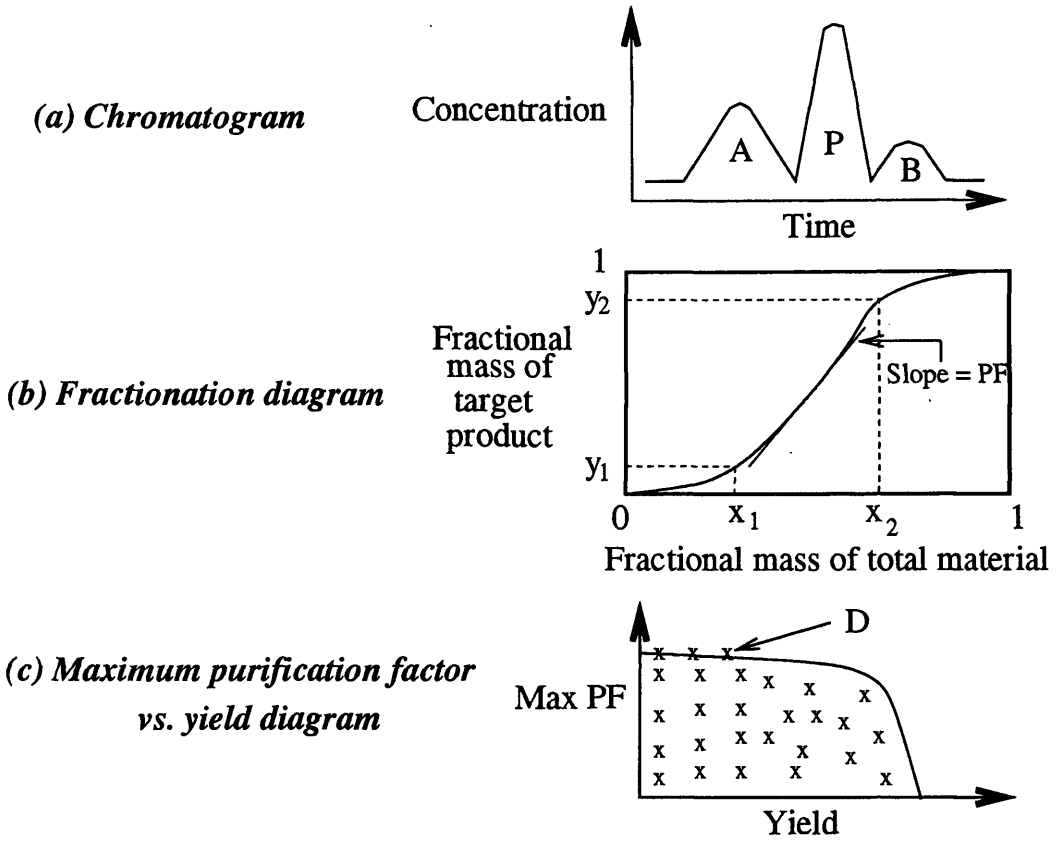

Figure F.1: Approach to achieve the maximum purification diagram from a chromatogram

$$\text{Area} = \frac{\frac{1}{2}(C_1 + C_2)}{t_2 - t_1} \tag{F.1}$$

The amount of each material, M_m (mg) (where subscript m = [P,A,B]), in a particular fraction is given by the product of the area under the curve of that component and the volumetric mobile phase flowrate F_c (ml/s):

$$\text{Amount of material, } M_m = \text{Area} \times F_c \tag{F.2}$$

The amounts of product ($M_{P,i}$), impurity A ($M_{A,i}$) and impurity B ($M_{B,i}$) in each interval i are calculated using Equation F.2. Hence, the total amount of material in interval i is the sum of all these quantities:

$$M_{T,i} = \sum_{i=1}^{n} M_{m,i} = M_{P,i} + M_{A,i} + M_{B,i} \tag{F.3}$$

For each interval, the arithmetic mean time t_m is defined as the time between the upper and lower limit of the interval i (n represents the total number of intervals):

$$t_m = \frac{1}{2}(t_i + t_{i+1}) \quad \forall i = 1, 2, \cdots, n \tag{F.4}$$

The fractionation diagram plots the changes in the cumulative fractional mass of the product (the component of interest) eluted as a function of the corresponding fractional total mass eluted. Hence, the axes of the fractional diagram are defined as:

Fractional mass of total material eluted,

$$X = \frac{\text{Cumulative mass of total material eluted at time t}}{\text{Total mass eluted at t} = \infty}$$

Fractional mass of product eluted,

$$Y = \frac{\text{Cumulative mass of product eluted at time t}}{\text{Total mass of product eluted at t} = \infty}$$

Mathematically, X and Y can be expressed as:

$$X = \frac{\sum_{i=1}^{n} M_{T,i}}{M_{T,Total}} \quad \forall i = 1, 2, \cdots, n \tag{F.5}$$

$$Y = \frac{\sum_{i=1}^{n} M_{P,i}}{M_{P,Total}} \quad \forall i = 1, 2, \cdots, n \tag{F.6}$$

where n is the total number of fractions, $M_{T,Total}$ is the total load of the feed sample, and $M_{P,Total}$ is the total amount of product component in the feed sample. Since X and Y are fractions, the values fall in the range between 0 and 1. A theoretical fractionation diagram can then be plotted as shown in Figure F.1(b).

F.2 Purification factor

Having defined the fractionation diagram, the purification factor (PF) can now be calculated to illustrate the performance of the operation. The purification factor is

defined as the ratio between the final purity of the product after purification to the starting purity of the feed sample:

$$PF = \frac{\text{Final purity of product}}{\text{Initial purity of total feed load}} = \frac{\left[\frac{M_P^{t_{end}} - M_P^{t_{start}}}{M_T^{t_{end}} - M_T^{t_{start}}}\right]}{\left[\frac{M_{P,Total}}{M_{T,Total}}\right]} \tag{F.7}$$

Equation F.7 can be rearrange to give:

$$PF = \frac{\left[\frac{M_P^{t_{end}}}{M_{P,Total}} - \frac{M_P^{t_{start}}}{M_{P,Total}}\right]}{\left[\frac{M_T^{t_{end}}}{M_{T,Total}} - \frac{M_T^{t_{start}}}{M_{T,Total}}\right]} \tag{F.8}$$

where the subscripts P and T denote the *product* fraction and *total* feed sample, respectively, and the superscripts t_{start} and t_{end} are the points of the starting and end collection times, respectively. The terms $\frac{M_T}{M_{T,Total}}$ and $\frac{M_P}{M_{P,Total}}$ define the x-axis (X) and y-axis (Y) in the fractionation diagram, respectively. Equation F.8 is in fact the gradient of the fractionation diagram between any two points corresponding to the start and end of product collection in the chromatogram (Refer to Figure F.1(b) for an example of the purification factor). The purification factor always carries a value equal to or greater than 1.0, as 1.0 reflects the situation where *no purification* is achieved.

F.3 Maximum purification factor diagram

It is possible to select the chromatogram at points from any positions along the fractionation curve that satisfy the following criterion: the vertical distance between any two points gives the product yield; the slope of the tangent between the two points is the value of purification factor corresponding to that yield. By varying the position of the collection points, a plot of purification factor against yield can then be produced. The plot obtained represents the set of all the possible values of purification factors achievable for any combination of cut points (These are represented by "x" in Figure F.1(c)). The range of yields share a rather inverse relationship with

the purification factors *i.e.* low yields have high purification factors. The engineer has to select conditions that maximise the purification factor for a given yield or to determine the best yield that can be achieved for a specific maximum purification factor.

In order to systematically generate the relationship between the maximum purification factor and yield, an incremental-searching-type computer algorithm was used by Ngiam (2002). All purification factors achievable for each yield were searched and compared to select the *maximum* purification factor value corresponding to that particular yield using an existing *Matlab* code by Ngiam (2002) (Refer to the maximum purification factor value D in Figure F.1(c)). This allows for the relationship between the maximum purification factor against the yield to be plotted.

In an ideal chromatographic separation, the highest possible product purity that can be achieved is 100%. Therefore, the highest theoretical value for the maximum purification factor for a given separation system, with an initial product purity of x percent is given as:

$$\text{Maximum purification factor, } PF_{max} = \frac{100}{x} \tag{F.9}$$

For instance, if the initial purity of the sample loaded is 20%, the largest value of the maximum purification factor in any selected fraction would be 20.

Appendix G

Relative error analysis for predicted elution profiles

In Chapter 4, a simple error analysis of the CSS models against the dynamic SMB model is presented here. These results demonstrate that the CSS (Switch) model is a more suitable model to use in predicting the SMB profiles.

The relative error calculation for the concentration profiles of the SMB models used in this work is as follows:

$$\frac{C^{dynamic}(i,z) - C^{CSS}(i,z)}{C^{dynamic}(i,z)} \times 100\% \qquad \text{(G.1)}$$

where $C^{dynamic}$ and C^{CSS} are the concentrations of component i along the axial direction z, for the dynamic SMB model and CSS SMB models, respectively.

This relative error is calculated across the elution profiles in the SMB unit for components 1 and 2 and are shown in the Figures G.1 amd G.2, respectively for both the CSS (Switch) and CSS (Cycle) models. .

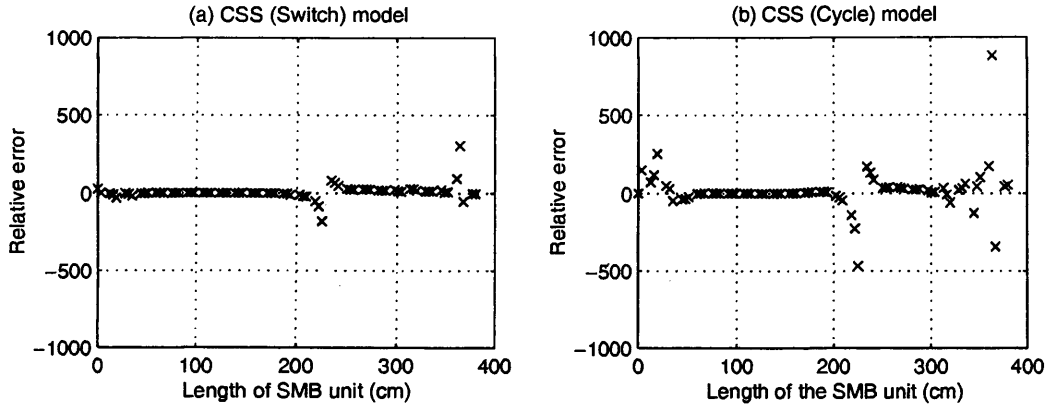

Figure G.1: Relative error of the CSS models for Component 1

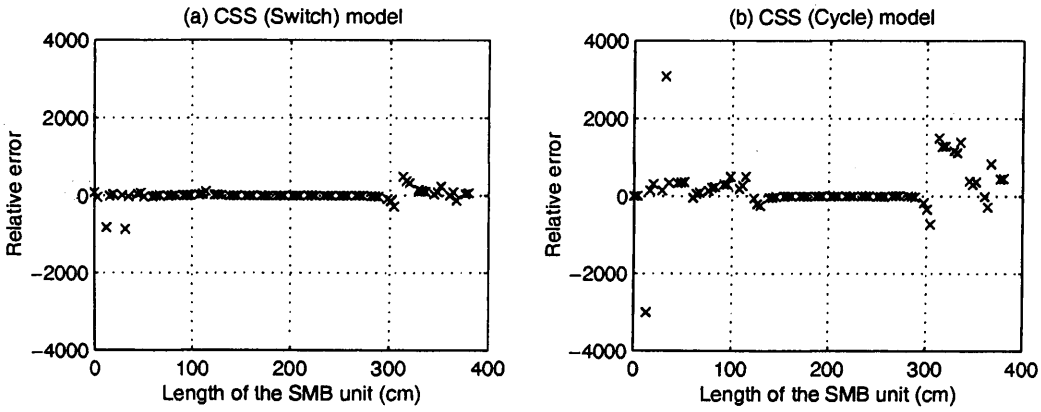

Figure G.2: Relative error of the CSS models for Component 2

For convenience, the graphs plotted on the same axes (for each component). Table G.1 shows the fraction of plots in each graph that meets the criteria of relative errors of 5% and less.

Component	**CSS (Switch) model**	**CSS (Cycle) model**
1	0.466	0.315
2	0.411	0.246

Table G.1: Comparison of relative error for the CSS (Switch) and CSS (Cycle)model

Table G.1 shows that the CSS (Cycle) model has a greater proportion of error compared to the CSS (Switch) model for both components, and Figures G.1 and G.2 also show visually a greater spread of error in the CSS (Cycle) model, as compared to the CSS (Switch) model, particularly along the ends of the SMB unit. This suggest that the CSS (Switch) model is a more accurate model as compared to the CSS (Cycle) model.

Appendix H

Calculations in the systematic approach for optimisation

There are several calculations entailed in each section of the systematic approach outlined in Chapter 5. The main calculations featured are the scale-up calculations, chromatographic unit capital cost and cash flow calculations for each process. In this chapter, the calculations for all the chromatographic processes in the approach are summarised.

H.1 Scale-up calculations

In this section, the scale-up calculations are repeated for single column, single column with recycling policy, SMB and Varicol processes (the last two are treated as the same process for scale-up purposes).

Basis: 100 minutes per batch					
Scale up factor	**Flowrate** (cm^3/s)	**Diameter** (cm)	**Production** (g) **per batch**	**Annual number of batches**	**Total production** (kg **per year**)
Base case	0.0166	1.4	0.50	4800	2.40
10	1.66	14	50	4800	240
20	6.64	28	200	4800	960
30	14.94	42	450	4800	2160
40	26.56	56	800	4800	3840
21	**7.32**	**29.4**	**221**	**4800**	**1060**
22	8.03	30.8	242	4800	1160

Table H.1: The scaled-up parameters in the single chromatographic column unit; parameters in bold are used

Basis: 170 minutes per batch					
Scale up factor	**Flowrate** (cm^3/s)	**Diameter** (cm)	**Production** (g **per batch**	**Annual number of batches**	**Total production** (kg **per year**)
Base case	0.0166	1.4	0.50	2400	1.44
10	1.66	14	50	2880	144
20	6.64	28	200	2880	576
25	10.38	35	313	2880	900
30	14.94	42	450	2880	1296
40	26.56	56	800	2880	2300
27	**12.10**	**37.8**	**365**	**2880**	**1050**

Table H.2: The scaled-up parameters for the single chromatographic column with recycling policy; parameters in bold are used

Basis: 618 seconds per switch; 4944 seconds per cycle (8 switches)								
Scale up factor	**Feed flowrate** (cm^3/s)	**Desorbent flowrate** (cm^3/s)	**Extract flowrate** (cm^3/s)	**Recycle flowrate**	**Diameter** (cm)	**Production** (g) **per cycles**	**Number of cycles per year**	**Total production** (kg **per year**)
Base case	0.0166	0.0266	0.0233	0.0665	1.4	0.13	5820	0.75
10	1.66	2.66	2.33	6.65	14	410	5820	2390
5	0.415	0.665	0.5825	1.6625	7	103	5820	597
7	0.813	1.303	1.142	3.259	9.8	201	5820	1170
6.5	**0.701**	**1.124**	**0.984**	**2.810**	**9.1**	**173**	**5820**	**1010**

Table H.3: The scaled-up parameters for the multi-column chromatography processes, SMB and Varicol; parameters in bold are used

The calculations for Tables H.1, H.2 and H.3 are as follows:

$$\text{Scaled up flowrate} = \text{Base case flowrate} \times \text{Scale up factor}^2 \quad \text{(H.1)}$$

$$\text{Scaled up diameter} = \text{Base case diameter} \times \text{Scale up factor} \quad \text{(H.2)}$$

The injection time (t_{inj}) in the single column with recycle from the base case remains that same throughout scale-up at 602.4 seconds. This means that with the increased volumetric flowrate, the injected volume increases. In the multi-column processes, the switching periods for the SMB and the Varicol processes are kept at 618 seconds, whilst all the flowrates are increased according to the scale-up factor. In the SMB process, all nodes are switched one column in the direction of the flow of the mobile phase at the same time. In the Varicol process, all four flowrates are switched one column in the direction of the mobile phase at different times within the same switching period of the SMB process *i.e.* 618 seconds. To calculate the batch production and annual production, refer to Equations 5.3 and 5.4 in Chapter 5, respectively.

H.2 Capital cost calculations

The single column and the single column with recycle are regarded to have the same capital costs as the same equipment can be used to allow operation in either conventional elution or closed-loop recycling mode (Section 5.2.2). Similarly, the capital cost for the SMB and the Varicol processes are the same *provided the number of columns are the same.* The differences in the operation of the two processes is controlled by computer software hence no additional cost is assumed.

Chapter 5 employed a *delivery cost percentage* estimation method to determine the capital investment for each chromatographic alternative. In this section, the results for the both single and multi-column processes are shown in Tables H.4 and H.5.

Components	Percentage of delivered equipment cost	Estimated cost
Direct costs		
Purchased equipment delivered (including fabricated equipment, process machinery, pumps and compressors)		150, 000
Purchased-equipment installation	0.39	58, 500
Instrumentation (installed)	0.26	39, 000
Piping (installed)	0.31	46, 500
Electrical (installed)	0.1	15, 000
Buildings (including services)	0.29	43, 500
Yard improvements	0.12	18, 000
Service facilities (installed)	0.55	82, 500
Indirect costs		
Engineering and supervision	0.32	48, 000
Construction expense	0.34	51, 000
Legal expense	0.04	6, 000
Contractor's fee	0.19	28, 500
Contingency	0.37	55, 500
Total (FCI)		642, 000
Working capital*	0.75	112, 000
Total capital investment		**754, 500**

Table H.4: Estimated capital costs based on percentage of delivered-equipment cost method for a single column (Peters *et al.*, 2003)
(*or approximately 15% of total capital investment)

Components	Percentage of delivered equipment cost	Estimated cost
Direct costs		
Purchased equipment delivered (including fabricated equipment, process machinery, pumps and compressors)		300, 000
Purchased-equipment installation	0.39	117, 000
Instrumentation (installed)	**0.4**	120, 000
Piping (installed)	**0.4**	120, 000
Electrical (installed)	0.1	30, 000
Buildings (including services)	0.29	87, 200
Yard improvements	0.12	36, 600
Service facilities (installed)	0.55	165, 000
Indirect costs		
Engineering and supervision	**0.5**	150, 000
Construction expense	0.34	102, 200
Legal expense	0.04	12, 200
Contractor's fee	0.19	57, 200
Contingency	0.37	111, 600
Total (FCI)		1, 407, 000
Working capital*	0.75	225, 000
Total capital investment		**1, 632, 000**

Table H.5: Estimated capital costs based on percentage of delivered-equipment cost method for multi-column operation (Peters *et al.*, 2003)
(*or approximately 15% of total capital investment) Figures in bold indicate changes made to the estimates from Table H.4

In each process, alterations have been made primarily to the percentages in the instrumentation and controls and engineering and supervision sections to accommodate that these complex processes will have higher costs in these areas compared to the single chromatographic column unit. These alternations to the percentages are in bold in Table H.5.

H.3 Economic appraisal calculations

The calculations for the cash flows in Tables H.6, H.7 and H.8 are explained in this section along with some sample calculations from Table H.6.

Sample calculation for year 4 in the single column process (refer to Table H.6 and): Sales income = 2000× US \$10000 = US \$20 $\times 10^6$

Raw material costs = 2000× US \$ 7170 = U \$14.34 $\times 10^6$

Production costs = US \$760000

Net cash flow = Sales income - costs - investment

= (20 - 14.34 - 0.76)$\times 10^6$ = US \$4.9 $\times 10^6$

Discounted cash flow (at 15 per cent) in year 4 = $\frac{4.9\times 10^6}{(1+0.15)^4}$ = US \$2.80 $\times 10^6$

End of year	Forecast sales kg	Forecast selling price US $/kg	Raw material costs US $/kg	Production costs (US $) $\times 10^5$	Sales income (US $) $\times 10^6$	Net cash flow (US $) $\times 10^6$	Cumulative cash flow (US $) $\times 10^7$	Discounted cash flow 15% (US $) $\times 10^6$	Cumulative discounted cash flow (US $) $\times 10^7$
1	0	0	0	0	0	-0.755	-0.0755	-0.656	-0.0656
2	2020	10000	7170	6.07	5.02	4.91	0.415	3.71	0.305
3	2020	10000	7170	6.07	5.02	5.02	0.917	3.30	0.635
4	2020	10000	7170	6.07	5.02	5.02	1.42	2.87	0.922
5	2020	10000	7170	6.07	5.02	5.02	1.92	2.50	1.17
6	2020	10000	7170	6.07	5.02	5.02	2.42	2.17	1.39
7	2020	10000	7170	6.07	5.02	5.02	2.93	1.89	1.58
8	2020	10000	7170	6.07	5.02	5.02	3.43	1.64	1.74
9	2020	10000	7170	6.07	5.02	5.02	3.93	1.43	1.88
10	2020	10000	7170	6.07	5.02	5.02	4.43	1.24	2.01
11	2020	10000	7170	6.07	5.02	5.02	4.93	1.08	2.12
12	2020	10000	7170	6.07	5.02	5.02	5.43	0.938	2.21
13	2020	10000	7170	6.07	5.02	5.02	5.94	0.816	2.29
14	2020	10000	7170	6.07	5.02	5.02	6.44	0.709	2.36
15	2020	10000	7170	6.07	5.02	5.02	6.94	0.617	2.42

Table H.6: Economic appraisal for the single chromatographic column unit

End of year	Forecast sales kg	Forecast selling price US $/kg	Raw material costs US $/kg	Production costs (US $) $\times 10^5$	Sales income (US $) $\times 10^6$	Net cash flow (US $) $\times 10^6$	Cumulative cash flow (US $) $\times 10^7$	Discounted cash flow 15% (US $) $\times 10^6$	Cumulative discounted cash flow (US $) $\times 10^7$
1	0	0	0	0	0	-1.63	-0.163	-1.42	-0.142
2	2020	10000	7170	2.78	5.42	5.19	0.356	3.96	0.251
3	2020	10000	7170	2.78	5.42	5.42	0.898	3.56	0.607
4	2020	10000	7170	2.78	5.42	5.42	1.44	3.10	0.917
5	2020	10000	7170	2.78	5.42	5.42	1.98	2.69	1.19
6	2020	10000	7170	2.78	5.42	5.42	2.52	2.34	1.42
7	2020	10000	7170	2.78	5.42	5.42	3.07	2.04	1.62
8	2020	10000	7170	2.78	5.42	5.42	3.61	1.77	1.80
9	2020	10000	7170	2.78	5.42	5.42	4.15	1.54	1.96
10	2020	10000	7170	2.78	5.42	5.42	4.69	1.34	2.09
11	2020	10000	7170	2.78	5.42	5.42	5.23	1.16	2.21
12	2020	10000	7170	2.78	5.42	5.42	5.78	1.01	2.31
13	2020	10000	7170	2.78	5.42	5.42	6.32	0.881	2.40
14	2020	10000	7170	2.78	5.42	5.42	6.86	0.766	2.47
15	2020	10000	7170	2.78	5.42	5.42	7.40	0.666	2.54

Table H.7: Economic appraisal for the SMB chromatograhic unit

End of year	Forecast sales kg	Forecast selling price US $/kg	Raw material costs US $/kg	Production costs (US $) $\times 10^5$	Sales income (US $) $\times 10^6$	Net cash flow (US $) $\times 10^6$	Cumulative cash flow (US $) $\times 10^7$	Discounted cash flow 15% (US $) $\times 10^6$	Cumulative discounted cash flow (US $) $\times 10^7$
1	0	0	0	0	0	-1.63	-0.163	-1.42	-0.142
2	2020	10000	7170	3.74	5.34	5.12	0.349	3.87	0.245
3	2020	10000	7170	3.74	5.34	5.34	0.883	3.51	0.597
4	2020	10000	7170	3.74	5.34	5.34	1.42	3.05	0.902
5	2020	10000	7170	3.74	5.34	5.34	1.95	2.66	1.17
6	2020	10000	7170	3.74	5.34	5.34	2.49	2.31	1.40
7	2020	10000	7170	3.74	5.34	5.34	3.02	2.01	1.60
8	2020	10000	7170	3.74	5.34	5.34	3.55	1.75	1.77
9	2020	10000	7170	3.74	5.34	5.34	4.09	1.52	1.93
10	2020	10000	7170	3.74	5.34	5.34	4.62	1.32	2.06
11	2020	10000	7170	3.74	5.34	5.34	5.16	1.15	2.17
12	2020	10000	7170	3.74	5.34	5.34	5.69	0.999	2.27
13	2020	10000	7170	3.74	5.34	5.34	6.23	0.868	2.36
14	2020	10000	7170	3.74	5.34	5.34	6.76	0.755	2.44
15	2020	10000	7170	3.74	5.34	5.34	7.29	0.657	2.50

Table H.8: Economic appraisal for the Varicol chromatographic unit

Figures H.1 and H.2 are plots from Tables H.6, H.7 and H.8. Figure H.1(a) show the cumulative cash flow diagram (without considering the effect of the time value of money) for all the processes, and Figure H.1(b) shows the effect on time on the net cash flow of the processes. Figure H.2 shows the cumulative discounted cash flow diagram for all the alternatives and is discussed in Chapter 5.

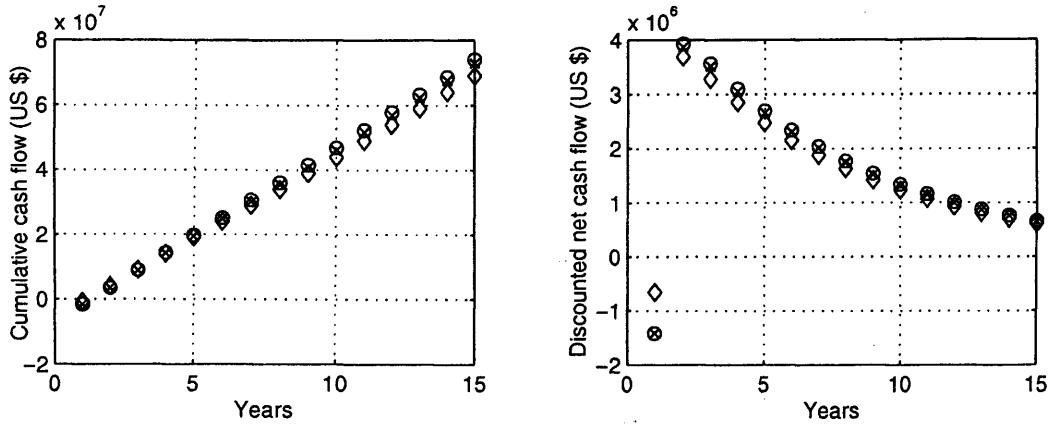

Figure H.1: (a) Cumulative cash flow diagram, (b) Discounted net cash flow diagram

◇: Single column, ○: SMB unit and ×: Varicol unit

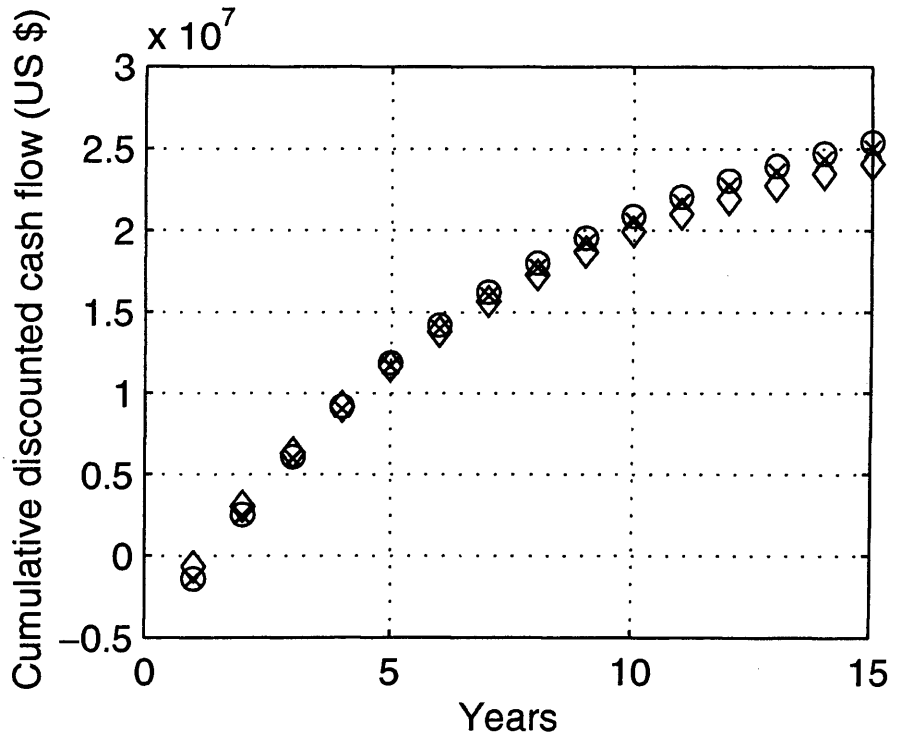

Figure H.2: Cumulative discounted net cash flow diagram

◇: Single column, ○: SMB unit and ×: Varicol unit

Appendix I

Economic evaluation of chromatographic processes

An economic objective function is involved in the optimisation and subsequent process selection of the different chromatographic techniques in Chapter 5, and some form of economic evaluation is thus necessary. In this chapter, important terms used in Chapter 5 are defined.

I.1 Introduction

Chapter 5 established that an economic comparison of the single and multi-column chromatographic processes is the only fair basis of comparison of these techniques. This means that some means of comparing the different economic performances of these processes is required. The processes differ widely in scope, operating policies and capital cost, and this requires sophisticated evaluation techniques to decide between them. Some important economic evaluation techniques and criteria used in Chapter 5 to judge economic performance are outlined in this appendix.

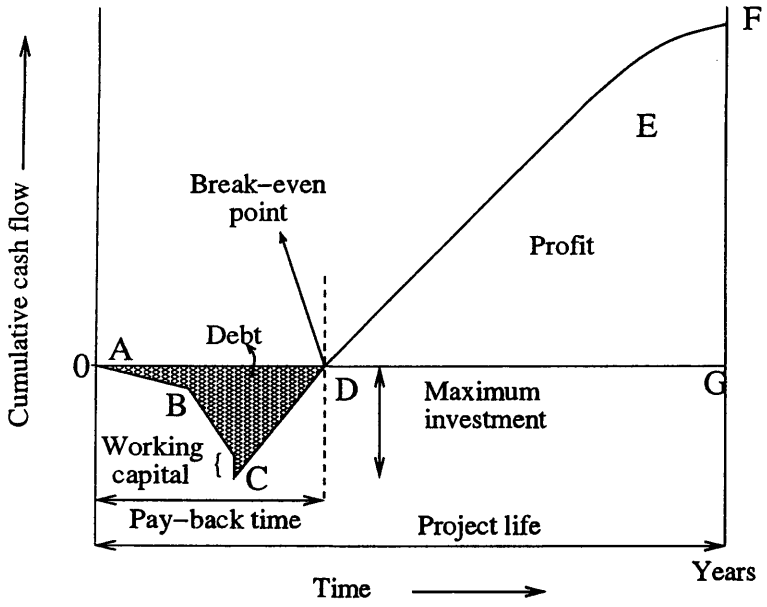

Figure I.1: A project cash-flow diagram (Sinnott, 2001)

I.2 Cash flow (CF)

The flow of cash is what sustains any commercial organisation and can be likened to the material flows in a process plant. The inputs, or investments, are necessary to pay for research and development, plate design and construction, and plant operation. The outputs are the products to be sold, whilst cash returns are recycled to the organisation from the profits earned (Sinnott, 2001). The *net cash flow* at any time is the difference between earnings and expenditure. Figure I.1 shows a *cash-flow diagram* of the forecast cumulative net cash flow over the life of the plant.

The cash flows in the cash-flow diagram are based on estimates of the investment, operating costs, sales volume and sales price of a particular project. Thus, the cash flow diagram gives a clear picture of the resources required for the project and the timing of the earnings, with the characteristic regions as illustrated in Figure I.1.

I.3 Discounted cash flow (DCF)

In Figure I.1, the value of the net cash flow in the year in which it occurred is shown. The figures on the *y-axis* reflect the "future worth" of the project: the cumulative "net future worth". Any money earned can be reinvested as soon as it is available to start earning a return. This means that the money earned in the early years of the project are more important than that earned in the later years. This "time value of money" can be displayed using a variation of compound interest formula.

The net cash flow in each year of the project can be brought to its "present value" at the start of the project by discounting it at some chosen compound interest rate. The *Net Present Value* (NPV) of cash flow in the year n is given by:

$$\text{NPV} = \frac{\text{Estimated net cash flow in year } n \text{ (NFW)}}{(1+r)^n} \tag{I.1}$$

where r is the discount rate (interest rate) in per cent, divided by 100.

$$\text{Total NPV of project} = \sum_{n=1}^{n=t} \frac{NFW}{(1+r)^n} \tag{I.2}$$

where t is the life of the project (in years).

The discount rate is chosen to reflect the earning power of money. It would be approximately equivalent to the current interest rate that the money would earn if invested. Note that the total NPV will be less than the total NFW as it reflects the time value of money and pattern of earnings over the life of the project.

I.4 Payback time

Payback time is the time required after the start of the project to pay off the initial investment from income: point D on Figure I.1. It is a useful criteria for judging projects that have a short life, or when capital is available only for a short time. As a criterion of investment performance, however, it does not by definition consider the performance of the project after the pay-back period.

I.5 Other considerations

There are other factors which also affect the cash flow analysis and these differ depending on the country and government policies employed. They may thus be taken into account at the user's discretion. In this work, these factors have not been included in the economic analysis, as the focus is the comparison of the performance of the processes and any changes in tax, depreciation and inflation are regarded to affect the processes in the same way.

I.5.1 Tax

Taxes on profits are not constant and depend on government policies. In recent years, the profit tax has been running at around 33 per cent and this can be used to estimated the cash flow after tax (Sinnott, 2001).

I.5.2 Depreciation

Depreciation of the investment (*i.e.* its devaluation over time) is inevitable. Its rates, however, depend on government policy, and the accounting practices of the particular company. In development areas, the government may sometimes allow higher depreciation rates for tax purposes or pay capital grants to encourage investment in such areas.

I.5.3 Inflation

Inflation depreciates money in a manner similar to, but different from, the idea of discounting to allow for the time value of money. The effect of inflation on the net cash flow in future years can be allowed for in a similar manner to the NPV calculation in Equation I.1 using an inflation rate in place or, or added to the discount rate r. However, it is difficult to decide what the inflation rate is likely to be in future years, and the inflation may well affect the sales price, operating

costs and raw material prices differently. It is possible to make a decision between alternative projects without formally considering inflation, as inflation is likely to affect the predictions made for both projects in a similar way.